

Electronic Theses and Dissertations, 2004-2019

2006

Modeling Of Atmospheric Refraction Effects On Traffic Noise Propagation

Ahmed El-Aassar
University of Central Florida

 Part of the [Environmental Engineering Commons](#)
Find similar works at: <https://stars.library.ucf.edu/etd>
University of Central Florida Libraries <http://library.ucf.edu>

This Doctoral Dissertation (Open Access) is brought to you for free and open access by STARS. It has been accepted for inclusion in Electronic Theses and Dissertations, 2004-2019 by an authorized administrator of STARS. For more information, please contact STARS@ucf.edu.

STARS Citation

El-Aassar, Ahmed, "Modeling Of Atmospheric Refraction Effects On Traffic Noise Propagation" (2006).
Electronic Theses and Dissertations, 2004-2019. 1123.
<https://stars.library.ucf.edu/etd/1123>

**MODELING OF ATMOSPHERIC REFRACTION EFFECTS ON
TRAFFIC NOISE PROPAGATION**

by

AHMED EL-AASSAR
B.S. Cairo University, 1995
M.S. The University of Birmingham, England, 1997
M.S. University of Central Florida, 2002

A dissertation submitted in partial fulfillment of the requirements
for the degree of Doctor of Philosophy in Environmental Engineering
in the College of Engineering and Computer Science
at the University of Central Florida
Orlando, Florida

Fall Term
2006

Major Professor: Roger Wayson

ABSTRACT

Traffic noise has been shown to have negative effects on exposed persons in the communities along highways. Noise from transportation systems is considered a nuisance in the U.S. and the government agencies require a determination of noise impacts for federally funded projects. There are several models available for assessing noise levels impacts. These models vary from simple charts to computer design models. Some computer models, i.e. Standard Method In Noise Analysis (STAMINA), the Traffic Noise Model (TNM) and the UCF Community Noise Model (CNM), have been used to predict geometric spreading, atmospheric absorption, diffraction, and ground impedance. However, they have largely neglected the atmospheric effects on noise propagation in their algorithms.

The purpose of this research was to better understand and predict the meteorological effects on traffic noise propagation through measurements and comparison to acoustic theory. It should be noted that this represents an approach to incorporate refraction algorithms affecting outdoor noise propagation that must also work with algorithms for geometric spreading, ground effects, diffraction, and turbulence.

The new empirical model for predicting atmospheric refraction shows that wind direction is a significant parameter and should be included in future modeling for atmospheric refraction. To accomplish this, the model includes a “wind shear” and “lapse

rate” terms instead of wind speed and temperature as previously needed for input of the most used models. The model is an attempt to explain atmospheric refraction by including the parameters of wind direction, wind shear, and lapse rate that directly affect atmospheric refraction.

My Wife Dalia

for her support and love

ACKNOWLEDGMENTS

I would like to express my deep gratitude to my supervisor Dr. Roger Wayson, for his helpful guidance, discussion and encouragement throughout my research. I would like to thank the other members of my committee: Dr. David Cooper, Dr. Essam Radwan, and Dr. Cynthia Young for their thorough review and helpful comments on my dissertation. Special thanks for Dr. John Macdonald for his valuable suggestions and sincere help during the course of this study.

Finally, this research is dedicated to mom and Dad for their support. I hope that I have fulfilled their dream.

TABLE OF CONTENTS

LIST OF FIGURES	ix
LIST OF TABLES	xi
CHAPTER 1 INTRODUCTION	1
CHAPTER 2 LITERATURE REVIEW	4
Sound Wave	5
Geometric Spreading	9
Ground Effects	13
Atmospheric Absorption	33
Refraction	38
Turbulence	49
Diffraction	53
Sound Propagation Models and Research	57
Summary of Literature Review	64
CHAPTER 3 METHODOLOGY	66
CHAPTER 4 ANALYSIS	89
Measured Data	89
Downwind Group	93
Crosswind Group	97
Upwind Group	100

ISO 9613-2.....	111
Downwind Group.....	114
Crosswind Group	118
Upwind Group	121
Summary	124
ISO 9613-2 (with Meteorological Correction)	138
Downwind Group.....	142
Crosswind Group	146
Upwind Group	149
Summary	152
ISO 9613-2 (with Wayson Refraction Model).....	166
Downwind Group.....	170
Crosswind Group	174
Upwind Group	176
Summary	178
Traffic Noise Model (TNM 2.5).....	191
Downwind Group.....	192
Crosswind Group	195
Upwind Group	197
Summary	199

Development of An Empirical Refraction Model.....	202
CHAPTER 5 CONCLUSIONS	229
CHAPTER 6 RECOMMENDATIONS.....	235
REFERENCES	237

LIST OF FIGURES

Figure 1: Different Types of Sources Generate Different Types of Wave Propagation...	10
Figure 2: Geometry of Direct and Reflected Sound Rays	14
Figure 3: Relative Sound Pressure Levels Measured 15.2 m from a Point Source and 1.2 m Above an Acoustically Hard Ground. Results Are for Four Different Source Heights	18
Figure 4: Relative Sound Pressure Levels Measured 5 m from a Point Source at the Surface of an Acoustically Soft Ground. Results are for Four Different Receives Heights	19
Figure 5: Excess Attenuation for Propagation from a Point Source over Mown Grass. The Calculated Curves Show the Contribution of the Various Waves.....	23
Figure 6: Excess Attenuation for Propagation from a Point Source over Mown Grass ...	25
Figure 7: Excess Attenuation Plots for Different Ground Surfaces, cgs Rayls	29
Figure 8: Spectra of Contribution to the Absorption Coefficient	36
Figure 9: Sound Propagation Across Boundary Between Layers with Different Velocities	39
Figure 10: Sound Refraction in Boundary Layer.....	40
Figure 11: Variation of Temperature in the Vicinity of a Flat Ground Surface	41
Figure 12: Typical Atmospheric Temperature Gradients	43
Figure 13: Diagram of Testing Location	70
Figure 14: Diagram of Testing Positions.....	70
Figure 15: Geometry of a Site for Calculation of Segments Contribution to Sound Level	75
Figure 16: Ground Effect Attenuation Output from Macdonald Program	86
Figure 17: Time Series of Wind Speed with Time Selected Shown by Brackets (U-wind) in (mph).....	92
Figure 18: Comparison of Measured Sound Levels for Each of the Three Groups dB(A)	105
Figure 19: Difference in Sound Level between Ref and Microphones dB(A)	107
Figure 20: Difference in Sound Level between Microphones dB(A).....	109
Figure 21: Difference Between Measured and Predicted Sound Levels for Downwind Group	115
Figure 22: Difference Between Measured and Predicted Sound Levels for Crosswind Group	120
Figure 23: Difference Between Measured and Predicted Sound Levels for Upwind Group	123
Figure 24: Average Difference Between Reference and Microphone Positions	126
Figure 25: Average Difference Between Measured and Predicted Sound levels	127

Figure 26: Difference Between Measured and Predicted Sound Levels for Downwind Group	144
Figure 27: Difference Between Measured and Predicted Sound Levels for Crosswind Group	148
Figure 28: Difference Between Measured and Predicted Sound Levels for Upwind Group	151
Figure 29: Average Difference Between Reference and Microphone Positions	153
Figure 30: Average Difference Between Measured and Predicted Sound Levels.....	155
Figure 31: Difference Between Measured and Predicted Sound Levels for Downwind Group	171
Figure 32: Difference Between Measured and Predicted Sound Levels for Crosswind Group	175
Figure 33: Difference Between Measured and Predicted Sound Levels for Upwind Group	176
Figure 34: Average Difference Between Reference and Microphone Positions	179
Figure 35: Average Difference between Measured and Predicted Sound levels.....	180
Figure 36: Difference Between Measured and Predicted Sound Levels for Downwind Group	193
Figure 37: Difference Between Measured and Predicted Sound Levels for Crosswind Group	196
Figure 38: Difference Between Measured and Predicted Sound Levels for Upwind Group	199
Figure 39: Average Difference between Measured and Predicted Sound levels.....	200
Figure 40: Attenuation due to Ground Effects.....	207
Figure 41: Scatter plot of Refraction Attenuation for both the Empirical Model and Wayson Method	227

LIST OF TABLES

Table 1: Values of Effective Flow Resistivity for Different Ground Surfaces.....	28
Table 2: “A” Weighting of Octave Band Levels	32
Table 3: Turbulence Characteristics for Various Richardson Number.....	51
Table 4: Number of Data Points Analyzed.....	92
Table 5: Summary of Wind Speed (mph) for Downwind Group	94
Table 6: Summary of Temperature for Downwind Group	95
Table 7: Summary of Sound Levels (dB) for Downwind Group.....	96
Table 8: Summary of Wind Speed (mph) for Crosswind Group	98
Table 9: Summary of Temperature for Crosswind Group	98
Table 10: Summary of Sound Levels (dB) for Crosswind Group	99
Table 11: Summary of Wind Speed (mph) for Upwind Group	101
Table 12: Summary of Temperature for Upwind Group	101
Table 13: Summary of Sound Power Levels (dB) for Upwind Group	102
Table 14: Downwind Group Sound Pressure Levels dB(A).....	104
Table 15: Crosswind Group Sound Pressure Levels dB(A)	104
Table 16: Upwind Group Sound Pressure Levels dB(A).....	105
Table 17: Difference in Sound Levels between Ref and Microphones dB(A).....	106
Table 18: Difference in Sound Pressure Levels between Microphones dB(A)	108
Table 19: Attenuation (dB) for Microphones in Downwind Group	112
Table 20: Attenuation (dB) for Microphones in Crosswind Group.....	113
Table 21: Attenuation (dB) for Microphones in Upwind Group	113
Table 22: Difference between Measured and Predicted Sound levels dB(A)	116
Table 23: Difference between Measured and Predicted Sound levels dB(A) for Crosswind Group	119
Table 24: Difference between Measured and Predicted Sound levels dB(A) for Upwind Group	122
Table 25: Average Difference Between Reference and Microphone Positions dB(A) ..	125
Table 26: Average Difference Between Measured and Predicted Sound levels dB(A) .	127
Table 27: Difference Between Measured & Predicted Octave Band Sound Levels dB(A)	129
Table 28: Difference Between Measured & Predicted Octave Band Sound levels dB(A)	132
Table 29: Difference Between Measured & Predicted Octave Band Sound levels dB(A)	134
Table 30: Summary of Difference Between Measured and Predicted Octave Band Sound Levels.....	136
Table 31: Attenuation (dB) for Microphones in Downwind Group	139
Table 32: Attenuation (dB) for Microphones in Crosswind Group.....	140

Table 33: Attenuation (dB) for Microphones in Upwind Group	141
Table 34: Difference between Measured and Predicted Sound levels dB(A) for Downwind Group.....	143
Table 35: Difference between Measured and Predicted Sound levels dB(A) for Crosswind Group	147
Table 36: Difference between Measured and Predicted Sound levels dB(A) for Upwind Group	150
Table 37: Average Difference Between Reference and Microphone Positions dB(A) ..	154
Table 38: Average Difference Between Measured and Predicted Sound Levels dB(A)	154
Table 39: Difference Between Measured & Predicted Octave Band Sound levels dB(A)	157
Table 40: Difference Between Measured & Predicted Octave Band Sound levels dB(A)	160
Table 41: Difference Between Measured & Predicted Octave Band Sound levels dB(A)	162
Table 42: Summary of Difference Between Measured and Predicted Octave Band Sound Levels.....	164
Table 43: Attenuation (dB) for Microphones in Downwind Group	167
Table 44: Attenuation (dB) for Microphones in Crosswind Group.....	168
Table 45: Attenuation (dB) for Microphones in Upwind Group	169
Table 46: Difference between Measured and Predicted Sound levels dB(A) for Downwind Group.....	172
Table 47: Difference between Measured and Predicted Sound levels dB(A) for Crosswind Group	174
Table 48: Difference between Measured and Predicted Sound levels dB(A) for Upwind Group	177
Table 49: Average Difference Between Reference and Microphone Positions dB(A) ..	179
Table 50: Average Difference between Measured and Predicted Sound levels dB(A) ..	180
Table 51: Difference Between Measured & Predicted Octave Band Sound levels dB(A)	182
Table 52: Difference Between Measured & Predicted Octave Band Sound levels dB(A)	185
Table 53: Difference Between Measured & Predicted Octave Band Sound levels dB(A)	187
Table 54: Summary of Difference Between Measured and Predicted Octave Band Sound Levels.....	189
Table 55: Hourly Traffic Counts for All Three Groups.....	192
Table 56: Difference between Measured and Predicted Sound levels dB(A) for Downwind Group.....	194

Table 57: Difference between Measured and Predicted Sound levels dB(A) for Crosswind Group	195
Table 58: Difference between Measured and Predicted Sound levels dB(A) for Upwind Group	198
Table 59: Average Difference between Measured and Predicted Sound levels dB(A)..	200
Table 60: Sample of Reference Sound Levels dB	203
Table 61: Sample of Mic 1 Sound Levels dB.....	203
Table 62: Sample of Mic 2 Sound Levels dB.....	204
Table 63: Sample of Mic 3 Sound Levels dB.....	204
Table 64: Sample of Mic 4 Sound Levels dB.....	205
Table 65: Attenuation due to Geometric Spreading dB.....	205
Table 66: Attenuation due to Atmospheric Absorption dB	206
Table 67: Attenuation due to Ground Effects dB	207
Table 68: Attenuation due to A-weighted dB.....	208
Table 69: The Sum of All Attenuations dB(A).....	208
Table 70: Sound Level Difference Between Reference & Mic 1 Downwind Group dB(A)	209
Table 71: Sound Level Difference Between Reference & Mic 2 Downwind Group dB(A)	210
Table 72: Sound Level Difference Between Reference & Mic 3 Downwind Group dB(A)	210
Table 73: Sound Level Difference Between Reference & Mic 4 Downwind Group dB(A)	211
Table 74: Sound Level Difference Between Reference & Mic 1 Crosswind Group dB(A)	212
Table 75: Sound Level Difference Between Reference & Mic 2 Crosswind Group dB(A)	212
Table 76: Sound Level Difference Between Reference & Mic 3 Crosswind Group dB(A)	213
Table 77: Sound Level Difference Between Reference & Mic 4 Crosswind Group dB(A)	213
Table 78: Sound Level Difference Between Reference & Mic 1 Upwind Group dB(A)	214
Table 79: Sound Level Difference Between Reference & Mic 2 Upwind Group dB(A)	214
Table 80: Sound Level Difference Between Reference & Mic 3 Upwind Group dB(A)	215
Table 81: Sound Level Difference Between Reference & Mic 4 Upwind Group dB(A)	215
Table 82: Sample of Data used for Empirical Model Development for the 63 Hz	217
Table 83: Refraction Attenuation Empirical Model for Each Frequency.....	219
Table 84: Data Collected in Texas by Wayson [Wayson, 1989].....	223
Table 85: Comparison Between Empirical Model Predicted Refraction Attenuation and Wayson Calculated Refraction Attenuation.....	225

CHAPTER 1

INTRODUCTION

Noise is a nuisance for many people and has been shown to have negative effects on exposed persons. This is particularly true for the communities along highways. The government has recognized such complaints and has passed several acts. In 1969 The National Environmental Policy Act (NEPA) was enacted and requires the assessment of environmental impacts for all federally funded projects, including noise. Moreover, some states and local agencies may call for more strict requirements. In 1972, The Noise Control Act included provisions to regulate maximum level standards for railway sources, trucks and buses. Two years later, the Environmental Protection Agency established sound levels goals at communities in order to protect its residences. In 1982 the Federal Highway Administration (FHWA) issued an important regulation related to highway traffic noise. These regulations, 23CFR772 “Procedures for Abatement of highway Traffic and Construction Noise” standardized traffic noise analysis procedures and required the use of FHWA noise prediction methodology. This required the prediction techniques to be ever more accurate. Methods required for assessing noise levels impacts have varied from simple charts to computer design models since the enactment of 23CFR772. In 1977 [FHWA, 1977] the FHWA issued a comprehensive methodology for estimating the noise levels along highways. Several computer models based on this FHWA methodology have been used; SNAP (Simplified Noise Analysis

Program) [Rudder, 1979], STAMINA (Standard Method In Noise Analysis) [Bowlby, 1983], the Traffic Noise Model (TNM) [Anderson, 1998] and the UCF CNM (Community Noise Model) [Wayson, 1997]. These models have been widely used to predict traffic noise along the highways, with TNM being the most recent methodology advocated by the FHWA. These algorithms have successfully predicted geometric spreading, atmospheric absorption, diffraction and ground impedance. The algorithms included for sound wave propagation through the atmosphere only include atmospheric absorption for weather effects. One key parameter missing in these models is atmospheric refraction. Refraction is due to wind shear, lapse rate, and turbulence and is the largest source of error remaining in the models.

Studies have been conducted to measure traffic noise along highways and have been used to establish existing noise levels, assess the effectiveness of noise barriers and to validate the prediction models. Usually, these measurements are carried out for a very short term, which does not provide long term accuracy assessments of the effects of weather conditions, atmospheric absorption and diffraction or shielding. More specific measurements, using the scientific method, need to be done to allow better quantification of these effects, especially refraction.

The purpose of this research will be to better understand the meteorological effects on traffic noise propagation through measurements and comparison to acoustic theory. It should be noted that this represents an approach to incorporate all refraction algorithms that must also work with algorithms for geometric spreading, ground effects,

refraction, and turbulence, affecting outdoor noise propagation. The methodology that was used is presented in this dissertation.

CHAPTER 2

LITERATURE REVIEW

Before electrical and wireless communications became common on the tactical level, the sound of battle was often the quickest and most efficient method by which a commander could judge the course of a battle. Reviewing military history, the first incidence of unusual acoustics due to atmospheric conditions occurred during the Four-Day battle in 1666. The naval battle was fought between Holland and England, and sounds of the battle were heard clearly at many points throughout England but not at intervening points. There are several similar acoustical phenomena that took place during the Civil War. Some of the battles, during which these events occurred, affected the commander decision and probably the outcome of the war. One of these battles, Gettysburg, happened on the hot and sunny July 2nd, 1863. General Lee, from the Confederate Army, had a plan for dislodging the Union Army from its perch along a series of ridges and hills. The plan was for General Longstreet to attack first, followed by General Ewell. However, for a long time after Longstreet had begun his attack, Ewell heard nothing and hence didn't move his troops, as a result Longstreet was defeated. Ewell inability to hear the artillery appears to stem first from the shielding effects of Cemetery Ridge and the hills between the Confederate forces. More importantly, the hot temperatures near ground probably caused a dramatic upward refraction of sound waves, further reducing the ability of General Ewell to hear the sounds of the battle. Upon

hitting, another warm layer higher up, these waves could be refracted back downwards and were clearly audible in Pittsburgh, 150 miles from Gettysburg. This same phenomenon affects traffic noise.

This chapter describes the physical phenomenon that have an effect on outdoor traffic noise propagation. Sound wave propagation outdoors is determined by the acoustic properties of the ground surface, the shape of the terrain, the properties of the air and the characteristics of the sound source. This chapter discusses each of these factors that affect traffic noise propagation. Moreover, a brief discussion of the traffic noise propagation models and the atmospheric models for sound propagation is included.

Sound Wave

Sound is the sensation produced in the organs of hearing by certain pressure variations or vibrations in the air caused by a vibration at a source. The sources cause molecules of air to vibrate creating regions of compression and rarefaction. This causes a wavelike process through the elastic media of air. There are several sources of transportation sound; trains, tire/pavement interaction for automobiles, exhaust and engine noise from trucks. In outdoor sound propagation, the ground surface acts as a boundary and is often considered an absorbing plane. A wave consists of three essential components, amplitude, frequency and phase. The wave propagation through an elastic medium is controlled by the linear wave equation shown in Equation (1).

$$\nabla^2 \mathbf{u} - c^{-2} U_{tt} = 0 \quad (1)$$

$$\nabla^2 \mathbf{u} = U_{xx} + U_{yy} + U_{zz} \quad (3 \text{ dimensions})$$

Where:

U_{xx} = is second order differential equation in the X-direction

U_{yy} = is second order differential equation in the Y-direction

U_{zz} = is second order differential equation in the Z-direction

This homogeneous wave equation contains the function, u , which is a function of space and time, the speed of sound in the medium, c , and the Laplacian operator, ∇^2 .

Equation (2) includes an expression for a simple plane wave, u that is a function of a single spatial coordinate, x , and oscillates with an angular frequency ω .

$$u = Ae^{i(kx - \omega t)} = A[\cos(kx - \omega t) + i \sin(kx - \omega t)] \quad (2)$$

MacDonald [MacDonald, 2002] has described that Equation (2) has been written in Euler notation; normally it is expressed in the exponential form with the implication that the real part of the wave, the cosine term, is the one of physical interest. The term, k , is the wave number and is also called the spatial frequency since it describes the oscillation in the spatial coordinate. The term t is simply the time of propagation, while A is a peak amplitude term.

The wave equation can be reduced to the Helmholtz equation, which is shown in Equation 3. The Equation is used to solve for the scalar velocity potential field, Φ , produced by a sound source. The Helmholtz equation is the typical differential equation that controls acoustic radiation potential.

$$\begin{aligned}\nabla^2 u + k^2 u &= 0 \\ k &= \omega / c\end{aligned}\tag{3}$$

The solution of the differential equation is dependent on the boundary conditions of its application. Some of these conditions are, body conditions where the potential (Dirichlet conditions) or flux (Neumann conditions) which are defined at the surface of a radiating body.

The sound pressure, p , is correlated with the velocity potential through the following Equation (4)

$$p = \nabla \cdot \Phi = -i\omega\rho_o\Phi \quad (4)$$

Where:

ρ_o = characteristic density of air

Φ = scalar velocity

∇ = Laplacian operator

D'Alembert has explained this equation, through a one dimensional linear wave equation. The equation consisted of two opposite traveling waves that have the shape of the initial displacement and half the amplitude of the initial displacement. The d'Alembert solution is given in Equation (5).

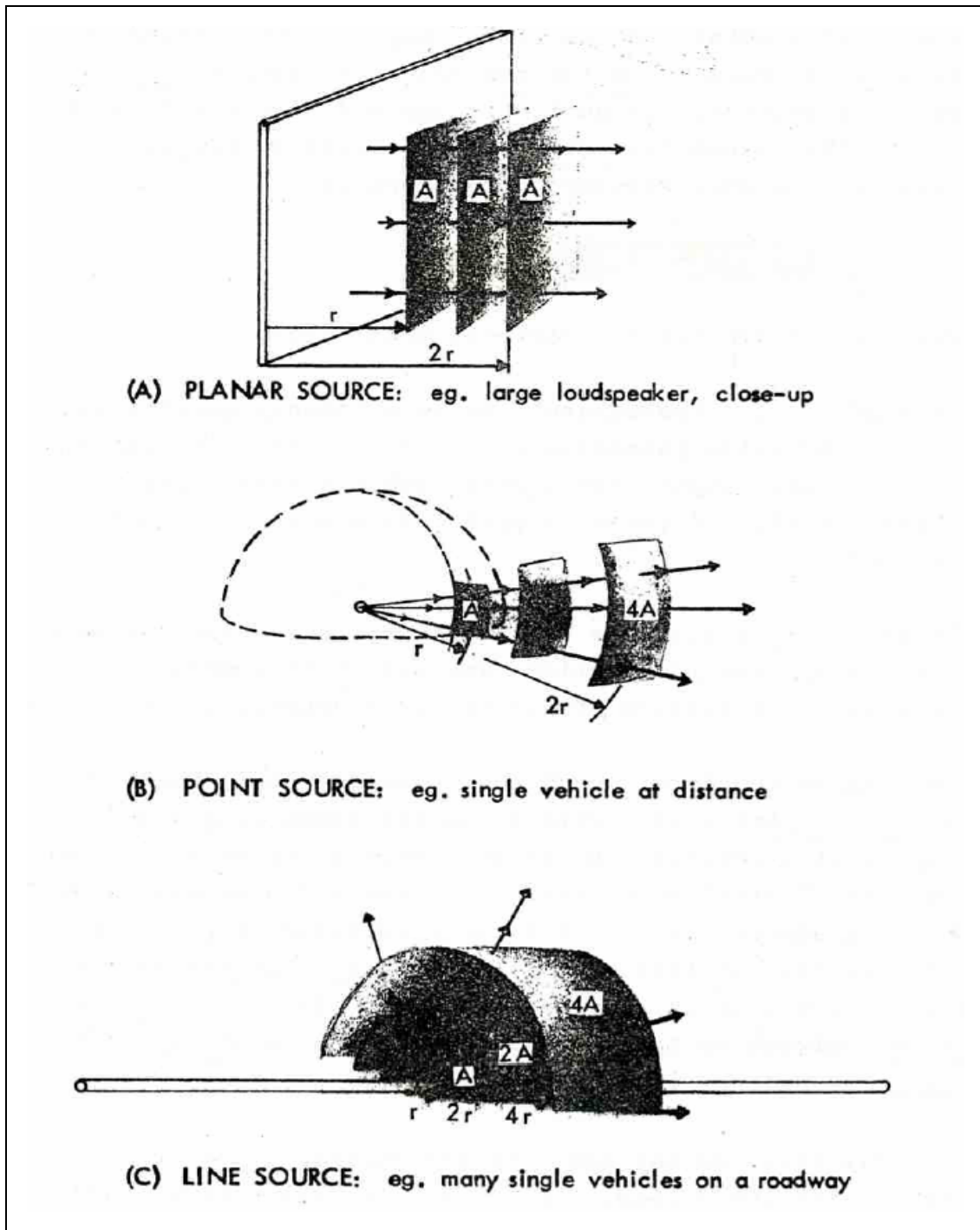
$$u(x,t) = \frac{1}{2}[f(x-ct) + f(x+ct)] + \frac{1}{2c} \int_{x-ct}^{x+ct} g(\tau) d\tau \quad (5)$$

By choosing appropriate coordinate system and boundary conditions, solutions to the two and three dimensional wave equation are possible. Solving the higher order wave equation for simple boundary conditions could be accomplished by separation of variables and transform techniques. It is difficult, in general, to solve the wave equation for the boundary conditions encountered in transportation noise without the use of numerical analysis techniques such as boundary element methods.

The sound wave propagation through free space was explained in the previous section, but we must also contemplate the cases of refraction due to nonhomogeneities in the atmosphere, spreading of the wave as it propagates outward from the source, absorption of sound energy due to a boundary with a finite impedance, diffraction of sound waves due to bending around objects and the loss of energy due to propagation in the open field, and geometric spreading which is described next.

Geometric Spreading

Geometric spreading is the event of the wave front moves away from it is source. For a planar source, the wave moves parallel and there is little or no energy loss for cases where the source-receiver distance is very small compared to the size of the source, as shown in Figure 1. Generally, waves spread in all three dimensions when the sound source is small compared to the distances being considered. For a spherical point source, the wave moves away from the source as an ever increasing sphere and the total energy is distributed over the surface of the sphere and the sound level decreases as sound energy is spread over greater and greater spherical surface areas with increasing distances from the source (see Figure 1).



Source: [FHWA,1981]

Figure 1: Different Types of Sources Generate Different Types of Wave Propagation

The dependence on distance is then related to the changing surface area of the sphere ($4\pi r^2$). Equation 6 shows this relationship for sound pressure level (SPL) and has been developed by evaluating the sound intensity at two distances and calculating the difference due to geometric spreading.

$$A_{geo}^{point} = 10 \log\left(\frac{r}{D_{ref}}\right)^2 = 20 \log\left(\frac{r}{D_{ref}}\right) \quad (6)$$

Where:

A_{geo} = is the sound attenuation due to geometric spreading

r = distance from the source to receiver

D_{ref} = source measurement reference distance

At twice the distance from the source, the surface area of the wavefront is four times as large, and the sound pressure decreases by a factor of four. Since SPL or dB are on a logarithmic scale, the sound pressure level (SPL) decreases by 6 dB (decibels). For another doubling of distance, the sound pressure level decreases by another 6 dB. When the source is located exactly at the surface of a rigid infinitely hard ground that is flat, the sound spreads into a hemisphere instead of a complete sphere. This spread is still in three dimensions, and the level still decreases by 6 dB for doubling of distance but in

influential near the ground plane. This is due to the source being located exactly at the intersection of two or more rigid planes.

For line sources, such as dense automobile traffic, the dependence on distance is related to the circumference of the expanding cylinder ($2\pi r$) (see Figure 1). As the sound waves radiates cylindrically in two dimensions from the source, energy is once again spread and the attenuation due to distance can be calculated as shown in Equation 7, again by taking the difference at two distances.

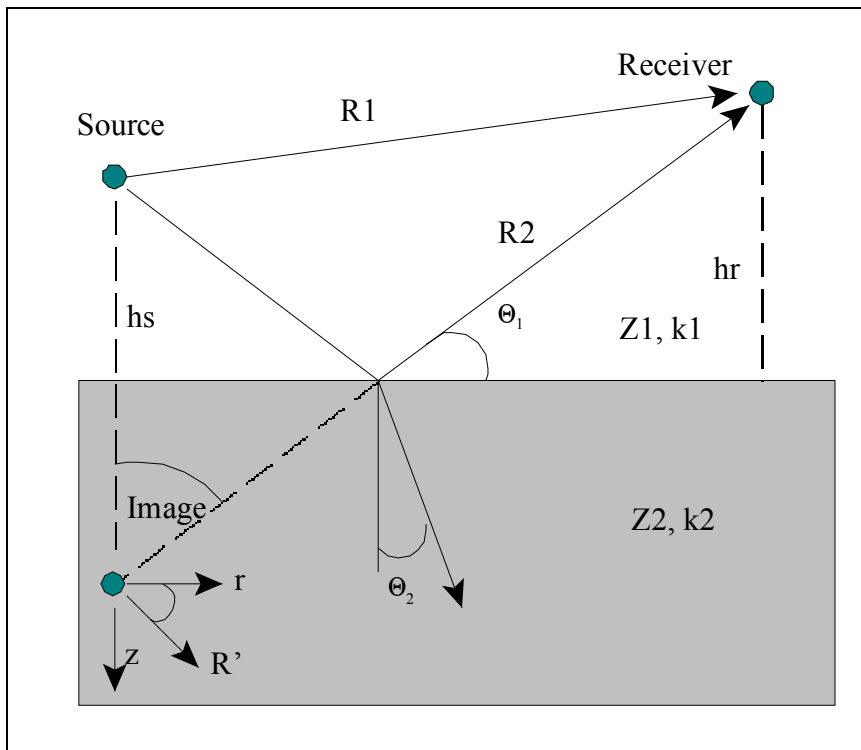
$$A_{geo}^{line} = 10 \log\left(\frac{r}{D_{ref}}\right) \quad (7)$$

For line sources, the sound pressure level decreases by 3 dB per doubling of distance, assuming that all distances are large compared with the spacing between sources, i.e. simulating line of cars. However, very near to the line source, the sound level depends only on distance to the nearest source because the other sources are relatively far away. Thus the maximum sound level still decreases by 6 dB per doubling of distance. As the distances become larger, about half the spacing between sources, the next nearest sources becomes significant and the sound pressure level decreases by 3 dB per double distance. This is also true when the sources are time-averaged along a line.

Ground Effects

Ground interference is due to the interaction of the sound waves with the ground surface. There are several interrelated phenomena whose magnitude or even existence depends on the value of the real and imaginary parts of the impedance of the ground surface. The theory was originally developed by Sommerfeld [Sommerfeld, 1909] for the propagation of electromagnetic waves near the earth surface. Rudnick [Rudnick, 1947] studied the propagation of acoustic waves along or near the boundary between air and a semi-infinite porous medium. Based on electromagnetic theory, he showed that the field of point source near to a plane boundary can be regarded as arising from the point source and the modified image located in the other medium. This resulted in an additional wave in the sound field called “ground wave”, which is the means by which the AM radio waves propagate.

In order to better explain the propagation phenomena above the plane, we should visualize the problem as a source near the ground that is radiating sound, a receiver located one or two meter above the ground, and a separation distance between source and receiver that is relatively large compared with their altitude above the ground. This is shown in Figure 2.



Source: [MacDonald, 2001]

Figure 2: Geometry of Direct and Reflected Sound Rays

This geometrical configuration consists of a direct path length “R1”, a reflected path length “R2”, a grazing angle “ θ_1 ” that the reflected sound ray makes with the surface. The media have complex acoustic impedance “Z”, propagation coefficient “k” and densities “ ρ ”. The acoustic impedance “Z” is described as the ratio of pressure and the normal component of the velocity at a point on the surface and is defined as shown in Equation 8.

$$Z_2 = \frac{\text{pressure}}{v_n} = \rho_2 c_2 \quad (8)$$

Where:

Z_2 = Acoustic impedance of the ground

Equation 9 may conveniently represent the amplitude reflection coefficient “ R_p ” for a plane wave of sound incident obliquely on a plane locally reacting surface.

$$R_p = \frac{\sin \theta_1 - \frac{Z_1}{Z_2}}{\sin \theta_1 + \frac{Z_1}{Z_2}} \quad (9)$$

The reflection coefficient varies with angle unless one of three extreme cases occurs. These cases are either “ $Z_1/Z_2 = 0$ ” which implies that the ground is infinitely hard (acoustically) and $R_p \rightarrow +1$ or “ $Z_1/Z_2 = \text{infinity}$ ” which implies that the ground is infinitely soft (acoustically) and $R_p \rightarrow -1$ or “ θ ” is constant which generally assumes that the incident waves are plane, reducing the mathematical complications. Rarely is one of these extreme conditions met in practice because no ground is infinitely hard or infinitely soft, and the angle of incidence is never constant for all elements of the ground surface.

The ground impedance and surface roughness varies considerably, such as the difference between vegetation and an asphalt road. These surfaces, based on the angle of

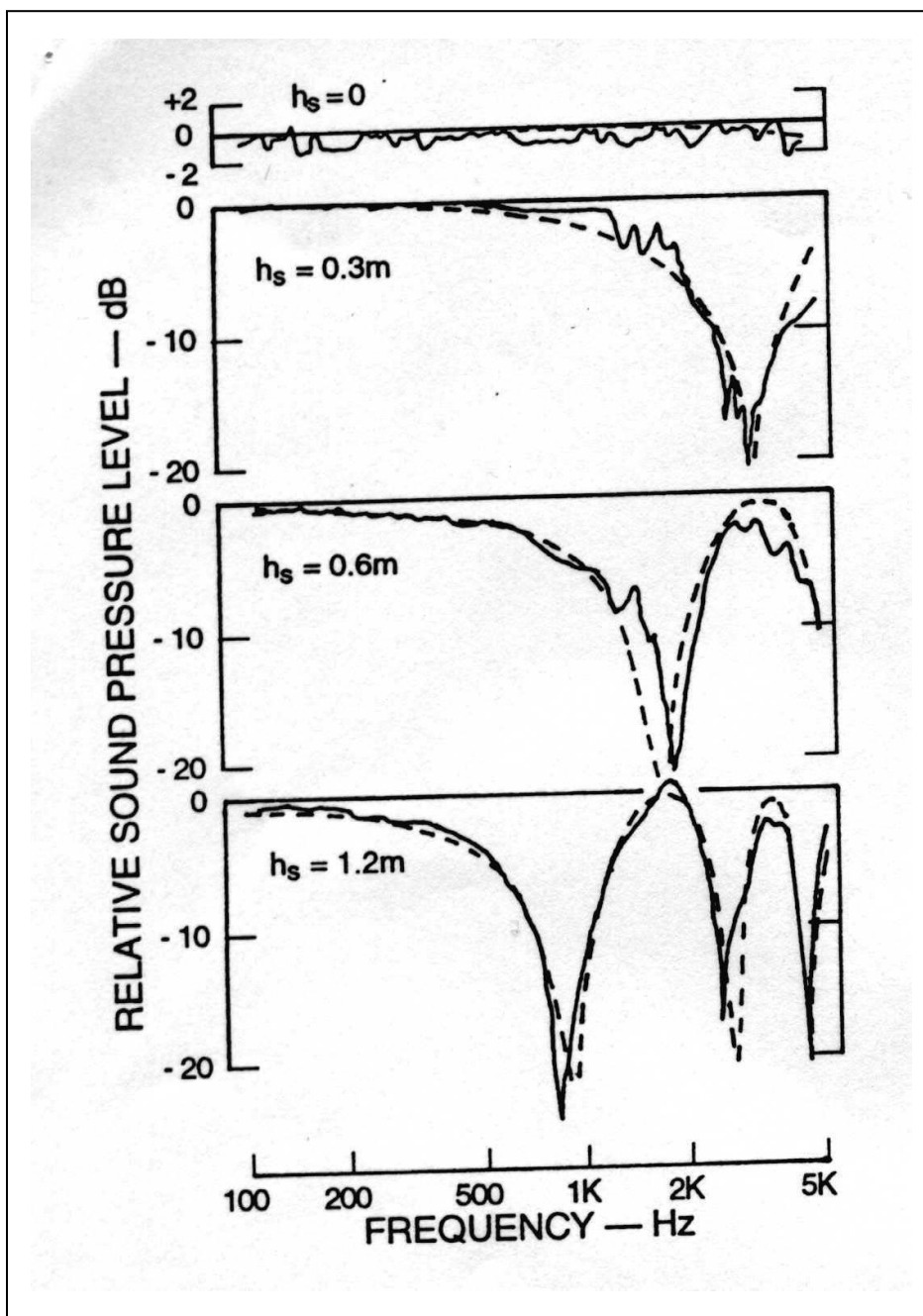
incidence, will have an effect on the reflected waves and the absorption of the wave. For example, the reflection will be minimum on very soft ground, where it will be maximum on hard surface. Averaging methods are routinely applied to overcome this difficulty.

Sound wave is the sum of a direct and a reflected wave. Embleton [Embleton, 1976] has explained that the difference in path length will introduce a phase delay, which is in addition to the phase delay caused by atmospheric attenuation and spherical spreading. Nevertheless, it introduces a phase delay $k\Delta r$, into the reflected path, where k is the wave number and Δr is the difference in path length between the direct and reflected waves. This phase delay is additional to phase changes produced during reflection on the ground surface.

When the propagation is above an acoustically hard surface, such as asphalt or concrete, it can be assumed $Z_1/Z_2 = 0$, $R_p \rightarrow +1$ and there is no phase change on reflection. The observed results are due entirely to the difference in path lengths between the source and the receiver. Embleton [Embleton, 1976] showed that at a certain frequency, the path length difference is about half the wavelength and the phase difference approaches odd multiples of 180° , $(2n-1)\Pi$, destructive interference occurs and a minimum appears in the sound pressure spectrum as shown in Figure 3. The figure shows that the two fields, direct and reflected, add perfectly at the ground surface, apart from the minor fluctuations due to atmospheric turbulence.

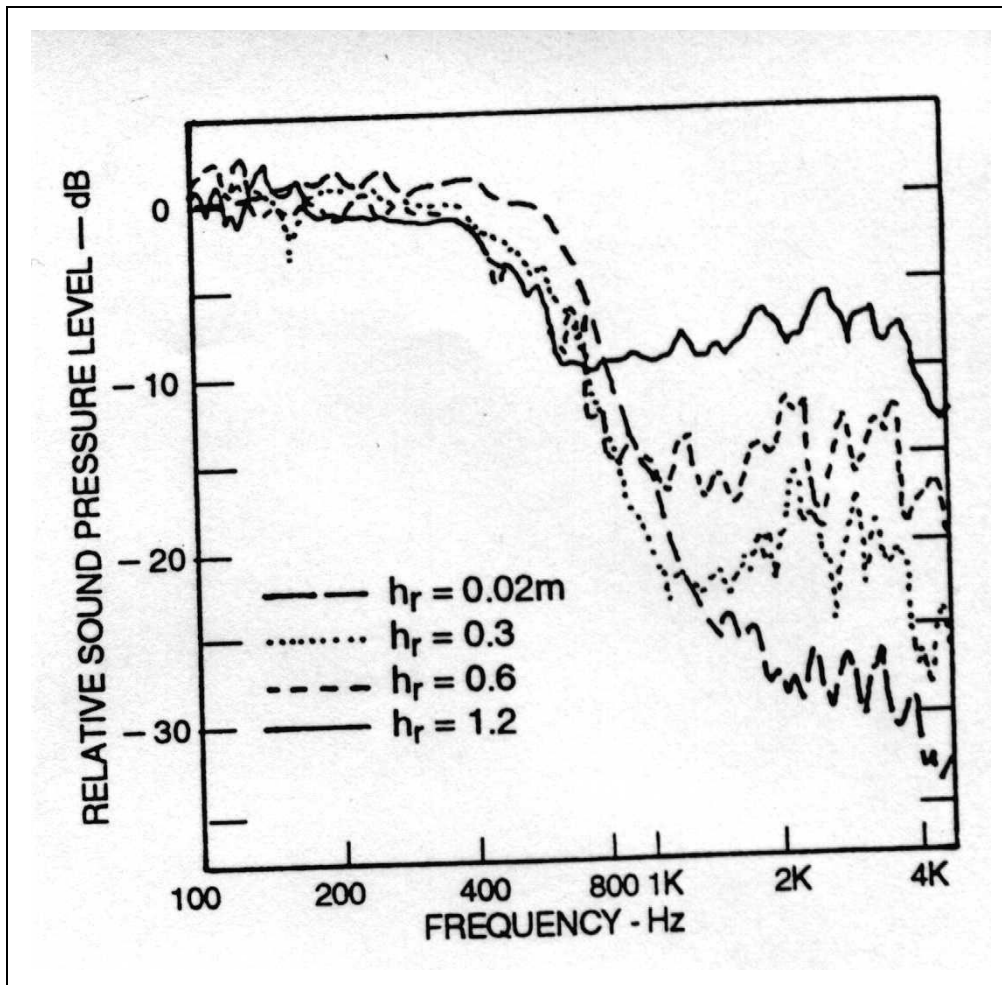
When the source and receiver are both very near the ground, and the sine of the incident angle approaches zero, then the reflection coefficient will be approximately

negative one. Consequently, the received sound pressure level should therefore be low at all frequencies since the reflected field should essentially cancel the direct field. However, measurements show that at grazing incidence, the sound pressure level is full strength below 800 Hz as shown in Figure 4. Acousticians call this the effect of the ground wave.



Source: [Embleton, 1976]

Figure 3: Relative Sound Pressure Levels Measured 15.2 m from a Point Source and 1.2 m Above an Acoustically Hard Ground. Results Are for Four Different Source Heights



Source: [Embleton, 1976]

Figure 4: Relative Sound Pressure Levels Measured 5 m from a Point Source at the Surface of an Acoustically Soft Ground. Results are for Four Different Receive Heights

The ground wave is that part of the reflected sound field that is not accounted for by the plane wave reflection coefficient, and it occurs whenever the incident waves are not plane. Rudnick [Rudnick, 1947] examined this problem and proposed using a point source representation with spherical incident waves, while the form of the reflected wave is determined by boundary conditions rather than the simple reflection coefficient.

Based on the fact that the velocity potentials for the direct and reflected waves could be defined as a sum of cylindrical waves [Rudnick, 1947], Norton [Norton, 1936] developed a function known as the “boundary loss factor”, $F(w)$. $F(w)$ is defined as the spectral shape of the ground waves and includes a complex error function. The term “ w ” is called the numeric distance and contains the amplitude and phase of the image source. Equation 10 describes the boundary loss factor and the numerical distance, as they show that the wavefront is plane as R_2 becomes very large and $F(w)$ approaches zero. Hence, it could be concluded that the solution approximate a plane wave for large distances or large heights above the ground. If the surface is infinitely hard (Z_2 is infinite) then $F(w)$ is unity then total reflection exists. In all other cases, $F(w)$ is a function of several variables including impedance, incident angle and distance.

$$F(w) = 1 + i2\sqrt{w}e^{-w} \int_{-i\sqrt{w}}^{\infty} e^{-u^2} du \quad (10)$$

$$w = \left(\frac{1}{2}ikr_1\right) \left(\sin \Theta + \frac{Z_1}{Z_2}\right)^2$$

For small values of w , $F(w)$ approaches unity regardless of the sign or value of the reflection coefficient. This occurs when the distance, R_2 , and the frequency are small or when Z_2 is much larger than Z_1 .

Equation 11 shows that a combination of the direct and reflected waves using the boundary loss factor, reflection coefficient and numerical distance would help in

explaining the sound field. Equation 11 is one form of the equation developed by Weyl and Van Der Pol [Weyl, 1919; Van Der Pol, 1935]. The term $[(1-R_p) F(w) \exp(ikR_2)/R_2]$ in the equation has been called the ground wave. One item of extreme importance for $F(w)$ is that it determines the spectral shape of the ground wave.

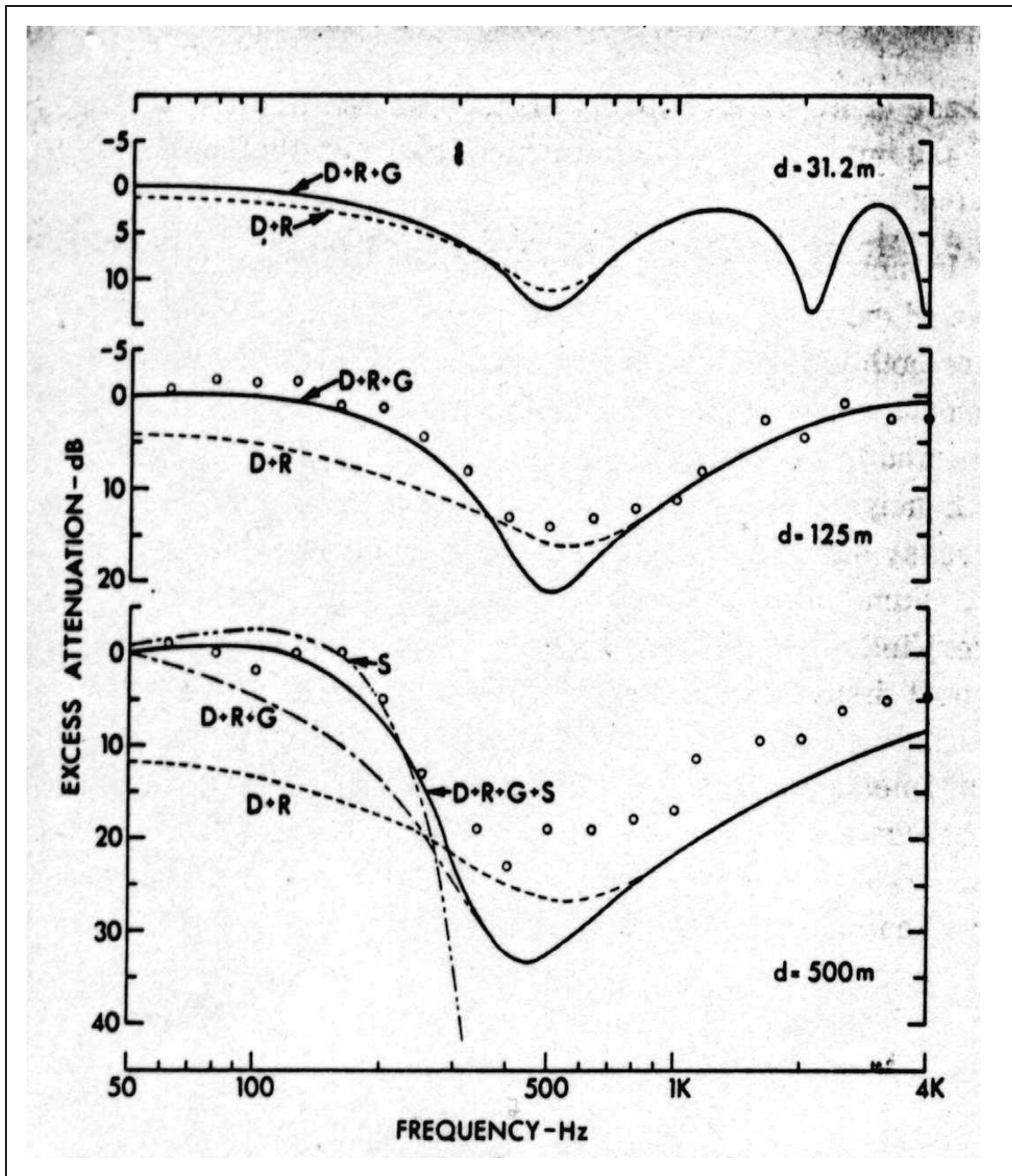
$$\Phi = \frac{e^{ik_1 R_1}}{R_1} + \frac{e^{ik_1 R_2}}{R_2} [(1 - R_p) F(w) + R_p] \quad (11)$$

Wenzel [Wenzel, 1974] has proposed that the existence of surface waves is explained by the observation of negative excess attenuation. By solving for the surface wave in electromagnetic theory, Wait [Wait, 1970] has shown an answer similar to those in acoustics. Specifically, that the surface wave produces a ducting of sound energy which produce an intensification of the wave field near the boundary due to the finite-impedance effect.

MacDonald [MacDonald, 2002] has indicating that in describing the wave propagation, we should assume that a shadow region caused by the finite impedance of the ground surface exists when the source is near the ground. The vertical extent of the region depends on the surface impedance. This shadow region is penetrated by a ground wave at low frequencies, the upper cutoff frequency of the ground wave being determined by the magnitude of the ground impedance and by horizontal range. This shadow region due to ground impedance is different from the shadow regions produced

by refraction due to atmospheric and wind gradients or by diffraction over and around objects. This shadow region is provided by the finite ground impedance, as sound wave propagates in air at close proximity to the ground their amplitude will decrease exponentially with height and travels with a velocity lower than that in free space. This is due to surface waves, which is a concentration of sound energy occurring above a surface when the acoustic impedance of the surface exceeds its acoustic resistance. Parkin and Scholes [Parkin and Scholes, 1964 & 1965] have first noted the existence of the surface wave when measurements were taken over grass covered fields in England. A few years later, this was confirmed by observing negative excess attenuation [Wait, 1970; Wenzel, 1974; Donato 76].

Piercy *et al.* [Piercy, 1976] has tried to explain all phenomena describing the sound field for source and receiver both above the ground. He showed the contribution of the direct D, reflected R, ground G, and surface S waves as shown in Figure 5.



Source: [Piercy, 1976]

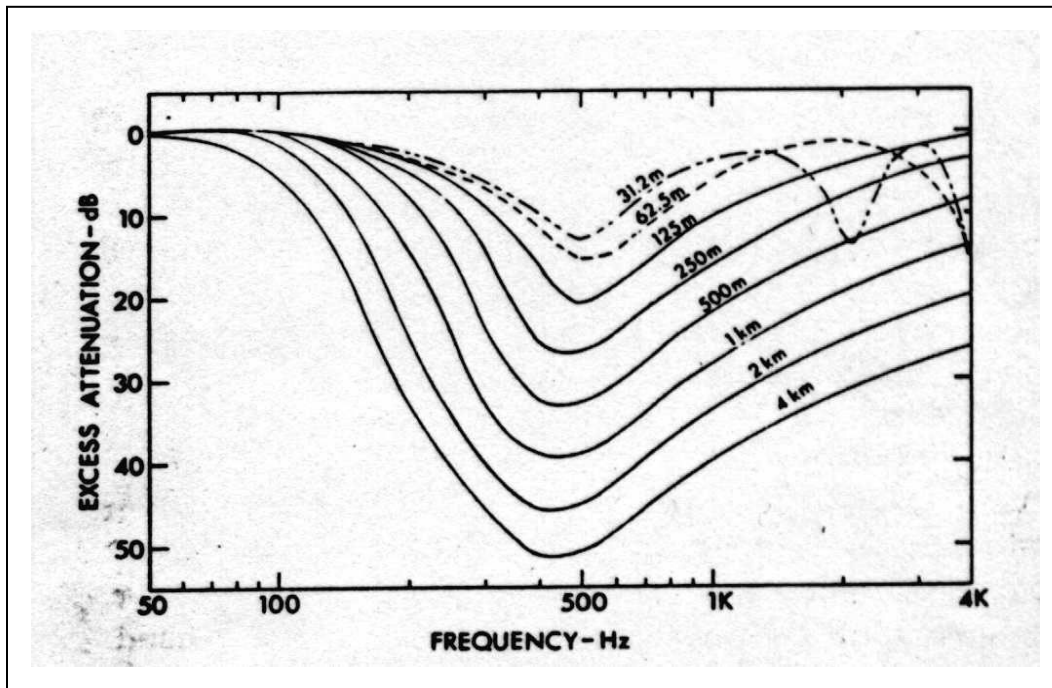
Figure 5: Excess Attenuation for Propagation from a Point Source over Mown Grass. The Calculated Curves Show the Contribution of the Various Waves

Piercy compared the different curves to measurements conducted from jet noise at comparable distances by Parkin [Parkin, 1965]. For short distances between source and receiver, the grazing angle Θ is sufficiently large. Hence, the direct and reflected waves only, no significant contribution from ground waves, are good approximation of the exact solution. Moreover, the grazing angle is too large for a surface wave to be significant. For frequencies greater than 1 kHz the effect of the path length difference between the direct and reflected waves is observed, which is in accordance with the theory regarding the presence of destructive interference, as the path length difference is significant.

As the source-receiver distance increases, it is noted that destructive interference is occurring at range greater than 4 kHz. Furthermore, as the grazing angle has decreased, a substantial contribution from the ground wave is clear at the low frequency range (50-500 Hz). At greater source-receiver distance, surface wave contribute to the solution as the ground wave in addition to the direct and reflected waves are not sufficient to present a solution for the field. This is indicated by the small enhancement (negative excess attenuation) observed at low frequency, which is in agreement with the theory described before by Wait, Wenzel [Wait, 1970; Wenzel, 1974].

Generally, the broadening of the shadow zone to higher frequencies is evident and has continued with increasing distance, which is indicated by the excess attenuation of 35 dB at 500 m and is also shown in Figure 6. Piercy [Piercy, 1977] concluded that the primary effect is a shadow zone caused by the finite acoustic impedance of the ground surface. The shadow zone is penetrated at low frequencies by ground and surface waves.

In addition, at higher frequencies, the shadow zone is penetrated by constructive interference for source and receiver above the boundary.



Source: [Piercy, 1977]

Figure 6: Excess Attenuation for Propagation from a Point Source over Mown Grass

A suitable descriptor of the ground surface is its specific impedance, normalized to the characteristic impedance for sound waves in air, ρc . Accurate measurement of normalized specific acoustic impedance is difficult not only because turbulence and other atmospheric effects, but also measurement techniques that can be used for higher frequencies often do not work at low frequencies, and vice versa.

Tillotson [Tillotson, 1965] measured the excess loss of sound pressure level during propagation over snow-covered fields and deduced the values of complex impedance of the layers of snow. Then Dickinson *et al.* [Dickinson, 1970] developed a technique of moving a microphone along a vertical path in the free field above the surface so as to leave the ground surface undisturbed, and obtained reliable results over a range of frequencies (200- 1 kHz). Later on, Aylor [Aylor, 1971] showed that the ground and the root system of the plants were more significant than the vegetation above ground in affecting sound propagation across the field. Embleton *et al.* [Embleton, 1977] showed that using an oblique path instead of a vertical path more closely approximates the direction of sound propagation in commonly occurring situation, and they were able to obtain accurate measurement within the frequency range (400 – 4kHz). Later, Bass *et al.* [Bass, 1980] showed that transmission of sound through the atmosphere-ground interface could not be described solely in terms of the impedance ratio of the two media. Ground surfaces are neither rigid nor impervious to air flow. The ground surface is porous and hence there is a motion within the pores of the ground that is driven by the pressure and particle velocity fluctuations of the sound field in the atmosphere adjacent to the surface.

Several relations have been developed to explain the ground effects. Based on work carried by Delany and Bazley [Delany, 1970], Chessel [Chessel, 1977] established that ground effects could be explained by a single parameter, the flow resistivity of the ground. It was shown that porosity, flow resistivity, tortuosity, steady flow shape and dynamic shape factor would better explain these effects [Attenborough, 1980]. Flow

resistivity and porosity are the most significant parameters in distinguishing any type of surface and both can be joined into a single term that may be expressed as an “effective flow resistivity”, denoted by σ and given in terms of Rayls.

Table 1 describes some typical ground surfaces by their representative effective flow resistivity. The flow resistivity of the earth varies with the soil type and its exposure to weather, ranging from about 800 to 8000 kPa-s/m². The flow resistivity of asphalt increases with its age and use, when its surface has been sealed by dust and compaction the effective flow resistivity is about 30,000 cgs Rayls. Concrete has an effective flow resistivity similar to asphalt.

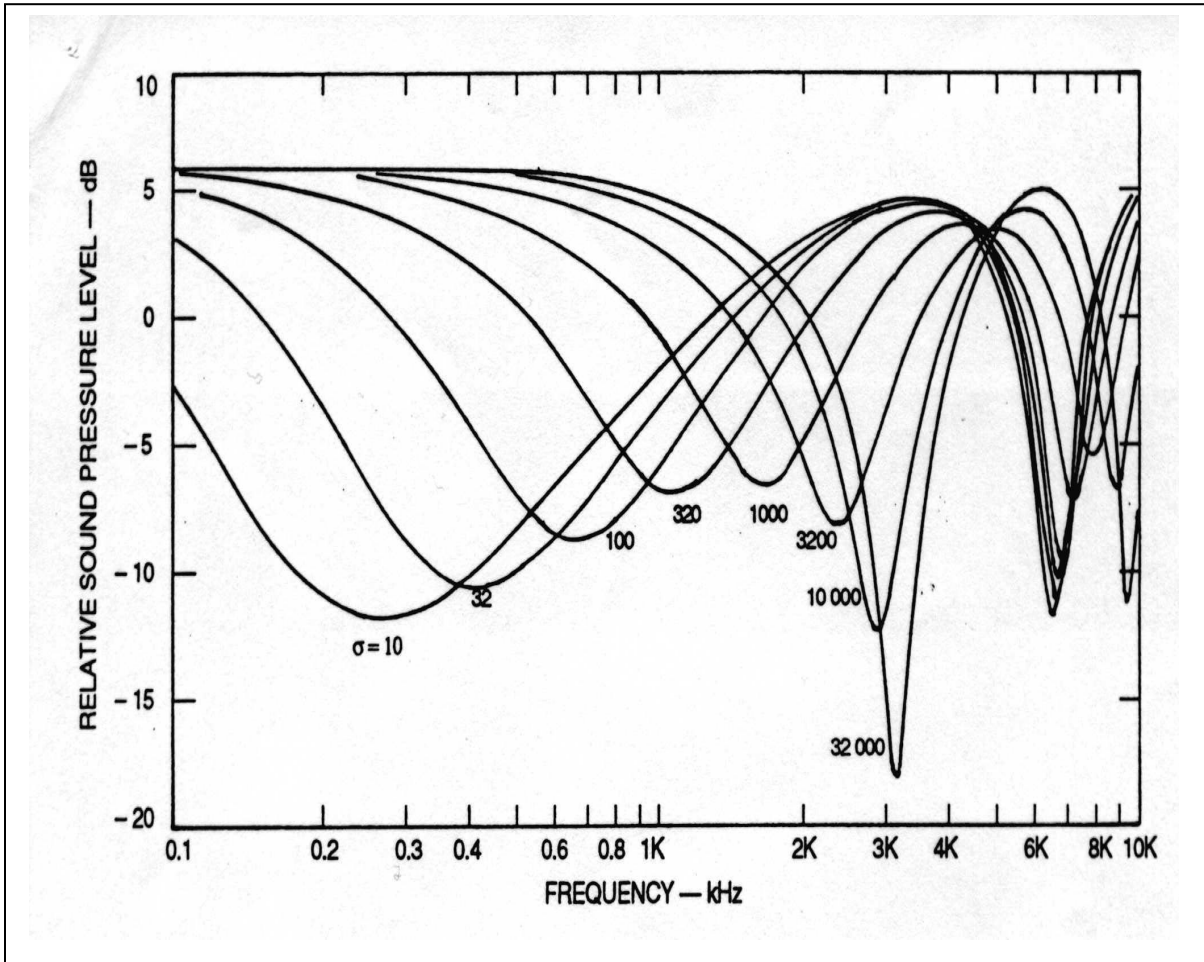
Table 1: Values of Effective Flow Resistivity for Different Ground Surfaces

Ground Surface Type	Effective Flow Resistivity (Rayls)
upper limit set by thermal conduction and viscosity	2×10^5 to 1×10^6
asphalt, sealed by dust and use	30000
very fine quarry dust, hard packed by vehicles	5000-20,000
earth, exposed and rain-packed	4000-8000
old dirt roadway, small stones and interstices filled by dust	2000-4000
thick layer of clean limestone chips, 0.01 to 0.025 m mesh	1500-4000
sandy silt, hard packed by vehicles	800-2500
roadside dirt, ill-defined, small rocks up to 0.01 m mesh	300-800
airport grass or old pasture	150-300
floor of evergreen forest	20-80
sugar snow	25-50
0.1 m new fallen snow, over older snow	10-30

Source: [Embleton, 1983]

Figure 7 shows several curves from the literature [Embleton, 1983] depicting the excess attenuation of sound pressure level due to the ground effect. These results were

obtained using the method of Equation (11). The 20,000 Rayls (cgs) hard surface curve displays a sharp dip at about 3.2 kHz. This dip location can be predicted knowing the geometry of the source and receiver which gives the path length difference.



Source: [Embleton, 1983]

Figure 7: Excess Attenuation Plots for Different Ground Surfaces, cgs Rayls

It should be noted that the phase between the two waves is affected and the minimal shifts to a lower frequency and becomes broader in case of absorptive ground. However, for reflective material, the spectra of the field at the receiver will have dominant sharp minima due to destructive interference between the direct and reflective waves, indicating little phase change on reflection.

Many empirical approaches are also used to predict the excess attenuation due to the ground interaction beside the theoretical methods. The Federal highway administration (FHWA) has in the past used a method known as the alpha factor in their methodology in the 108 report [Barry, 1978]. FHWA implemented this methodology in model called STAMINA [Bowlby, 1982], before including a method by Chessel in it is new traffic noise model (TNM) [Anderson, 1998]. The alpha factor method incorporates the ground effect into the geometrical spreading calculation as shown by Equation 12:

$$A_g \text{ (dB)} = 10 \log (r/D_{\text{ref}})^{1+\alpha} \quad (12)$$

Where:

α = empirical constant

α = 0.5 soft ground

α = 0.0 hard ground

This empirical method was found to fit measured results for specific conditions but was used in general for any ground type that was considered to be “soft”. This

method does not account for the frequency dependence of the phenomenon. This method was mainly used for overall “A” weighted reference sound pressure levels to save computer resources in the early 1980s by using simplified approach.

“A” weighting is a method that imitate the frequency response of the human ear at moderate intensities by attenuating low and high frequency levels while amplifying the 2000 and 4000 Hz band. This is accomplished by combining weighted octave band levels into a single number representation of the sound pressure level. Table 2 identifies the weighting for each octave band to produce an “A” weighted sound pressure level as indicated in the ANSI Standard S.14 [ANSI, 1983]. In order to express the overall “A” weighted sound pressure level, the octave band level contributions are logarithmically summed after the “A” weighting adjustment has been applied.

B and C scales are also used for loud and intense sounds, respectively. These scales use different weighting schemes to emphasize different frequency ranges. The “C” weighting scheme does not attenuate the lower frequencies nearly as much as the “A” weighting scheme and comparing the dB(A) and dB(C) levels from a sound level analyzer can be used to estimate the low frequency content of a source as explained by MacDonald [MacDonald, 2001].

Table 2: “A” Weighting of Octave Band Levels

Center Frequency (Hz)	Weighting Adjustment (dB)
31.5	-39
63	-26
125	-16
250	-9
500	-3
1000	0
2000	1
4000	1
8000	-1
16000	-7

Source: [ANSI, 1983]

In addition, the international standard ISO-9613:2 [ISO, 1996].accounts for ground effects. The ground effect excess attenuation is mainly a function of the mean effective propagation height and distance between the source and receiver. This method also corrects for overall “A” weighted sound pressure levels in the free field. This method was mainly developed for the downward curving propagation path that occurs during downwind conditions and assumes that the ground attenuation effect is primarily determined by the ground surfaces near the source and the receiver.

However, during outdoor noise propagation, atmospheric phenomena occur which may cause the unshielded noise levels to differ considerably from the levels that would be expected if only ground interference and geometric spreading were considered. Additionally, the atmospheric effects can change the angle the wave strikes the earth's surface, changing the ground effects. There are many examples of outdoor measurements that have an attenuation or amplification effects beyond that predicted for ground effects or geometric spreading and this thought to be the result of meteorological effects. Ignoring meteorological effects can affect barrier insertion loss modeling which shows up during measurements. The resulting differences (excess or reduced attenuation) can only be attributed to effects on the sound wave from the medium in which it is traveling (in this case, air). In clean air, the physical atmospheric mechanisms that can be identified as having a direct effect on noise levels are absorption, refraction, and turbulence [Ingard, 1953; Piercy, 1977].

Atmospheric Absorption

Absorption is caused by shear viscosity, thermal conductivity, mass diffusion, thermal diffusion, molecular rotational relaxation and molecular vibrational relaxation. Molecular absorption converts a small fraction of the energy of the sound wave into internal modes of vibration of the air which is dominated by oxygen and nitrogen molecules. There are time delays associated with this process of conversion and these

delays produce phase changes of the propagating waves. Research relying on direct measurements in the field, measurements of air absorption in the laboratory and general theory of the physical atmospheric absorption mechanisms has been extensive in this area. The review by Piercy [Piercy, 1977] summarizes this information, certain key findings have come from this extensive research. One such finding is that the attenuation by absorption can be considered a constant for a given distance along the propagation path. This tends to make atmospheric absorption more important with increasing distance. Ingard and Piercy [Ingard, 1953; Piercy, 1972] have established these findings from measurements in the laboratory and from general classical physics.

Kneser developed a theory that was based on the molecular attenuation of the classical absorption mechanisms (shear viscosity, thermal conductivity, mass diffusion thermal diffusion, and the absorption caused by the rotational relaxation of the molecules in air) and oxygen in the atmosphere [Kneser, 1940]. The model provided a good fit with measurement except at the lower frequency range. The disagreement between the measured data and the method first devised by Kneser at low frequencies was later explained [Piercy, 1969] to be due to the atmospheric nitrogen relaxation, which is significant at lower frequencies as shown in Figure 8.

The ANSI standard clarifies that the temperature, frequency and relative humidity are the three key variables that affect absorption. However, temperature does not directly have as significant an influence on absorption as water vapor but does so indirectly by

affecting the amount of water vapor in the air. Pressure affects absorption in similar way as temperature. The relevant Equations 13 - 18 for this model are given below.

$$A_{\text{atm}} = 8.686 f^2 [((1.84e-11)(T/T_0)^{0.5}) + C_1 + C_2] \quad (13)$$

Where:

$$A_{\text{atm}} = \text{dB/m}$$

$$C_1 = (T/T_0)^{5/2} [(0.01275 \exp(-2239.1/T))/(f_{rO} + (f^2/f_{rO}))]$$

$$C_2 = [(0.1068 \exp(-3352/T))/(f_{rN} + (f^2/f_{rN}))]$$

T_0 = reference air temperature 293.15 kelvin

T = ambient air temperature in kelvin

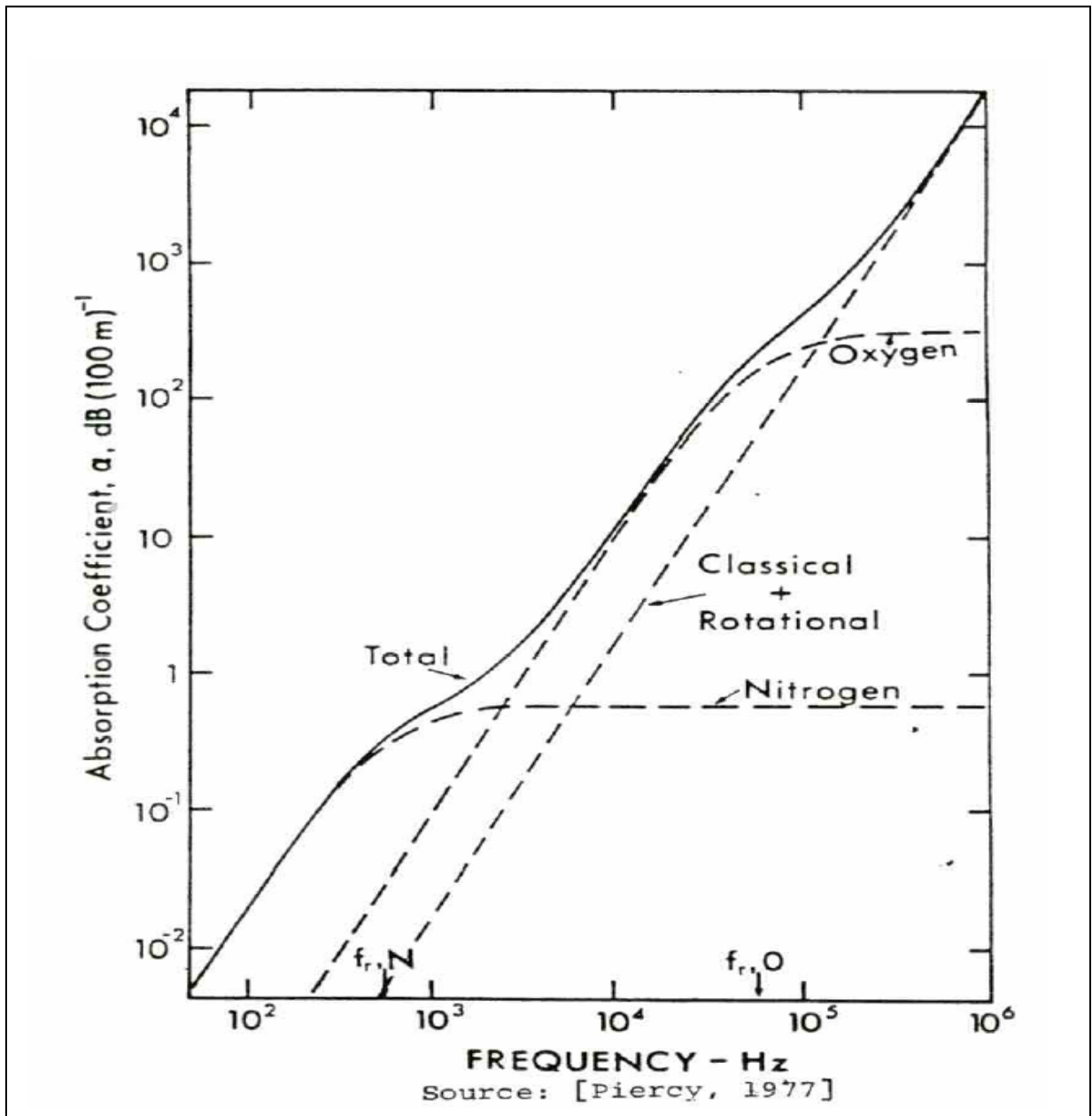
h = molar concentration of water vapor, percent

f = frequency, Hz

f_{rO} = oxygen relaxation frequency

f_{rN} = nitrogen relaxation frequency

$$f_{rO} = 24 + 4.04 h^* [(0.02+h)/(0.391+h)] \quad (14)$$



Source: [Wayson, 1989]

Figure 8: Spectra of Contribution to the Absorption Coefficient

$$f_{rN} = (T_o/T)^{0.5} [9 + 280 \ln \exp\{-4.17((T_o/T)^{1/3} - 1)\}] \quad (15)$$

$$h = RH * P_{\text{sat}}/P_{\text{sot}} \quad (16)$$

Where:

RH = relative humidity, percent

P_{sat} = saturation vapor pressure

P_{sot} = standard reference pressure, 101.325 kPa

$$P_{\text{sat}}/P_{\text{sot}} = 10^c \quad (17)$$

$$c = -6.8346 (T_{\text{o1}}/T) 1.261 + 4.6151 \quad (18)$$

Where:

T_{o1} = 273.16 kelvin, triple point isotherm temperature.

Sutherland developed an empirical method of calculating the atmospheric absorption coefficient. This method is valid up to 10 km, a frequency range of 50 to 10kHz and standard atmospheric conditions 20°C, using the new information on the role of nitrogen relaxation effect [Sutherland, 1974]. The American National Standards Institute approved this method [ANSI, 1978], and it was verified by over 850 laboratory measurements. However, outdoor measurement and the variable atmosphere cause a larger deviation in measurement values and a subsequent larger error than with laboratory

testing. The model is reported by ANSI to be accurate in outdoor conditions to within 10% from 0 to 40C [Sutherland, 1975]. The ANSI method is shown by Equation 19:

$$P = P_o e^{-\alpha s} \quad (19)$$

Where:

p = root-mean square amplitude of the acoustic pressure at distances, (Pa)

P_o = root-mean square amplitude of the acoustic pressure where $s= 0$ (at reference point), in Pa

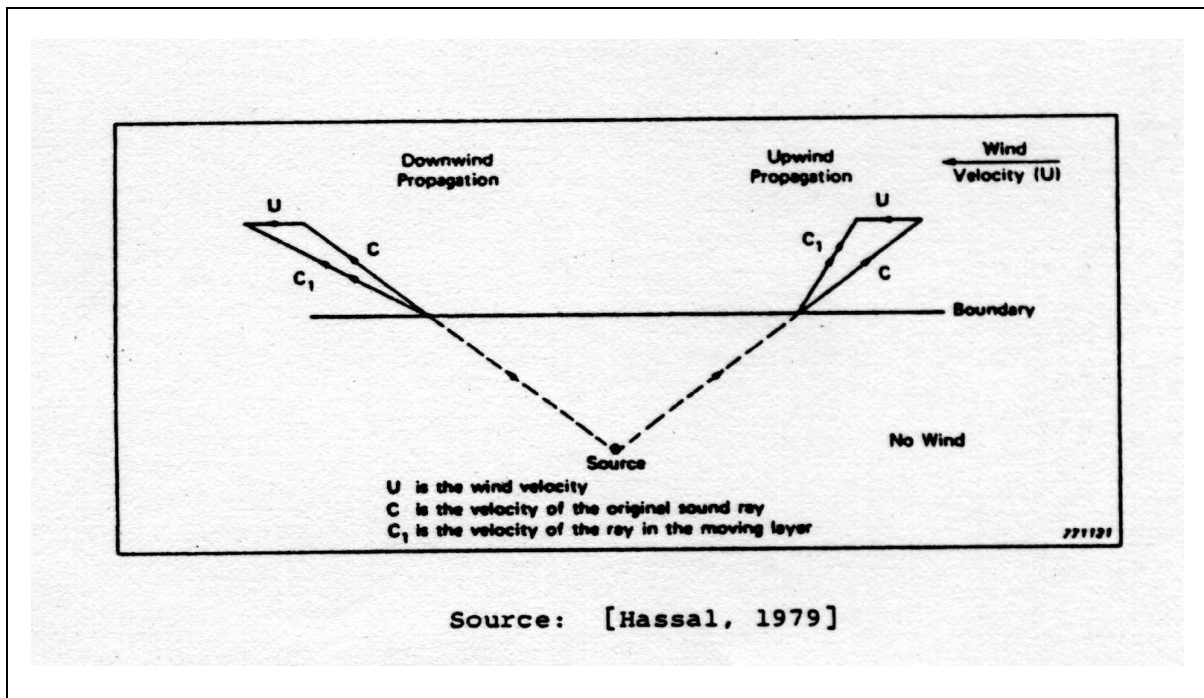
α = absorption coefficient (nepers per meter)

s = distance through which sound propagates (meters)

Refraction

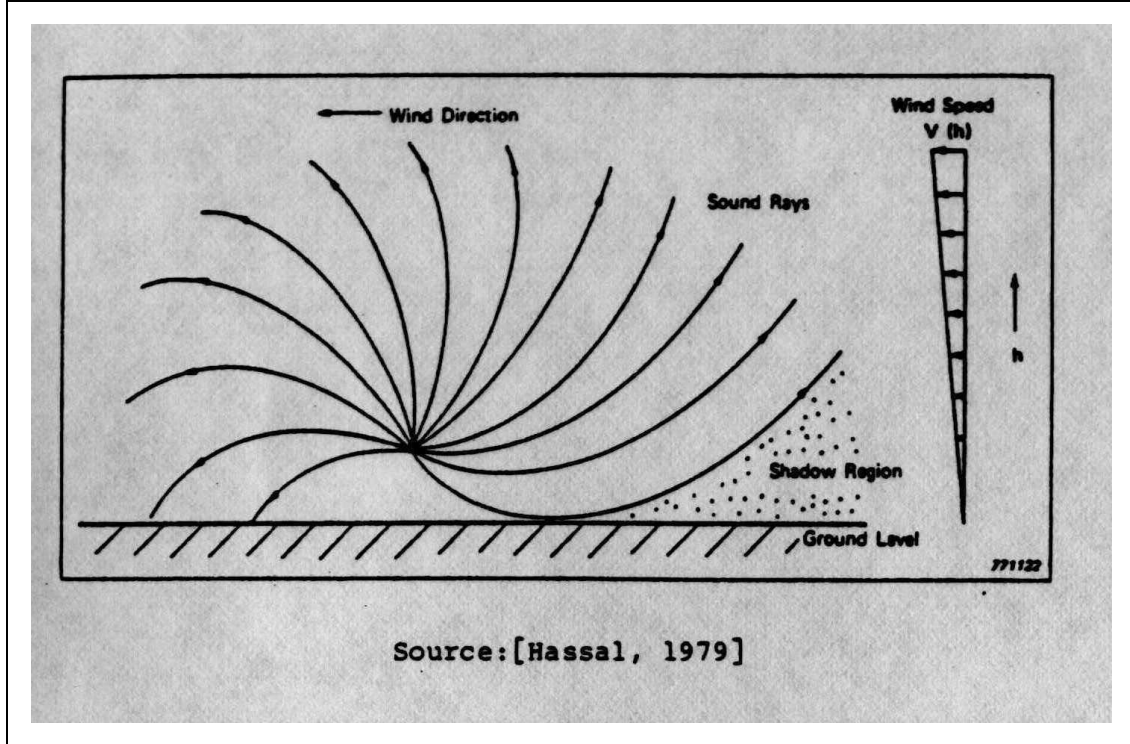
Refraction of sound in the atmosphere is the process of sound waves bending as they pass through localized differences in temperatures and wind speeds. This causes changes in the propagation media resulting in changes to the speed of sound in these localized regions and the wave bends in response much like optical wave bends as they pass from air into water. Figure 9 and 10 show the wind effects, as the wave, represented by the sound rays and vector constructions, impinges on the various layers of the wind gradient. The direction of propagation changes because the wave advances faster in a direction different from its previous direction. When entering a layer of air with a

different speed of sound, the wave is refracted toward the layer with the greater speed. Conversely, the wave is directed away from the interface when entering a region of lower speed. While, Figure 10 shows a simplified ray diagram of the effects on the noise propagation for upwind and downwind conditions.



Source: [Wayson, 1989]

Figure 9: Sound Propagation Across Boundary Between Layers with Different Velocities



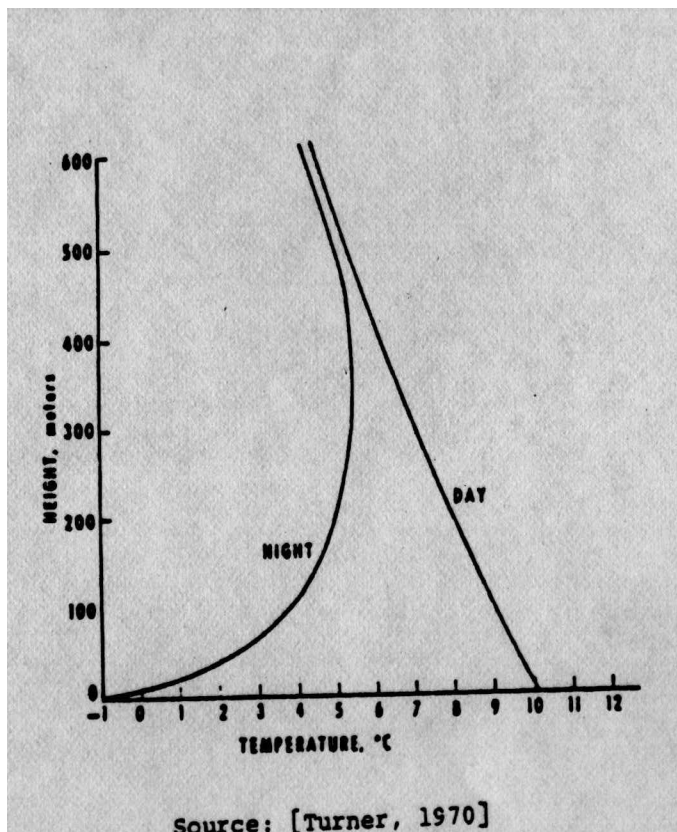
Source: [Wayson, 1989]

Figure 10: Sound Refraction in Boundary Layer

Wayson [Wayson, 1989] described these effects occur because the speed of sound is dependent only upon the medium in which it is propagated. A movement of this medium imposes a similar movement on its transport. If the sound has a component in the same direction as the wind, that vector component of the sound wave will be refracted toward the interface existing between the two velocity regions when entering an air layer with a lower speed, and away from the interface when entering a layer of greater speed. A reverse action occurs for those vector components of the sound wave that are moving toward the direction of the wind. It should be noted that the refraction produced by the

wind is zero when the vector component of the sound wave is directly crosswind and increases progressively as the direction of propagation parallels the wind vector.

Temperature gradients also cause refraction to occur. Figure 11 shows the difference between the temperature profile during the day and night. Contrary to the wind velocity, the temperature profiles vary much more during the day. Moreover, temperature is a scalar quantity and the sound refraction produced by temperature gradients is the same in all parallel directions to the ground plane.



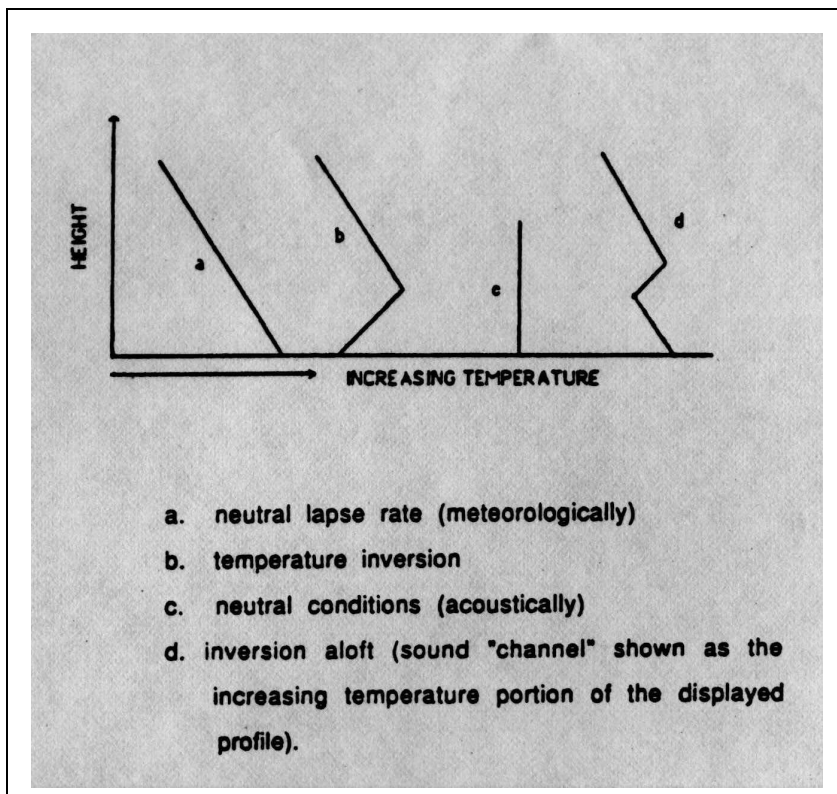
Source: [Wayson, 1989]

Figure 11: Variation of Temperature in the Vicinity of a Flat Ground Surface

The gradient of the thermal boundary layer is known as the lapse rate. An acoustically neutral lapse rate would be isothermal and have a constant temperature with height. An adiabatic lapse rate, which is neutral for atmospheric mixing of air pollutants, results in the temperature decreasing by 0.98 degrees Centigrade per 100 meters [Fleagle, 1963].

During the day, solar radiation heats the ground that in turn heats the air by conduction. As the air becomes cooler with increasing height, the speed of sound will decrease and the sound waves will bend towards the region with the lower speed of sound (cooler), for this case upwards forming a shadow zone. Conversely, the ground may cool faster than the atmosphere at night. Air near the earth surface is cooler and temperature may increase with height. This, as well as other conditions may cause an inverse lapse rate (inversion) and temperature increase with height. Under these conditions, the speed of sound is higher at greater elevations and the sound waves will bend downwards towards the region of lower speed sound during propagation and increased sound levels at the ground can occur.

Finally, an inversion aloft can cause sound waves to be refracted over considerable distances with little attenuation. Within the area of the inverse lapse rate, a channel is formed and the refraction of the noise keeps the sound waves in this narrow channel. As such, the noise level does not fall off with distance, as would be expected with geometric spreading. Figure 12 displays these different lapse rates.



Source: [Wayson, 1989]

Figure 12: Typical Atmospheric Temperature Gradients

Piercy [Piercy, 1977] developed a general picture of the refraction effects for distances less than 1500 meters. The noise sources were aircraft in a ground- to-ground configuration. The data was measured in one-third octave bands for distance of 110 meters and 615 meters. Piercy concluded that there was excess attenuation, due to refraction effects, after subtracting the losses from atmospheric absorption and spherical spreading. Moreover, Foss [Foss, 1978], investigated the meteorological effects on traffic noise propagation. He found that there are 25 dB differences between the upwind and downwind locations at a height of 1.2 m and 300 meters from the source. Even for a

moderate wind 1.8 m/s and at 46 m, 12 dB differences were reported. Below 500 Hz predictions worked well, but above 500 Hz predictions were increasingly in error.

Research carried out in Sweden by Larsson indicated positive correlation between meteorological parameters and traffic sound levels, but which varied with seasons and ground cover [Larsson, 1979]. During this study, Larson reported that different ground surfaces had no effect during downwind propagation and increased temperature gradient. However, the effect of ground cover seemed to be more significant in upwind conditions. He reported that extensive micro-meteorological measurements are needed for distances of 2 meters or more from a traffic route. In addition, the effects of meteorological variables increase with increased distance and can be readily observed, even at 25 meters. Finally, Larsson concluded that the wind and temperature gradients are of major importance in traffic noise propagation.

Parkin and Scholes [Parkin, 1965] showed significant effects from both positive and negative wind gradients for frequencies greater than 300Hz at 110 meters from the source. It was found that both the temperature and wind gradients effects were on the same order of magnitude. In later studies by Parkin and Scholes [Parkin, 1964; Scholes, 1971], it was noted that areas of temperature inversions would experience noise levels 15 to 20 dB above those predicted. Dickinson [Dickinson, 1976] has confirmed the work of both Parkin and Scholes in a research conducted on aircraft noise. Despite the fact that Parkin and Dickinson studies were on aircraft noise while Scholes was mainly concerned with measurement from highway traffic noise behind noise barriers, they both ended up

with similar results. This concurrence in results may lead to the use of work done on aircraft noise propagation in predicting highway traffic noise propagation.

Piercy [Piercy, 1977] summarized these results and concluded that attenuation could range from 0 dB, during downwind propagation or inverse lapse rate, to 20 dB during upwind propagation or normal lapse rates within the high frequency region ($f > 500\text{Hz}$). It should be emphasized that these large attenuations were consistent up to 61.5 meters from the source. While inside the central frequency region ($f = 250\text{-}500\text{ Hz}$), it was remarked that the refraction did not indicate any effects for short distances, which was attributed to the interaction of atmospheric effects and ground effects. However, within the low frequency region ($f < 200\text{Hz}$), it was demonstrated that temperature and wind gradients had an attenuation effects of 2-3 dB up to 100 meters from the source. Ingard [Ingard, 1953] noted that a significant enhancement to the lower frequencies will occur during downwind propagation or in inversion conditions.

Ground effects can have significant effects on noise attenuation. This is due to ground reflected waves interference (directed and reflected waves being out of phase along the ground), which will reduce a significant part of the A-weighted spectrum (1000 to 2500 Hz) at 7.5 meters and to the effect of absorption of the wave at the surface that is also frequency dependent. Another important factor is the angle of the incident waves that are affected by refraction [Embleton, 1976; 1980]. This causes a “shadow zone” due to wave cancellation. Traffic noise, emitted close to the earth surface can be greatly

affected by such ground effects. Furthermore, absorption and ground effects are interrelated because of the angle of incidence.

Wiener [Wiener, 1959] derived an empirical refraction relation for higher frequencies based on the assumption of linear vertical gradients. Later Delany [Delany, 1969] modified this model by using logarithmic profiles for temperature and wind gradients. In a study carried by Kriebel [Kriebel, 1972], an observed attenuation of 11 dB during short range propagation occurred. However, the short distance was not defined quantitatively and these models are not precise for lower frequencies.

In an effort to accurately predict the amount of refraction, Pierce [Pierce, 1981] modified a mathematical model derived by Gutenberg [Gutenberg, 1942], based on calculating the radius of curvature of a component of the wave neglecting the cross wind in Equation 20.

$$R_c = C / [(dc/dz) \sin\theta + dv_x / dz] \quad (20)$$

Where:

R_c = the radius of curvature of a vector component of the sound wave at any point

C = speed of sound in air

Z = height

θ = the angle of the vector component of the sound wave makes with the vertical

v_x = the horizontal component of the wind velocity (direction of sound propagation)

dc/dz = the effect of the temperature gradient

“ R_c ” will have a positive or negative value if downward or upward bending respectively. Equation 20 can be modified by neglecting the “ $\sin\theta$ ” component if the waves are propagating in nearly horizontal directions. This approximation is good within 3 to 4 percent accuracy for angles within 15 degrees of the horizontal. With this assumption, Equation 20 will be reduced to Equation 21:

$$R_c = C / [(d(c+v_x) / dz)] \quad (21)$$

Once the amount of ray curvature is predicted, divergence of sound rays can be calculated. The sound energy decreases with distance in direct proportion to the amount

of divergence between adjacent rays. Using geometric or ray acoustics the reduction in sound levels may be calculated.

In a study carried out by Wayson [Wayson, 1989], using meteorological equipment and multiple microphones to measure sound pressure level, relative humidity, and wind speed in the three coordinate axis, an empirical model for refraction was proposed. The calculations are meant to predict the excess attenuation due to refraction during positive and negative wind cases. Equations 22 and 23 are the empirical relations used for positive wind speed (wind moving from source to receiver) and negative wind speed (wind moving from receiver to the source) respectively. It should be noted that this model is based on observation up to 122 meters from the centerline of the facility and no barrier or other obstruction were present.

$$A_{\text{ref/Pos}} / \text{m} = (1/1000) * [-26.4 - 131.3\gamma + 23.4s - 1.2R_i - 38.6\sigma_w - 70.2\sigma_v + 73.7\sigma_u] \quad (22)$$

$$A_{\text{ref/Neg}} / \text{m} = (1/1000) * [33.4 - 107.3\gamma + 4.6s - 3.9R_i - 150.5\sigma_w - 15.6\sigma_v - 26.2\sigma_u] \quad (23)$$

Where:

γ = true lapse rate

S = wind speed, m/s

R_i = Richardson number

$\sigma_{u,v,w}$ = Standard deviation of wind speed in three coordinates

Turbulence

Turbulence is another atmospheric phenomena that could affect sound level due to turbulent refraction. Lumley [Lumley, 1964] explained that due to instabilities within the thermal and viscous boundary layers at the surface of the ground, eddies of approximately 1 mm in size are formed. Turbulence ranges from small amounts of activity on inversion nights to large amounts of mixing on windy summer afternoons with bright sunshine.

Two prime mechanisms exist in the boundary layer that creates turbulence: convection by mechanical mixing and thermal buoyancy. Mechanical mixing occurs due to wind gradients caused by obstructions and the surface roughness of the earth. Thermal effects occur when the ground heats and cools slower than the surrounding air.

Several studies were performed in order to evaluate the effect of turbulence on noise propagation, it was concluded there is a significant attenuation cause by

atmospheric turbulence [Brown, 1976] and including the middle and lower frequency range [Sutherland, 1971; Embleton, 1974].

One method for quantifying turbulence is the Richardson number [Richardson, 1920], as shown in Equation 24, which is a dimensionless parameter that incorporates both thermal and mechanical forces. The Richardson number is proportional to the rate of consumption of turbulent energy by buoyant forces divided by the rate of production of turbulent energy by wind shear. Table 3 shows typical turbulence characteristics for various Richardson numbers.

$$Ri = (g/T_A) \{(\gamma - \Gamma) / [(du/dz)^2]\} \quad (24)$$

Where:

Ri = Richardson number

g = gravitational acceleration

γ = true lapse rate

Γ = adiabatic lapse rate

T_A = absolute ambient temperature

du/dz = Wind shear component

Table 3: Turbulence Characteristics for Various Richardson Number

Richardson Number	Turbulence Characteristics
$Ri > 0.25$	No vertical mixing
$0.25 > Ri > 0$	Mechanical turbulence, weakened by stratification
$Ri = 0$	Mechanical turbulence only
$0 > Ri > -0.33$	Mechanical turbulence dominates convective mixing
$Ri < -0.04$	Convective mixing dominates mechanical mixing

Source: [Wark, 1976]

In order to better understand excess noise attenuation due to atmospheric effects, turbulence should be considered with wind speed and temperature gradients. The effects of turbulence, as with refraction from wind and temperature gradients, increase with distance and with frequency [Embleton, 1980]. Turbulence may act to both scatter sound and interact with other actions that depend on coherence (i.e. ground interference). The amount of noise “scattered” into the shadow zone is important in understanding the overall noise attenuation due to atmospheric effects, since it provides an understanding of noise barrier effectiveness due to scattered sound levels.

It was determined that the orientation of the source and receiver and the beam width of the source rather than the transport medium would have an effect on excess attenuation due to turbulence [Brown, 1976].

In an effort to measure turbulence and to determine the effects on noise propagation, Chernov [Chernov, 1960] and Tatarski [Tatarski, 1961 and 1971] have developed basic acoustic scatter models based on turbulent eddies. Tatarski showed that the mean square amplitude is proportional to a refractive index structure function “ C_n ”. This function is shown in Equation 25:

$$(C_n)^2 = \{[(C_T)^2 / 4 (T_0)^2] + [(C_v)^2 / (C_o)^2]\} \quad (25)$$

Where:

T_0 = absolute temperature

C_o = phase velocity

$(C_v)^2$ = mechanical turbulence structure

$(C_T)^2$ = thermal turbulence structure

$$(C_v)^2 = [(V_1 - V_2)^2 / (r)^{0.667}] \quad (26)$$

$$(C_T)^2 = [(T_1 - T_2)^2 / (r)^{0.667}] \quad (27)$$

Where:

V_1, V_2 = fluctuating wind velocities at 2 points separated by a distance r

T_1, T_2 = fluctuating temperatures at 2 points separated by a distance r

The problems with incorporating this model in a prediction scheme are obvious when trying to determine C_V and C_T . In summary, it can be seen that several mathematical models have been developed. However, Inconsistencies and prediction errors limit the effective use of these equations.

Diffraction

Noise barriers are used to abate sound level from traffic noise sources. The object of highway barrier design is to provide protection against traffic noise for residences along the highway. They are usually built to break the line of sight between the highway traffic and the affected residences.

The main purpose of a noise barrier is to create a shadow zone behind the barrier by diffracting the sound waves over the top and around the barrier. Barrier design is based on predicting diffraction effects, usually with the help of computer modeling. Several methods have been developed to model diffraction; they are divided into three different techniques. First, the empirical methods are developed from scale modeling and actual barriers; they are subject to error when applied toward other project locations and geometry. This is due to the fact that sound pressure levels are sensitive to atmospheric conditions such as temperature; wind velocity and thermal lapse rates, which are all site specific. Secondly are the approximate analytical methods developed from the diffraction theory, which is more general in its approach to predict sound level. Finally, the

numerical methods are used to solve the differential equation governing sound wave propagation. These latter methods are the least practiced due mainly to the complexity of the method requiring detailed input by the user.

The analytical methods have two approaches as explained by MacDonald [MacDonald, 2002], geometrical approximation methods and numerical methods that attempt to solve the wave equation in the presence of a barrier and absorptive boundary. Geometrical approximation uses the concepts of rays which describe the propagation path of acoustic wavefronts. A solution of the wave equation is the most rigorous mathematical method since it starts with a governing differential equation describing the sound field. However, the wave equation is generally difficult to solve with the boundary conditions that we encounter with a barrier and absorptive ground. Furthermore, the wave equation has a unique solution for different source-barrier-receiver geometry and therefore has to be evaluated for each project.

Wave optics principles and theories are the basis for the majority of the analytical methods of acoustic diffraction. Given that the electromagnetic theory for diffraction and propagation of waves is applicable to any process comprised of wavelike disturbances, the ideas of wave optics could be applied in the acoustic field. Geometric optics is a simpler approach to the diffraction phenomenon and does not seek to solve the wave equation but uses the ideas of approximating wavefronts as rays that are normal to the wavefronts and then following the path of the rays. The geometrical approach for optics and acoustics use the concept of shortest travel time over a path from Fermat's principle.

A coordinate system describes the positions of the source, barrier and receiver and allows calculation of the corresponding path length differences of the Huygen's wavelets. A superposition of the wavelets produces the total sound field at a receiver.

The shape of wave surface can be explained by assuming that each point of a diffracting surface emits a spherical wave as indicated in the Huygen's principle. Fresnel proved that Huygen's principle is an exact consequence of the differential equations of optics. Sommerfeld [Sommerfeld, 1964] derived Equation 28, starting with the Green's function solution to the wave equation to produce the diffraction integral below.

$$i\lambda\Phi_p = \int_S \frac{e^{ik(r_s+r_o)}}{r_s+r_o} \frac{\cos\theta_s + \cos\theta_o}{2} \Phi dS \quad (28)$$

Where:

Φ_p = the sound field at a point, p

Φ = the incident field

S= aperture surface

r_o = distance from diffracting edge to receiver

r_s = distance from diffracting edge to source

θ_o = angle from receiver to diffracting edge

θ_s = angle from source to diffracting edge

Equation 28 can be interpreted as a light wave falling on aperture S, with every element dS emitting a spherical wave $[1/r * \exp(ikr)]$ that has the amplitude and phase of the incident wave, Φ . The above integral has been formulated with the assumption that $kr \gg 1$, the same assumption made in the geometrical optics case.

Several researchers have attempted to develop models for diffraction. Based on the work of Sommerfeld [Sommerfeld, 1909], Keller [Keller, 1962] has advanced the idea of geometrical optics in wave equation solution, to include diffracted rays that hit the edges or corners of apertures and screens, which is Keller's geometrical theory of diffraction simplifies the formulas. Later, Kurze and Anderson [Kurze, 1971] simplified Keller's expression and developed Equation 29, which is satisfactory for low Fresnel numbers but requires a correction for large Fresnel numbers (N). The Fresnel number is a function of the angle the ray must make going over the barrier and can be approximated by using only the path length difference between direct and diffracted path divided by the wavelength.

$$A_{\text{diff}} = 5 \text{ dB} + 20 \log [(2 \pi N)^{1/2} / \tanh(2 \pi N)^{1/2}] \quad (29)$$

Other solutions have been proposed by Pierce [Pierce, 1972], DeJong [DeJong, 1984], Jonasson [Jonasson, 1972] and Embleton [Embleton, 1980], however, most of the computer models in use today employ the method of Kurze and Anderson. This approach

is popular because it is based on a single parameter, the Fresnel number and it is easy to use.

Several mathematical models and empirical formulas have been developed to measure the effects of absorption, wind speed gradients, temperature gradients, turbulence and diffraction on noise propagation. However, some models were inconsistent and were only valid within a certain frequency range. Moreover, many of these models were derived for noise from aircraft or only considering a point source, which will not provide accurate prediction when modeling traffic noise. Currently used highway modeling methodologies are discussed later in this chapter.

Sound Propagation Models and Research

Many models used in traffic noise research have largely ignored atmospheric effects. Newer models have included the traffic noise spectra and it is now possible to start and include atmospheric effects in a reasonable way. This is important because as we have just explained atmospheric phenomena could significantly affect sound levels attenuation beyond what is expected from geometric spreading and shielding from noise barriers. Some of these models will be discussed briefly hereafter.

One of the most popular highway noise prediction models has been the FHWA program STAMINA 2.0 and SNAP 1.1 [Bowlby, 1983; 1980 respectively], which are both based on the FHWA methodology [Barry, 1978]. During the 80's and 90's

STAMINA 2.0 were the most widely used until the development of FHWA traffic noise model TNM 1.0 & 1.1 in 1998. Despite the fact these models are widely used in prediction traffic noise levels, the main shortcoming is that these models have all failed to model atmospheric refraction effects due to temperature and wind gradients. However, they have included atmospheric absorption. A very simple form is used for STAMINA 2.0 as shown in Equation 30:

$$A = 5.4 (10^{-4} (2.35)^{(n-5)} r_{s-r}) \quad (30)$$

Where:

A = attenuation due to atmospheric absorption in dB

r_{s-r} = the source to receiver distance in feet

n = the octave band frequency index

Other studies have been specifically conducted to observe atmospheric effects other than absorption on highway noise traffic noise, but have either failed to provide accurate results or required additional analytical development or experimental validation.

Some efforts have tried to correlate a single weather parameter, which have proven to be sufficient for point sources but unsuccessful in modeling noise from line sources [Yoshihisa, 1984]. Various models have attempted to model noise levels at larger distances beyond the first or second row of homes along highways [De Jong, 1980; 1981]. Many of the papers reviewed have only modeled the noise levels at short distance

(i.e., 38 meters). In the Netherlands a model has been developed to allow for meteorological adjustment for long term equivalent traffic noise levels. This model, which corrects for downwind propagation is shown in Equation 31:

$$A_m = 3.5 \{1 - 10 [(Z_s + Z_r)/d]\} \quad (31)$$

Where:

A_m = sound level adjustment in dB ($A_m > 0$)

Z_s = source height

Z_r = receiver height

D = distance between source and receiver

Baker and Hemdal [Baker, 1980] have correlated atmospheric effects and passby trucks sound levels. Significant (1% confidence level) correlation coefficients varied from 0.23 to 0.83 for temperature, and 0.2 to 0.54 for relative humidity.

In 1977, when FHWA developed the methodology for noise prediction [FHWA, 1977] used in STAMINA. The STAMINA model used reference energy mean emission levels (REMELs) as a starting point. The reference levels are adjusted for traffic flow, including speed and volume, distance, finite roadway (section angle) and shielding. The FHWA method used the alpha factor method that combines spreading and ground attenuation into a single term. Barriers, rows of buildings and vegetation are forms of shielding. The barrier calculations follow the Kurze and Anderson method using

wavelength and path length difference to calculate the Fresnel number. In addition, this method is a function of ground type.

The FHWA traffic noise prediction method [FHWA 1977] used Equation (32) to predict one hour sound levels from highway sources.

$$L_{eq}(1 \text{ hr}) = L_o + 10\log(Ni\pi D_{ref}/SiT) + 10 \log(D_{ref}/D)^{1+\alpha} + 10\log[f(\phi_1, \phi_2)/ \pi](32)$$

Where:

L_o = reference level for single vehicle passby

Ni = vehicles per hour

Si = speed of vehicle, km/h

T = time, 1 hour average

α = ground type parameter (0=hard, 1=soft)

$f(\phi_1, \phi_2)$ = function to adjust for non-infinite line source

Notice that the exponent is “ $1+\alpha$ “, the “1” indicates that this is a line source approximation. MacDonald [MacDonald, 2002] has explained that the “ $(Ni\pi Do/SiT)$ ” term accounts for the traffic volume that passes the receiver per hour and the speed of travel. Speed is used to determine the REMEL value but the “ $(Ni\pi Do/SiT)$ ” also accounts for the time that vehicle in the passby event needed when developing time average values. Vehicles traveling at higher speeds do not provide the same overall energy with time to a receiver since the event is of shorter duration. The $f(\phi_1, \phi_2)$ term is

the angle formed by the receiver and the endpoints of the roadway. This term accounts for the non-infinite roadway and is negative since the $f(\phi_1, \phi_2)$ angle is always less than or equal to 180 degrees.

STAMINA calculates “A” weighted L_{eq} sound levels at receivers and includes geometric spreading, ground effects, barrier diffraction and atmospheric absorption. STAMINA uses REMEL curves based on L_{max} measurements for its sources. These sources include passenger cars, medium trucks and heavy trucks.

Equation 29 [Kurze, 1971] was used to account for barrier attenuation in STAMINA. The main parameter in Equation 29 is the Fresnel number (N), which is based on the path length difference, caused by the barrier. It should be noted that the path length distance is only a surrogate for the angle formed as the ray goes over the barrier.

$$A_{diff} = 5 \text{ dB} + 20 \log[(2 \pi N)^{1/2} / \tanh(2 \pi N)^{1/2}] \quad (29)$$

STAMINA calculates the ground attenuation and the barrier attenuation, and then chooses the smaller of the two values. Consequently, no insertion loss because its attenuation is lower than the ground attenuation, which results in a low height barrier. The insertion loss will be emphasized when the calculated barrier attenuation is greater than the calculated ground attenuation. However, over hard ground, STAMINA equates a barrier’s insertion loss to its barrier attenuation.

In recent years, FHWA developed a new model called the Traffic Noise Model (TNM) for predicting traffic noise. TNM is a relatively new traffic noise model created for the FHWA [Anderson, 1998] by a team led by Harris, Miller, Miller and Hanson, et al. TNM uses the method of modeling source contribution with reference levels that are adjusted by independent attenuation terms. TNM uses elemental triangles (x, y plane) formed between receivers and two endpoints on roadway or barrier segments to compute line source contributions. The smallest angle allowed for the elemental triangles is ten degrees. Attenuation terms are calculated in the z plane and at each leg of the triangle. TNM computes average vehicle speeds for an elemental triangle. Ground attenuation algorithms summarized by Chessel [Chessel, 1977] provide more accurate modeling of the ground surface. The TNM is essentially a free flow model but it does allow the user to model interrupted flow traffic using acceleration zones of equivalent energy. Vehicle emission reference levels used the by TNM account for accelerating vehicles, vehicles on grades and different pavement types. Sources have two source heights, at ground and above ground. Energy is distributed among these heights. Source levels and algorithms are based on one third octave band spectra.

The diffraction model is based on work described by DeJong [DeJong, 1983]. It accounts for diffraction from wedges, berms, barriers and impedance discontinuities. For complicated geometry and impedance discontinuities such as highways, TNM uses a ground impedance averaging scheme by Boulanger [Boulanger, 1957]

TNM uses a correction term to get free field sound pressure; this is used to remove ground effects due to measured REMELs so that TNM can calculate its own ground and diffraction effects.

The model does not account for atmospheric effects such as temperature and wind gradients but does calculate atmospheric absorption based on the well known ISO 9613 standard.

Wayson [Wayson, 1989] has mentioned that atmospheric phenomena may affect traffic noise levels even at very close proximity to the roadway. He determined the need to consider separating positive and negative perpendicular components of the wind when modeling atmospheric effects. In brief, all efforts to predict excess attenuation of traffic noise due to atmospheric effects are still being evaluated in an attempt an accurate widely used model.

Gilbert [Gilbert, 1989] has concluded that the parabolic equation method can accurately treat sound propagation in a realistic outdoor environment. However, the parabolic equation model used was limited to deterministic, range independent, sound speed profiles over a smooth ground surface. Consequently, the model did not take into account any mechanism that could weaken the shadow zone.

El-Aassar [El-Aassar, 2002] has shown that the meteorological effects maybe significant at short distances and those effects occur in cases of stronger lapse rates. This may also occur during cases of stronger wind shear, but data collected during this project were not sufficient to check these cases. The correlation was generally found at higher

frequencies. In the case of low frequencies, a change in ground effects caused by refraction was thought to be the reason. Temperature had more effect than wind for these measured sites according to the measurements.

Recently, Heinman [Heinman, 2003] has confirmed that the state of art algorithms do not consider meteorological influences. Moreover, downwind propagation is assumed as a standard in order to provide conservative estimates. Heinman suggested the introduction of meteorological classes which are representative of specific acoustical behaviors, e.g. upward or downward refraction. This idea is being researched through a European project named “HARMNOISE”. The procedure is based on a classification of relevant meteorological situations and the determination of long-term frequency distribution class. The latter is given by the local climate including mesoscale effects. Separate predictions of the immission are made for each class and the results are averaged after giving them the statistical weight according to their frequency of occurrence. However, Wayson [Wayson, 1989] has tried to explore a similar idea but he concluded that the procedure was not accurate in predicting outdoor noise levels.

Summary of Literature Review

In this chapter we have reviewed the physical mechanism that causes atmospheric effects on traffic noise propagation. In order to predict accurate traffic noise levels, we have determined that modeling atmospheric effect is very important and cannot be

ignored. Moreover, we have indicated that there is a strong relation between ground and atmospheric effects and that they should not be ignored when predicting noise levels. We have shown that atmospheric phenomena are very complicated to model due to the different factors; absorption, ground surface, seasonal variations, temperature and wind speeds, which need to be considered. In addition, we have shown the effort in modeling diffraction and we have found that the traffic noise models currently used (i.e. TNM) have largely neglected the atmospheric effects, except for atmospheric absorption. Likewise, many efforts have studied only the atmospheric effects at long distance from the source. Several of the relations were developed to model aircraft noise or other sources not primarily highway traffic noise. Finally, it has been shown that there is limited research carried that have tried to incorporate all mechanisms, i.e. geometric spreading, ground effects, refraction, and turbulence, affecting outdoor noise propagation.

Because of these shortcomings, there is a need to better understand the meteorological effects on traffic noise propagation through measurements and comparison to acoustic theory. There is a need for a model that incorporates all refraction algorithms that must also work with algorithms for geometric spreading, ground effects, refraction, and turbulence, affecting outdoor noise propagation. The methodology that will be used is presented in the next chapter.

CHAPTER 3

METHODOLOGY

The objective of this work was to develop a model to account for the effects of atmospheric parameters on sound propagation for traffic sources. This should result in better and more accurate prediction of traffic noise levels. This chapter discusses the methods and procedures that were derived to collect and model the raw data; including sound levels, meteorological and traffic data. As explained in the literature review, there are several physical mechanisms that affect outdoor noise propagation. These mechanisms are complicated, interrelated and include geometric spreading, ground impedance, atmospheric absorption, atmospheric refraction, and diffraction. Moreover, the majority of the research that has been performed on the prediction of traffic noise levels has ignored atmospheric effects (refraction). The error from atmospheric effects has been reported to be as high as 30 dB(A), which is a difference of three order of magnitude for the acoustic energy. When atmospheric refraction has been considered, it was often only for downwind propagation and conservative cases. In order to accurately predict noise levels, a more robust method must be included in the modeling process.

A common acoustic modeling approach is to assume that propagation effects are independent [Beranek, 1971]. With this assumption, these effects may be considered to act separately on the noise levels perceived by a receiver. Based on this assumption the noise level may be defined by the following Equation 33:

$$L_x = L_o + A_{\text{geo}} + A_b + L_r + A_e \quad (33)$$

Where:

L_x = Time averaged sound level at some distance x , in dB

L_o = Sound level at a reference distance

A_{geo} = Attenuation due to geometric spreading

A_b = Insertion loss due to diffraction

L_r = Increase in sound level due to reflection

A_e = Attenuation due to ground characteristics and environmental effects.

The term denoted (A_e) include three different attenuation parameters: attenuation due to ground effects, attenuation due to atmospheric absorption, and attenuation due to atmospheric refraction. The term (A_e) could be re-written as follow:

$$A_e = A_{\text{grd}} + A_{\text{abs}} + A_{\text{ref}} \quad (34)$$

Where:

A_{grd} = Attenuation due to ground effects

A_{abs} = Attenuation due to atmospheric absorption

A_{ref} = Attenuation due to atmospheric refraction

In order to study the effects of atmospheric refraction on outdoor noise propagation, the relationship between sound level (L_x) and A_{ref} need to be evaluated. All the terms in Equation 34 need to be quantified to the best extent possible.

The Federal Highway Administration (FHWA) uses a method to calculate reference emission levels (L_o) for estimating vehicle passby levels. Procedures have been developed to measure vehicle passbys at a reference sideline distance of usually fifty feet (15 m) from the center of the vehicle track. At this distance, refraction effects should be minimal and as such this distance is not suitable for this research. For the purpose of this research, sound levels were measured at various distance ranging from close to the highway as a reference position with minimal refraction effects and up to several hundred feet from the road where refraction effects should be significant. This should permit measurements of atmospheric effects as shown in Figure 13. The distances varied from 75 feet (23 m) to 780 feet (238 m) from the center of the highway as shown in Figure 14. The 75 foot location should not be significantly affected by refraction effects and can serve as a reference position and allow normalization due to highway traffic. This position was selected because it was as close to the source (near lane) that could be selected without being in the near field. Near field is defined as a distance smaller than one-quarter of the wavelength of interest close to the sound source. In this region, sound levels fluctuate drastically with small changes in distances from the source. The reference was chosen outside the near field so noise levels measurements would not be affected by this effect.

The sound levels were measured in 1/3 octave band sound levels. The measurements were done using five Cesvas 1/3 octave band analyzers and two Metrosonic dB308 overall sound level analyzers (used to measure broadband A-weighted sound levels). The 1/3 octave band analyzers provided sound levels for the various frequency 1/3 octave band from 20 Hertz to 10,000 Hertz. This enabled the observation of the effects of propagation parameters by frequency. Figure 14 shows that multiple microphone heights were employed, using portable towers. Of note are the distance and heights for each microphone.

Two 1/3 octave band analyzers (Mic1 and Mic2) were positioned at 5 feet (1.5 m) above the ground surface and two 1/3 octave band analyzers (Mic3 and Mic4) were positioned at 20 feet (6 m) above the ground surface. Mic 1 and Mic 3 were located a horizontal distance of 440 feet (134 m) from the center of the highway, while Mic 2 and Mic 4 were located at 780 feet (238 m) from the center of the highway. The overall analyzers (Mic5 and Mic6) were placed adjacent to Mic 1 and Mic 2 and at the same height 5 feet (1.5 m) as the 1/3 octave band analyzers for quality control purposes. Mic 5 and Mic 6 should record the same A-weighted levels as the 1/3 octave band analyzers.

In addition again for quality control Mic 7 (3rd microphone location in Figure 13) was located at 135 ft (41 m) south of S.R. 434 to ensure that traffic contribution from the road did not add substantially to the overall sound level measured. This permitted the analysis to only be based on noise propagation from S.R. 417. This was carried out by checking the sound levels between Mic 5 located at 556 ft (169 m) from S.R. 434 and

Mic 7, if they are within 12.5 dB, then they have an influence and the measurement periods will be removed from further consideration.



Figure 13: Diagram of Testing Location

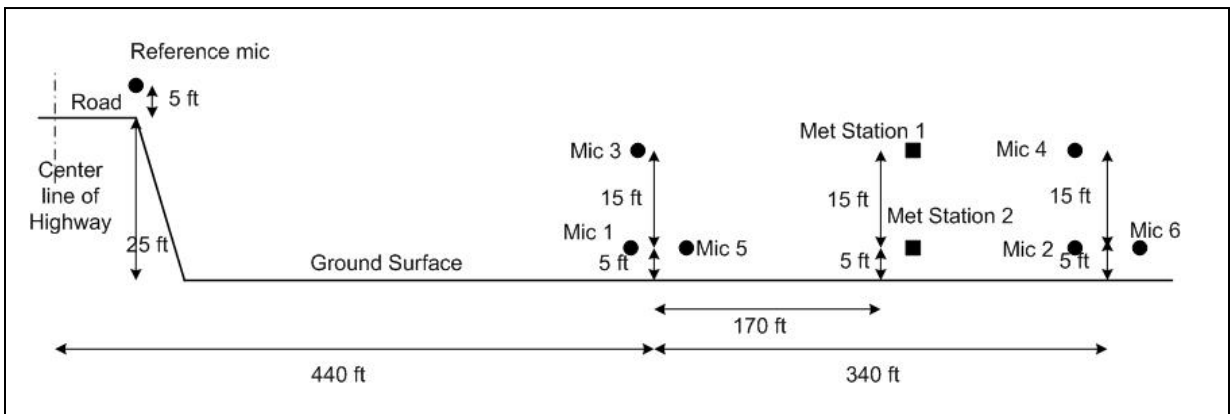


Figure 14: Diagram of Testing Positions

The meteorological instruments were situated in the available open areas away from and between the microphones to avoid any interference. Wind speed, direction, and temperature were collected at the heights of 5 feet (1.5 m) and 20 feet (6 m), as shown in Figure 14. By measuring at various heights, data collected allowed a better understanding of the changes between ground effects, wind shear and lapse rate with height. This provided more insight to how the sound levels were changing and allowed further evaluation of ground effects.

Wind speed and direction were measured by using U-V-W anemometers. U-V-W anemometers measure wind speed directly for the three orthogonal directions. The anemometers were oriented with the positive V-axis (Y in usual coordinate system) pointing to the north. The U-axis (X in a usual coordinate system) oriented to the east, which was perpendicular to the highway and in the primary plane of sound propagation. The W-axis (Z-axis) is perpendicular to the ground plane with the positive direction being upwards. The speed of rotation of the propellers on each axis allowed each wind vector to be recorded as direction and magnitude. Also, as explained in the literature review, wind shear is an important refraction parameter. In the case of downwind propagation (i.e. positive wind moving from source to receiver), the sound level at the receiver could increase due to sound wave bending downward as a result of change in sound wave velocity with height. The wave velocity is the sum of both the wind velocity vector and the original sound wave velocity. Similarly, in the case of upwind propagation (i.e. wind moving from receiver to source), the sound level at the receiver may be

attenuated creating a shadow zone, which is the result of the sound wave bending upwards as a result of sound wave velocity changes with height. Again, the wave velocity is the sum of both the wind velocity vector and the original sound wave velocity. The magnitude of the wind shear should be directly correlated to refraction based on theory. Moreover, low wind speeds, with a small change in speed with height, should have a smaller effect on the downward noise propagation. For accuracy polypropylene propellers, with very low stall speed of less than 1 mile-per-hour, were used. This allowed very low wind speeds to be measured.

Temperature data were collected using digital aspirated thermometers. Optical thermometers were used, attached inside a PVC housing vertically with the housing being 3 feet (0.9m) in length. At one end of the pipe a fan was used to maintain air flow around the thermometer in order to provide accurate reading of the air temperature and to minimize heat transfer to the sensor. The air flows over the thermometers were comparable to the same flow rate used in R.M.Young aspirated digital thermometers which is equal to 20 fps. The readings from both thermometers were taken before and after each sampling periods in order to ensure they had similar reading at the same height, and there was no difference between them. The thermometers were mounted at the same height as the anemometers, as shown in Figure 14, on separate portable towers.

Traffic data collection included vehicle speed, traffic volume, and vehicle mix, as these parameters are needed as input to determine the source strength. During the sampling period, the traffic data was manually counted during each sample period for

each direction of travel. Vehicle classifications were done at the same time using FHWA defined vehicle classes of cars, medium trucks, heavy trucks, buses and motorcycles. The traffic counts were conducted manually at 15 minutes periods. Speed data was collected using radar guns for accuracy.

The overall sound level meters as well as the 1/3 octave band analyzers were calibrated before and each sampling period to make sure consistency of the data measured during sampling periods. The calibration for the 1/3 octave band analyzers was carried at 1 KHz for 94 dB, while the calibration for the overall A-weighted sound level analyzers was conducted at 1 KHz for 102 dB. A difference in calibration reading before and after the sampling periods was acceptable if it fell within 0.2 dB.

The term A_{geo} in Equation 33, refers to geometric spreading of sound and can be predicted with an acceptable measure of accuracy. As previously described, due to geometric spreading alone, sound levels decrease roughly by a rate of 3 dB per doubling distance from line sources at short distances, while the fall off rate for point source is 6 dB per doubling of distance for short distances. Current methods show that these fall off rates are only approximate and change with distance from the source and ground types. More complex prediction techniques are needed for various propagation parameters. Fall off rates due to ground effects and geometric spreading can be modeled as reported by Chessel [Chessel, 1977] and has been widely used in several traffic noise models, including the FHWA Traffic Noise Model.

For the typical roadway with many vehicles in a line, we cannot simply limit our concern to a small, nearby segment because the other farther segments all along the line often contribute significantly to the overall sound level. It is important to determine the section of the highway that will contribute to the sound level at a receiver away from the roadways. Figure 15 shows the geometry of the site that will be evaluated to determine the contributing segment distance. The evaluation is based on Equation 35, which is the equation used to determine attenuation due to geometric spreading. It should be noted that Equation 35 is for point sources, however it is applied in line source calculation because traffic is modeled as an infinite number of point sources. This will be a conservative analysis since other factors could cause an even greater fall off rate.

$$\Delta L = 10 \log (D_o/D)^2 \quad (35)$$

Where:

ΔL = Difference in sound level between two receivers

D_o = Distance at reference receiver

D = Distance at moving receiver

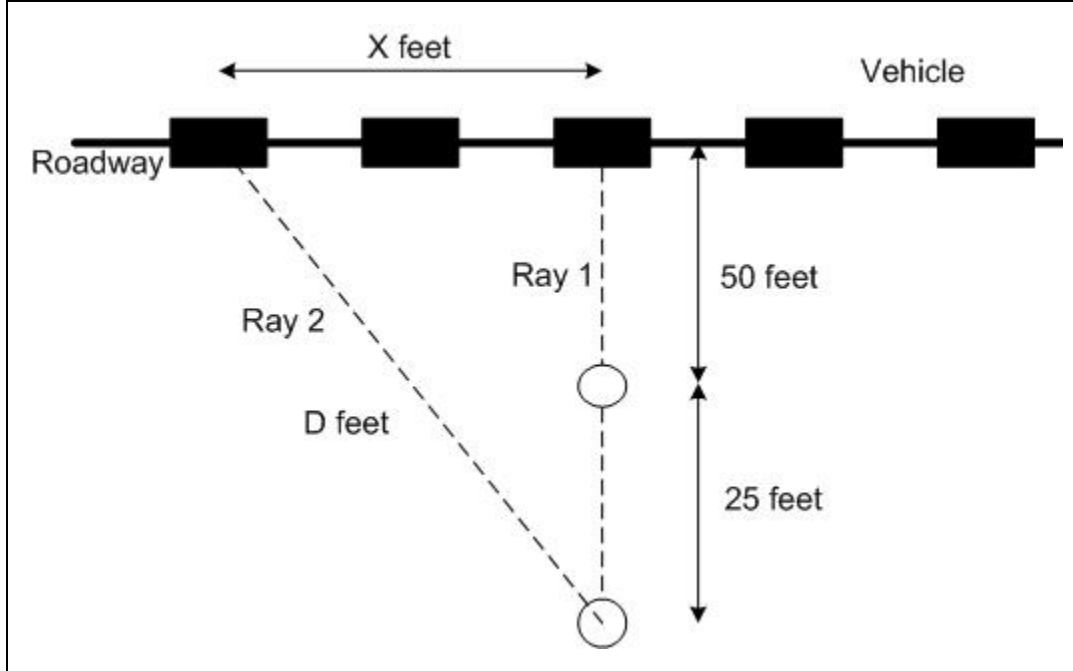


Figure 15: Geometry of a Site for Calculation of Segments Contribution to Sound Level

A 12.5 dB difference in sound level between two sources would mean that the lower sound level is not significantly contributing to the overall sound. This occurs because of the logarithmic way in which dB are added. In order to determine the highway segment contributing sound level to the receiver, the reference microphone location for this research is at 75 feet (23 m) from the center line of the highway, and was compared to a receiver location at a distance 50 feet (15 m) from the highway, which is the distance used as a preferred Reference positions for all measurements according to FHWA, as shown in Figure 15. Based on Equation 35, the sound level at the receiver from a single vehicle, based on ray 1, will decrease by 3.5 dB from the original sound pressure level (SPL) as shown in Equation 36. Equation 37 was used to achieve a 16 dB between the

two sources for ray 1 and 2, the sound level for Receiver 2 based on ray 2 was calculated. Hence the new distance based on the 75 feet (23 m) could be calculated. Based on Equation 37, the distance “X” shown in Figure 15 is equal to 139 feet (42 m). Accordingly, the highway segment contributing to the sound level at a receiver 75 feet (23 m) from the highway has been calculated to have a total segment length of 278 feet (85 m), centered at the Reference receiver.

$$\Delta L_1 = 10 \log (50/75)^2 = \text{SPL} - 3.5 \text{ dB} \quad (36)$$

$$\Delta L_2 = 10 \log (25/D)^2 = \text{SPL} - 16 \text{ dB} \quad (37)$$

This means that the zone of influence of vehicles contributing to the sound level is just less than 140 feet (43 m) in each direction for this Reference receiver. As such, a line source is considered approximately 280 feet (86 m) long.

The roadways selected for study have speed limits ranging from 30 to 60 mph, which are equivalent to 44 and 88 ft/s respectively. At this speed, the time needed for a vehicle to pass through this segment length of 280, estimated previously, is calculated as shown in Equations 38 and 39:

$$\text{Time} = 280 / 44 = 6 \text{ seconds (for speed of 30 mph)} \quad (38)$$

$$\text{Time} = 280 / 88 = 3 \text{ seconds (for speed of 60 mph)} \quad (39)$$

Based on these calculations, the smallest sample time for a data collection period should not be less than 6 seconds for lower speed roadways. For conservative purposes, no sample period will be less than ten seconds, which will allow monitoring and counting all vehicles passing through the segmenting contributing sound level energy to the receiver. This analysis was important for the Reference microphone, since we want to ensure that the distance chosen will be beyond any refraction attenuation effects.

The term A_b in Equation 33, refers to the diffraction of sound due to a barrier or large adjacent object and has been explored in the literature [Pierce, 1972]. Presence of such an object would complicate the sound level modeling process. Moreover, the term L_r in Equation 33, refers to reflection from large solid objects may act to significantly increase noise levels at receiver adding further complications. For the purpose of this research, through careful location selection, an open field was selected and used to avoid obstacles in the propagation path and to minimize the diffraction and reflection effects described above.

The last term in Equation 33, A_e , refers to attenuation due to ground characteristics and environmental effects and has been expanded to account for these effects in Equation 34. Atmospheric absorption A_{abs} , the second term in Equation 34, can be predicted by the ANSI method [Sutherland, 1975]. Additionally, The first term in Equation 34, ground attenuation A_{grd} cannot be neglected in calculating excess

attenuation. As pointed out in the literature review [Embleton, 1983], ground effects could significantly affect sound levels. It depends on the angle of the wave striking the ground, and this angle is to a certain extent affected by atmospheric refraction. Hence, ground effects must be considered concurrently with atmospheric refraction. The area chosen for the research had minimum grass, soft ground, in order to minimize any reflection from the ground and subsequently minimizing ground effects. Estimation of ground effects were accomplished by modeling of measurements using a custom program that was developed by MacDonald [MacDonald, 2001].

A large database was compiled that includes the 1/3 octave band sound levels, the different weather parameters discussed previously and traffic data. The meteorological data collected for each tower included the U-V-W wind vector at two heights, and temperature at two heights. Then, lapse rate, which is the difference between the temperature at the higher and lower meteorological station divided by the vertical distance between the thermometers, was calculated. Also, wind shear was calculated, which is the difference between the wind vector in the propagation path between the anemometers at the higher and lower meteorological station divided by the vertical distance between the anemometers.

Based on statistical analysis and data previously collected by Wayson [Wayson, 1989] an experimental design analysis was conducted. Considering a 2x3 (two level of wind and 3 levels for temperature) experiment, the sample period needed to be

statistically significant using a 95% confidence interval was calculated, using Equation 40:

$$t_{\alpha/2} * (s_{\beta}/\sqrt{n}) = H \quad (40)$$

Where:

$t_{\alpha/2}$ = t-test for 95% confidence interval

s_{β} = standard error for interaction term in the model

n = sample size

H = half-width of a confidence interval

Regression analysis was used and the standard error for the interaction term $s_{\beta} = 0.15$. Based on $t_{\alpha/2} = 2.447$ (6 df) and assuming $H = 0.1$, the number of sample period required to be statistically significant is 14. As a result, more than fourteen sample periods would be desired during this research. The research was carried out during different weather conditions in order to provide the suitable conditions to observe atmospheric refraction during downwind / upwind conditions and different lapse rate including inversions. Measurements were conducted for long periods of time in an effort to account for the above stated conditions. However, prevailing weather conditions, during the measurements periods resulted in only one upwind condition and few inversion cases.

Several prediction schemes were evaluated as part of the analysis. The first two schemes were based on determining sound pressure level at the receivers using the ISO 9613-2 method with and without the meteorological correction factor. The third scheme was a combination of the ISO method and the Wayson refraction empirical model. The final scheme was an evaluation based on a comparison between the measured value and TNM 2.5.

The ISO 9613-2 specifies a prediction method for calculating outdoor sound levels. Attenuation of sound during propagation outdoors is included in order to predict the sound level at various distances and conditions from a variety of sources. Equation 41 was used to calculate sound pressure level at a receiver location for the eight octave bands with nominal midband frequencies from 63 Hz to 8 KHz.

$$L_{fT} = L_w + D_c - A \quad (41)$$

Where:

L_{fT} = Time averaged sound level at some distance x, in dB

L_w = Sound level at a reference distance

D_c = Directivity correction

A = Attenuation that occurs during propagation from source to receiver

Correction due to directivity was assumed to be equal to zero, since the sound source is freely radiating into open free field. The attenuation term A in Equation 41 is for environmental, diffraction and miscellaneous effects is given by Equation 42:

$$A = A_{\text{div}} + A_{\text{atm}} + A_{\text{gr}} + A_{\text{bar}} + A_{\text{misc}} \quad (42)$$

Where:

A_{div} = Attenuation due to geometrical divergence

A_{atm} = Attenuation due to atmospheric absorption

A_{gr} = Attenuation due to ground effect

A_{bar} = Attenuation due to a barrier

A_{misc} = Attenuation due to miscellaneous other effects

The attenuation term A in Equation 42 is similar to the attenuation previously stated in Equations 34 and 35 developed by Beranek [Beranek, 1971].

The fifth term A_{misc} in Equation 42 refers to attenuation due to propagation through foliage, industrial sites, and areas of houses. For the purpose of this research, the fourth and fifth terms “ $A_{\text{bar}} + A_{\text{misc}}$ ” are not applicable since the test location is an open field and there were no barriers or any obstruction between the source and the receiver.

The first term in Equation 42 is for geometric spreading or divergence and is determined as expressed by Equation 43. Of note is that this equation is the same as Equation 12 presented in the literature review.

$$A_{\text{div}} = [10 \log (d/d_0)] \text{ dB} \quad (43)$$

Where:

d = distance from the source to the receiver (m)

d_0 = reference distance (=1m)

The second term in Equation 42 is for atmospheric absorption attenuation, varied for each nominal frequency and is determined by Equation 44.

$$A_{\text{atm}} = \alpha d/1000 \quad (44)$$

Where:

d = distance from the source to the receiver (m)

α = atmospheric attenuation coefficient (dB/km)

The third terms in Equation 42 is for ground effect attenuation, varied for each nominal frequency and is determined using Equations 45.

$$A_{\text{gr}} = A_s + A_r + A_m \quad (45)$$

Where:

A_s = attenuation within the source region ($30h_s$)

A_r = attenuation within the receiver region ($30h_r$)

A_m = attenuation within the middle region (distance between source and receiver)

Finally, there is a meteorological correction factor in dB (C_{met}) which is used in calculation of sound pressure level over a long period of time (several months) when using the ISO method, as shown in Equation 46.

$$C_{met} = C_o [1 - 10 (h_s + h_r) / d_p] \quad (46)$$

Where:

h_s = source height

h_r = receiver height

d_p = distance between the source and receiver projected to the horizontal ground plane

C_o = a factor that depends on local meteorological statistics for wind speed and direction, and temperature gradients

The values of C_o used for this research are shown in Table 3. The ISO method specifies that in cases of unfavorable conditions, which the wind blowing from the receiver to the source the value should be 2 dB. While in favorable conditions, based on the percentage of time the wind is blowing toward the receiver the number varies from 0.5 to 1 dB.

Table 3: Values of local meteorological correction C_o

Groups	Downwind	Crosswind	Upwind
C_o	0.75	1	2

The Wayson [Wayson, 1989] empirical model was developed to predict the excess attenuation due to refraction during positive and negative wind cases. Previously shown in Equations 22 and 23 are the empirical relations that were used for positive wind speed (wind moving from source to receiver) and negative wind speed (wind moving from receiver to the source) respectively.

$$A_{\text{ref/Pos}} / \text{m} = (1/1000) * [-26.4 - 131.3\gamma + 23.4s - 1.2R_i - 38.6\sigma_w - 70.2\sigma_v + 73.7\sigma_u] \quad (22)$$

$$A_{\text{ref/Neg}} / \text{m} = (1/1000) * [33.4 - 107.3\gamma + 4.6s - 3.9R_i - 150.5\sigma_w - 15.6\sigma_v - 26.2\sigma_u] \quad (23)$$

Where:

γ = true lapse rate

S = wind speed, m/s

R_i = Richardson number

$\sigma_{u,v,w}$ = Standard deviation of wind speed in three coordinates

Based on these methods, the difference between predicted and measured should be minimal if the methods work well. However, it is understood from the literature review that each of these methods has constraints. For example the Wayson empirical model was based on observation up to 400 feet (122 m) from the centerline of the facility. Moreover, the ISO method is developed for downwind propagation.

In order to evaluate these conditions and needs for further adjustments, this research included wind measurement both in upwind and downwind cases. Furthermore, the receivers were located at 440 feet (134 m) and 780 feet (238 m) from the source and at two elevations 5 feet (1.5 m) and 20 feet (6 m).

Normalization of the data was done by a direct comparison of the close Reference position where refraction effects should be minimal to the different receiver positions after correcting for all other propagation effects that were previously described. The normalized difference between predicted and measured is expected to be due only to atmospheric refraction since all other propagation effects were individually accounted for. By using of the difference between the Reference position and the farther microphone locations, varying traffic effects on the sound levels are greatly reduced so this variable need to be considered.

The following steps were applied to determine the effects due only to refraction. First was to adjust for geometric spreading by subtracting 7.7 dBA from the sound level of the Reference position when calculating effects for the microphone located at 440 feet (134 m). Also, adjust for geometric spreading by subtracting 10.2 dBA from the sound level of the Reference position when calculating effects for the microphone located at 780 feet (238 m). Then, correction for atmospheric absorption was done using Equation 44 from the ISO method. The final step was to adjust for excess attenuation caused by ground effects. The excess attenuation was calculated by a custom program developed by MacDonald as part of his dissertation [MacDonald, 2001].The program results were

verified against published ground attenuation results presented by Embleton [Embleton, 1976]. Figure 16 shows the output from MacDonald custom program. The source and the receivers are at 1.2m above the ground, and they are 15.2 m apart, with effective flow resistivity for a hard ground of 30000 cgs Rayls. The results are comparable to the output from Embleton [Embleton, 1976] as shown in Figure 16. The slight difference in the numbers could be attributed to the different way of interpolation between the two methods.

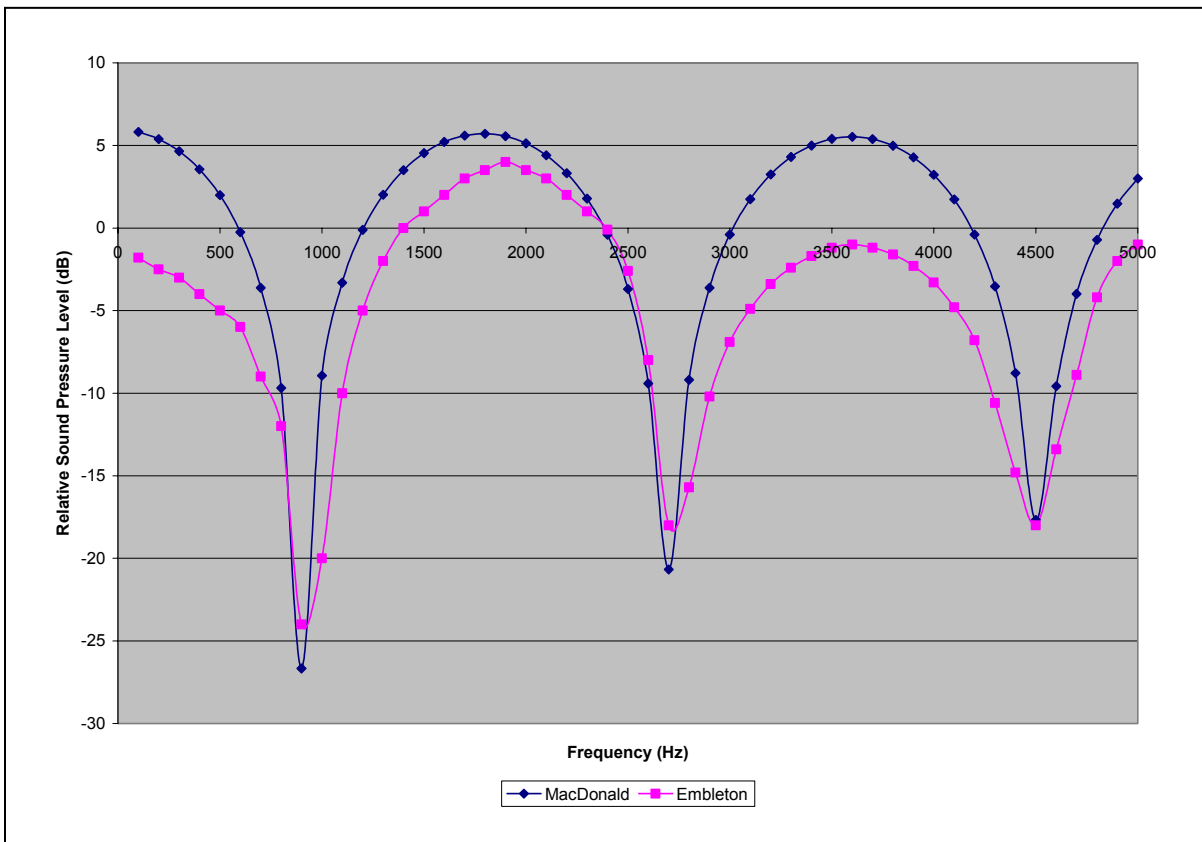


Figure 16: Ground Effect Attenuation Output from Macdonald Program

After subtracting these attenuations from the Reference microphone position, the normalized difference is the difference between the calculated Reference remainder and the other microphone positions. Any remaining difference should only be due to atmospheric refraction if it is assumed the models are accurate. Thus, an empirical model incorporating the measured parameters (wind shear, and lapse rate) was developed based on the derived refraction differences.

Statistical methods, i.e. hypothesis testing to determine significant parameter, multiple regression analysis for model building and other suitable statistical method (i.e. stepwise regression and backward elimination) were employed to correlate the attenuation due to atmospheric refraction with the different atmospheric parameters, which included wind shear, wind speed and lapse rate.

The methodology format selected is shown in Equation 47:

$$A_{\text{ref}} = A * (f(\text{lapse rate}))^b + C * (f(\text{wind shear}))^d + G * (f(\text{wind speed}))^h \quad (47)$$

This format was selected because it includes the weather parameters that have been shown to be the most significant in refraction effects based on the literature review. The normalized difference was used to develop the empirical model. In developing the algorithm, the need for transformation of the dependent variable was checked, the need for higher order function for the independent variables was checked, and the overall

empirical model and the independent variables were tested for significance. The best empirical model was used to predict the refraction for the other microphones positions. Then, the measured sound level and the predicted sound levels from the new empirical model are compared.

In summary, the purpose of this research was to represent an approach to incorporate a refraction algorithm that must also work with algorithms for geometric spreading, ground effects, refraction, and turbulence, affecting outdoor noise propagation from traffic.

CHAPTER 4

ANALYSIS

This chapter will discuss the sound level and atmospheric parameters measured at the test location and the subsequent analysis. A comparison to the FHWA TNM and the ISO 9613-2 outdoor sound propagation prediction methods is presented to determine the difference between the measured and predicted sound levels for these established models. This chapter will also evaluate the ISO meteorological correction factor and the refraction empirical model developed by Wayson to determine if this reduces the difference between measured and predicted sound levels. Furthermore, this chapter presents the steps in developing an empirical model, based on measured parameters (wind shear, wind speed, and lapse rate) to account for the atmospheric refraction.

Measured Data

Sound levels and meteorological data were collected at the test location for 18 days from 15 October, 2005 to 18 November, 2005. The measurement periods varied between 4 to 8 hours each day with selected sample periods that were analyzed in detail ranging from 15 to 20 minutes. Sound levels, wind speed and temperature were recorded every second. During the measurements periods, the majority of the wind prevailing conditions were downwind from the source to receiver (from the roadway and toward

microphone locations Mic 1 to Mic 4). Only on one day did the wind conditions change to an upwind condition (from microphone locations Mic 1 to Mic 4 and toward the roadway) for the whole day. Traffic volumes and vehicles speeds were measured concurrently with the sound levels for both direction and the on-ramp.

Once data were collected, formatted, quality controlled by including all noise data from the 1/3 octave band sound level analyzers, where their calibrations did not vary before and after the sampling periods. Also, the same was conducted for the overall A-weighted octave band analyzers. In the event that any of the microphones portable towers has fallen all data for this time period was rejected. Moreover, the data collected on the last day, where the meteorological portable towers have fallen to the ground due to high wind, were not included in the analysis.

Once data was reviewed, the analysis was begun. It was determined that the data could be divided into three distinct wind groupings: downwind, crosswind and upwind. Several samples were selected from the overall data taken, each sample ranged from 15 to 20 minutes (900 to 1200 data points). To determine these samples, for each measurement day, the wind speed and wind direction were plotted versus time to determine the time periods where wind speed was relatively constant as shown in Figure 17. Figure 17 is representative of Sample 2 for the Upwind Group, and this sample is indicated by the portion within the brackets shown on the Figure 17. Times when the wind speed (U-wind component) was relatively constant were isolated and chosen a good sample of periods for further analysis. This procedure was conducted for all sample

periods for all the groups. As with previous research [Embleton, 1976], it was indicated that downwind and upwind conditions have different refraction effects. The data collected has indicated that wind shear was more dominant, and lapse rate variation was minimal as will be shown later. Hence, wind shear was chosen as the main factor in data analysis. The data was divided into three groups: the Downwind Group, the Crosswind Group and the Upwind Group. This was done based on the wind direction by looking at the plots of the U-wind versus time and the wind direction as function of the propagation path, then separating the data recorded into these three groups. The number of data points analyzed in each group is shown in Table 4.

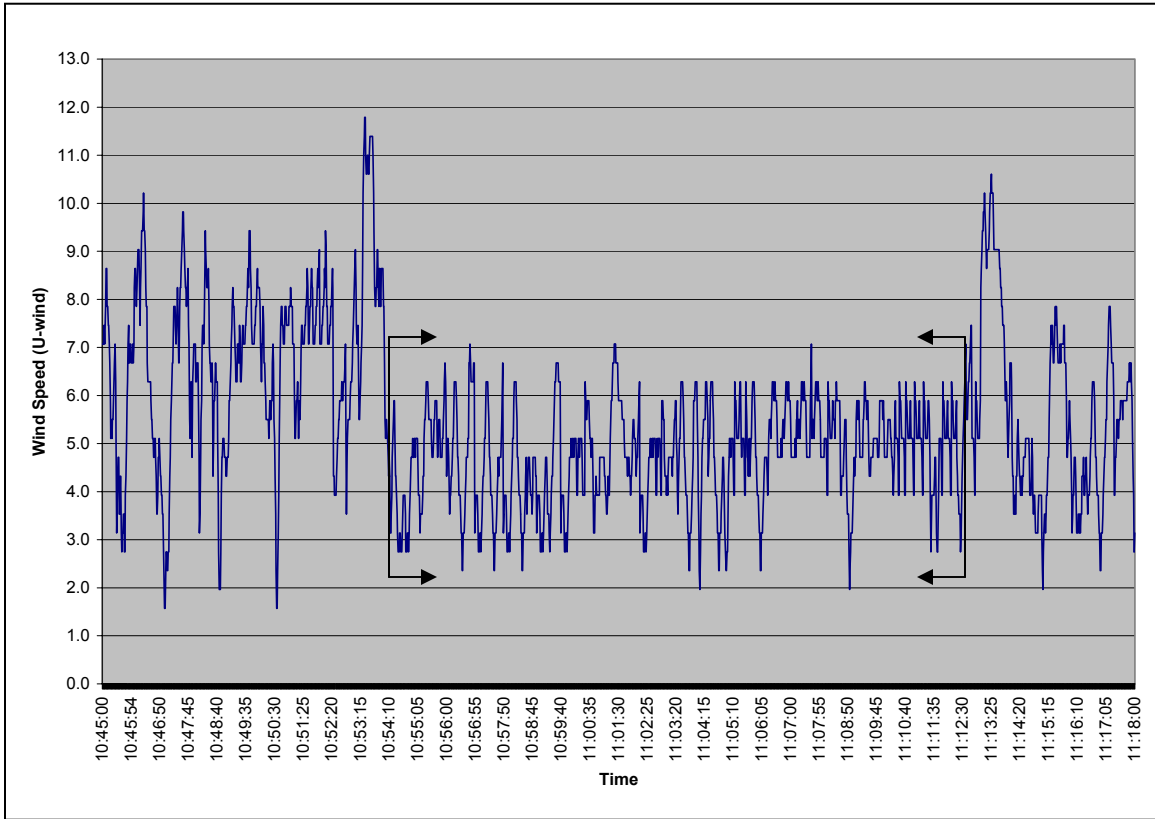


Figure 17: Time Series of Wind Speed with Time Selected Shown by Brackets (U-wind) in (mph)

Table 4: Number of Data Points Analyzed

	Downwind				Crosswind				Upwind			
	Date	Time	points	Lapse Rate	Date	Time	points	Lapse Rate	Date	Time	points	Lapse Rate
Sample 1	10/28	15:45-16:01	960	Normal	10/31	8:42-9:00	1080	Normal	11/10	10:35-10:50	900	Inversion
Sample 2	10/28	16:12-16:30	1080	Normal	10/31	9:10-9:25	900	Normal	11/10	10:55-11:12	1020	Inversion
Sample 3	10/28	16:33-16:53	1200	Normal	10/31	9:40-9:59	1140	Normal	11/10	11:17-11:33	960	Inversion
Sample 4	10/28	17:01-17:17	990	Normal	N/A	N/A	N/A	N/A	11/10	13:03	900	Normal
Sample 5	10/29	13:56-14:14	1080	Inversion	N/A	N/A	N/A	N/A	N/A	N/A	N/A	N/A
Sample 6	10/29	15:20-15:35	900	Normal	N/A	N/A	N/A	N/A	N/A	N/A	N/A	N/A

Downwind Group

The Downwind Group is the downwind condition (wind blowing from the source to the receivers). After plotting the wind speed component (U) versus time, six sample periods ranging from 15- 20 minutes were chosen because these six samples had the best cases where the downwind condition was apparent. Due to the time constraints on the equipment use and the loss of portable towers towards the end of the project, only these six samples were considered for this group. The U-wind component is the wind blowing in the same path as the sound propagation path from the source to the receivers. The summary of these six sample periods is shown in Table 5. For each sample the average and standard deviation is shown for the U, V, W anemometer directions described in the previous chapter. The U-wind direction is perpendicular to the propagation path and the wind will be cross-blowing (i.e. neither toward the source or the receivers). Thus, the effect of downwind or upwind refraction effects will be minimized. It should be noted that the larger the wind in this direction, the lower the effect of the downwind refraction effects.

The temperature measurements are shown in Table 6. The measured data indicates a downwind conditions and a strong lapse rate for all samples except Sample 5. These temperature data correspond to the same sampling periods chosen due to wind conditions. The average and standard deviation were derived and are shown for each sample. It should be noted that Sample 5 is an inversion case. The inversion case

corresponds to the strongest wind sample (Sample 5) within the downwind group. This case will be analyzed individually in an effort to better understand the impact on the wind refraction effects, and how the refraction effects for this case will differ from the other five samples.

Table 5: Summary of Wind Speed (mph) for Downwind Group

		Anemometer 20 ft (6 m)					Anemometer 5 ft (1.5 m)				
		U (mph)	V (mph)	W (mph)	Spd. (mph)	Angle °	U (mph)	V (mph)	W (mph)	Spd. (mph)	Angle °
Sample 1	<i>Avg</i>	2	5.4	-0.1	6.1	31	2.7	5.1	0.2	6	38
	<i>Stdv</i>	1.6	1.7	1	1.7	NE	1.4	1.5	0.6	1.7	NE
Sample 2	<i>Avg</i>	2.6	7.2	-0.3	8	31	2.4	6.4	0.2	7.2	34
	<i>Stdv</i>	1.8	2.1	1	2	NE	1.6	1.8	0.7	1.7	NE
Sample 3	<i>Avg</i>	2.6	8.5	-0.6	9.1	28	2.4	7.4	0.2	8	29
	<i>Stdv</i>	1.7	1.9	1	1.9	NE	1.4	1.6	0.7	1.5	NE
Sample 4	<i>Avg</i>	3.3	7.2	-0.5	8.3	35	3.4	6.5	0.1	7.5	37
	<i>Stdv</i>	1.8	2	1	1.8	NE	1.7	1.8	0.7	1.8	NE
Sample 5	<i>Avg</i>	5.7	7.3	-0.1	9.5	39	4.8	5.2	-0.1	7.3	43
	<i>Stdv</i>	1.7	2.2	0.9	1.8	NE	1.5	1.7	0.7	1.4	NE
Sample 6	<i>Avg</i>	4.4	7.2	0.2	8.7	32	3.6	5	0.1	6.4	36
	<i>Stdv</i>	1.6	2	1	1.9	NE	1.5	1.7	0.7	1.5	NE

Table 6: Summary of Temperature for Downwind Group

		Thermometer 20 ft (6m)		Thermometer 5 ft (1.5 m)		Lapse Rate
		°C	°F	°C	°F	°C / m
Sample 1	<i>Avg</i>	28.3	83.0	29.1	84.4	-0.175
	<i>Stdv</i>	0.1	0.1	0.0	0.0	N/A
Sample 2	<i>Avg</i>	28.2	82.7	28.7	83.7	-0.109
	<i>Stdv</i>	0.1	0.1	0.1	0.1	N/A
Sample 3	<i>Avg</i>	28.0	82.5	28.4	83.2	-0.087
	<i>Stdv</i>	0.1	0.1	0.1	0.1	N/A
Sample 4	<i>Avg</i>	27.9	82.2	28.0	82.4	-0.022
	<i>Stdv</i>	0.1	0.1	0.2	0.2	N/A
Sample 5	<i>Avg</i>	25.7	78.3	25.4	77.8	0.066
	<i>Stdv</i>	0.1	0.1	0.1	0.1	N/A
Sample 6	<i>Avg</i>	23.8	74.9	24.1	75.5	-0.066
	<i>Stdv</i>	0.0	0.0	0.0	0.0	N/A

As previously described, sound pressure level was measured using five microphone locations. Two microphones (Mic 1 and Mic 2) were positioned at 5 feet (1.5 m) above the ground at 440 feet (134 m) and 780 feet (238 m) from the center line of the roadway respectively. Another two microphones (Mic 3 and Mic 4) were positioned at 20 feet (6 m) above the ground at 440 feet (134 m) and 780 feet (238 m) from the center line of the roadway respectively. A Reference microphone (Ref) was positioned at 5 feet (1.5 m) above the ground at 75 feet (23 m) from the center line of the roadway. This position was selected because it was as close to the source (near lane) that could be selected without being in the near field. The corresponding measured sound levels for each octave band frequency for the six sample periods are shown in Table 7.

Table 7: Summary of Sound Levels (dB) for Downwind Group

		Frequency (Hz)							
		63	125	250	500	1k	2k	4k	8k
Sample 1	Ref	70.8	69.0	66.9	66.7	66.9	60.9	52.7	45.3
	Mic 1	65.5	62.0	52.1	51.0	53.4	47.3	39.4	38.7
	Mic 2	65.4	61.0	56.5	55.9	56.6	49.5	41.2	39.3
	Mic 3	63.5	59.5	48.3	46.3	52.6	44.6	36.8	38.2
	Mic 4	63.0	58.0	51.5	51.6	53.6	46.7	40.1	39.2
Sample 2	Ref	69.5	71.8	68.1	72.8	70.0	63.0	54.2	45.9
	Mic 1	64.3	63.6	53.0	52.9	54.0	48.3	39.4	38.7
	Mic 2	64.0	61.4	57.4	57.5	57.5	50.6	41.5	39.3
	Mic 3	63.0	62.6	52.4	48.9	53.4	45.8	37.0	38.2
	Mic 4	61.9	59.0	53.6	54.9	54.5	47.7	40.4	39.2
Sample 3	Ref	74.4	74.0	67.7	73.2	69.4	63.3	54.7	46.0
	Mic 1	67.2	63.2	53.1	53.3	54.3	48.9	40.5	38.7
	Mic 2	66.8	61.3	57.0	57.4	57.9	51.4	42.5	39.5
	Mic 3	65.4	61.5	51.8	50.0	53.6	46.4	37.6	38.2
	Mic 4	64.2	58.8	53.8	54.4	54.8	48.4	40.9	39.4
Sample 4	Ref	74.3	72.4	67.2	68.5	69.2	63.0	54.3	46.4
	Mic 1	72.4	61.9	51.2	51.6	54.5	48.3	39.6	38.8
	Mic 2	72.1	59.2	56.0	55.5	57.6	50.9	41.5	39.5
	Mic 3	68.8	59.4	48.3	47.8	53.9	46.0	36.8	38.2
	Mic 4	67.8	56.3	52.5	52.4	54.8	47.9	40.2	39.2
Sample 5	Ref	65.2	68.2	63.3	62.9	65.3	60.1	52.5	46.9
	Mic 1	60.3	58.3	49.3	46.4	50.3	44.2	37.6	38.8
	Mic 2	61.5	57.2	52.6	50.8	54.1	47.1	40.0	39.2
	Mic 3	59.3	57.0	48.2	42.7	49.9	42.8	35.9	38.2
	Mic 4	61.1	55.8	49.6	47.8	51.0	44.3	38.9	38.8
Sample 6	Ref	64.9	68.1	64.7	63.4	65.4	60.7	53.0	44.4
	Mic 1	59.3	66.0	52.7	47.7	50.9	44.8	37.2	38.6
	Mic 2	58.8	62.6	57.4	51.8	54.1	47.6	40.1	39.1
	Mic 3	60.0	61.3	49.3	44.9	50.9	43.7	36.8	38.2
	Mic 4	62.8	59.4	55.6	48.8	51.4	44.8	40.4	38.9

Crosswind Group

The Crosswind Group represents the cross-wind condition (i.e. V-wind) that is the wind is blowing perpendicular the propagation path of the sound from the source to the receivers. After plotting the wind speed and direction versus time, three sample periods were chosen. Again, only three samples have been chosen because these samples had the best cases where the U-wind component was small. Due to the time constraints on the equipment use and the loss of portable towers towards the end of the project, only these three samples were consistent with a low U-wind component. The summary of the three sample periods is shown in Table 8. For each sample the average and standard deviation is shown for U, V, W anemometer directions described in the previous chapter. The measured data indicates that on average the wind speed is lighter than the Downwind Group for all three samples, but the most important aspect is the U-wind is small. The summary of the temperature results are shown in Table 9. These temperature data correspond to the same sampling periods chosen by wind condition, and the average and standard deviation are shown for each sample.

Table 8: Summary of Wind Speed (mph) for Crosswind Group

		Anemometer 20 ft (6 m)					Anemometer 5 ft (1.5 m)				
		U (mph)	V (mph)	W (mph)	Spd. (mph)	Angle °	U (mph)	V (mph)	W (mph)	Spd. (mph)	Angle °
Sample 1	<i>Avg</i>	1.0	2.6	0.2	2.9	23	0.2	2.2	0.1	2.3	7
	<i>Stdv</i>	0.6	1.0	0.4	0.9	NNE	0.7	0.9	0.2	0.7	NNE
Sample 2	<i>Avg</i>	1.2	3.8	0.3	4.1	18	0.1	3.5	0.0	3.5	4
	<i>Stdv</i>	0.5	1.0	0.4	0.9	NNE	0.5	0.9	0.3	0.9	NNE
Sample 3	<i>Avg</i>	0.7	3.7	0.2	3.9	11	0.3	3.4	0.1	3.5	5
	<i>Stdv</i>	0.6	1.0	0.4	0.9	NNE	0.6	1.0	0.3	1.0	NNE

Table 9: Summary of Temperature for Crosswind Group

		Thermometer 20 ft (6 m)		Thermometer 5 ft (1.5)		Lapse Rate
		°C	°F	U	V	°C / m
Sample 1	<i>Avg</i>	21.6	70.9	22.3	72.1	-0.153
	<i>Stdv</i>	0.2	0.2	0.2	0.2	N/A
Sample 2	<i>Avg</i>	23.2	73.9	24.1	76.4	-0.197
	<i>Stdv</i>	0.2	0.2	0.2	0.2	N/A
Sample 3	<i>Avg</i>	25.3	77.6	26.4	79.6	-0.241
	<i>Stdv</i>	0.2	0.2	0.2	0.2	N/A

Sound pressure level was measured using the same five microphone locations as described before. The corresponding measured sound levels for each octave band frequency for the three samples are shown in Table 10.

Table 10: Summary of Sound Levels (dB) for Crosswind Group

		Frequency (Hz)							
		63	125	250	500	1k	2k	4k	8k
Sample 1	Ref	72.3	73.1	70.9	70.2	68.2	62.7	55.3	48.1
	Mic 1	68.0	63.3	54.5	52.4	53.4	50.5	42.8	39.4
	Mic 2	67.5	61.4	59.1	58.0	57.5	52.0	43.8	40.2
	Mic 3	64.6	59.9	50.6	44.3	49.7	47.5	39.2	38.8
	Mic 4	63.7	57.9	52.6	54.0	52.6	47.4	40.7	39.4
Sample 2	Ref	68.6	72.2	66.7	67.9	67.4	62.2	54.8	49.3
	Mic 1	66.1	59.7	50.1	48.4	50.7	45.7	41.7	39.6
	Mic 2	65.7	57.9	54.8	55.3	55.8	49.3	43.7	40.6
	Mic 3	62.1	56.7	46.7	42.1	48.1	44.3	37.4	39.0
	Mic 4	61.7	54.7	49.0	51.4	51.3	45.4	41.6	39.6
Sample 3	Ref	71.7	69.9	66.7	67.9	66.5	61.2	53.7	50.2
	Mic 1	67.2	59.5	51.1	48.6	49.6	45.6	42.8	41.7
	Mic 2	67.4	58.2	55.3	55.2	54.9	50.0	45.7	43.9
	Mic 3	61.9	56.8	47.6	41.8	46.0	42.8	37.7	38.6
	Mic 4	61.3	55.4	49.6	51.1	49.8	44.8	41.1	40.0

Upwind Group

The Upwind Group is the upwind condition (wind blowing from the receivers to the source). After plotting the wind speed and direction versus time, four sample periods were chosen. Again, only four samples could be chosen because these samples had the best cases where the upwind condition was apparent. Moreover, the upwind condition occurred only one day during the measurements periods. Due to the time constraints and the loss of portable towers towards the end of the project, only these four samples were considered. The summary of these four sample periods is shown in Table 11. For each sample the average and standard deviation is shown for U, V, W anemometer directions described in the previous chapter. The summary of the temperature results are shown in Table 12. The measured data indicates an upwind conditions and an inversion lapse rate, except Sample 4. This case (sample 4) is a normal lapse rate that will be analyzed individually in an effort to better understand the impact on the wind refraction effects, and how the refraction effects for this case will differ from the other three samples. These temperature data correspond to the same sampling periods chosen by wind condition, and the average and standard deviation are shown for each sample.

Table 11: Summary of Wind Speed (mph) for Upwind Group

		Anemometer 20 ft (6 m)					Anemometer 5 ft (1.5 m)				
		U (mph)	V (mph)	W (mph)	Spd. (mph)	Angle °	U (mph)	V (mph)	W (mph)	Spd. (mph)	Angle °
Sample 1	<i>Avg</i>	-9.4	0.6	0.2	9.4	274	-5.6	0.5	0.1	5.7	274
	<i>Stdv</i>	0.9	0.5	0.2	1	WNW	0.9	0.5	0.2	0.8	W
Sample 2	<i>Avg</i>	-7.3	1.4	0.1	7.5	281	-5.5	0.7	0.2	5.7	278
	<i>Stdv</i>	0.7	0.4	0.2	0.6	WNW	0.9	0.5	0.2	0.7	WNW
Sample 3	<i>Avg</i>	-3.3	4.2	0.2	5.5	318	-3.1	4.2	0.1	5.4	321
	<i>Stdv</i>	0.4	0.4	0.2	0.4	NW	0.5	0.4	0.2	0.5	Nw
Sample 4	<i>Avg</i>	-5.2	5	0.1	7.4	314	-4.3	4.6	0.2	6.6	316
	<i>Stdv</i>	0.9	1	0.5	0.7	NW	0.8	1	0.5	0.7	NW

Table 12: Summary of Temperature for Upwind Group

		Thermometer 20 ft (6 m)		Thermometer 5 ft (1.5 m)		Lapse Rate
		°C	°F	°C	°F	°C / m
Sample 1	<i>Avg</i>	28.6	83.5	27.7	81.9	0.197
	<i>Stdv</i>	0.0	0.0	0.2	0.1	N/A
Sample 2	<i>Avg</i>	28.5	83.3	27.5	81.5	0.219
	<i>Stdv</i>	0.1	0.1	0.1	0.1	N/A
Sample 3	<i>Avg</i>	28.0	82.5	27.7	81.8	0.066
	<i>Stdv</i>	0.0	0.0	0.0	0.0	N/A
Sample 4	<i>Avg</i>	28.2	82.7	29.5	85.1	-0.284
	<i>Stdv</i>	0.1	0.1	0.0	0.0	N/A

Sound pressure level was measured using the five microphone locations as described before. The corresponding measured sound levels for each octave band frequency for the six samples are shown in Table 13.

Table 13: Summary of Sound Power Levels (dB) for Upwind Group

		Frequency (Hz)							
		63	125	250	500	1k	2k	4k	8k
Sample 1	Ref	70.1	67.7	66.5	68.7	67.4	61.4	54.0	46.0
	Mic 1	61.1	56.7	47.2	44.2	45.9	41.6	38.0	38.8
	Mic 2	68.2	58.3	53.9	53.2	55.1	48.0	42.2	40.2
	Mic 3	65.8	54.3	47.1	38.2	44.1	38.8	36.0	38.3
	Mic 4	63.8	52.1	48.4	44.9	46.9	42.0	38.1	37.8
Sample 2	Ref	68.7	68.1	66.9	69.8	64.7	59.6	55.9	50.8
	Mic 1	61.2	56.6	48.6	45.4	45.5	42.2	37.3	38.7
	Mic 2	59.9	55.1	53.1	54.7	54.1	47.8	42.2	39.7
	Mic 3	57.7	51.8	43.2	38.0	42.0	37.7	35.7	38.1
	Mic 4	55.1	50.1	44.8	45.5	45.1	40.0	38.0	37.4
Sample 3	Ref	74.2	70.6	64.3	66.7	65.7	59.5	55.8	47.6
	Mic 1	64.1	57.9	49.4	47.9	48.8	45.5	43.5	39.4
	Mic 2	63.3	56.1	53.7	52.6	53.7	46.8	42.6	39.8
	Mic 3	60.9	53.6	45.0	40.3	43.7	40.2	38.6	38.1
	Mic 4	58.6	50.9	46.2	46.9	47.2	41.7	39.3	37.5
Sample 4	Ref	69.6	68.5	70.9	64.7	64.4	59.5	52.6	45.2
	Mic 1	65.9	55.8	50.2	44.4	47.1	43.9	41.2	38.9
	Mic 2	66.0	55.3	56.2	53.1	53.1	47.1	42.7	39.5
	Mic 3	63.5	53.7	45.0	39.6	43.6	39.4	35.9	38.2
	Mic 4	61.8	51.6	47.7	45.6	46.5	41.5	38.4	37.3

The sound levels for all three groups are summarized and A-weighted values of the samples for each group have been computed and are shown in Tables 14-16.

Sample 5 in Table 14 represents the only inversion lapse rate case within the downwind group (temperature increase with height). Sample 5 has strong wind conditions leading to greater wind shear, and it was expected to increase sound level even more because of the inversion lapse rate that occurred during this sample period.

Moreover, the lower microphone locations Mic 1 and Mic 2 seem to have been affected by different ground effects when compared to the other five sample periods. This might be due to different incident angle to the ground caused by the combination of downwind and inversion conditions.

Sample 4 in Table 16 represents the only normal lapse rate case within the upwind group. All other sample periods occur during inversion (negative lapse rate). The effect of upwind conditions and normal lapse rate in this case was expected to increase sound levels at the higher microphone locations. However, the data show that the difference in sound levels between the upper and lower microphone locations were comparable to the other three sample periods. The difference for Sample 4 was 5.2 dB(A), while the difference for the other 3 samples was 5.8 dB(A). Moreover, the sound level at the lower microphone locations Mic 1 and Mic 2 seem to have increased by 0.5 dB(A), this is likely due different ground effects.

Figure 18 illustrates the average of the measured sound levels for each of three groups. It is shown that there is small variation at the Reference microphone which is expected because this measurement location was very close to the source where attenuation refraction effects would be small. Moreover, Figure 18 shows that the Upwind Group sound levels are lower than the other two groups for all microphone positions, which is also expected since during upwind conditions, the wind tend to bend the sound waves upward hence reducing sound level at the microphones. Downwind values are always greater than upwind.

The finding that the Reference microphone has minimal refraction effects reinforces the assumption that the Reference microphone would not be affected by refraction effects. This helps to show that this assumption in normalization of the data in order to account for refraction effects between Reference and other microphone locations was justified.

Table 14: Downwind Group Sound Pressure Levels dB(A)

	Sample 1	Sample 2	Sample 3	Sample 4	Sample 5	Sample 6	Average
Ref	69.9	73.7	73.7	72.0	68.0	68.4	71.0
Mic 1	56.4	57.3	57.7	57.4	53.2	55.2	56.2
Mic 2	54.6	55.9	56.1	55.9	52.2	53.5	54.7
Mic 3	59.4	60.5	60.8	60.2	56.5	57.4	59.1
Mic 4	56.2	57.7	57.8	57.3	53.6	54.8	56.2

Table 15: Crosswind Group Sound Pressure Levels dB(A)

	Sample 1	Sample 2	Sample 3	Average
Ref	72.3	70.8	70.2	71.1
Mic 1	57.7	54.3	54.2	55.4
Mic 2	53.9	51.5	50.4	51.9
Mic 3	61.1	58.8	58.7	59.5
Mic 4	56.4	54.7	53.9	55.0

Table 16: Upwind Group Sound Pressure Levels dB(A)

	Sample 1	Sample 2	Sample 3	Sample 4	Average
Ref	70.8	70.1	69.2	68.7	69.7
Mic 1	50.3	50.4	53.4	51.8	51.5
Mic 2	48.6	46.4	48.4	48.0	47.9
Mic 3	57.8	57.4	56.6	56.7	57.1
Mic 4	50.7	49.1	50.8	50.3	50.2

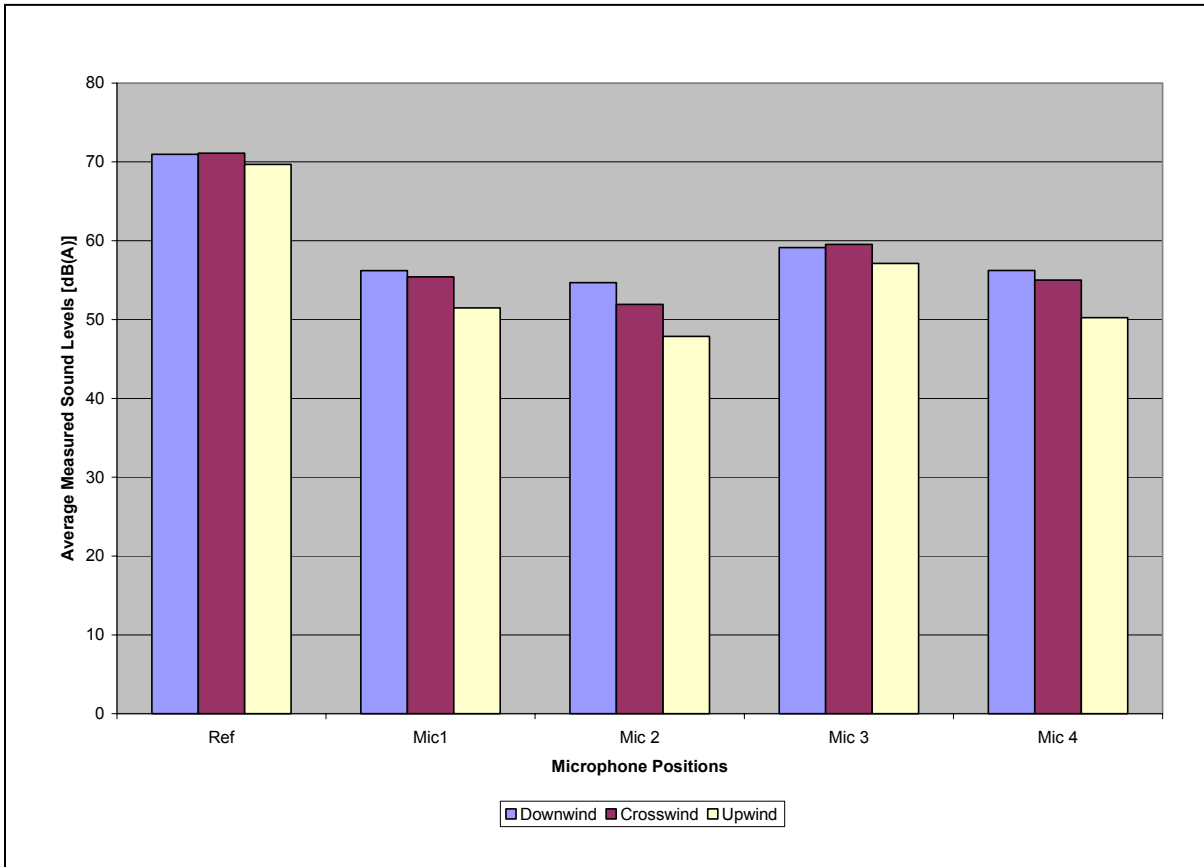


Figure 18: Comparison of Measured Sound Levels for Each of the Three Groups dB(A)

From these measurements, it was apparent that a detailed comparison was needed which is shown hereafter. Table 17 and Figure 19 show the difference in sound levels between the Reference and the microphone locations Mic 1, Mic 2, Mic 3 and Mic 4. The data illustrate larger difference between Reference and the microphone locations for the Upwind Group than the Downwind and Crosswind Groups. This information follows expected trends that during upwind conditions (Upwind Group), the sound waves tend to bend upwards and the acoustic energy is redirected. This results in reduced sound levels at the microphone locations as compared to the Reference and the microphone locations. During downwind conditions (Downwind Group) the sound waves should bend downward due to wind shear thus increasing the sound levels at the microphone locations. Hence, the difference between the Reference and the microphone locations has decreased.

Table 17: Difference in Sound Levels between Ref and Microphones dB(A)

Groups	Difference Ref- Mic 1	Difference Ref- Mic 2	Difference Ref- Mic 3	Difference Ref- Mic 4
Downwind	14.8	16.3	11.8	14.7
Crosswind	15.7	19.2	11.6	16.1
Upwind	18.2	21.9	12.6	19.5

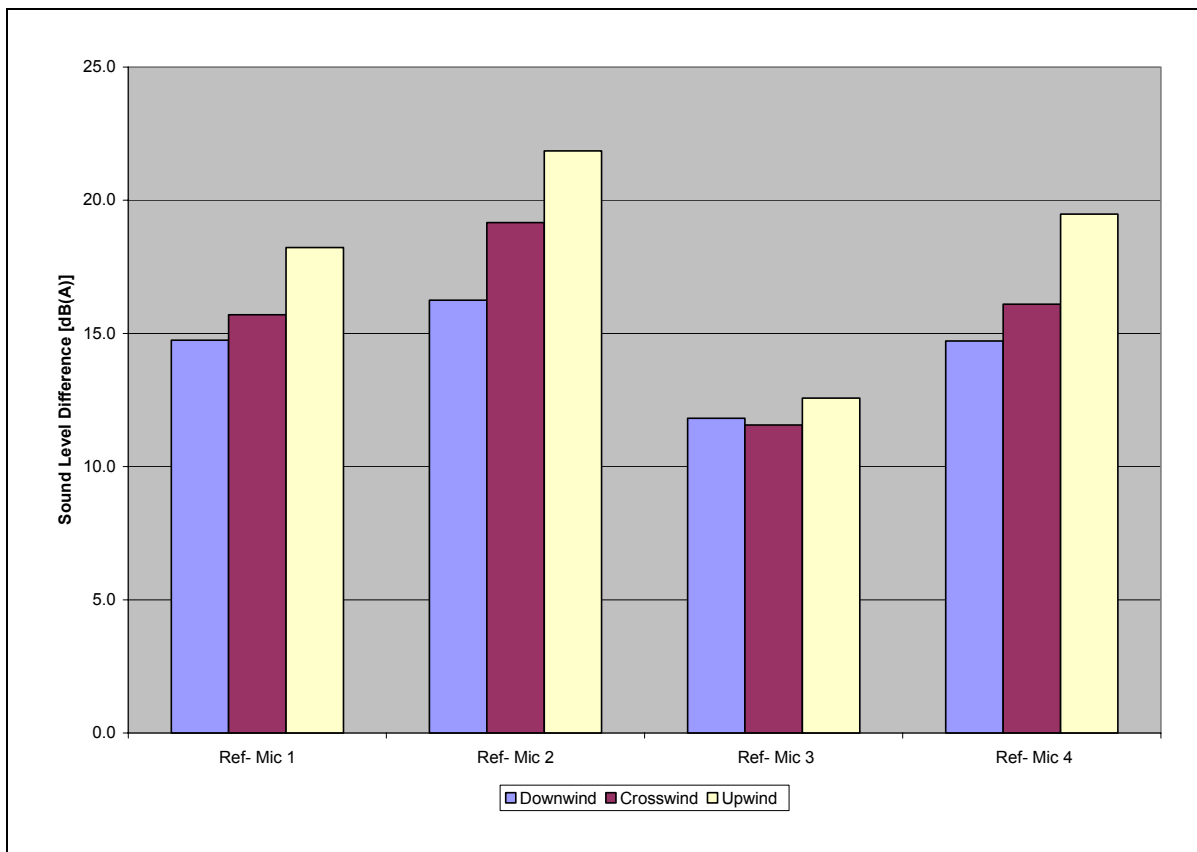


Figure 19: Difference in Sound Level between Ref and Microphones dB(A)

As would be expected, the difference in sound level between the Reference and microphone locations for each of Mic 2 and Mic 4 is larger than the difference in sound level between the Reference and microphone locations for each of Mic 1 and Mic 3 respectively. This is due to a geometric spreading and a reduction in sound levels at the further microphone locations (i.e. Mic 2 and Mic 4) as we move away from the source. However, this difference on average of 3 dB(A) might not be attributed only to distance

and might also include attributable to ground effects interaction as at great distance from the source.

Table 18 and Figure 20 show the difference between the sound levels of Mic 1 and Mic 2 (the position closest to the ground) for Downwind Group is 1.5 dB(A), which is lower than the 3.5 dB(A) and 3.6 dB(A) for the same microphones for both the Crosswind and Upwind Groups respectively. This information most likely is a function of the interaction of the downwind conditions causing the sound waves to bend downwards and the ground effects changing accordingly as the incident wave angle to the ground changes. This angle is affected by wind shear and lapse rate variations between the three groups. Hence, these effects may have tended to reduce the difference between the two microphones at ground level for the Downwind Group more than in the Crosswind and the Upwind Groups respectively.

Table 18: Difference in Sound Pressure Levels between Microphones dB(A)

	Mic 1- Mic 2	Mic 3- Mic 4
Downwind	1.5	2.9
Crosswind	3.5	4.5
Upwind	3.6	6.9

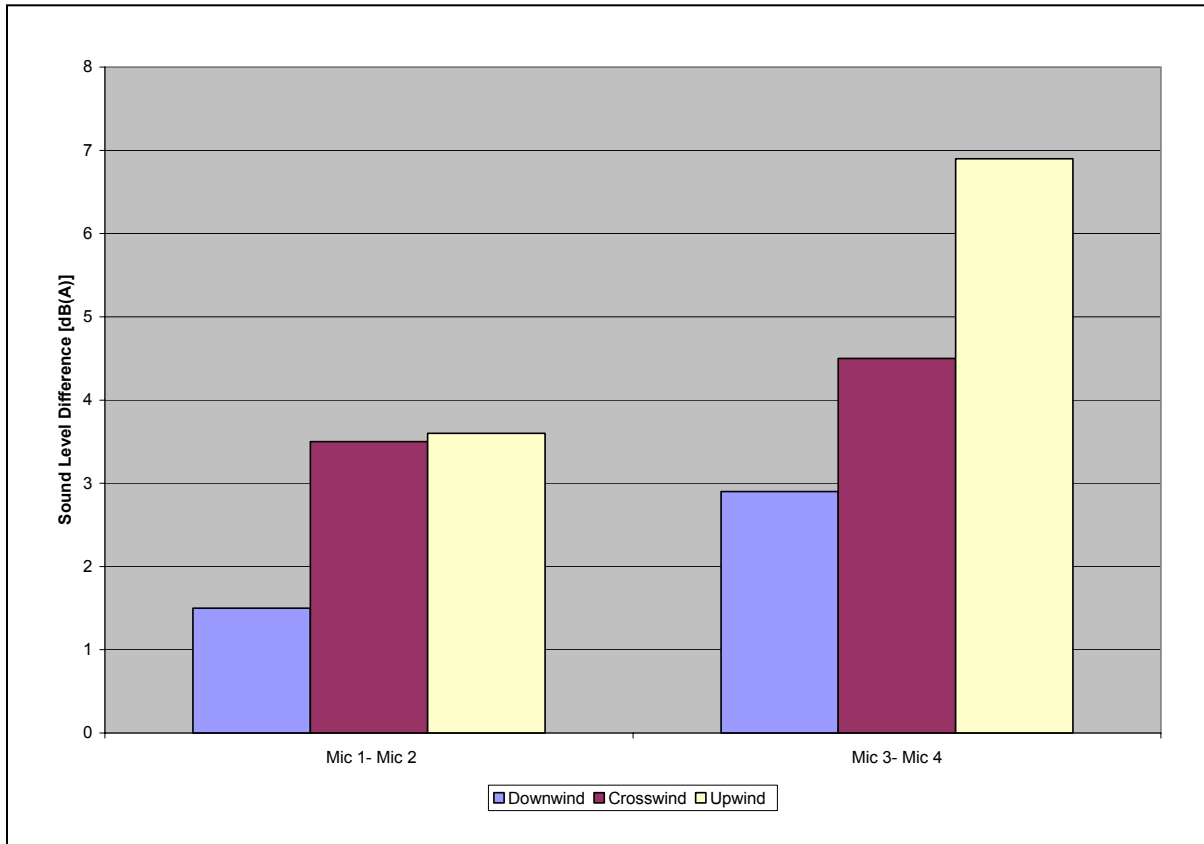


Figure 20: Difference in Sound Level between Microphones dB(A)

The difference between the sound levels of Mic 3 and Mic 4 (at the higher position) for Downwind Group is 2.9 dB(A), which is lower than the 4.5 dB(A) and 6.9 dB(A) for the same microphones for both the Crosswind and Upwind Groups respectively. Just as the other microphone positions, this information reinforces the theory of refraction effects for the downwind conditions the waves are bend downwards and in upwind conditions the sound waves bends upwards.

It should be noted that the source (i.e. highway) was elevated. The highway was 25 feet (7.6 m) higher than the ground level. This location was selected partially due to

this reason because ground effects are significantly reduced. This allowed a greater effort to be applied in calculating refraction effects although it is obvious ground effects provide significant effects which had to be taken in account during the final analysis.

ISO 9613-2

The ISO 9613-2 specifies an engineering method for calculating the attenuation of sound during propagation outdoors in order to predict the sound level at a distance from a variety of sources. The basic equation used in modeling is Equation 42 which was detailed in the previous chapter literature review. Other alternatives for predicting outdoor propagation, CONCAWE and NORD2000 were not evaluated since there was too little literature reported. The ISO 9613-2 method is still the most accepted for predicting outdoor sound propagation.

The main attenuation parameters included are: attenuation due to divergence (A_{div}), attenuation due to atmospheric absorption (A_{atm}), and attenuation due to ground effects (A_{gr}). A_{div} is based on the basic equation for point source attenuation as was previously illustrated in Equation 44. A_{atm} is based on atmospheric attenuation coefficient “ α ” which is dependent on temperature and relative humidity. The “ α ” values are listed in the ISO 9613-1 that covers a range of temperature from -20°C (-4°F) to 50°C (122°F) for a range of humidity from 10% to 100%. A_{gr} consists of three regions; the first is the ground attenuation within the source region (A_s), the second is the ground attenuation within the receiver region (A_r) and the third is the ground attenuation within the middle region (A_m). The source and receiver regions are a function of 30 times the source and receivers heights respectively. The middle region is the distance between the source and

receiver regions. In this research, the ISO method ground effect correction was set to zero.

Tables 19-21 present the calculated attenuation in dB, based on Equation 42, for each microphone position of the three groups Downwind, Crosswind, and Upwind. Afterward, a summary of the sound levels predicted by the ISO9613-2 method is shown for each group and a comparison to the measured sound levels for each microphone evaluated.

Table 19: Attenuation (dB) for Microphones in Downwind Group

Attenuation		Frequency (Hz)							
		63	125	250	500	1k	2k	4k	8k
Mic 1	A _{div}	7.7	7.7	7.7	7.7	7.7	7.7	7.7	7.7
	A _{atm}	0.0	0.0	0.2	0.5	0.9	1.6	3.3	9.8
	A _{gr}	-5.0	1.3	14.6	17.7	5.3	0.0	0.0	0.0
	Sum	2.7	9.1	22.4	25.8	13.9	9.3	11.0	17.5
Mic 2	A _{div}	10.2	10.2	10.2	10.2	10.2	10.2	10.2	10.2
	A _{atm}	0.0	0.1	0.3	0.8	1.7	2.8	5.8	17.4
	A _{gr}	-5.4	2.5	15.5	18.8	5.6	0.0	0.0	0.0
	Sum	4.8	12.7	26.0	29.8	17.5	13.0	16.0	27.5
Mic 3	A _{div}	7.7	7.7	7.7	7.7	7.7	7.7	7.7	7.7
	A _{atm}	0.0	0.0	0.2	0.5	0.9	1.6	3.3	9.8
	A _{gr}	-3.0	3.1	8.3	13.0	4.7	0.0	0.0	0.0
	Sum	4.7	10.8	16.2	21.2	13.3	9.3	11.0	17.5
Mic 4	A _{div}	10.2	10.2	10.2	10.2	10.2	10.2	10.2	10.2
	A _{atm}	0.0	0.1	0.3	0.8	1.7	2.8	5.8	17.4
	A _{gr}	-3.7	6.1	8.9	13.9	5.0	0.0	0.0	0.0
	Sum	6.5	16.4	19.3	24.9	16.8	13.0	16.0	27.5

Table 20: Attenuation (dB) for Microphones in Crosswind Group

Attenuation		Frequency (Hz)							
		63	125	250	500	1k	2k	4k	8k
Mic 1	A _{div}	7.7	7.7	7.7	7.7	7.7	7.7	7.7	7.7
	A _{atm}	0.0	0.0	0.2	0.4	0.8	1.4	3.1	9.8
	A _{gr}	-5.0	1.3	14.6	17.7	5.3	0.0	0.0	0.0
	Sum	2.7	9.1	22.4	25.8	13.8	9.1	10.8	17.5
Mic 2	A _{div}	10.2	10.2	10.2	10.2	10.2	10.2	10.2	10.2
	A _{atm}	0.0	0.1	0.3	0.8	1.4	2.4	5.5	17.5
	A _{gr}	-5.4	2.5	15.5	18.8	5.6	0.0	0.0	0.0
	Sum	4.8	12.7	25.9	29.7	17.2	12.6	15.7	27.6
Mic 3	A _{div}	7.7	7.7	7.7	7.7	7.7	7.7	7.7	7.7
	A _{atm}	0.0	0.0	0.2	0.4	0.8	1.4	3.1	9.8
	A _{gr}	-3.0	3.1	8.3	13.0	4.7	0.0	0.0	0.0
	Sum	4.7	10.8	16.2	21.2	13.1	9.1	10.8	17.5
Mic 4	A _{div}	10.2	10.2	10.2	10.2	10.2	10.2	10.2	10.2
	A _{atm}	0.0	0.1	0.3	0.8	1.4	2.4	5.5	17.5
	A _{gr}	-3.7	6.1	8.9	13.9	5.0	0.0	0.0	0.0
	Sum	6.5	16.4	19.3	24.8	16.5	12.6	15.7	27.6

Table 21: Attenuation (dB) for Microphones in Upwind Group

Attenuation		Frequency (Hz)							
		63	125	250	500	1k	2k	4k	8k
Mic 1	A _{div}	7.7	7.7	7.7	7.7	7.7	7.7	7.7	7.7
	A _{atm}	0.0	0.0	0.2	0.5	0.9	1.6	3.3	9.8
	A _{gr}	-5.0	1.3	14.6	17.7	5.3	0.0	0.0	0.0
	Sum	2.7	9.1	22.4	25.8	13.9	9.3	11.0	17.5
Mic 2	A _{div}	10.2	10.2	10.2	10.2	10.2	10.2	10.2	10.2
	A _{atm}	0.0	0.1	0.3	0.8	1.7	2.8	5.8	17.4
	A _{gr}	-5.4	2.5	15.5	18.8	5.6	0.0	0.0	0.0
	Sum	4.8	12.7	26.0	29.8	17.5	13.0	16.0	27.5
Mic 3	A _{div}	7.7	7.7	7.7	7.7	7.7	7.7	7.7	7.7
	A _{atm}	0.0	0.0	0.2	0.5	0.9	1.6	3.3	9.8
	A _{gr}	-3.0	3.1	8.3	13.0	4.7	0.0	0.0	0.0
	Sum	4.7	10.8	16.2	21.2	13.3	9.3	11.0	17.5
Mic 4	A _{div}	10.2	10.2	10.2	10.2	10.2	10.2	10.2	10.2
	A _{atm}	0.0	0.1	0.3	0.8	1.7	2.8	5.8	17.4
	A _{gr}	-3.7	6.1	8.9	13.9	5.0	0.0	0.0	0.0
	Sum	6.5	16.4	19.3	24.9	16.8	13.0	16.0	27.5

The different attenuation factors vary depending on distance between receivers and the source within each group as can be expected using Equations 43-45. Comparing the attenuation between the different groups, it can be determined that the attenuation factor (α value) within the atmospheric absorption A_{atm} term changes very little for the sample groups. Changes among the frequencies ranged only 1% to 10% for the different groups. This is due to the small change in temperatures and relative humidity for the days included in this study.

Downwind Group

For the analysis, the first step was to determine adjustments for propagation effects calculated by the ISO method. This was done by summing all the attenuation factors presented in Table 19. Then, A-weighted adjustments were applied for each corresponding frequency band and subtracted from the measured sound levels at the Reference microphone (Ref.) to calculate the predicted sound levels for the different microphone locations: Mic 1, Mic 2, Mic 3 and Mic 4.

Table 22 and Figure 21 show the measured sound levels dB(A), the predicted sound levels dB(A) using the ISO 9613-2 method and the difference between the two methods for each microphone within the Downwind Group. The last part of the table shows the average of the six samples within the Downwind Group, and highlights the

average difference between measured and predicted sound levels for the various microphones. It can be seen that the average error for all samples is within 2 dB(A).

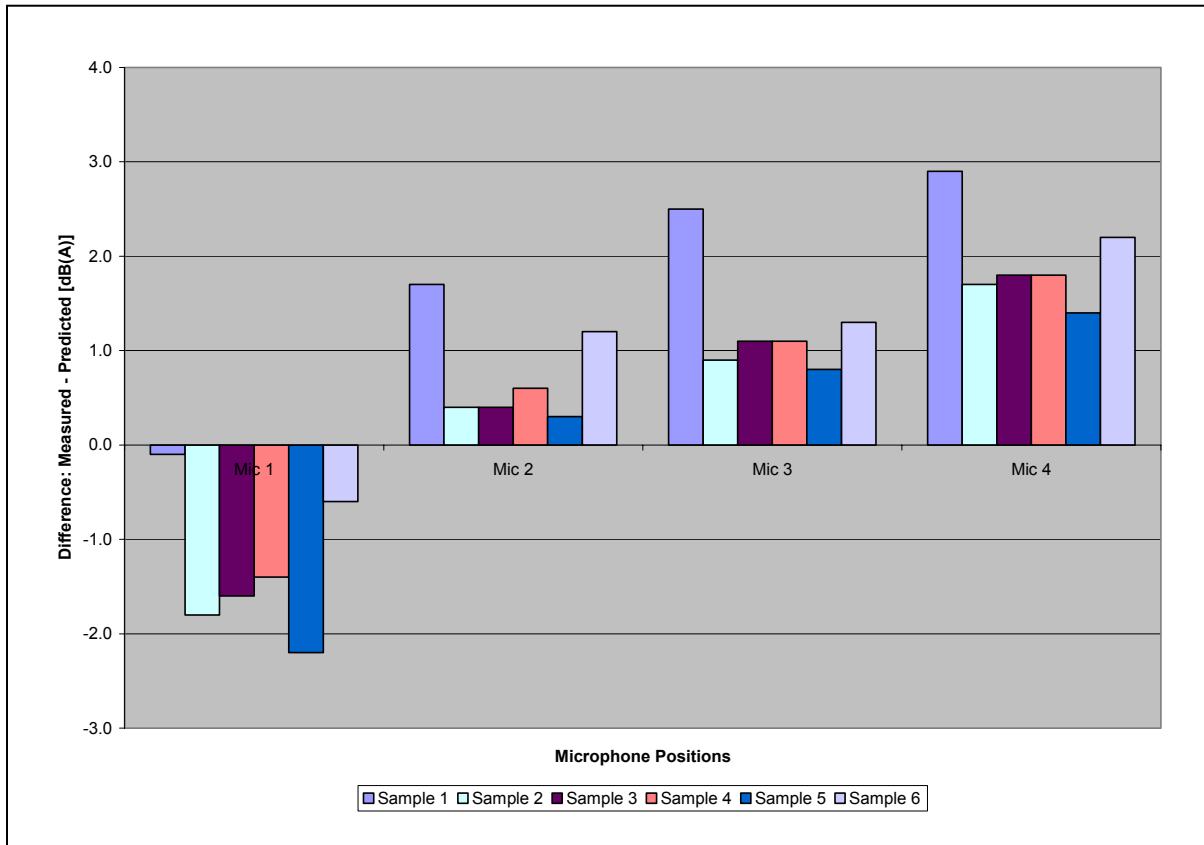


Figure 21: Difference Between Measured and Predicted Sound Levels for Downwind Group

Table 22: Difference between Measured and Predicted Sound levels dB(A)

		Measured	ISO	Difference
Sample 1	Ref	69.9	69.9	0.0
	Mic 1	56.4	56.5	-0.1
	Mic 2	54.6	52.9	1.7
	Mic 3	59.4	56.9	2.5
	Mic 4	56.2	53.3	2.9
Sample 2	Ref	73.7	73.7	0.0
	Mic 1	57.3	59.1	-1.8
	Mic 2	55.9	55.5	0.4
	Mic 3	60.5	59.6	0.9
	Mic 4	57.7	56.0	1.7
Sample 3	Ref	73.7	73.7	0.0
	Mic 1	57.7	59.3	-1.6
	Mic 2	56.1	55.7	0.4
	Mic 3	60.8	59.7	1.1
	Mic 4	57.8	56.0	1.8
Sample 4	Ref	72.0	72.0	0.0
	Mic 1	57.4	58.8	-1.4
	Mic 2	55.9	55.3	0.6
	Mic 3	60.2	59.1	1.1
	Mic 4	57.3	55.5	1.8
Sample 5	Ref	68.0	68.0	0.0
	Mic 1	53.2	55.4	-2.2
	Mic 2	52.2	51.9	0.3
	Mic 3	56.5	55.7	0.8
	Mic 4	53.6	52.2	1.4
Sample 6	Ref	68.4	68.4	0.0
	Mic 1	55.2	55.8	-0.6
	Mic 2	53.5	52.3	1.2
	Mic 3	57.4	56.1	1.3
	Mic 4	54.8	52.6	2.2
Average	Ref	71.0	71.0	0.0
	Mic 1	56.2	57.5	-1.3
	Mic 2	54.7	53.9	0.8
	Mic 3	59.1	57.9	1.3
	Mic 4	56.2	54.3	2.0

It should be noted that the predicted sound levels for the ISO method do not include any attenuation factors based on refraction. Comparing the measured and predicted values from the ISO method shows that on average the ISO method is over-predicting for Mic 1, while under-predicting for Mic 2, Mic 3 and Mic 4. Furthermore, it is presented that the difference between measured and predicted sound levels increased with the receivers that are the furthest from the source indicating the increased prediction error with distance. In downwind conditions the sound waves should bend downward towards the ground, thus increasing the sound levels above the normal levels. This should be even more apparent in Sample 5 due to the occurrence of the inversion which tends to bend the sound waves downward as well. The downward refraction effects are more noticeable in the increased difference at Mic 3 and Mic 4 where the differences in ground effects seem to be important. Of interest is Sample 5, where there is a combination between a strong wind condition and inversion. This case has shown that inversion lapse rate has amplified the downward wind refraction effects as shown by the reduction in the sound level difference between the Reference microphone and the other microphone location to be 14dB(A) compared to an average of 16 dB(A) for the other sample periods. Also, the inversion has most likely caused the ground effects to vary from the other sample periods within the group. This would result in increased sound levels for the microphone positions, and hence reducing the difference between measured and predicted sound levels when compared to other sample periods as shown in Figure 21. Furthermore, the ISO method seems to be over predicting for Mic 1, this is likely due to

diffraction effects at the edge of the road, which was not modeled, thus providing shielding and reducing measured sound level at Mic 1.

Crosswind Group

Table 23 and Figure 22 present the measured sound levels dB(A), the predicted sound levels dB(A) using the ISO 9613-2 method and the difference between the two methods for each microphone within the Crosswind Group. The last part of the table shows the average of the three samples within the Crosswind Group, and highlights the average difference between measured and predicted sound levels for the various microphones. It can be seen that the average error for all sample ranges from -2.3 to 1.5 dB(A).

Table 23: Difference between Measured and Predicted Sound levels dB(A) for Crosswind Group

		Measured	ISO	Difference
Sample 1	Ref	72.3	72.3	0.0
	Mic 1	57.7	58.5	-0.8
	Mic 2	53.9	55.0	-1.1
	Mic 3	61.1	58.9	2.2
	Mic 4	56.4	55.4	1.0
Sample 2	Ref	70.8	70.8	0.0
	Mic 1	54.3	57.7	-3.4
	Mic 2	51.5	54.2	-2.7
	Mic 3	58.8	58.0	0.8
	Mic 4	54.7	54.4	0.3
Sample 3	Ref	70.2	70.2	0.0
	Mic 1	54.2	56.8	-2.6
	Mic 2	50.4	53.3	-2.9
	Mic 3	58.7	57.2	1.5
	Mic 4	53.9	53.6	0.3
Average	Ref	71.1	71.1	0.0
	Mic 1	55.4	57.7	-2.3
	Mic 2	51.9	54.2	-2.2
	Mic 3	59.5	58.0	1.5
	Mic 4	55.0	54.5	0.5

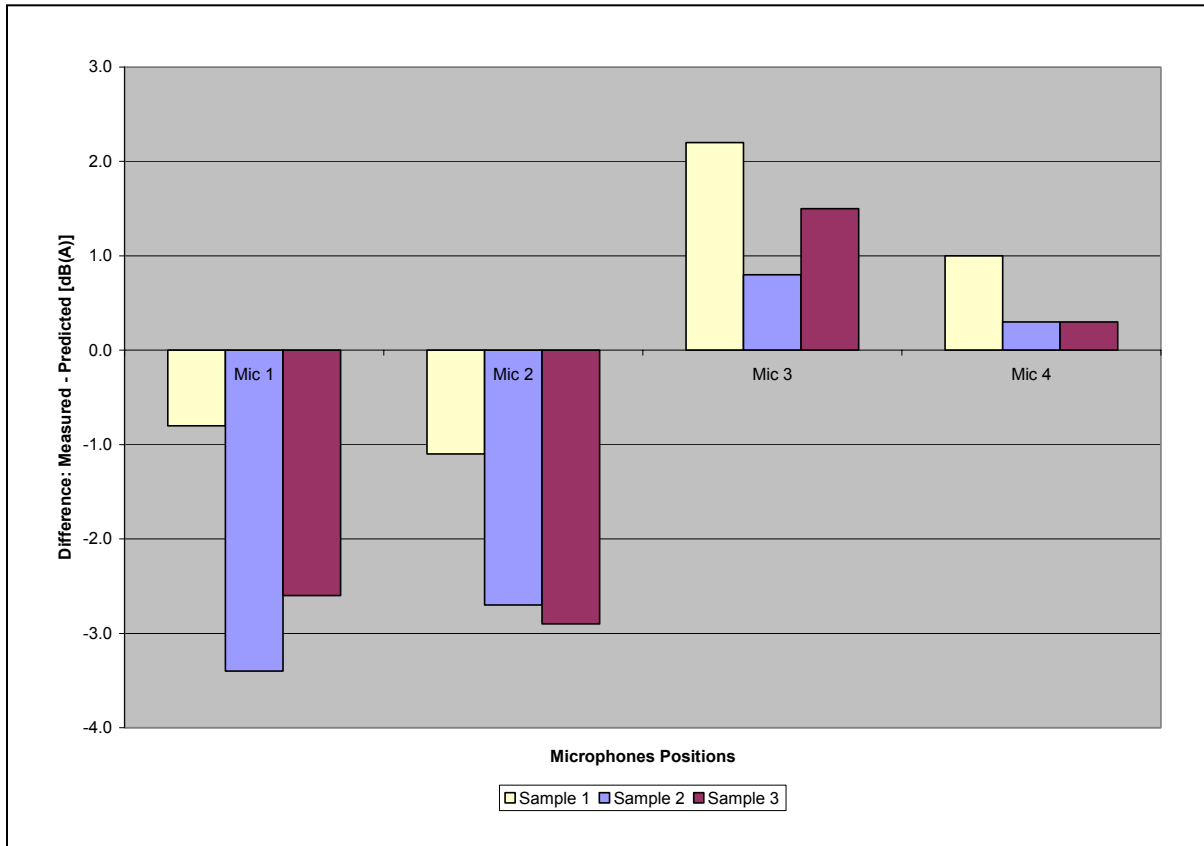


Figure 22: Difference Between Measured and Predicted Sound Levels for Crosswind Group

As previously noted, the above predicted sound levels, using ISO 9613, do not include any attenuation factors based on refraction. It is shown that on average the ISO method is over-predicting for Mic 1 and Mic 2, while under-predicting for Mic 3 and Mic 4. Crosswind conditions are wind that blows perpendicular to the propagation path between the source and the receivers. Also, the main aspect is that U-wind component is small, thus refraction effects is minimal. Of note is that the difference between measured and predicted sound levels decreased with the receivers that are the furthest from the source. This was not the trend in the Downwind Group but expected here for the

Crosswind Group. The sound waves propagation is not affected as much by refraction where it is less prone to waves being forced to bend either downward or upward due to wind shear. Moreover, lapse rate effects might still be present and might contribute to downward bending occurring in all sample periods.

Upwind Group

Table 24 and Figure 23 present the difference between the measured sound levels dB(A) and the predicted sound levels dB(A) using the ISO 9613-2 method for the Upwind Group. The last part of the table shows the average of the four samples within the Upwind Group, and highlights the average difference between measured and predicted sound levels for the various microphones. It is shown that on average the difference is within 4.4 dB(A).

Table 24: Difference between Measured and Predicted Sound levels dB(A) for Upwind Group

		Measured	ISO	Difference
Sample 1	Ref	70.8	70.8	0.0
	Mic 1	50.3	57.0	-6.7
	Mic 2	48.6	53.3	-4.7
	Mic 3	57.8	57.4	0.4
	Mic 4	50.7	53.8	-3.1
Sample 2	Ref	70.1	70.1	0.0
	Mic 1	50.4	55.3	-4.9
	Mic 2	46.4	51.6	-5.2
	Mic 3	57.4	55.9	1.5
	Mic 4	49.1	52.1	-3.0
Sample 3	Ref	69.2	69.2	0.0
	Mic 1	53.4	56.0	-2.6
	Mic 2	48.4	52.5	-4.1
	Mic 3	56.6	56.2	0.4
	Mic 4	50.8	52.5	-1.7
Sample 4	Ref	68.7	68.7	0.0
	Mic 1	51.8	55.0	-3.2
	Mic 2	48.0	51.3	-3.3
	Mic 3	56.7	55.5	1.2
	Mic 4	50.3	51.9	-1.6
Average	Ref	69.7	69.7	0.0
	Mic 1	51.5	55.8	-4.4
	Mic 2	47.9	52.2	-4.3
	Mic 3	57.1	56.3	0.9
	Mic 4	50.2	52.6	-2.3

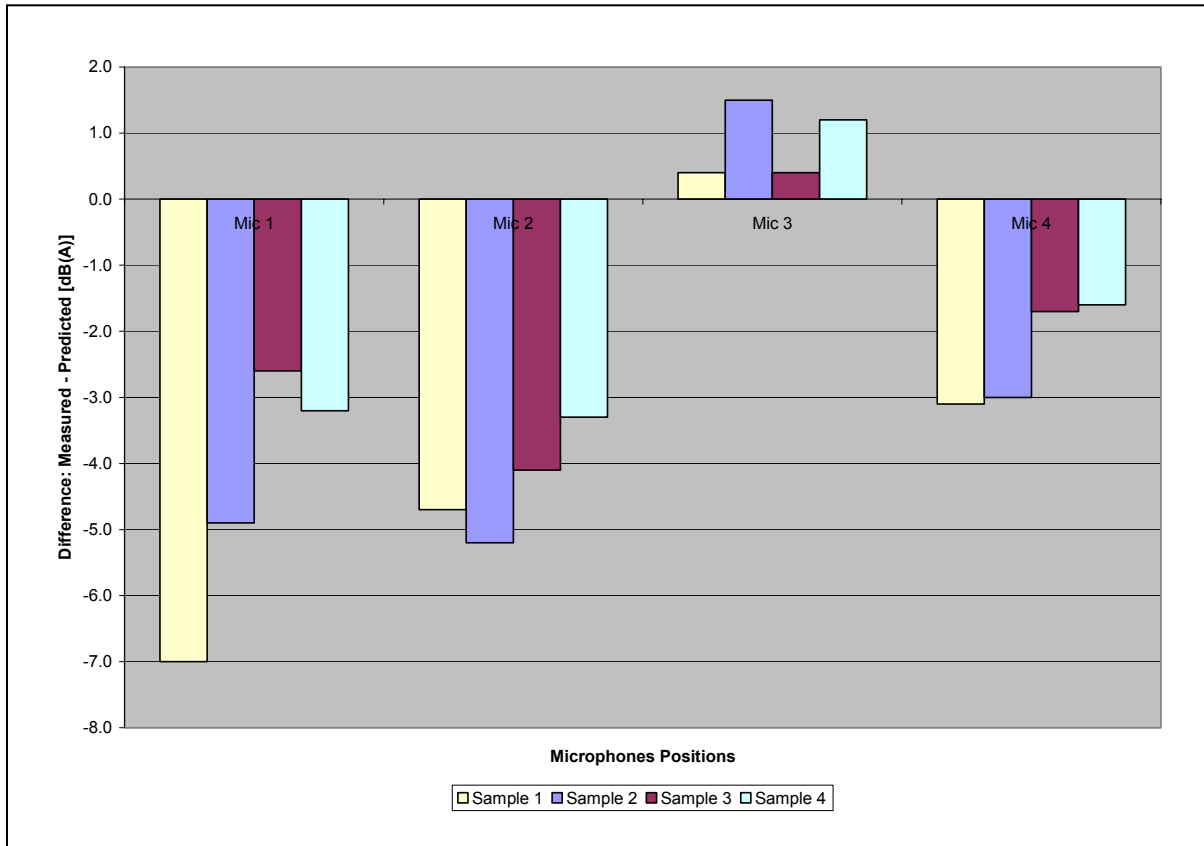


Figure 23: Difference Between Measured and Predicted Sound Levels for Upwind Group

Again, the sound levels do not include any attenuation factors based on refraction. It is shown that on average the ISO method is generally over-predicting for Mic 1, Mic 2 and Mic 4, while the method is under-predicting for Mic 3. The ISO 9613-2 method was developed to predict sound levels in downwind conditions. In upwind conditions sound waves should bend upward away from the ground, thus decreasing the sound levels below the normal levels. The sound waves bending upward are noticeable in the increased difference at Mic 1 and Mic 2 due both to refraction and ground effects affecting the sound levels as shown by the increased sound levels at the higher

microphone locations. Moreover, inversion lapse rates have occurred for Samples 1 – 3, which should have increased the sound levels at the lower microphone positions. However, the upward refraction effect from the wind shear would appear to be more dominant than the inversion lapse rate effect because of the large difference, 5 dB(A) for the Upwind Group compared to 2 dB(A) for the Downwind and Crosswind Groups, between measured and predicted sound at Mic 1 and Mic 2 near the ground which seems to indicate that the inversions lapse rate were negated by the upward refraction effects. In Sample 4, the normal lapse rate case should have increased the sound levels at the higher microphone locations; and this was amplified by the dominant upward refraction effects. This was shown by the reduction in the difference between measured and predicted sound levels for Sample 4 when compared to other sample periods as shown in Figure 23.

Summary

Table 25 and Figure 24 show the average difference in sound levels between the Reference and the microphone locations Mic 1, Mic 2, Mic 3 and Mic 4. The data illustrate small difference between the three groups when calculating the difference between the Reference and the microphone locations. This information demonstrates that the ISO method is treating all groups the same way. It should be noted that no correction

based on atmospheric conditions are included and as such the ISO method used does not account for refraction effects.

The average sound levels difference between the Reference and the microphone positions is almost the same for the lower and higher microphone locations at each tower. This is due to the fact that ISO 9613-2 method assumes that for soft ground effects correction is equal to zero in the middle region between the source and the receiver regions. Hence, the predicted ground effects are similar for the higher and lower microphone positions and only distances seems to make a difference. In reality, this is not the case for the measurements were the ground effects are different for the different heights.

Table 25: Average Difference Between Reference and Microphone Positions dB(A)

	Ref- Mic 1	Ref- Mic 2	Ref- Mic 3	Ref- Mic 4
Downwind	13.5	17.0	13.1	16.7
Crosswind	13.4	16.9	13.1	16.6
Upwind	13.8	17.5	13.5	17.1

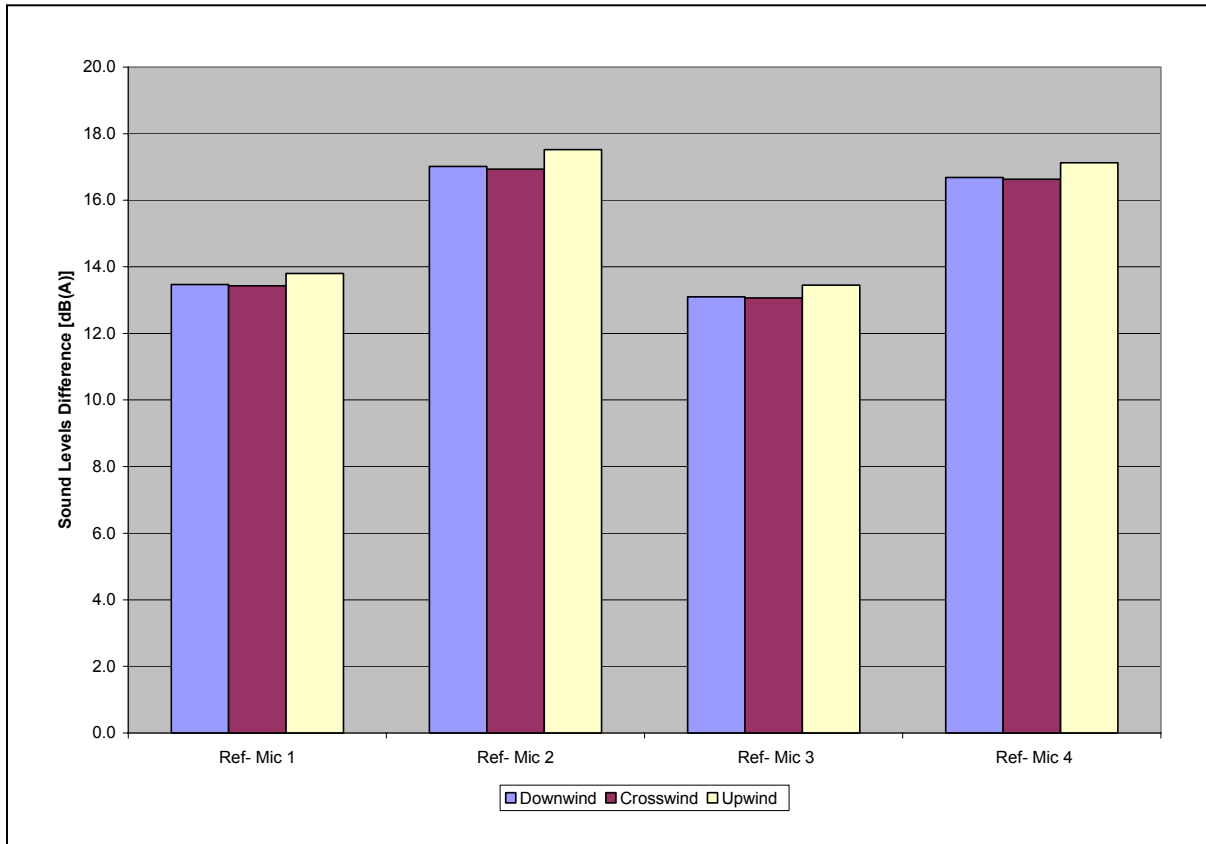


Figure 24: Average Difference Between Reference and Microphone Positions

Figure 25 and Table 26 present the summary of the average difference between measured and predicted sound levels dB(A) using the ISO 9613-2 method with no meteorological corrections factors applied.

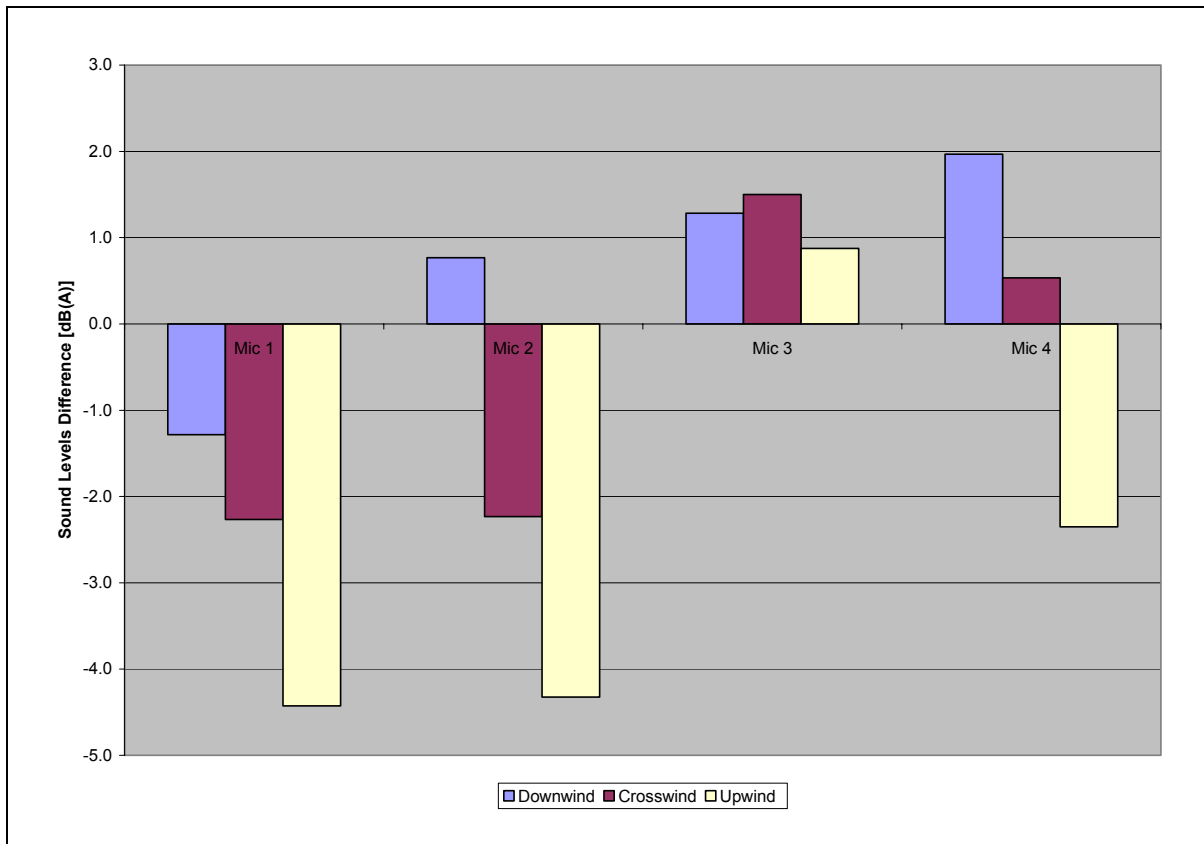


Figure 25: Average Difference Between Measured and Predicted Sound levels

Table 26: Average Difference Between Measured and Predicted Sound levels dB(A)

	Downwind	Crosswind	Upwind
Mic 1	-1.3	-2.3	-4.4
Mic 2	0.8	-2.2	-4.3
Mic 3	1.3	1.5	0.9
Mic 4	2.0	0.5	-2.3

Table 26 shows that the Upwind Group, followed by the Crosswind Group, provides the largest difference between the measured and predicted sound levels. This is due to the fact that the ISO method was developed for downwind conditions and so as

expected, does not do as good in crosswind and upwind conditions. Figure 25 shows that the microphones nearest to the ground, Mic 1 and Mic 2, show the largest variations among the different receivers. This is most likely due to the ground effects not being predicted correctly contributing to the greater microphone sound levels variations.

Tables 27 - 29 presents the difference between the measured octave band sound levels in dB(A) and the predicted octave band sound levels in dB(A) using the ISO 9613-2 method for the Downwind, Crosswind and Upwind Groups respectively.

Table 27, for the Downwind Group, shows that the ISO method on average is under-predicting for octave band that have center frequencies of 125 Hz, 250 Hz, 500 Hz, 1 KHz, and 8 KHz for the majority of the microphone locations with exception Mic 1 at 1 KHz. While, the ISO method is over-predicting for the octave band sound levels in the 63 Hz, 2 KHz, and 4 KHz bands for the majority of the microphone locations with exception Mic 4 at 4 KHz. At Mic 4, the ISO method seems to be under-predicting. It is shown that the difference between measured and predicted octave band sound levels ranged from 0.5 to 22 dB(A).

Table 27: Difference Between Measured & Predicted Octave Band Sound Levels dB(A)

			Frequency (Hz)							
			63	125	250	500	1k	2k	4k	8k
Sample 1	Mic 1	Measured	39.3	45.9	43.5	47.8	53.4	48.5	40.4	37.6
		ISO	42.1	43.9	35.5	37.9	52.9	52.7	42.8	26.8
		Difference	-2.8	2.0	8.0	9.9	0.5	-4.2	-2.4	10.8
	Mic 2	Measured	37.3	43.4	39.7	43.1	52.6	45.8	37.8	37.1
		ISO	40.0	40.2	32.0	33.9	49.4	49.0	37.7	16.7
		Difference	-2.7	3.1	7.7	9.2	3.2	-3.1	0.0	20.4
	Mic 3	Measured	39.2	44.9	47.9	52.7	56.6	50.7	42.2	38.2
		ISO	40.1	42.1	41.7	42.5	53.6	52.7	42.8	26.8
		Difference	-0.9	2.8	6.2	10.2	3.0	-1.9	-0.5	11.4
	Mic 4	Measured	36.8	41.9	42.9	48.4	53.6	47.9	41.1	38.1
		ISO	38.3	36.6	38.6	38.8	50.1	49.0	37.7	16.7
		Difference	-1.5	5.2	4.3	9.6	3.6	-1.1	3.3	21.4
Sample 2	Mic 1	Measured	38.1	47.5	44.4	49.7	54.0	49.5	40.4	37.6
		ISO	40.8	46.8	36.7	43.9	56.0	54.7	44.3	27.4
		Difference	-2.7	0.7	7.7	5.8	-2.0	-5.2	-3.9	10.2
	Mic 2	Measured	36.8	46.5	43.8	45.7	53.4	47.0	38.0	37.1
		ISO	38.7	43.1	33.2	39.9	52.5	51.0	39.2	17.4
		Difference	-1.9	3.4	10.6	5.7	0.9	-4.0	-1.3	19.7
	Mic 3	Measured	37.8	45.3	48.8	54.3	57.5	51.8	42.5	38.2
		ISO	38.8	45.0	43.0	48.6	56.7	54.7	44.3	27.4
		Difference	-0.9	0.3	5.8	5.8	0.8	-2.9	-1.8	10.7
	Mic 4	Measured	35.7	42.9	45.0	51.7	54.5	48.9	41.4	38.1
		ISO	37.0	39.5	39.8	44.9	53.2	51.0	39.2	17.4
		Difference	-1.3	3.5	5.2	6.8	1.4	-2.1	2.2	20.8
Sample 3	Mic 1	Measured	41.0	47.1	44.5	50.1	54.3	50.1	41.5	37.6
		ISO	45.7	49.0	36.3	44.4	55.5	55.1	44.8	27.5
		Difference	-4.7	-1.8	8.2	5.8	-1.2	-5.0	-3.3	10.1
	Mic 2	Measured	39.2	45.4	43.2	46.8	53.6	47.6	38.6	37.1
		ISO	43.7	45.3	32.8	40.4	52.0	51.4	39.7	17.4
		Difference	-4.5	0.1	10.4	6.4	1.7	-3.8	-1.2	19.7
	Mic 3	Measured	40.6	45.2	48.4	54.2	57.9	52.6	43.5	38.4
		ISO	43.7	47.2	42.5	49.0	56.1	55.1	44.8	27.5
		Difference	-3.1	-2.0	5.9	5.2	1.8	-2.5	-1.2	10.9
	Mic 4	Measured	38.0	42.7	45.2	51.2	54.8	49.6	41.9	38.3
		ISO	41.9	41.7	39.4	45.3	52.6	51.4	39.7	17.4
		Difference	-3.9	1.0	5.8	5.9	2.2	-1.8	2.1	20.8

			Ferequency							
			63	125	250	500	1k	2k	4k	8k
Sample 4	Mic 1	Measured	46.2	45.8	42.6	48.4	54.5	49.5	40.6	37.7
		ISO	45.6	47.3	35.8	39.7	55.2	54.8	44.3	28.0
		Difference	0.6	-1.6	6.8	8.8	-0.8	-5.3	-3.7	9.7
	Mic 2	Measured	42.6	43.3	39.7	44.6	53.9	47.2	37.8	37.1
		ISO	43.6	43.7	32.2	35.7	51.7	51.1	39.3	17.9
		Difference	-1.0	-0.3	7.4	9.0	2.1	-3.9	-1.5	19.2
	Mic 3	Measured	45.9	43.1	47.4	52.3	57.6	52.1	42.5	38.4
		ISO	43.6	45.6	42.0	44.3	55.9	54.8	44.3	28.0
		Difference	2.3	-2.4	5.4	8.0	1.7	-2.7	-1.8	10.4
	Mic 4	Measured	41.6	40.2	43.9	49.2	54.8	49.1	41.2	38.1
		ISO	41.8	40.0	38.9	40.6	52.4	51.1	39.3	17.9
		Difference	-0.3	0.2	5.0	8.6	2.4	-2.0	1.9	20.2
Sample 5	Mic 1	Measured	34.3	42.3	40.3	43.4	50.3	45.2	38.6	37.8
		ISO	36.5	43.2	31.9	34.1	51.6	52.0	42.4	26.8
		Difference	-2.2	-0.9	8.4	9.3	-1.2	-6.8	-3.7	11.0
	Mic 2	Measured	33.3	41.0	39.2	39.7	49.9	43.8	36.9	37.2
		ISO	34.4	39.5	28.4	30.2	48.2	48.5	37.2	15.4
		Difference	-1.1	1.4	10.8	9.5	1.8	-4.7	-0.3	21.7
	Mic 3	Measured	35.5	41.2	43.6	47.8	54.1	48.1	41.0	38.2
		ISO	34.5	41.4	38.1	38.8	52.2	52.0	42.4	26.8
		Difference	1.0	-0.2	5.4	9.0	1.9	-3.9	-1.4	11.4
	Mic 4	Measured	35.1	39.8	40.6	44.8	51.0	45.3	39.9	37.8
		ISO	32.7	35.9	35.0	35.1	48.8	48.5	37.2	15.4
		Difference	2.4	3.9	5.6	9.8	2.2	-3.2	2.7	22.4
Sample 6	Mic 1	Measured	33.3	50.0	43.7	44.7	50.9	45.8	38.2	37.6
		ISO	36.2	43.1	33.3	34.6	51.7	52.7	42.9	24.2
		Difference	-2.9	6.9	10.4	10.2	-0.8	-6.9	-4.7	13.4
	Mic 2	Measured	34.0	45.3	40.3	41.9	50.9	44.7	37.8	37.2
		ISO	34.2	39.5	29.7	30.6	48.3	49.1	37.8	12.9
		Difference	-0.2	5.8	10.6	11.3	2.6	-4.4	0.1	24.3
	Mic 3	Measured	32.8	46.6	48.4	48.8	54.1	48.6	41.1	38.1
		ISO	34.2	41.3	39.5	39.2	52.3	52.7	42.9	24.2
		Difference	-1.4	5.3	8.9	9.6	1.8	-4.1	-1.8	13.9
	Mic 4	Measured	36.8	43.4	46.6	45.8	51.4	45.8	41.4	37.9
		ISO	32.5	35.8	36.3	35.5	49.0	49.1	37.8	12.9
		Difference	4.3	7.6	10.2	10.3	2.4	-3.4	3.6	25.0

			Frequency (Hz)							
			63	125	250	500	1k	2k	4k	8k
Average	Mic 1	Measured	38.7	46.4	43.2	47.4	52.9	48.1	39.9	37.7
		ISO	41.1	45.5	34.9	39.1	53.8	53.7	43.6	26.8
		Difference	-2.5	0.9	8.3	8.3	-0.9	-5.6	-3.6	10.9
	Mic 2	Measured	37.2	44.1	41.0	43.6	52.4	46.0	37.8	37.1
		ISO	39.1	41.9	31.4	35.1	50.3	50.0	38.5	16.3
		Difference	-1.9	2.3	9.6	8.5	2.0	-4.0	-0.7	20.8
	Mic 3	Measured	38.6	44.4	47.4	51.7	56.3	50.7	42.2	38.2
		ISO	39.2	43.8	41.2	43.7	54.5	53.7	43.6	26.8
		Difference	-0.5	0.6	6.3	8.0	1.8	-3.0	-1.4	11.5
	Mic 4	Measured	37.3	41.8	44.0	48.5	53.4	47.8	41.1	38.1
		ISO	37.4	38.3	38.0	40.0	51.0	50.0	38.5	16.3
		Difference	-0.1	3.6	6.0	8.5	2.4	-2.3	2.6	21.8

Table 28, for the Crosswind Group, shows that the ISO 9613-2 method on average is over-predicting for the octave band that have center frequencies of 63 Hz, 125 Hz, 1 KHz, 2 KHz, and 4 KHz for microphone locations Mic 1 and Mic 2. While, the ISO method is shown to under-predict for the octave band centered at 250 Hz, 500 Hz, and 8 KHz for microphone locations Mic 1 and Mic 2, which are closer to the ground. In addition, the data show that the method is over-predicting for the octave band that have center frequencies of 63 Hz, and 2 KHz for microphone locations Mic 3 and Mic 4 with exception Mic 3 at 63 Hz. While, the ISO method is shown to under-predict for the octave band centered at 125 Hz, 250 Hz, 500 Hz, 1 KHz, 4 KHz, and 8 KHz for microphone locations Mic 3 and Mic 4 with exception Mic 3 at 125 Hz, which are high above the ground. It is shown that the difference between measured and predicted octave band sound levels ranged from as low as 0.5 dB(A) to as high as 18 dB(A). Moreover, the difference is smaller than the Downwind Group since this is the Crosswind Group and the

refraction effects are less thus reducing the difference between predicted and measured sound levels.

Table 28: Difference Between Measured & Predicted Octave Band Sound levels dB(A)

			Frequency (Hz)							
			63	125	250	500	1k	2k	4k	8k
Sample 1	Mic 1	Measured	41.8	47.2	45.9	49.2	53.4	51.7	43.8	38.3
		ISO	43.6	48.0	39.5	41.5	54.4	54.7	45.5	29.6
		Difference	-1.7	-0.8	6.4	7.8	-1.0	-3.0	-1.7	8.7
	Mic 2	Measured	38.4	43.8	42.0	41.1	49.7	48.7	40.2	37.7
		ISO	41.5	44.4	35.9	37.5	51.0	51.2	40.6	19.5
		Difference	-3.1	-0.5	6.1	3.6	-1.3	-2.5	-0.3	18.2
	Mic 3	Measured	41.3	45.3	50.5	54.8	57.5	53.2	44.8	39.1
		ISO	41.6	46.3	45.7	46.1	55.0	54.7	45.5	29.6
		Difference	-0.3	-1.0	4.8	8.7	2.5	-1.5	-0.7	9.5
	Mic 4	Measured	37.5	41.8	44.0	50.8	52.6	48.6	41.7	38.3
		ISO	39.8	40.7	42.6	42.4	51.6	51.2	40.6	19.5
		Difference	-2.3	1.0	1.4	8.3	0.9	-2.6	1.1	18.8
Sample 2	Mic 1	Measured	39.9	43.6	41.5	45.2	50.7	46.9	42.7	38.5
		ISO	39.9	47.1	35.3	39.1	53.6	54.1	45.0	30.8
		Difference	0.0	-3.5	6.2	6.1	-2.9	-7.2	-2.3	7.7
	Mic 2	Measured	35.9	40.6	38.1	38.9	48.1	45.5	38.4	37.9
		ISO	37.9	43.4	31.7	35.1	50.2	50.6	40.1	20.7
		Difference	-2.0	-2.9	6.4	3.8	-2.1	-5.1	-1.7	17.2
	Mic 3	Measured	39.5	41.8	46.2	52.1	55.8	50.5	44.7	39.5
		ISO	37.9	45.4	41.5	43.7	54.2	54.1	45.0	30.8
		Difference	1.5	-3.5	4.7	8.4	1.6	-3.6	-0.3	8.7
	Mic 4	Measured	35.5	38.6	40.4	48.2	51.3	46.6	42.6	38.5
		ISO	36.1	39.8	38.4	40.1	50.8	50.6	40.1	20.7
		Difference	-0.7	-1.2	2.1	8.2	0.5	-4.0	2.5	17.8
Sample 3	Mic 1	Measured	41.0	43.4	42.5	45.4	49.6	46.8	43.8	40.6
		ISO	42.9	44.8	35.3	39.1	52.7	53.2	43.9	31.7
		Difference	-2.0	-1.4	7.1	6.3	-3.1	-6.4	-0.1	8.9
	Mic 2	Measured	35.7	40.7	39.0	38.6	46.0	44.0	38.7	37.5
		ISO	40.9	41.2	31.8	35.1	49.3	49.6	39.0	21.6
		Difference	-5.2	-0.5	7.2	3.4	-3.3	-5.6	-0.2	15.9
	Mic 3	Measured	41.2	42.1	46.7	52.0	54.9	51.2	46.7	42.8
		ISO	41.0	43.1	41.6	43.7	53.4	53.2	43.9	31.7
		Difference	0.2	-1.0	5.1	8.3	1.6	-2.0	2.8	11.1
	Mic 4	Measured	35.1	39.3	41.0	47.9	49.8	46.0	42.1	38.9
		ISO	39.2	37.6	38.4	40.1	50.0	49.6	39.0	21.6
		Difference	-4.0	1.8	2.6	7.8	-0.2	-3.7	3.1	17.3

			Frequency (Hz)							
			63	125	250	500	1k	2k	4k	8k
Average	Mic 1	Measured	40.9	44.7	43.3	46.6	51.2	48.5	43.4	39.1
		ISO	42.1	46.7	36.7	39.9	53.6	54.0	44.8	30.7
		Difference	-1.2	-1.9	6.6	6.7	-2.3	-5.5	-1.4	8.4
	Mic 2	Measured	36.7	41.7	39.7	39.5	47.9	46.1	39.1	37.7
		ISO	40.1	43.0	33.1	35.9	50.2	50.5	39.9	20.6
		Difference	-3.4	-1.3	6.6	3.6	-2.2	-4.4	-0.8	17.1
	Mic 3	Measured	40.6	43.1	47.8	53.0	56.1	51.7	45.4	40.5
		ISO	40.2	44.9	42.9	44.5	54.2	54.0	44.8	30.7
		Difference	0.5	-1.8	4.9	8.5	1.9	-2.3	0.6	9.8
	Mic 4	Measured	36.0	39.9	41.8	49.0	51.2	47.0	42.2	38.6
		ISO	38.4	39.4	39.8	40.9	50.8	50.5	39.9	20.6
		Difference	-2.3	0.5	2.0	8.1	0.4	-3.4	2.3	18.0

Table 29, for the Upwind Group, shows that the ISO 9613-2 method on average is over-predicting for the octave band that have center frequencies 63 Hz, 125 Hz, 1 KHz, 2 KHz, and 4 KHz for the majority of the microphone locations with exception Mic 3 at 1 KHz. While, the ISO method is shown to under-predict for the octave band centered at 250 Hz, 500 Hz, and 8 KHz for the majority of the microphone locations with exception Mic 4 at 250 Hz. It is shown that the difference between measured and predicted octave band sound levels ranged from as low as 1 dB(A) to as high as 18 dB(A).

Table 29: Difference Between Measured & Predicted Octave Band Sound levels dB(A)

			Frequency (Hz)							
			63	125	250	500	1k	2k	4k	8k
Sample 1	Mic 1	Measured	35.1	40.7	38.2	41.2	45.9	42.6	39.0	37.8
		ISO	41.4	42.6	35.1	39.8	53.4	53.1	44.0	27.5
		Difference	-6.2	-1.9	3.1	1.4	-7.5	-10.5	-5.1	10.2
	Mic 2	Measured	39.8	38.3	38.1	35.2	44.1	39.8	37.0	37.3
		ISO	39.3	38.9	31.5	35.8	49.9	49.4	39.0	17.5
		Difference	0.5	-0.6	6.6	-0.7	-5.8	-9.6	-2.0	19.8
	Mic 3	Measured	42.2	42.3	44.9	50.2	55.1	49.0	43.2	39.2
		ISO	39.4	40.9	41.3	44.5	54.1	53.1	44.0	27.5
		Difference	2.8	1.5	3.6	5.8	1.0	-4.1	-0.8	11.7
	Mic 4	Measured	37.8	36.1	39.4	41.9	46.9	43.0	39.1	36.8
		ISO	37.6	35.3	38.1	40.8	50.6	49.4	39.0	17.5
		Difference	0.2	0.7	1.3	1.2	-3.7	-6.4	0.1	19.3
Sample 2	Mic 1	Measured	35.2	40.6	39.6	42.4	45.5	43.2	38.3	37.7
		ISO	40.0	43.1	35.5	41.0	50.7	51.3	45.9	32.3
		Difference	-4.8	-2.4	4.1	1.4	-5.2	-8.1	-7.6	5.4
	Mic 2	Measured	31.7	35.8	34.2	35.0	42.0	38.7	36.7	37.1
		ISO	37.9	39.4	31.9	37.0	47.2	47.6	40.9	22.3
		Difference	-6.2	-3.6	2.3	-2.0	-5.2	-8.9	-4.2	14.8
	Mic 3	Measured	33.9	39.1	44.1	51.7	54.1	48.8	43.2	38.7
		ISO	38.0	41.3	41.7	45.6	51.4	51.3	45.9	32.3
		Difference	-4.1	-2.2	2.3	6.1	2.7	-2.5	-2.7	6.4
	Mic 4	Measured	29.1	34.1	35.8	42.5	45.1	41.0	39.0	36.4
		ISO	36.2	35.8	38.6	41.9	47.9	47.6	40.9	22.3
		Difference	-7.1	-1.7	-2.8	0.6	-2.7	-6.7	-1.9	14.2
Sample 3	Mic 1	Measured	38.1	41.9	40.4	44.9	48.8	46.5	44.5	38.4
		ISO	45.4	45.6	32.9	37.9	51.8	51.2	45.8	29.1
		Difference	-7.3	-3.7	7.4	7.0	-3.0	-4.8	-1.3	9.3
	Mic 2	Measured	34.9	37.6	36.0	37.3	43.7	41.2	39.6	37.1
		ISO	43.4	41.9	29.4	33.9	48.2	47.5	40.8	19.0
		Difference	-8.5	-4.3	6.7	3.4	-4.5	-6.3	-1.2	18.1
	Mic 3	Measured	37.3	40.1	44.7	49.6	53.7	47.8	43.6	38.8
		ISO	43.5	43.8	39.2	42.5	52.4	51.2	45.8	29.1
		Difference	-6.2	-3.6	5.6	7.1	1.2	-3.4	-2.2	9.7
	Mic 4	Measured	32.6	34.9	37.2	43.9	47.2	42.7	40.3	36.5
		ISO	41.7	38.3	36.0	38.8	48.9	47.5	40.8	19.0
		Difference	-9.1	-3.4	1.2	5.1	-1.7	-4.8	-0.5	17.5

			Frequency (Hz)							
			63	125	250	500	1k	2k	4k	8k
Sample 4	Mic 1	Measured	39.9	39.8	41.2	41.4	47.1	44.9	42.2	37.9
		ISO	40.9	43.5	39.5	35.9	50.5	51.3	42.6	26.7
		Difference	-1.0	-3.6	1.8	5.6	-3.5	-6.4	-0.4	11.2
	Mic 2	Measured	37.5	37.7	36.0	36.6	43.6	40.4	36.9	37.2
		ISO	38.9	39.8	35.9	31.9	47.0	47.6	37.6	16.6
		Difference	-1.3	-2.1	0.1	4.7	-3.4	-7.2	-0.7	20.5
	Mic 3	Measured	40.0	39.3	47.2	50.1	53.1	48.1	43.7	38.5
		ISO	38.9	41.7	45.7	40.5	51.2	51.3	42.6	26.7
		Difference	1.1	-2.4	1.5	9.6	2.0	-3.2	1.1	11.8
	Mic 4	Measured	35.8	35.6	38.7	42.6	46.5	42.5	39.4	36.3
		ISO	37.1	36.2	42.6	36.8	47.6	47.6	37.6	16.6
		Difference	-1.3	-0.6	-3.9	5.8	-1.2	-5.1	1.8	19.7
Average	Mic 1	Measured	37.1	40.8	39.8	42.5	46.8	44.3	41.0	37.9
		ISO	41.9	43.7	35.7	38.6	51.6	51.7	44.6	28.9
		Difference	-4.8	-2.9	4.1	3.8	-4.8	-7.4	-3.6	9.0
	Mic 2	Measured	36.0	37.4	36.1	36.0	43.4	40.0	37.5	37.2
		ISO	39.9	40.0	32.2	34.6	48.1	48.0	39.6	18.8
		Difference	-3.9	-2.6	3.9	1.4	-4.7	-8.0	-2.0	18.3
	Mic 3	Measured	38.3	40.2	45.2	50.4	54.0	48.4	43.4	38.8
		ISO	39.9	41.9	42.0	43.3	52.3	51.7	44.6	28.9
		Difference	-1.6	-1.7	3.2	7.1	1.7	-3.3	-1.2	9.9
	Mic 4	Measured	33.8	35.2	37.8	42.8	46.4	42.3	39.4	36.5
		ISO	38.2	36.4	38.8	39.6	48.7	48.0	39.6	18.8
		Difference	-4.3	-1.2	-1.0	3.2	-2.3	-5.8	-0.1	17.7

Table 30 show that there is no significant difference between the three groups when comparing the difference between measured and predicted octave band sound levels. This is likely due to the fact that the ISO method does not include any meteorological correction. Moreover, when analyzing the results from using the ISO-method to predict octave band sound levels. It was expected that the difference should increase by frequency since refraction effects increases at higher frequency. However, it appears that the ISO method works well in the middle frequencies but does not do as well

at both the low and high frequencies. This is most likely an inability to handle the ground effects properly and that refraction effects are not included.

Table 30: Summary of Difference Between Measured and Predicted Octave Band Sound Levels

		63	125	250	500	1k	2k	4k	8k
Mic 1	Downwind	-2.5	0.9	8.3	8.3	-0.9	-5.6	-3.6	10.9
	Crosswind	-1.2	-1.9	6.6	6.7	-2.3	-5.5	-1.4	8.4
	Upwind	-4.8	-2.9	4.1	3.8	-4.8	-7.4	-3.6	9.0
Mic 2	Downwind	-1.9	2.3	9.6	8.5	2.0	-4.0	-0.7	20.8
	Crosswind	-3.4	-1.3	6.6	3.6	-2.2	-4.4	-0.8	17.1
	Upwind	-3.9	-2.6	3.9	1.4	-4.7	-8.0	-2.0	18.3
Mic 3	Downwind	-0.5	0.6	6.3	8.0	1.8	-3.0	-1.4	11.5
	Crosswind	0.5	-1.8	4.9	8.5	1.9	-2.3	0.6	9.8
	Upwind	-1.6	-1.7	3.2	7.1	1.7	-3.3	-1.2	9.9
Mic 4	Downwind	-0.1	3.6	6.0	8.5	2.4	-2.3	2.6	21.8
	Crosswind	-2.3	0.5	2.0	8.1	0.4	-3.4	2.3	18.0
	Upwind	-4.3	-1.2	-1.0	3.2	-2.3	-5.8	-0.1	17.7

All these analysis observations point to limitations in the ISO 9613 methodology. The ISO 9613-2 method was mainly developed for downwind conditions, which explains the large difference between predicted and measured sound levels corresponding to the Upwind and the Crosswind Groups. Although this method is used widely in outdoor sound propagation sound level prediction, it appears it does not predict well the traffic noise sources in this situation. The method has been primarily developed for industrial locations and point sources, while traffic noise is modeled as a line source and perhaps this is part of the problem. Furthermore, the noise source from the highway is elevated 25 feet (7.6 m) above the ground. The ISO 9613-2 method assumes that for soft ground, the

ground effect is equal to zero in the middle region between the source and the receiver regions for most of the frequencies and this may not be occurring. This has also likely contributed to the difference (over/under-predicting) between measured and predicted octave band sound levels as shown in Tables 23, 25 and 27. All of these factors contributed to the inaccurate modeling of propagation effects, hence large error occurred in the predicted sound levels.

The ISO9613-2 method also may include the meteorological correction factors. This factor, by name implies it will account for refraction caused by wind gradient and lapse rates. However, as will be discussed, these are not inputs to the model. Use of this option was also considered and discussed in the next section.

ISO 9613-2 (with Meteorological Correction)

The ISO 9613-2 may be used with a meteorological correction term (C_{met}). This term was defined in Equation 46. C_{met} is a factor based on source and receiver heights, in addition to local meteorological conditions factor C_o , with values being shown previously in Chapter 3, Table 3 for the three different groups. Tables 31 – 33 present the calculated different attenuation in dB for each microphone positions of the three groups Downwind, Crosswind and Upwind. Afterward, a summary of the sound levels predicted by the ISO9613-2 with the meteorological correction factor applied is presented for each group and a comparison to the measured sound levels for each microphone evaluated.

Table 31: Attenuation (dB) for Microphones in Downwind Group

Attenuation		Frequency (Hz)							
		63	125	250	500	1k	2k	4k	8k
Mic 1	A _{div}	7.7	7.7	7.7	7.7	7.7	7.7	7.7	7.7
	A _{atm}	0.0	0.0	0.2	0.5	0.9	1.6	3.3	9.8
	A _{gr}	-5.0	1.3	14.6	17.7	5.3	0.0	0.0	0.0
	C _{met}	0.7	0.7	0.7	0.7	0.7	0.7	0.7	0.7
	Sum	3.4	9.7	23.1	26.5	14.6	9.9	11.6	18.2
Mic 2	A _{div}	10.2	10.2	10.2	10.2	10.2	10.2	10.2	10.2
	A _{atm}	0.0	0.1	0.3	0.8	1.7	2.8	5.8	17.4
	A _{gr}	-5.4	2.5	15.5	18.8	5.6	0.0	0.0	0.0
	C _{met}	0.7	0.7	0.7	0.7	0.7	0.7	0.7	0.7
	Sum	5.5	13.4	26.7	30.5	18.2	13.7	16.7	28.2
Mic 3	A _{div}	7.7	7.7	7.7	7.7	7.7	7.7	7.7	7.7
	A _{atm}	0.0	0.0	0.2	0.5	0.9	1.6	3.3	9.8
	A _{gr}	-3.0	3.1	8.3	13.0	4.7	0.0	0.0	0.0
	C _{met}	0.4	0.4	0.4	0.4	0.4	0.4	0.4	0.4
	Sum	5.1	11.2	16.6	21.6	13.7	9.7	11.4	17.9
Mic 4	A _{div}	10.2	10.2	10.2	10.2	10.2	10.2	10.2	10.2
	A _{atm}	0.0	0.1	0.3	0.8	1.7	2.8	5.8	17.4
	A _{gr}	-3.7	6.1	8.9	13.9	5.0	0.0	0.0	0.0
	C _{met}	0.6	0.6	0.6	0.6	0.6	0.6	0.6	0.6
	Sum	7.0	16.9	19.9	25.5	17.4	13.5	16.6	28.1

Table 32: Attenuation (dB) for Microphones in Crosswind Group

Attenuation		Frequency (Hz)							
		63	125	250	500	1k	2k	4k	8k
Mic 1	A_{div}	7.7	7.7	7.7	7.7	7.7	7.7	7.7	7.7
	A_{atm}	0.0	0.0	0.2	0.4	0.8	1.4	3.1	9.8
	A_{gr}	-5.0	1.3	14.6	17.7	5.3	0.0	0.0	0.0
	C_{met}	0.9	0.9	0.9	0.9	0.9	0.9	0.9	0.9
	Sum	3.6	10.0	23.3	26.7	14.7	9.9	11.7	18.4
Mic 2	A_{div}	10.2	10.2	10.2	10.2	10.2	10.2	10.2	10.2
	A_{atm}	0.0	0.1	0.3	0.8	1.4	2.4	5.5	17.5
	A_{gr}	-5.4	2.5	15.5	18.8	5.6	0.0	0.0	0.0
	C_{met}	0.9	0.9	0.9	0.9	0.9	0.9	0.9	0.9
	Sum	5.7	13.7	26.9	30.7	18.1	13.5	16.6	28.6
Mic 3	A_{div}	7.7	7.7	7.7	7.7	7.7	7.7	7.7	7.7
	A_{atm}	0.0	0.0	0.2	0.4	0.8	1.4	3.1	9.8
	A_{gr}	-3.0	3.1	8.3	13.0	4.7	0.0	0.0	0.0
	C_{met}	0.5	0.5	0.5	0.5	0.5	0.5	0.5	0.5
	Sum	5.2	11.3	16.7	21.7	13.6	9.6	11.3	18.0
Mic 4	A_{div}	10.2	10.2	10.2	10.2	10.2	10.2	10.2	10.2
	A_{atm}	0.0	0.1	0.3	0.8	1.4	2.4	5.5	17.5
	A_{gr}	-3.7	6.1	8.9	13.9	5.0	0.0	0.0	0.0
	C_{met}	0.8	0.8	0.8	0.8	0.8	0.8	0.8	0.8
	Sum	7.2	17.1	20.1	25.6	17.3	13.3	16.4	28.4

Table 33: Attenuation (dB) for Microphones in Upwind Group

Attenuation		Frequency (Hz)							
		63	125	250	500	1k	2k	4k	8k
Mic 1	A _{div}	7.7	7.7	7.7	7.7	7.7	7.7	7.7	7.7
	A _{atm}	0.0	0.0	0.2	0.5	0.9	1.6	3.3	9.8
	A _{gr}	-5.0	1.3	14.6	17.7	5.3	0.0	0.0	0.0
	C _{met}	1.8	1.8	1.8	1.8	1.8	1.8	1.8	1.8
	Sum	4.5	10.8	24.2	27.6	15.7	11.0	12.7	19.3
Mic 2	A _{div}	10.2	10.2	10.2	10.2	10.2	10.2	10.2	10.2
	A _{atm}	0.0	0.1	0.3	0.8	1.7	2.8	5.8	17.4
	A _{gr}	-5.4	2.5	15.5	18.8	5.6	0.0	0.0	0.0
	C _{met}	1.9	1.9	1.9	1.9	1.9	1.9	1.9	1.9
	Sum	6.6	14.6	27.8	31.7	19.3	14.8	17.9	29.4
Mic 3	A _{div}	7.7	7.7	7.7	7.7	7.7	7.7	7.7	7.7
	A _{atm}	0.0	0.0	0.2	0.5	0.9	1.6	3.3	9.8
	A _{gr}	-3.0	3.1	8.3	13.0	4.7	0.0	0.0	0.0
	C _{met}	1.1	1.1	1.1	1.1	1.1	1.1	1.1	1.1
	Sum	5.8	11.9	17.3	22.3	14.4	10.4	12.1	18.6
Mic 4	A _{div}	10.2	10.2	10.2	10.2	10.2	10.2	10.2	10.2
	A _{atm}	0.0	0.1	0.3	0.8	1.7	2.8	5.8	17.4
	A _{gr}	-3.7	6.1	8.9	13.9	5.0	0.0	0.0	0.0
	C _{met}	1.5	1.5	1.5	1.5	1.5	1.5	1.5	1.5
	Sum	8.0	17.8	20.8	26.4	18.3	14.4	17.5	29.0

The different attenuation factors vary depending on distance between receivers and source within each group due to the prediction scheme shown in Equations 43-46. Comparing the attenuation between the different groups, it can be determined that the attenuation factor (α value) within the atmospheric absorption A_{atm} term had changed among the frequencies by only 1% to 10% for the different groups. This is due to the small change in temperatures and relative humidity for the days included in this study.

Downwind Group

The analysis consists of applying all the attenuation factors: A_{div} , A_{atm} , A_{gr} , and C_{met} . A-weighted adjustments were then applied for each corresponding octave band frequency. The A-weighted adjusted attenuation factors were subtracted from the measured sound levels at the Reference microphone (Ref.) to calculate the predicted sound levels for the different microphone locations: Mic 1, Mic 2, Mic 3 and Mic 4.

Table 34 and Figure 26 present the measured sound levels dB(A), the predicted sound levels dB(A) using the ISO 9613-2 method (meteorological correction) and the difference between the two methods for each microphone within the Downwind Group. The last part of the table shows the average of the six samples within the Downwind Group, and highlights the average difference between measured and predicted sound levels for the various microphones. It is shown that on average the difference is within 2.6 dB(A).

Table 34: Difference between Measured and Predicted Sound levels dB(A) for Downwind Group

		Measured	ISO-Cmet	Difference
Sample 1	Ref	69.9	69.9	0.0
	Mic 1	56.4	55.9	0.5
	Mic 2	54.6	52.2	2.4
	Mic 3	59.4	56.5	2.9
	Mic 4	56.2	52.7	3.5
Sample 2	Ref	73.7	73.7	0.0
	Mic 1	57.3	58.4	-1.1
	Mic 2	55.9	54.8	1.1
	Mic 3	60.5	59.2	1.3
	Mic 4	57.7	55.4	2.3
Sample 3	Ref	73.7	73.7	0.0
	Mic 1	57.7	58.6	-0.9
	Mic 2	56.1	55.0	1.1
	Mic 3	60.8	59.3	1.5
	Mic 4	57.8	55.5	2.3
Sample 4	Ref	72.0	72.0	0.0
	Mic 1	57.4	58.2	-0.8
	Mic 2	55.9	54.6	1.3
	Mic 3	60.2	58.7	1.5
	Mic 4	57.3	54.9	2.4
Sample 5	Ref	68.0	68.0	0.0
	Mic 1	53.2	54.8	-1.6
	Mic 2	52.2	51.2	1.0
	Mic 3	56.5	55.3	1.2
	Mic 4	53.6	51.6	2.0
Sample 6	Ref	68.4	68.4	0.0
	Mic 1	55.2	55.2	0.0
	Mic 2	53.5	51.6	1.9
	Mic 3	57.4	55.7	1.7
	Mic 4	54.8	52.0	2.8
Average	Ref	71.0	71.0	0.0
	Mic 1	56.2	56.9	-0.7
	Mic 2	54.7	53.2	1.5
	Mic 3	59.1	57.5	1.7
	Mic 4	56.2	53.7	2.6

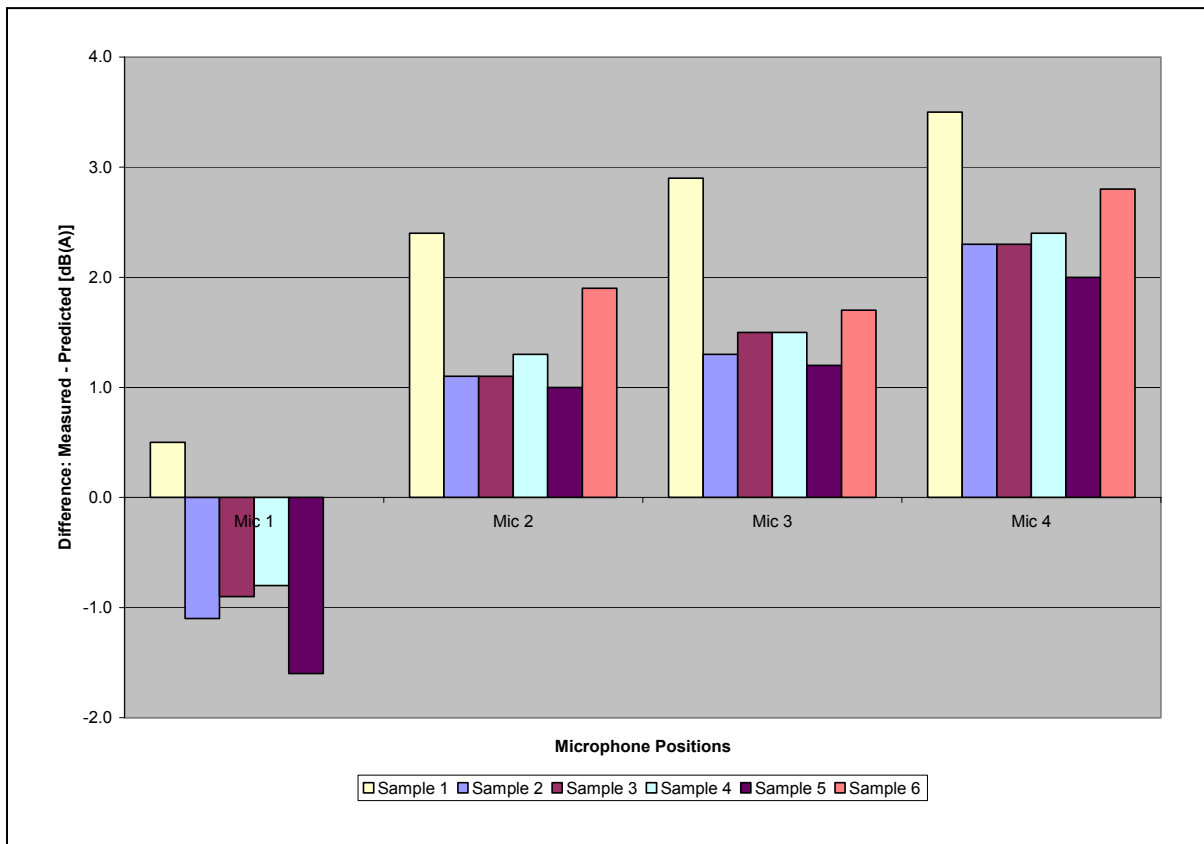


Figure 26: Difference Between Measured and Predicted Sound Levels for Downwind Group

It is shown that the ISO method is primarily over-predicting for Mic 1, while in one case (sample 6) there is no difference, and in another case (sample 1) the sound level is under-predicted. Under-predicting occurred at Mic 2, Mic 3 and Mic 4 for all sample periods. The over prediction at Mic 1 might be due to shielding from the edge of the pavement for Mic 1. This would add diffraction effects that have not been included in the modeling. In general the difference between measured and predicted sound levels increased for the receivers further from the source, which would tend to indicate the effect of varying ground and refraction effects not being included. In downwind

conditions the sound waves should bend downward towards the ground, thus increasing the sound levels above the normal levels. The downward refraction is noticeable by the increased difference between the measured and predicted sound levels at Mic 3 and Mic 4 compared to Mic 1 and Mic 2 which are near the ground.

Although the ISO 9613-2 method meteorological correction factor has been applied, the error was only reduced for Mic 1, while it has increased for Mic 2, Mic 3 and Mic 4. This is thought to be explained by the fact that the correction factor is directly depended on the source and receiver heights, and does not directly include any parameters that explicit functions of wind shear or lapse rates. Neither does it account for how these variables could change ground effects. The C_o term is a number that only varies from 0 to 2 and is based on percentage of time the wind is blowing in favorable conditions. This was true and a valid variable for the downwind conditions which is the standard case for the way the model was derived. However, it does not apply well for cases with upwind or crosswind conditions. As such, the model did not predict accurately sound levels accurately.

Of interest is Sample 5, where there is a combination between a strong wind condition and inversion. This case has shown that inversion lapse rate has amplified the downward wind refraction effects as shown by the sound level difference between the Reference microphone and the other microphone locations, with sound level difference is 14 dB(A) for sample 5 compared to an average sound level difference of 16 dB(A) for the other sample period. Also, the inversion has caused ground effects to vary from the other

sample periods within the group, thus increasing the sound levels for the microphone positions, and hence reducing the difference between measured and predicted sound levels when compared to other sample periods as shown in Figure 26.

Crosswind Group

Table 35 and Figure 27 present the measured sound levels dB(A), the predicted sound levels dB(A) using the ISO 9613-2 method (with the meteorological correction applied) and the difference between the two methods for each microphone within the Crosswind Group. The last part of the table shows the average of the three samples within the Crosswind Group, and highlights the average difference between measured and predicted sound levels for the various microphones.

Table 35: Difference between Measured and Predicted Sound levels dB(A) for Crosswind Group

		Measured	ISO-Cmet	Difference
Sample 1	Ref	72.3	72.3	0.0
	Mic 1	57.7	57.7	0.0
	Mic 2	53.9	54.1	-0.2
	Mic 3	61.1	58.4	2.7
	Mic 4	56.4	54.6	1.8
Sample 2	Ref	70.8	70.8	0.0
	Mic 1	54.3	57.0	-2.7
	Mic 2	51.5	53.2	-1.7
	Mic 3	58.8	57.5	1.3
	Mic 4	54.7	53.7	1.0
Sample 3	Ref	70.2	70.2	0.0
	Mic 1	54.2	55.9	-1.7
	Mic 2	50.4	52.4	-2.0
	Mic 3	58.7	56.7	2.0
	Mic 4	53.9	52.9	1.0
Average	Ref	71.1	71.1	0.0
	Mic 1	55.4	56.9	-1.5
	Mic 2	51.9	53.2	-1.3
	Mic 3	59.5	57.5	2.0
	Mic 4	55.0	53.7	1.3

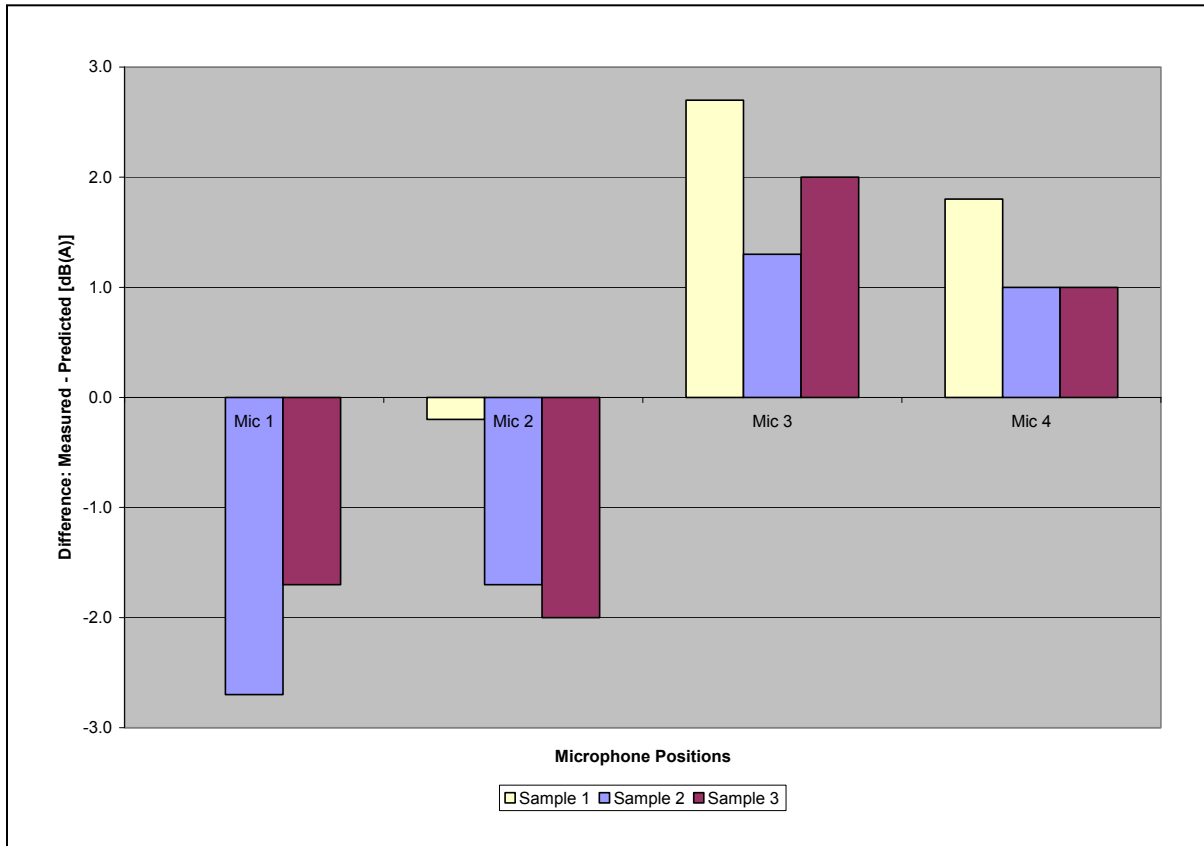


Figure 27: Difference Between Measured and Predicted Sound Levels for Crosswind Group

It is shown that the ISO method is primarily over-predicting for Mic 1 and Mic 2, while in one case (sample 1, Mic 1) there is no difference. Under-predicting occurs at Mic 3 and Mic 4 for all sample periods. Furthermore, on average the difference between measured and predicted sound levels has been reduced with distance for the receivers that are the furthest from the source. This was not the trend in the Downwind Group but was expected here since the U-wind component is smaller for the Crosswind Group and during the crosswind condition the wind is blowing perpendicular to the propagation path

between the source and the receiver. Thus, no strong refraction effects due to wind shear are expected at the microphones furthest from the source.

Upwind Group

Table 36 and Figure 28 present the measured sound levels dB(A), the predicted sound levels dB(A) using the ISO 9613-2 method (with the meteorological correction) and the difference between the two methods for each microphone within the Upwind Group. The last part of the table shows the average of the three samples within the Upwind Group, and highlights the average difference between measured and predicted sound levels for the various microphones. It is shown that on average the difference is within 2.6 dB(A).

Table 36: Difference between Measured and Predicted Sound levels dB(A) for Upwind Group

		Measured	ISO-Cmet	Difference
Sample 1	Ref	70.8	70.8	0.0
	Mic 1	50.3	55.2	-4.9
	Mic 2	48.6	51.5	-2.9
	Mic 3	57.8	56.3	1.5
	Mic 4	50.7	52.3	-1.6
Sample 2	Ref	70.1	70.1	0.0
	Mic 1	50.4	53.5	-3.1
	Mic 2	46.4	49.7	-3.3
	Mic 3	57.4	54.7	2.7
	Mic 4	49.1	50.6	-1.5
Sample 3	Ref	69.2	69.2	0.0
	Mic 1	53.4	54.3	-0.9
	Mic 2	48.4	50.6	-2.2
	Mic 3	56.6	55.1	1.5
	Mic 4	50.8	51.0	-0.2
Sample 4	Ref	68.7	68.7	0.0
	Mic 1	51.8	53.2	-1.4
	Mic 2	48.0	49.5	-1.5
	Mic 3	56.7	54.4	2.3
	Mic 4	50.3	50.4	-0.1
Average	Ref	69.7	69.7	0.0
	Mic 1	51.5	54.1	-2.6
	Mic 2	47.9	50.3	-2.5
	Mic 3	57.1	55.1	2.0
	Mic 4	50.2	51.1	-0.8

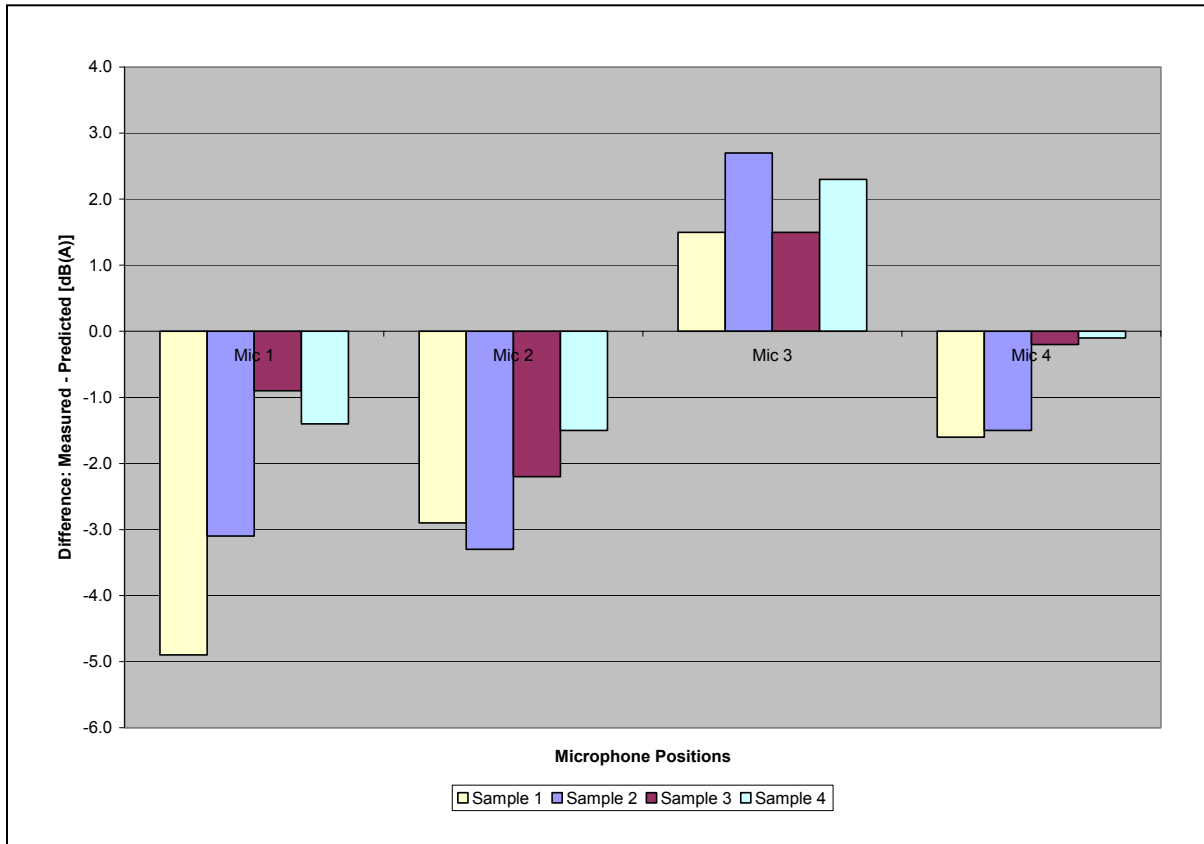


Figure 28: Difference Between Measured and Predicted Sound Levels for Upwind Group

It is shown that the ISO method is over-predicting for Mic 1, Mic 2 and Mic 4, while the method is under-predicting for Mic 3. The ISO 9613-2 method was developed to accurately predict sound levels in downwind conditions. In upwind conditions sound waves should bend upward away from the ground, thus decreasing the sound levels below the normal levels and this is not accounted for. The sound waves bending upward are more noticeable in the increased difference in sound level at Mic 1 and Mic 2. In addition, it is shown that the difference between measured and predicted sound levels is

larger at the lower microphones near the ground. This could be explained by increased ground effects.

In Sample 4, the normal lapse rate case should have increased the sound levels at the higher microphone locations; and this was shown by the reduction in the difference between measured and predicted sound levels for Sample 4 when compared to other sample periods as shown in Figure 28.

Summary

Table 37 and Figure 29 show the average difference in sound levels between the Reference and the other microphone locations (Mic 1, Mic 2, Mic 3 and Mic 4). The data illustrate small difference between the Downwind and the Crosswind Groups when calculating the difference between the Reference and the microphone locations, while the numbers are slightly higher for the difference between the Reference and the microphone positions for the Upwind Group. The increased difference in sound level for the upwind conditions is most likely due to the application of the meteorological correction factor, which was developed for downwind conditions. This is shown by the increased difference between measured and predicted in sound levels for upwind conditions as shown in Figure 30.

The average sound levels difference between the Reference and the microphone positions is almost the same for the lower and higher microphone locations in the ISO 9613 predictions. This is due to the fact that ISO 9613-2 method assumes that for soft ground the ground effect correction is equal to zero in the middle region between the source, and the receiver regions. Hence, the ground effects are similar for the higher and lower microphone positions.

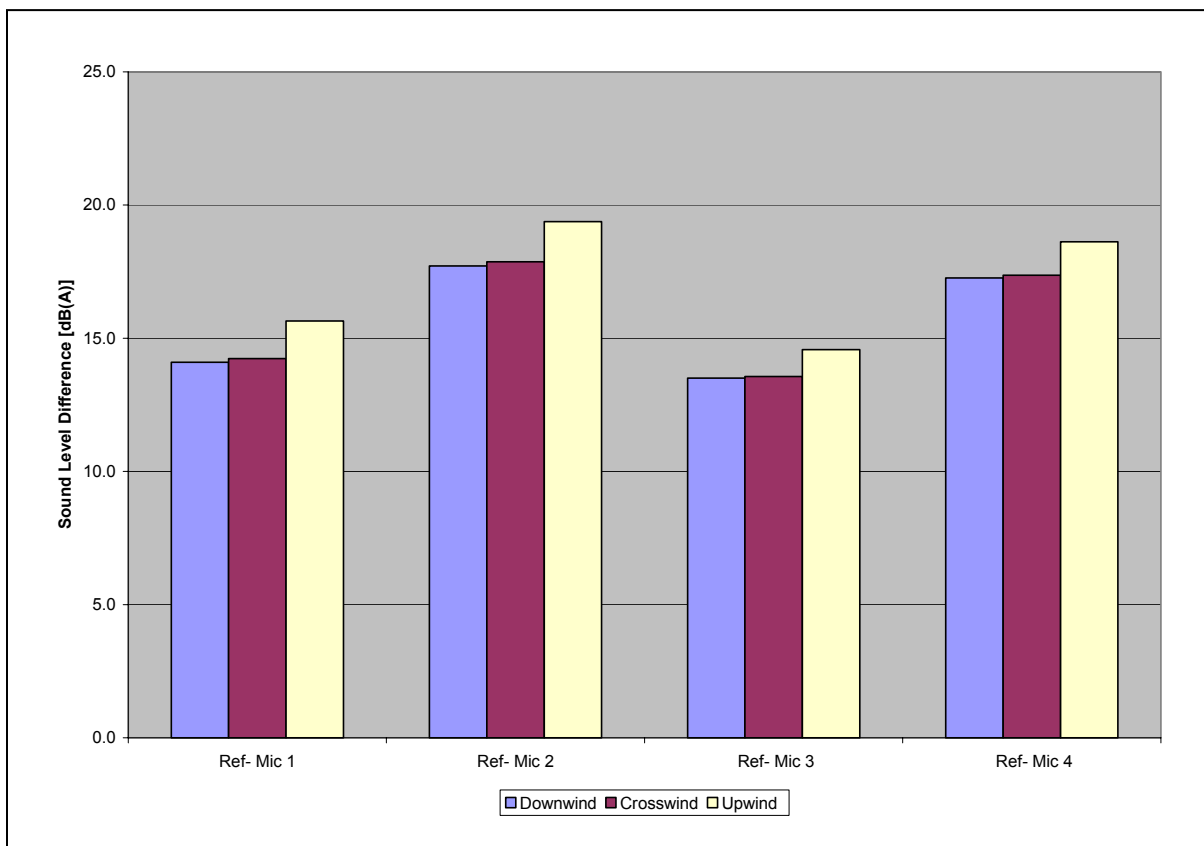


Figure 29: Average Difference Between Reference and Microphone Positions

Table 37: Average Difference Between Reference and Microphone Positions dB(A)

	Ref- Mic 1	Ref- Mic 2	Ref- Mic 3	Ref- Mic 4
Downwind	14.1	17.7	13.5	17.3
Crosswind	14.2	17.9	13.6	17.4
Upwind	15.7	19.4	14.6	18.6

Table 38 and Figure 30 present the summary of the difference between measured and predicted sound levels dB(A) using the ISO 9613-2 method with meteorological corrections factors applied.

Table 38: Average Difference Between Measured and Predicted Sound Levels dB(A)

	Downwind	Crosswind	Upwind
Mic 1	-0.7	-1.5	-2.6
Mic 2	1.5	-1.3	-2.5
Mic 3	1.7	2.0	2.0
Mic 4	2.6	1.3	-0.8

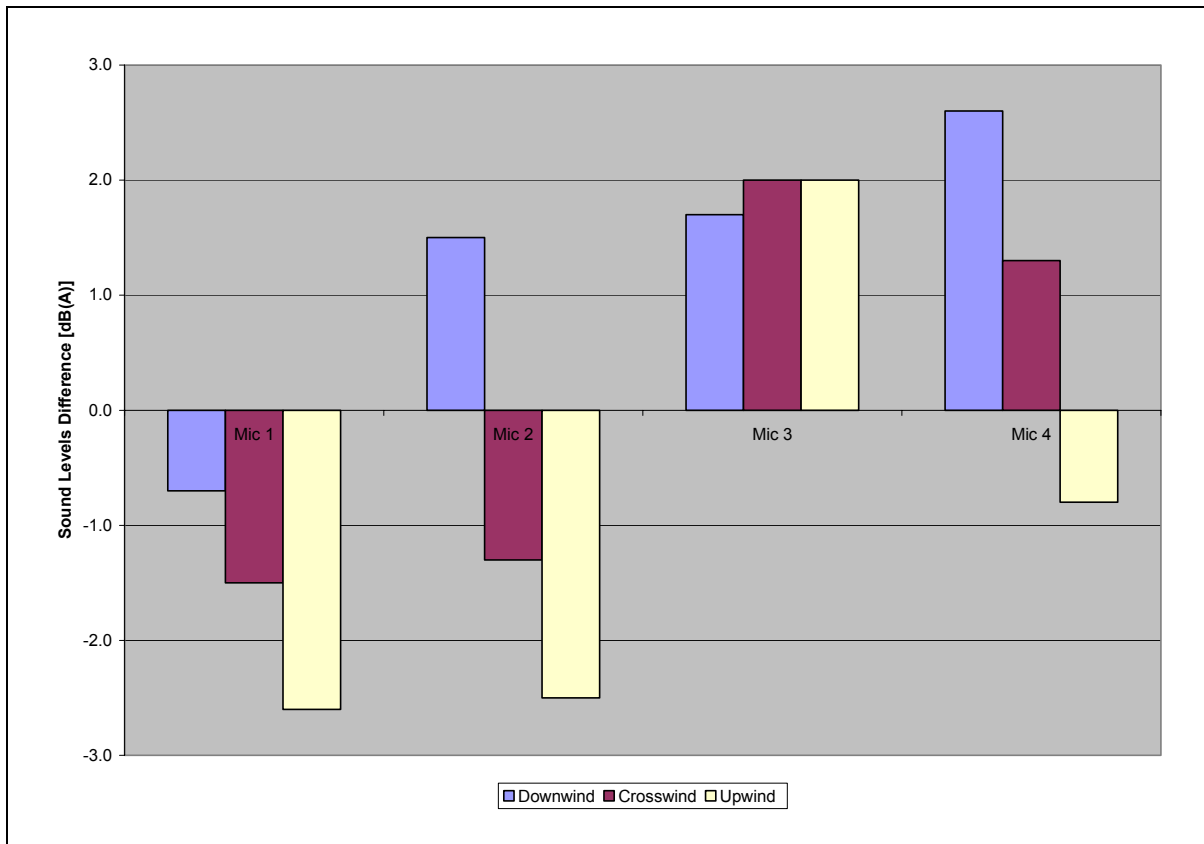


Figure 30: Average Difference Between Measured and Predicted Sound Levels

It is shown that applying the meteorological correction factors has reduced the overall average difference for Mic 1 and Mic 2, while difference increased between measured and predicted sound level for Mic 3 and Mic 4 for the Downwind and Crosswind Groups. This is likely due to less ground effect at the higher microphone locations which resulted in higher difference between measured and predicted sound levels as shown in Figure 30. The lack of any wind shear and lapse rates in the meteorological correction did not successfully result in substantially reducing the difference between measured and predicted sound levels. This is likely due to the fact

that the correction factor is directly depended on the source and receiver heights, and does not directly include any parameters that explicit functions of wind shear or lapse rates. This is also confirmed by the similarity of the prediction results for both the ISO method and the ISO method with meteorological factors applied, where the correction factor did not have an effect.

Tables 39 - 41 present the difference between the measured octave band sound levels in dB(A) and the predicted octave band sound levels in dB(A) using the ISO 9613-2 method with the meteorological correction factor included for the Downwind, Crosswind, and Upwind Groups respectively.

Table 39, for the Downwind Group, shows that this method is on average over-predicting for the octave band that have center frequencies 63 Hz, 2 KHz, and 4 KHz for the majority of the microphone locations, except Mic 4 at 4 KHz. While, the ISO method is shown to under-predict for the octave band centered at frequencies 125 Hz, 250 Hz, 500 Hz, 1 KHz and 8 KHz for the majority of the microphone locations, except Mic 1 at 1 KHz. It is shown that the difference between measured and predicted octave band sound levels ranged from as low as 0.3 dB(A) to as high as 22 dB(A).

Table 39: Difference Between Measured & Predicted Octave Band Sound levels dB(A)

			Frequency (Hz)							
			63	125	250	500	1k	2k	4k	8k
Sample 1	Mic 1	Measured	39.3	45.9	43.5	47.8	53.4	48.5	40.4	37.6
		ISO-Cmet	41.4	43.2	34.8	37.2	52.3	52.0	42.1	26.1
		Difference	-2.1	2.6	8.7	10.6	1.1	-3.5	-1.7	11.5
	Mic 2	Measured	37.3	43.4	39.7	43.1	52.6	45.8	37.8	37.1
		ISO-Cmet	39.3	39.5	31.3	33.2	48.7	48.3	37.0	16.0
		Difference	-2.0	3.8	8.4	9.9	3.9	-2.4	0.7	21.1
	Mic 3	Measured	39.2	44.9	47.9	52.7	56.6	50.7	42.2	38.2
		ISO-Cmet	39.7	41.7	41.3	42.1	53.2	52.3	42.3	26.4
		Difference	-0.4	3.2	6.6	10.6	3.4	-1.5	-0.1	11.8
	Mic 4	Measured	36.8	41.9	42.9	48.4	53.6	47.9	41.1	38.1
		ISO-Cmet	37.7	36.1	38.0	38.2	49.5	48.4	37.2	16.1
		Difference	-1.0	5.8	4.9	10.1	4.1	-0.5	3.9	22.0
Sample 2	Mic 1	Measured	38.1	47.5	44.4	49.7	54.0	49.5	40.4	37.6
		ISO-Cmet	40.1	46.1	36.1	43.3	55.4	54.0	43.6	26.8
		Difference	-2.0	1.4	8.3	6.4	-1.3	-4.6	-3.2	10.8
	Mic 2	Measured	36.8	46.5	43.8	45.7	53.4	47.0	38.0	37.1
		ISO-Cmet	38.0	42.4	32.5	39.2	51.8	50.3	38.5	16.7
		Difference	-1.2	4.1	11.3	6.4	1.6	-3.3	-0.6	20.4
	Mic 3	Measured	37.8	45.3	48.8	54.3	57.5	51.8	42.5	38.2
		ISO-Cmet	38.4	44.6	42.6	48.2	56.3	54.3	43.8	27.0
		Difference	-0.5	0.7	6.3	6.2	1.3	-2.5	-1.4	11.1
	Mic 4	Measured	35.7	42.9	45.0	51.7	54.5	48.9	41.4	38.1
		ISO-Cmet	36.5	38.9	39.3	44.3	52.6	50.4	38.7	16.8
		Difference	-0.8	4.0	5.8	7.4	2.0	-1.5	2.7	21.3
Sample 3	Mic 1	Measured	41.0	47.1	44.5	50.1	54.3	50.1	41.5	37.6
		ISO-Cmet	45.0	48.3	35.6	43.7	54.8	54.4	44.1	26.8
		Difference	-4.1	-1.2	8.9	6.5	-0.5	-4.3	-2.6	10.8
	Mic 2	Measured	39.2	45.4	43.2	46.8	53.6	47.6	38.6	37.1
		ISO-Cmet	43.0	44.6	32.1	39.7	51.3	50.7	39.0	16.7
		Difference	-3.8	0.8	11.1	7.1	2.4	-3.1	-0.5	20.4
	Mic 3	Measured	40.6	45.2	48.4	54.2	57.9	52.6	43.5	38.4
		ISO	43.7	47.2	42.5	49.0	56.1	55.1	44.8	27.5
		Difference	-3.1	-2.0	5.9	5.2	1.8	-2.5	-1.2	10.9
	Mic 4	Measured	38.0	42.7	45.2	51.2	54.8	49.6	41.9	38.3
		ISO	41.9	41.7	39.4	45.3	52.6	51.4	39.7	17.4
		Difference	-3.9	1.0	5.8	5.9	2.2	-1.8	2.1	20.8

			Frequency (Hz)							
			63	125	250	500	1k	2k	4k	8k
Sample 4	Mic 1	Measured	46.2	45.8	42.6	48.4	54.5	49.5	40.6	37.7
		ISO	45.6	47.3	35.8	39.7	55.2	54.8	44.3	28.0
		Difference	0.6	-1.6	6.8	8.8	-0.8	-5.3	-3.7	9.7
	Mic 2	Measured	42.6	43.3	39.7	44.6	53.9	47.2	37.8	37.1
		ISO	43.6	43.7	32.2	35.7	51.7	51.1	39.3	17.9
		Difference	-1.0	-0.3	7.4	9.0	2.1	-3.9	-1.5	19.2
	Mic 3	Measured	45.9	43.1	47.4	52.3	57.6	52.1	42.5	38.4
		ISO	43.6	45.6	42.0	44.3	55.9	54.8	44.3	28.0
		Difference	2.3	-2.4	5.4	8.0	1.7	-2.7	-1.8	10.4
	Mic 4	Measured	41.6	40.2	43.9	49.2	54.8	49.1	41.2	38.1
		ISO	41.8	40.0	38.9	40.6	52.4	51.1	39.3	17.9
		Difference	-0.3	0.2	5.0	8.6	2.4	-2.0	1.9	20.2
Sample 5	Mic 1	Measured	34.3	42.3	40.3	43.4	50.3	45.2	38.6	37.8
		ISO	36.5	43.2	31.9	34.1	51.6	52.0	42.4	26.8
		Difference	-2.2	-0.9	8.4	9.3	-1.2	-6.8	-3.7	11.0
	Mic 2	Measured	33.3	41.0	39.2	39.7	49.9	43.8	36.9	37.2
		ISO	34.4	39.5	28.4	30.2	48.2	48.5	37.2	15.4
		Difference	-1.1	1.4	10.8	9.5	1.8	-4.7	-0.3	21.7
	Mic 3	Measured	35.5	41.2	43.6	47.8	54.1	48.1	41.0	38.2
		ISO	34.5	41.4	38.1	38.8	52.2	52.0	42.4	26.8
		Difference	1.0	-0.2	5.4	9.0	1.9	-3.9	-1.4	11.4
	Mic 4	Measured	35.1	39.8	40.6	44.8	51.0	45.3	39.9	37.8
		ISO	32.7	35.9	35.0	35.1	48.8	48.5	37.2	15.4
		Difference	2.4	3.9	5.6	9.8	2.2	-3.2	2.7	22.4
Sample 6	Mic 1	Measured	33.3	50.0	43.7	44.7	50.9	45.8	38.2	37.6
		ISO	36.2	43.1	33.3	34.6	51.7	52.7	42.9	24.2
		Difference	-2.9	6.9	10.4	10.2	-0.8	-6.9	-4.7	13.4
	Mic 2	Measured	34.0	45.3	40.3	41.9	50.9	44.7	37.8	37.2
		ISO	34.2	39.5	29.7	30.6	48.3	49.1	37.8	12.9
		Difference	-0.2	5.8	10.6	11.3	2.6	-4.4	0.1	24.3
	Mic 3	Measured	32.8	46.6	48.4	48.8	54.1	48.6	41.1	38.1
		ISO	34.2	41.3	39.5	39.2	52.3	52.7	42.9	24.2
		Difference	-1.4	5.3	8.9	9.6	1.8	-4.1	-1.8	13.9
	Mic 4	Measured	36.8	43.4	46.6	45.8	51.4	45.8	41.4	37.9
		ISO	32.5	35.8	36.3	35.5	49.0	49.1	37.8	12.9
		Difference	4.3	7.6	10.2	10.3	2.4	-3.4	3.6	25.0

			Frequency (Hz)							
			63	125	250	500	1k	2k	4k	8k
Average	Mic 1	Measured	38.7	46.4	43.2	47.4	52.9	48.1	39.9	37.7
		ISO	41.1	45.5	34.9	39.1	53.8	53.7	43.6	26.8
		Difference	-2.5	0.9	8.3	8.3	-0.9	-5.6	-3.6	10.9
	Mic 2	Measured	37.2	44.1	41.0	43.6	52.4	46.0	37.8	37.1
		ISO	39.1	41.9	31.4	35.1	50.3	50.0	38.5	16.3
		Difference	-1.9	2.3	9.6	8.5	2.0	-4.0	-0.7	20.8
	Mic 3	Measured	38.6	44.4	47.4	51.7	56.3	50.7	42.2	38.2
		ISO	39.2	43.8	41.2	43.7	54.5	53.7	43.6	26.8
		Difference	-0.5	0.6	6.3	8.0	1.8	-3.0	-1.4	11.5
	Mic 4	Measured	37.3	41.8	44.0	48.5	53.4	47.8	41.1	38.1
		ISO	37.4	38.3	38.0	40.0	51.0	50.0	38.5	16.3
		Difference	-0.1	3.6	6.0	8.5	2.4	-2.3	2.6	21.8

Table 40, for the Crosswind Group, shows that the ISO 9613-2 method on average is over-predicting for the octave band that have center frequencies 63 Hz, 125 Hz, 1 KHz, 2 KHz, and 4 KHz for microphone locations Mic 1 and Mic 2, except Mic 2 at 4 KHz. While, the ISO method is shown on average to under-predict for the octave band centered at frequencies 250 Hz, 500 Hz, and 8 KHz for microphone locations Mic 1 and Mic 2, which are closer to the ground. In addition, the data show that on average the method is over-predicting for the octave band that have center frequencies 63 Hz, and 2 KHz) for microphone locations Mic 3 and Mic 4, except Mic 3 at 63 Hz. While, the ISO method is shown to under-predict for the octave band centered at 125 Hz, 250 Hz, 500 Hz, 1 KHz, 4 KHz, and 8 KHz for microphone locations Mic 3 and Mic 4, which are high above the ground. It is shown that the difference between measured and predicted octave band sound levels ranged from as low as 0.3 dB(A) to as high as 19 dB(A).

Table 40: Difference Between Measured & Predicted Octave Band Sound levels dB(A)

			Frequency (Hz)							
			63	125	250	500	1k	2k	4k	8k
Sample 1	Mic 1	Measured	41.8	47.2	45.9	49.2	53.4	51.7	43.8	38.3
		ISO-Cmet	42.7	47.1	38.6	40.6	53.5	53.8	44.6	28.7
		Difference	-0.8	0.1	7.3	8.7	-0.1	-2.1	-0.8	9.6
	Mic 2	Measured	38.4	43.8	42.0	41.1	49.7	48.7	40.2	37.7
		ISO-Cmet	40.6	43.4	35.0	36.6	50.0	50.2	39.6	18.6
		Difference	-2.2	0.4	7.0	4.5	-0.3	-1.6	0.6	19.1
	Mic 3	Measured	41.3	45.3	50.5	54.8	57.5	53.2	44.8	39.1
		ISO-Cmet	41.1	45.8	45.2	45.6	54.5	54.2	45.0	29.1
		Difference	0.2	-0.5	5.3	9.2	3.0	-1.0	-0.2	10.0
	Mic 4	Measured	37.5	41.8	44.0	50.8	52.6	48.6	41.7	38.3
		ISO-Cmet	39.0	40.0	41.8	41.7	50.9	50.4	39.8	18.8
		Difference	-1.6	1.8	2.2	9.1	1.7	-1.8	1.9	19.6
Sample 2	Mic 1	Measured	39.9	43.6	41.5	45.2	50.7	46.9	42.7	38.5
		ISO-Cmet	39.0	46.2	34.4	38.2	53.0	53.2	44.1	29.9
		Difference	0.9	-2.7	7.1	7.0	-2.3	-6.3	-1.4	8.6
	Mic 2	Measured	35.9	40.6	38.1	38.9	48.1	45.5	38.4	37.9
		ISO-Cmet	36.9	42.5	30.8	34.2	49.2	49.6	39.2	19.8
		Difference	-1.0	-1.9	7.3	4.7	-1.1	-4.2	-0.8	18.1
	Mic 3	Measured	39.5	41.8	46.2	52.1	55.8	50.5	44.7	39.5
		ISO-Cmet	37.4	44.9	41.0	43.2	53.7	53.6	44.5	30.3
		Difference	2.0	-3.0	5.2	8.9	2.1	-3.1	0.2	9.2
	Mic 4	Measured	35.5	38.6	40.4	48.2	51.3	46.6	42.6	38.5
		ISO-Cmet	35.4	39.1	37.6	39.3	50.1	49.8	39.4	20.0
		Difference	0.1	-0.5	2.8	8.9	1.3	-3.2	3.3	18.6
Sample 3	Mic 1	Measured	41.0	43.4	42.5	45.4	49.6	46.8	43.8	40.6
		ISO-Cmet	42.1	44.0	34.4	38.2	51.8	52.3	43.0	30.8
		Difference	-1.1	-0.5	8.0	7.2	-2.2	-5.5	0.8	9.8
	Mic 2	Measured	35.7	40.7	39.0	38.6	46.0	44.0	38.7	37.5
		ISO-Cmet	40.0	40.2	30.8	34.2	48.4	48.7	38.0	20.7
		Difference	-4.2	0.4	8.1	4.4	-2.4	-4.6	0.7	16.8
	Mic 3	Measured	41.2	42.1	46.7	52.0	54.9	51.2	46.7	42.8
		ISO-Cmet	40.5	42.6	41.1	43.2	52.9	52.7	43.4	31.2
		Difference	0.7	-0.5	5.6	8.8	2.1	-1.5	3.3	11.6
	Mic 4	Measured	35.1	39.3	41.0	47.9	49.8	46.0	42.1	38.9
		ISO-Cmet	38.4	36.8	37.7	39.3	49.2	48.9	38.2	20.8
		Difference	-3.3	2.5	3.3	8.6	0.6	-2.9	3.9	18.1

			Frequency (Hz)							
			63	125	250	500	1k	2k	4k	8k
Average	Mic 1	Measured	40.9	44.7	43.3	46.6	51.2	48.5	43.4	39.1
		ISO-Cmet	41.2	45.8	35.8	39.0	52.8	53.1	43.9	29.8
		Difference	-0.3	-1.0	7.5	7.6	-1.6	-4.6	-0.5	9.3
	Mic 2	Measured	36.7	41.7	39.7	39.5	47.9	46.1	39.1	37.7
		ISO-Cmet	39.1	42.1	32.2	35.0	49.2	49.5	39.0	19.7
		Difference	-2.5	-0.4	7.5	4.5	-1.3	-3.5	0.2	18.0
	Mic 3	Measured	40.6	43.1	47.8	53.0	56.1	51.7	45.4	40.5
		ISO-Cmet	39.7	44.4	42.4	44.0	53.7	53.5	44.3	30.2
		Difference	1.0	-1.3	5.4	9.0	2.4	-1.8	1.1	10.3
	Mic 4	Measured	36.0	39.9	41.8	49.0	51.2	47.0	42.2	38.6
		ISO-Cmet	37.6	38.6	39.0	40.1	50.1	49.7	39.1	19.9
		Difference	-1.6	1.3	2.8	8.9	1.2	-2.7	3.0	18.7

Table 41, for the Upwind Group, shows that the ISO 9613-2 method on average is over-predicting for the octave band that have center frequencies 63 Hz, 125 Hz, 1 KHz, 2 KHz, and 4 KHz for microphone locations Mic 1 and Mic 2. While, the ISO method is shown to under-predict for the octave band centered at 250 Hz, 500 Hz, and 8 KHz for microphone locations Mic 1 and Mic 2, which are closer to the ground. In addition, the data show that on average the method is over-predicting for the octave band that have center frequencies 63 Hz, and 2 KHz for microphone locations Mic 3 and Mic 4 which are high above the ground. While, the ISO method is shown to under-predict for the octave band centered at 125 Hz, 250 Hz, 500 Hz, 1 KHz, 4 KHz, and 8 KHz for microphone locations Mic 3 and Mic 4, except Mic 3 at 63 Hz and 4 KHz, Mic 4 at 1 KHz. It is shown that the difference between measured and predicted octave band sound levels ranged from as low as 0.3 dB(A) to as high as 19 dB(A).

Table 41: Difference Between Measured & Predicted Octave Band Sound levels dB(A)

			Frequency (Hz)							
			63	125	250	500	1k	2k	4k	8k
Sample 1	Mic 1	Measured	35.1	40.7	38.2	41.2	45.9	42.6	39.0	37.8
		ISO-Cmet	39.6	40.8	33.3	38.1	51.7	51.4	42.3	25.8
		Difference	-4.4	-0.1	4.9	3.2	-5.7	-8.8	-3.3	12.0
	Mic 2	Measured	39.8	38.3	38.1	35.2	44.1	39.8	37.0	37.3
		ISO-Cmet	37.4	37.1	29.6	34.0	48.0	47.6	37.1	15.6
		Difference	2.4	1.2	8.4	1.2	-3.9	-7.7	-0.1	21.7
	Mic 3	Measured	42.2	42.3	44.9	50.2	55.1	49.0	43.2	39.2
		ISO-Cmet	38.3	39.7	40.2	43.4	53.0	52.0	42.9	26.4
		Difference	3.9	2.6	4.7	6.9	2.1	-3.0	0.3	12.8
	Mic 4	Measured	37.8	36.1	39.4	41.9	46.9	43.0	39.1	36.8
		ISO-Cmet	36.1	33.8	36.6	39.3	49.1	48.0	37.5	16.0
		Difference	1.7	2.2	2.8	2.7	-2.2	-4.9	1.6	20.8
Sample 2	Mic 1	Measured	35.2	40.6	39.6	42.4	45.5	43.2	38.3	37.7
		ISO-Cmet	38.2	41.3	33.7	39.2	49.0	49.5	44.2	30.6
		Difference	-3.0	-0.7	5.9	3.1	-3.4	-6.3	-5.8	7.2
	Mic 2	Measured	31.7	35.8	34.2	35.0	42.0	38.7	36.7	37.1
		ISO-Cmet	36.1	37.5	30.1	35.1	45.3	45.7	39.0	20.4
		Difference	-4.3	-1.7	4.1	-0.1	-3.4	-7.1	-2.3	16.7
	Mic 3	Measured	33.9	39.1	44.1	51.7	54.1	48.8	43.2	38.7
		ISO-Cmet	36.9	40.2	40.6	44.5	50.3	50.2	44.8	31.2
		Difference	-3.0	-1.1	3.4	7.2	3.8	-1.4	-1.6	7.5
	Mic 4	Measured	29.1	34.1	35.8	42.5	45.1	41.0	39.0	36.4
		ISO-Cmet	34.7	34.3	37.1	40.4	46.4	46.1	39.4	20.8
		Difference	-5.6	-0.2	-1.3	2.1	-1.3	-5.2	-0.5	15.7
Sample 3	Mic 1	Measured	38.1	41.9	40.4	44.9	48.8	46.5	44.5	38.4
		ISO-Cmet	43.7	43.8	31.1	36.1	50.0	49.5	44.0	27.3
		Difference	-5.6	-1.9	9.2	8.8	-1.2	-3.0	0.5	11.1
	Mic 2	Measured	34.9	37.6	36.0	37.3	43.7	41.2	39.6	37.1
		ISO-Cmet	41.5	40.0	27.5	32.0	46.4	45.7	38.9	17.1
		Difference	-6.6	-2.4	8.6	5.3	-2.6	-4.4	0.7	19.9
	Mic 3	Measured	37.3	40.1	44.7	49.6	53.7	47.8	43.6	38.8
		ISO-Cmet	42.4	42.7	38.0	41.4	51.3	50.1	44.7	28.0
		Difference	-5.1	-2.5	6.7	8.2	2.3	-2.3	-1.1	10.8
	Mic 4	Measured	32.6	34.9	37.2	43.9	47.2	42.7	40.3	36.5
		ISO-Cmet	40.2	36.8	34.5	37.3	47.4	46.1	39.3	17.5
		Difference	-7.6	-1.9	2.7	6.6	-0.2	-3.4	1.0	19.0

			Frequency (Hz)							
			63	125	250	500	1k	2k	4k	8k
Sample 4	Mic 1	Measured	39.9	39.8	41.2	41.4	47.1	44.9	42.2	37.9
		ISO-Cmet	39.1	41.7	37.7	34.1	48.7	49.5	40.8	24.9
		Difference	0.7	-1.9	3.5	7.4	-1.7	-4.6	1.4	13.0
	Mic 2	Measured	37.5	37.7	36.0	36.6	43.6	40.4	36.9	37.2
		ISO-Cmet	37.0	37.9	34.1	30.0	45.1	45.7	35.7	14.7
		Difference	0.5	-0.2	1.9	6.6	-1.5	-5.4	1.1	22.4
	Mic 3	Measured	40.0	39.3	47.2	50.1	53.1	48.1	43.7	38.5
		ISO-Cmet	37.8	40.6	44.6	39.4	50.1	50.2	41.5	25.6
		Difference	2.2	-1.3	2.6	10.7	3.1	-2.1	2.2	12.9
	Mic 4	Measured	35.8	35.6	38.7	42.6	46.5	42.5	39.4	36.3
		ISO-Cmet	35.6	34.7	41.1	35.3	46.1	46.1	36.1	15.1
		Difference	0.2	0.9	-2.4	7.3	0.3	-3.6	3.3	21.2
Average	Mic 1	Measured	37.1	40.8	39.8	42.5	46.8	44.3	41.0	37.9
		ISO-Cmet	40.1	41.9	34.0	36.9	49.8	50.0	42.8	27.1
		Difference	-3.1	-1.1	5.9	5.6	-3.0	-5.7	-1.8	10.8
	Mic 2	Measured	36.0	37.4	36.1	36.0	43.4	40.0	37.5	37.2
		ISO-Cmet	38.0	38.1	30.3	32.8	46.2	46.2	37.7	17.0
		Difference	-2.0	-0.8	5.8	3.2	-2.8	-6.2	-0.2	20.2
	Mic 3	Measured	38.3	40.2	45.2	50.4	54.0	48.4	43.4	38.8
		ISO-Cmet	38.8	40.8	40.9	42.2	51.2	50.6	43.5	27.8
		Difference	-0.5	-0.6	4.4	8.2	2.8	-2.2	-0.1	11.0
	Mic 4	Measured	33.8	35.2	37.8	42.8	46.4	42.3	39.4	36.5
		ISO-Cmet	36.7	34.9	37.3	38.1	47.2	46.6	38.1	17.3
		Difference	-2.9	0.3	0.5	4.7	-0.8	-4.3	1.4	19.2

Table 42 shows the results for both the ISO method and the ISO method with meteorological correction included seem to be similar. This indicates that the meteorological correction factor applied did not minimize the difference between the measured and predicted sound levels. This is likely due to the fact that the correction factor is directly depended on the source and receiver heights, and does not directly include any parameters that explicit functions of wind shear or lapse rates.

Moreover, when analyzing the results from using the ISO-method to predict octave band sound levels. It was expected that the difference should increase by frequency since refraction effects increases at higher frequency. However, it appears that the ISO method works well in the middle frequencies but does not do as well at both the low and high frequencies. This is most likely an inability to handle the ground effects properly and that refraction effects are not included.

Table 42: Summary of Difference Between Measured and Predicted Octave Band Sound Levels

		63	125	250	500	1k	2k	4k	8k
Mic 1	Downwind	-1.8	1.5	8.9	8.9	-0.3	-4.9	-2.9	11.6
	Crosswind	-0.3	-1.0	7.5	7.6	-1.6	-4.6	-0.5	9.3
	Upwind	-3.1	-1.1	5.9	5.6	-3.0	-5.7	-1.8	10.8
Mic 2	Downwind	-1.2	3.0	10.3	9.2	2.7	-3.3	0.0	21.5
	Crosswind	-2.5	-0.4	7.5	4.5	-1.3	-3.5	0.2	18.0
	Upwind	-2.0	-0.8	5.8	3.2	-2.8	-6.2	-0.2	20.2
Mic 3	Downwind	-0.1	1.0	6.7	8.4	2.3	-2.6	-1.0	11.9
	Crosswind	1.0	-1.3	5.4	9.0	2.4	-1.8	1.1	10.3
	Upwind	-0.5	-0.6	4.4	8.2	2.8	-2.2	-0.1	11.0
Mic 4	Downwind	0.5	4.1	6.6	9.0	2.9	-1.7	3.2	22.3
	Crosswind	-1.6	1.3	2.8	8.9	1.2	-2.7	3.0	18.7
	Upwind	-2.9	0.3	0.5	4.7	-0.8	-4.3	1.4	19.2

It should be reiterated that this method was not primarily derived to model traffic noise sources. The ISO method requires that the ground be fairly flat or have a uniform slope between source and receiver for accurate prediction and this case has been met. However, the surface characteristics vary for this location. All of these factors contribute

to the inaccurate modeling of ground effects, hence the difference in predicted sound levels.

This analysis indicates that a correction for true atmospheric refraction due to wind shear and lapse rate is needed. The following section will illustrate the results when combining the ISO9613-2 method with the Wayson refraction empirical model that was developed to account for refraction caused by wind gradient and lapse rates.

ISO 9613-2 (with Wayson Refraction Model)

The empirical model developed by Wayson [Wayson, 1989], was used to predict the excess attenuation due to refraction during positive and negative wind cases measured for this research. Equations 22 and 23 are the empirical relations used for positive wind speed (wind moving from source to receiver) and negative wind speed (wind moving from receiver to the source) respectively.

This section will combine the attenuation predicted by the ISO 9613-2 with the Wayson empirical refraction model. Tables 43 – 45 present the calculated different attenuation in dB for each microphone positions of the three groups: Downwind, Crosswind and Upwind. Afterward, a summary of the sound levels predicted by the ISO9613-2 with the Wayson refraction model attenuation applied is presented for each group and a comparison to the measured sound levels for each microphone evaluated.

Table 43: Attenuation (dB) for Microphones in Downwind Group

Attenuation		Frequency (Hz)							
		63	125	250	500	1k	2k	4k	8k
Mic 1	A_{div}	7.7	7.7	7.7	7.7	7.7	7.7	7.7	7.7
	A_{atm}	0.0	0.0	0.2	0.5	0.9	1.6	3.3	9.8
	A_{gr}	-5.0	1.3	14.6	17.7	5.3	0.0	0.0	0.0
	A_{ref}	-0.7	-0.7	-0.7	-0.7	-0.7	-0.7	-0.7	-0.7
	Sum	2.0	8.3	21.7	25.1	13.2	8.5	10.2	16.8
Mic 2	A_{div}	10.2	10.2	10.2	10.2	10.2	10.2	10.2	10.2
	A_{atm}	0.0	0.1	0.3	0.8	1.7	2.8	5.8	17.4
	A_{gr}	-5.4	2.5	15.5	18.8	5.6	0.0	0.0	0.0
	A_{ref}	-1.3	-1.3	-1.3	-1.3	-1.3	-1.3	-1.3	-1.3
	Sum	3.5	11.4	24.7	28.5	16.2	11.7	14.7	26.2
Mic 3	A_{div}	7.7	7.7	7.7	7.7	7.7	7.7	7.7	7.7
	A_{atm}	0.0	0.0	0.2	0.5	0.9	1.6	3.3	9.8
	A_{gr}	-3.0	3.1	8.3	13.0	4.7	0.0	0.0	0.0
	A_{ref}	-1.9	-1.9	-1.9	-1.9	-1.9	-1.9	-1.9	-1.9
	Sum	2.8	9.0	14.3	19.3	11.4	7.4	9.1	15.6
Mic 4	A_{div}	10.2	10.2	10.2	10.2	10.2	10.2	10.2	10.2
	A_{atm}	0.0	0.1	0.3	0.8	1.7	2.8	5.8	17.4
	A_{gr}	-3.7	6.1	8.9	13.9	5.0	0.0	0.0	0.0
	A_{ref}	-3.4	-3.4	-3.4	-3.4	-3.4	-3.4	-3.4	-3.4
	Sum	3.1	13.0	16.0	21.5	13.4	9.6	12.6	24.2

Table 44: Attenuation (dB) for Microphones in Crosswind Group

Attenuation		Frequency (Hz)							
		63	125	250	500	1k	2k	4k	8k
Mic 1	A _{div}	7.7	7.7	7.7	7.7	7.7	7.7	7.7	7.7
	A _{atm}	0.0	0.0	0.2	0.4	0.8	1.4	3.1	9.8
	A _{gr}	-5.0	1.3	14.6	17.7	5.3	0.0	0.0	0.0
	A _{ref}	-1.3	-1.3	-1.3	-1.3	-1.3	-1.3	-1.3	-1.3
	Sum	1.4	7.8	21.1	24.5	12.5	7.8	9.5	16.2
Mic 2	A _{div}	10.2	10.2	10.2	10.2	10.2	10.2	10.2	10.2
	A _{atm}	0.0	0.1	0.3	0.8	1.4	2.4	5.5	17.5
	A _{gr}	-5.4	2.5	15.5	18.8	5.6	0.0	0.0	0.0
	A _{ref}	-2.2	-2.2	-2.2	-2.2	-2.2	-2.2	-2.2	-2.2
	Sum	2.6	10.5	23.7	27.5	15.0	10.4	13.5	25.4
Mic 3	A _{div}	7.7	7.7	7.7	7.7	7.7	7.7	7.7	7.7
	A _{atm}	0.0	0.0	0.2	0.4	0.8	1.4	3.1	9.8
	A _{gr}	-3.0	3.1	8.3	13.0	4.7	0.0	0.0	0.0
	A _{ref}	-1.6	-1.6	-1.6	-1.6	-1.6	-1.6	-1.6	-1.6
	Sum	3.1	9.2	14.6	19.6	11.5	7.5	9.2	15.9
Mic 4	A _{div}	10.2	10.2	10.2	10.2	10.2	10.2	10.2	10.2
	A _{atm}	0.0	0.1	0.3	0.8	1.4	2.4	5.5	17.5
	A _{gr}	-3.7	6.1	8.9	13.9	5.0	0.0	0.0	0.0
	A _{ref}	-2.6	-2.6	-2.6	-2.6	-2.6	-2.6	-2.6	-2.6
	Sum	3.9	13.8	16.7	22.2	13.9	10.0	13.1	25.0

Table 45: Attenuation (dB) for Microphones in Upwind Group

Attenuation		Frequency (Hz)							
		63	125	250	500	1k	2k	4k	8k
Mic 1	A_{div}	7.7	7.7	7.7	7.7	7.7	7.7	7.7	7.7
	A_{atm}	0.0	0.0	0.2	0.5	0.9	1.6	3.3	9.8
	A_{gr}	-5.0	1.3	14.6	17.7	5.3	0.0	0.0	0.0
	A_{ref}	5.3	5.3	5.3	5.3	5.3	5.3	5.3	5.3
	Sum	8.0	14.3	27.7	31.1	19.2	14.5	16.2	22.8
Mic 2	A_{div}	10.2	10.2	10.2	10.2	10.2	10.2	10.2	10.2
	A_{atm}	0.0	0.1	0.3	0.8	1.7	2.8	5.8	17.4
	A_{gr}	-5.4	2.5	15.5	18.8	5.6	0.0	0.0	0.0
	A_{ref}	8.5	8.5	8.5	8.5	8.5	8.5	8.5	8.5
	Sum	13.3	21.3	34.5	38.4	26.0	21.5	24.5	36.1
Mic 3	A_{div}	7.7	7.7	7.7	7.7	7.7	7.7	7.7	7.7
	A_{atm}	0.0	0.0	0.2	0.5	0.9	1.6	3.3	9.8
	A_{gr}	-3.0	3.1	8.3	13.0	4.7	0.0	0.0	0.0
	A_{ref}	5.4	5.4	5.4	5.4	5.4	5.4	5.4	5.4
	Sum	10.1	16.3	21.6	26.6	18.7	14.7	16.4	22.9
Mic 4	A_{div}	10.2	10.2	10.2	10.2	10.2	10.2	10.2	10.2
	A_{atm}	0.0	0.1	0.3	0.8	1.7	2.8	5.8	17.4
	A_{gr}	-3.7	6.1	8.9	13.9	5.0	0.0	0.0	0.0
	A_{ref}	8.2	8.2	8.2	8.2	8.2	8.2	8.2	8.2
	Sum	14.6	24.5	27.5	33.0	24.9	21.1	24.1	35.7

Comparing the attenuation between the different groups, it can be determined that the attenuation factor (α value) within the atmospheric absorption A_{atm} term had changed by only 1% to 10% for the different groups. This is due to the small change in temperatures and relative humidity for the days included in this study. The refraction term, A_{ref} varied from -0.7 dB to -3.4 dB for the downwind conditions, while A_{ref} varied from 5.3 dB to 8.5 dB for the upwind conditions. As previously shown in the analysis of the measured data section, wind shear was more dominant than lapse rates due to the

small variation in lapse rate during the measurement periods. Hence, it is expected there will be an increase in sound levels for all microphones for the Downwind Group as the sound waves will bend downward increasing sound levels at the microphones. As for Upwind Group, which is an upwind condition, it was expected that the results will show attenuation in sound level because the sound waves will tend to bend upwards thus reducing sound levels at the microphones. Hence, a reduction in sound level is expected for all microphones within the Upwind Group.

Downwind Group

The analysis consists of applying all the attenuation factors: A_{div} , A_{atm} , A_{gr} , and A_{ref} . A_{ref} is the attenuation refraction correction based on the Wayson empirical model. A-weighted adjustments were then applied for each corresponding frequency. Each frequency contribution was then logarithmically summed to derive A-weighted sound level correction factors. The A-weighted adjusted attenuation factors were applied to the measured sound levels at the Reference microphone (Ref.) to calculate the predicted sound levels for the different microphone locations: Mic 1, Mic 2, Mic 3 and Mic 4.

Figure 31 and Table 46 present the measured sound levels dB(A), the predicted sound levels dB(A) using the ISO 9613-2 method (with the Wayson refraction empirical model) and the difference between the two methods for each microphone within the Downwind Group. The last part of the table shows the average of the six samples within

the Downwind Group, and highlights the average difference between measured and predicted sound levels for the various microphones. It is shown that on average the difference is within 1.9 dB(A).

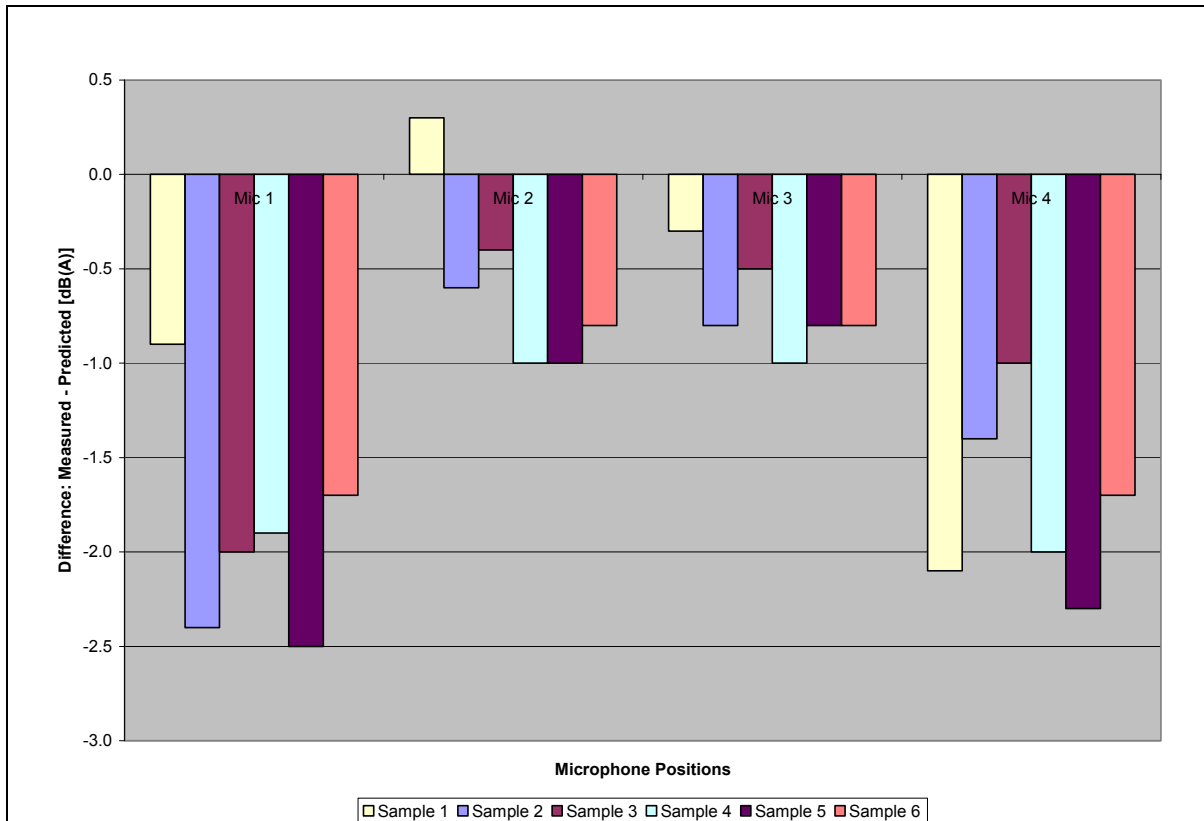


Figure 31: Difference Between Measured and Predicted Sound Levels for Downwind Group

Table 46: Difference between Measured and Predicted Sound levels dB(A) for Downwind Group

		Measured	ISO-wayson	Difference
Sample 1	Ref	69.9	69.9	0.0
	Mic 1	56.4	57.3	-0.9
	Mic 2	54.6	54.3	0.3
	Mic 3	59.4	59.7	-0.3
	Mic 4	56.2	58.3	-2.1
Sample 2	Ref	73.7	73.7	0.0
	Mic 1	57.3	59.7	-2.4
	Mic 2	55.9	56.5	-0.6
	Mic 3	60.5	61.3	-0.8
	Mic 4	57.7	59.1	-1.4
Sample 3	Ref	73.7	73.7	0.0
	Mic 1	57.7	59.7	-2.0
	Mic 2	56.1	56.5	-0.4
	Mic 3	60.8	61.3	-0.5
	Mic 4	57.8	58.8	-1.0
Sample 4	Ref	72.0	72.0	0.0
	Mic 1	57.4	59.3	-1.9
	Mic 2	55.9	56.9	-1.0
	Mic 3	60.2	61.2	-1.0
	Mic 4	57.3	59.3	-2.0
Sample 5	Ref	68.0	68.0	0.0
	Mic 1	53.2	55.7	-2.5
	Mic 2	52.2	53.2	-1.0
	Mic 3	56.5	57.3	-0.8
	Mic 4	53.6	55.9	-2.3
Sample 6	Ref	68.4	68.4	0.0
	Mic 1	55.2	56.9	-1.7
	Mic 2	53.5	54.3	-0.8
	Mic 3	57.4	58.2	-0.8
	Mic 4	54.8	56.5	-1.7
Average	Ref	71.0	71.0	0.0
	Mic 1	56.2	58.1	-1.9
	Mic 2	54.7	55.3	-0.6
	Mic 3	59.1	59.8	-0.7
	Mic 4	56.2	58.0	-1.7

It is shown that this method is over-predicting for all microphones locations, except Sample 2, Mic 2 where it is under-predicting. After application of the Wayson empirical method, the difference between the measured and predicted sound levels has been reduced to within 1 dB(A) for Mic 2 and Mic 3, and reduced to within 2 dB(A) for Mic 1 and Mic 4. The inaccuracy in modeling ground effects might have contributed to the larger difference for the microphone positions near the ground. Overall, it is shown that the use of the Wayson method reduced the difference between measured and predicted sound levels in downwind conditions.

Of interest is Sample 5, where there is a combination between a strong wind condition and inversion. This case has shown that inversion lapse rate has amplified the downward wind refraction effects. Also, the inversion has caused ground effects to vary from the other sample periods within the group, thus increasing the sound levels for the microphone positions, and hence slightly reducing the difference between measured and predicted sound levels when compared to other sample periods.

Also, it is shown that the difference between the measured and predicted sound level is larger (-2.5 and -1 dB(A)) for Mic 1 and Mic 2 respectively compared with the other five sample periods. This is may also be attributed to the increase of refraction due to the effects of both downward refraction effects and inversion lapse rate.

Crosswind Group

Table 47 and Figure 32 present the measured sound levels dB(A), the predicted sound levels dB(A) using the ISO 9613-2 method (with the Wayson refraction empirical model) and the difference between the two methods for each microphone within the Crosswind Group. The last part of the table shows the average of the three samples within the Crosswind Group, and highlights the average difference between measured and predicted sound levels for the various microphones.

Table 47: Difference between Measured and Predicted Sound levels dB(A) for Crosswind Group

		Measured	ISO-wayson	Difference
Sample 1	Ref	72.3	72.3	0.0
	Mic 1	57.7	60.2	-2.5
	Mic 2	53.9	58.0	-4.1
	Mic 3	61.1	61.9	-0.8
	Mic 4	56.4	57.8	-1.4
Sample 2	Ref	70.8	70.8	0.0
	Mic 1	54.3	58.9	-4.6
	Mic 2	51.5	56.3	-4.8
	Mic 3	58.8	59.1	-0.3
	Mic 4	54.7	56.3	-1.6
Sample 3	Ref	70.2	70.2	0.0
	Mic 1	54.2	57.7	-3.5
	Mic 2	50.4	54.8	-4.4
	Mic 3	58.7	59.3	-0.6
	Mic 4	53.9	55.2	-1.3
Average	Ref	71.1	71.1	0.0
	Mic 1	55.4	58.9	-3.5
	Mic 2	51.9	56.4	-4.4
	Mic 3	59.5	60.1	-0.6
	Mic 4	55.0	56.4	-1.4

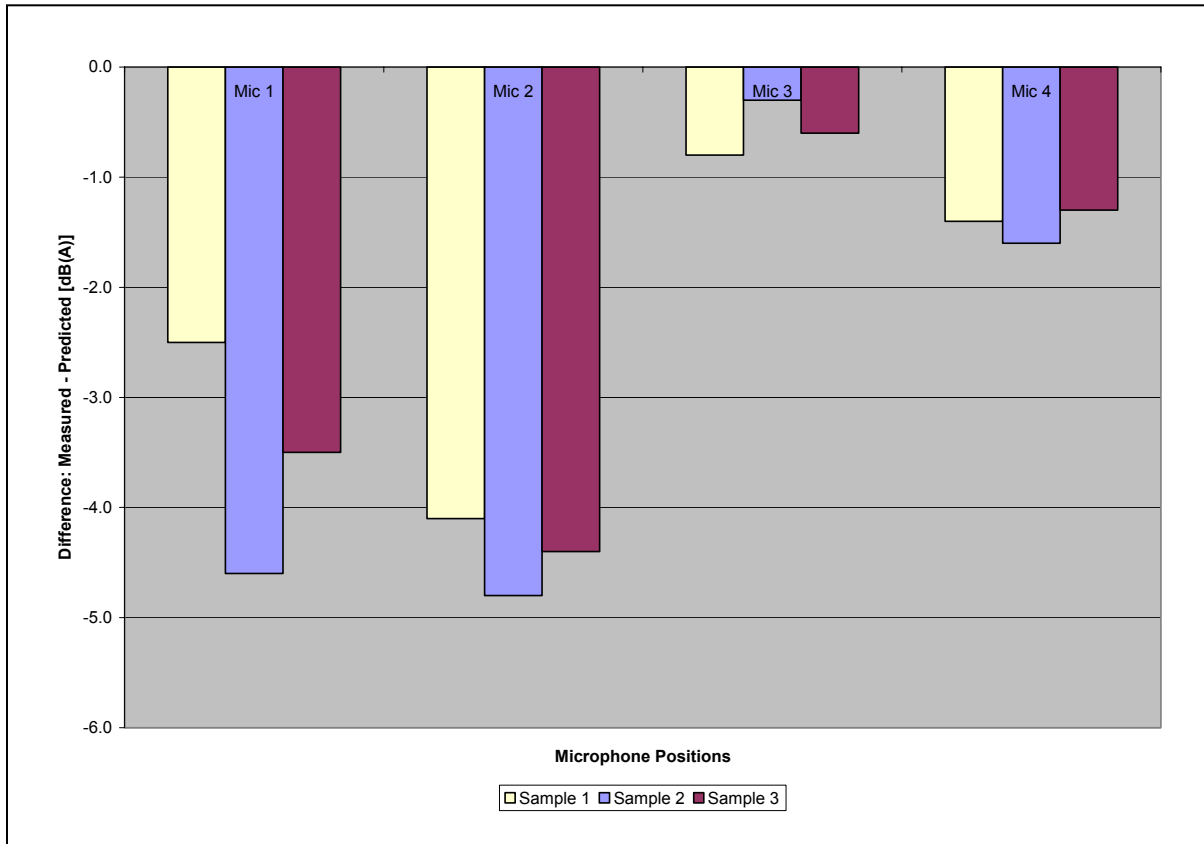


Figure 32: Difference Between Measured and Predicted Sound Levels for Crosswind Group

It is shown that this method results in over-prediction for all microphones positions. The difference between measured and predicted sound levels remains large for Mic 1 and Mic 2, while the difference is reduced to within 1.5 dBA for Mic 3 and Mic 4. It is shown that this combination has reduced the difference between measured and predicted sound levels for microphones farther above the ground, i.e. Mic 3 and Mic 4, which are outside the boundary of the ground effects.

Upwind Group

Table 48 and Figure 33 present the measured sound levels dB(A), the predicted sound levels dB(A) using the ISO 9613-2 method (with the Wayson refraction empirical model included) and the difference between the two methods for each microphone within the Upwind Group. The last part of the table shows the average of the four samples within the Upwind Group, and highlights the average difference between measured and predicted sound levels for the various microphones.

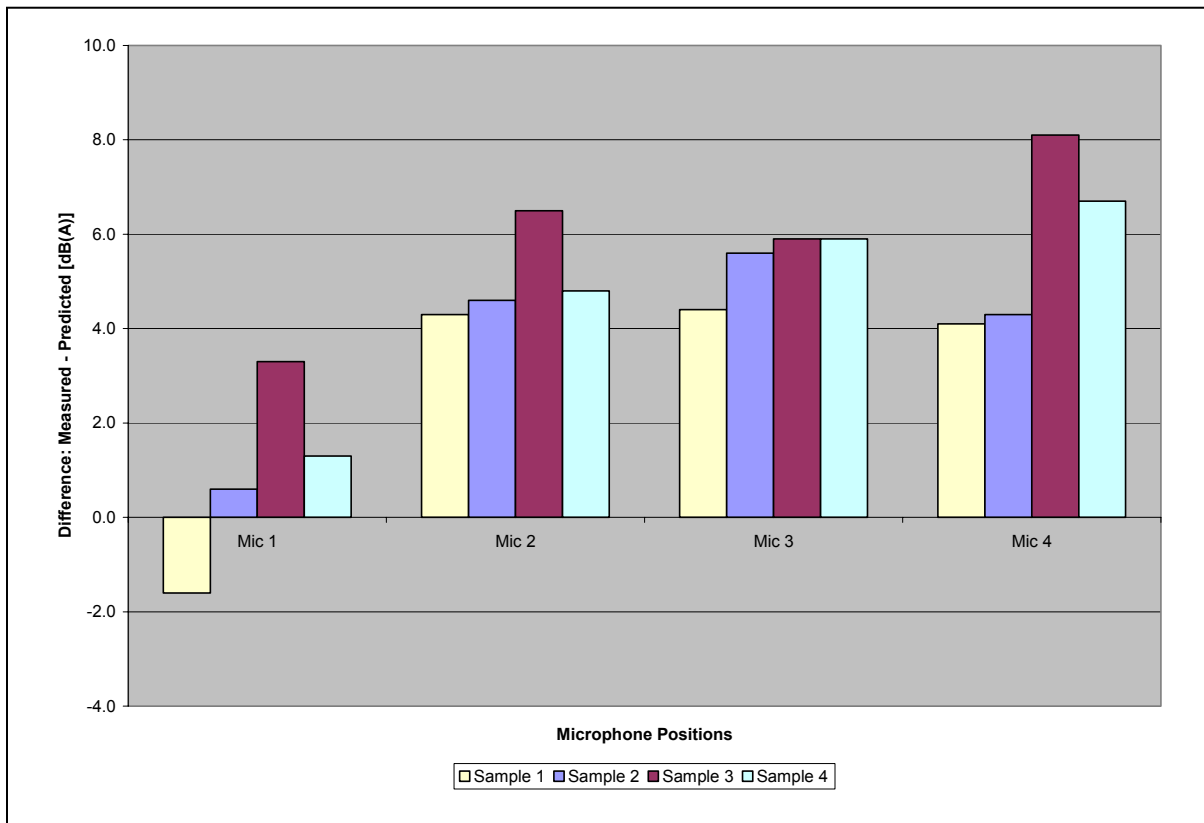


Figure 33: Difference Between Measured and Predicted Sound Levels for Upwind Group

Table 48: Difference between Measured and Predicted Sound levels dB(A) for Upwind Group

		Measured	ISO-wayson	Difference
Sample 1	Ref	70.8	70.8	0.0
	Mic 1	50.3	51.9	-1.6
	Mic 2	48.6	44.3	4.3
	Mic 3	57.8	53.4	4.4
	Mic 4	50.7	46.6	4.1
Sample 2	Ref	70.1	70.1	0.0
	Mic 1	50.4	49.8	0.6
	Mic 2	46.4	41.8	4.6
	Mic 3	57.4	51.8	5.6
	Mic 4	49.1	44.8	4.3
Sample 3	Ref	69.2	69.2	0.0
	Mic 1	53.4	50.1	3.3
	Mic 2	48.4	41.9	6.5
	Mic 3	56.6	50.7	5.9
	Mic 4	50.8	42.7	8.1
Sample 4	Ref	68.7	68.7	0.0
	Mic 1	51.8	50.5	1.3
	Mic 2	48.0	43.2	4.8
	Mic 3	56.7	50.8	5.9
	Mic 4	50.3	43.6	6.7
Average	Ref	69.7	69.7	0.0
	Mic 1	51.5	50.6	0.9
	Mic 2	47.9	42.8	5.1
	Mic 3	57.1	51.7	5.5
	Mic 4	50.2	44.4	5.8

It is shown that this method is under-predicting for all microphones position, except for Sample 1, Mic 1 where it is over-predicting. Moreover, it is presented that the difference between measured and predicted sound levels varies from acceptable to too large for all microphones, ranging from 1 dB(A) to 6 dB(A) for different microphone

locations. Furthermore, on average the difference between measured and predicted sound levels for the majority of the microphone in the Upwind Group is larger than the other Groups because only one case of upwind conditions has occurred during the study period.

In Sample 4, the normal lapse rate case should have increased the sound levels at the higher microphone locations; and this was amplified by the dominant upward refraction effects. This was shown by the reduction in the difference between measured and predicted sound levels for Sample 4 when compared to other sample periods as shown in Figure 33.

Summary

Table 49 and Figure 34 show the average difference in sound levels between the Reference and the microphone locations Mic 1, Mic 2, Mic 3 and Mic 4. The data illustrate small difference between the Downwind and the Crosswind Groups when calculating the difference between the Reference and the microphone locations, while the numbers are significantly higher for the difference between the Reference and the microphone positions for the Upwind Group. The larger difference occurring in the upwind group might be attributed to the inaccurate results obtained when using the Wayson empirical refraction model in upwind conditions. This is likely due to the fact that the Wayson model did not include many upwind cases when the model was

developed, hence the large difference between the measured and predicted in sound levels when compared to the same results for the Downwind and the Crosswind Groups

Table 49: Average Difference Between Reference and Microphone Positions dB(A)

	Ref- Mic 1	Ref- Mic 2	Ref- Mic 3	Ref- Mic 4
Downwind	12.9	15.7	11.1	13.0
Crosswind	12.2	14.7	11.0	14.7
Upwind	19.1	26.9	18.0	25.3

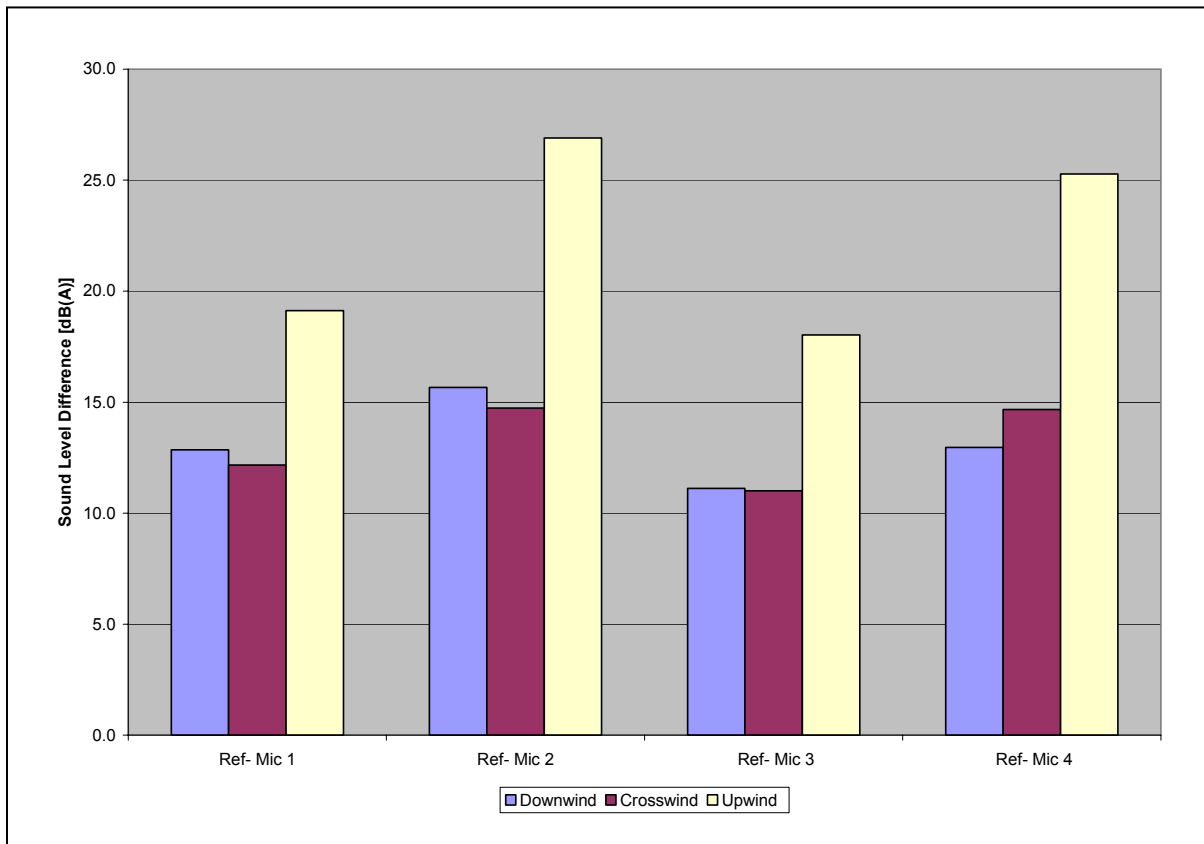


Figure 34: Average Difference Between Reference and Microphone Positions

Table 50 and Figure 35 present the summary of the average difference between measured and predicted sound levels dB(A) using the ISO 9613-2 method with the Wayson refraction empirical model attenuation applied.

Table 50: Average Difference between Measured and Predicted Sound levels dB(A)

	Downwind	Crosswind	Upwind
Mic 1	-1.9	-3.5	0.9
Mic 2	-0.6	-4.4	5.1
Mic 3	-0.7	-0.6	5.5
Mic 4	-1.7	-1.4	5.8

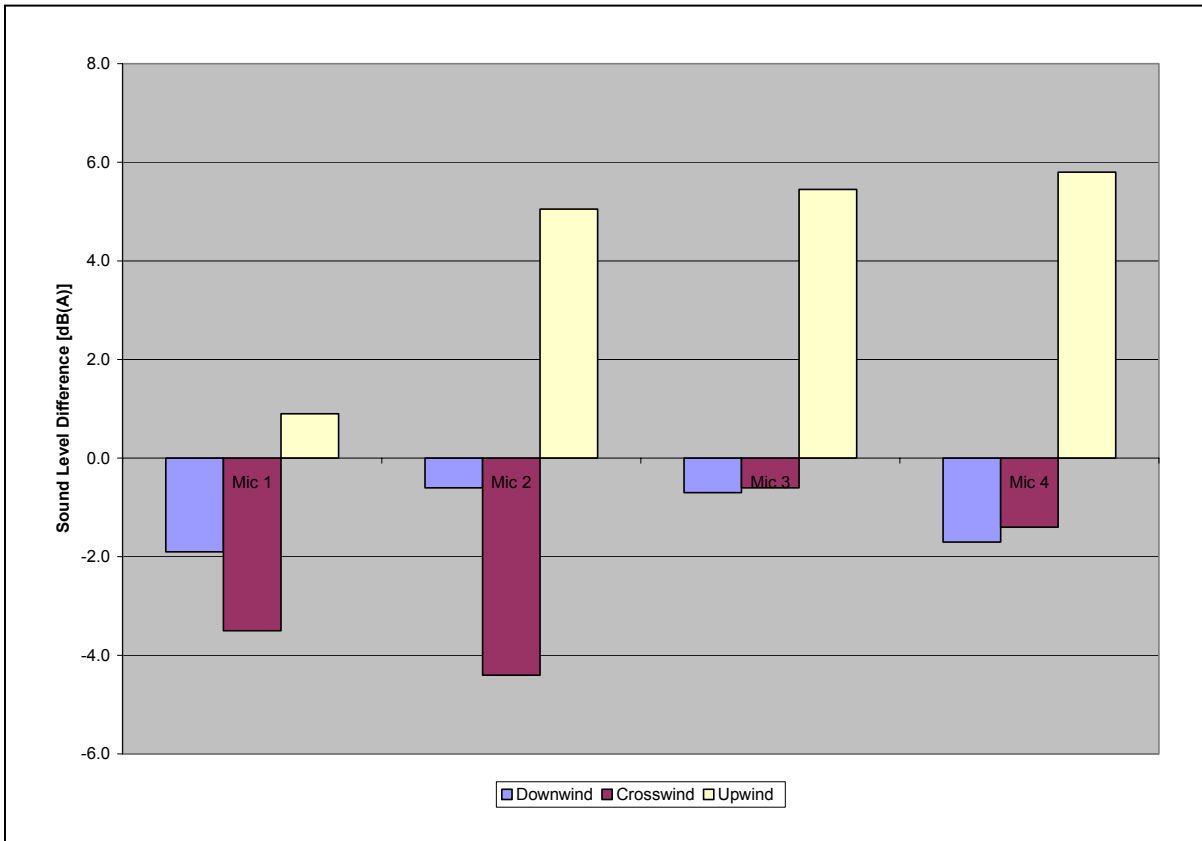


Figure 35: Average Difference between Measured and Predicted Sound levels

It is shown that combining the ISO 9613-2 method with Wayson refraction empirical model has worked well and reduced the difference between measured and predicted sound levels for the downwind conditions (the Downwind Group) and to some extent in the crosswind conditions (the Crosswind Group). Meanwhile, this combination has reduced the difference between predicted and measured sound levels but has under-predicted for upwind conditions.

Tables 51 - 53 present the difference between the measured octave band sound levels in dB(A) and the predicted octave band sound levels in dB(A) using the ISO 9613-2 method (with the Wayson refraction empirical model included) for the Downwind, Crosswind and Upwind Groups respectively.

Table 51, for the Downwind Group, shows that this method on average is over-predicting for the octave band that have center frequencies 63 Hz, 1 KHz, 2 KHz, and 4 KHz for the majority of the microphone locations, except Mic 2 and Mic 3 at 1 KHz. While, the method is shown to under-predict for the octave band centered at 125 Hz, 250 Hz, 500 Hz, and 8 KHz for the majority of the microphone locations, except Mic 3 at 125 Hz. It is shown that the difference between measured and predicted octave band sound levels ranged from 0 to 19 dB(A).

Table 51: Difference Between Measured & Predicted Octave Band Sound levels dB(A)

			Frequency (Hz)							
			63	125	250	500	1k	2k	4k	8k
Sample 1	Mic 1	Measured	39.3	45.9	43.5	47.8	53.4	48.5	40.4	37.6
		ISO-Wayson	42.9	44.7	36.3	38.7	53.7	53.5	43.6	27.6
		Difference	-3.6	1.2	7.2	9.1	-0.3	-5.0	-3.2	10.0
	Mic 2	Measured	37.3	43.4	39.7	43.1	52.6	45.8	37.8	37.1
		ISO-Wayson	41.4	41.6	33.4	35.3	50.8	50.4	39.1	18.1
		Difference	-4.1	1.7	6.3	7.8	1.8	-4.5	-1.4	19.0
	Mic 3	Measured	39.2	44.9	47.9	52.7	56.6	50.7	42.2	38.2
		ISO-Wayson	42.9	44.9	44.5	45.3	56.4	55.5	45.6	29.6
		Difference	-3.7	0.0	3.4	7.4	0.2	-4.7	-3.3	8.6
	Mic 4	Measured	36.8	41.9	42.9	48.4	53.6	47.9	41.1	38.1
		ISO-Wayson	43.3	41.6	43.6	43.8	55.1	54.0	42.7	21.7
		Difference	-6.5	0.2	-0.7	4.6	-1.4	-6.1	-1.7	16.4
Sample 2	Mic 1	Measured	38.1	47.5	44.4	49.7	54.0	49.5	40.4	37.6
		ISO-Wayson	41.4	47.4	37.3	44.5	56.6	55.3	44.9	28.0
		Difference	-3.3	0.1	7.1	5.2	-2.6	-5.8	-4.5	9.6
	Mic 2	Measured	36.8	46.5	43.8	45.7	53.4	47.0	38.0	37.1
		ISO-Wayson	39.7	44.1	34.2	40.9	53.5	52.0	40.2	18.4
		Difference	-2.9	2.4	9.6	4.7	-0.1	-5.0	-2.3	18.7
	Mic 3	Measured	37.8	45.3	48.8	54.3	57.5	51.8	42.5	38.2
		ISO-Wayson	40.5	46.7	44.7	50.3	58.4	56.4	46.0	29.1
		Difference	-2.6	-1.4	4.1	4.1	-0.9	-4.6	-3.5	9.0
	Mic 4	Measured	35.7	42.9	45.0	51.7	54.5	48.9	41.4	38.1
		ISO-Wayson	40.1	42.6	42.9	48.0	56.3	54.1	42.3	20.5
		Difference	-4.4	0.4	2.1	3.7	-1.7	-5.2	-0.9	17.7
Sample 3	Mic 1	Measured	41.0	47.1	44.5	50.1	54.3	50.1	41.5	37.6
		ISO-Wayson	46.1	49.4	36.7	44.8	55.9	55.5	45.2	27.9
		Difference	-5.1	-2.2	7.8	5.4	-1.6	-5.4	-3.7	9.7
	Mic 2	Measured	39.2	45.4	43.2	46.8	53.6	47.6	38.6	37.1
		ISO-Wayson	44.5	46.1	33.6	41.2	52.8	52.2	40.5	18.2
		Difference	-5.3	-0.7	9.6	5.6	0.9	-4.6	-2.0	18.9
	Mic 3	Measured	40.6	45.2	48.4	54.2	57.9	52.6	43.5	38.4
		ISO-Wayson	45.3	48.8	44.1	50.6	57.7	56.7	46.4	29.1
		Difference	-4.7	-3.6	4.3	3.6	0.2	-4.1	-2.8	9.3
	Mic 4	Measured	38.0	42.7	45.2	51.2	54.8	49.6	41.9	38.3
		ISO-Cmet	44.7	44.5	42.2	48.1	55.4	54.2	42.5	20.2
		Difference	-6.7	-1.8	3.0	3.1	-0.6	-4.6	-0.7	18.0

			Frequency (Hz)							
			63	125	250	500	1k	2k	4k	8k
Sample 4	Mic 1	Measured	46.2	45.8	42.6	48.4	54.5	49.5	40.6	37.7
		ISO-Wayson	46.1	47.8	36.3	40.2	55.7	55.3	44.8	28.5
		Difference	0.1	-2.1	6.3	8.3	-1.3	-5.8	-4.2	9.2
	Mic 2	Measured	42.6	43.3	39.7	44.6	53.9	47.2	37.8	37.1
		ISO-Wayson	45.2	45.3	33.8	37.3	53.3	52.7	40.9	19.5
		Difference	-2.6	-1.9	5.8	7.4	0.5	-5.5	-3.1	17.6
	Mic 3	Measured	45.9	43.1	47.4	52.3	57.6	52.1	42.5	38.4
		ISO-Wayson	45.7	47.7	44.1	46.4	58.0	56.9	46.4	30.1
		Difference	0.2	-4.5	3.3	5.9	-0.4	-4.8	-3.9	8.3
	Mic 4	Measured	41.6	40.2	43.9	49.2	54.8	49.1	41.2	38.1
		ISO-Wayson	45.6	43.8	42.7	44.4	56.2	54.9	43.1	21.7
		Difference	-4.1	-3.6	1.2	4.8	-1.4	-5.8	-1.9	16.4
Sample 5	Mic 1	Measured	34.3	42.3	40.3	43.4	50.3	45.2	38.6	37.8
		ISO-Wayson	37.4	44.1	32.8	35.0	52.5	52.9	43.3	27.7
		Difference	-3.1	-1.8	7.5	8.4	-2.1	-7.7	-4.6	10.1
	Mic 2	Measured	33.3	41.0	39.2	39.7	49.9	43.8	36.9	37.2
		ISO-Wayson	36.1	41.2	30.1	31.9	49.9	50.2	38.9	17.1
		Difference	-2.8	-0.3	9.1	7.8	0.1	-6.4	-2.0	20.0
	Mic 3	Measured	35.5	41.2	43.6	47.8	54.1	48.1	41.0	38.2
		ISO-Wayson	36.1	43.0	39.7	40.4	53.8	53.6	44.0	28.4
		Difference	-0.6	-1.8	3.8	7.4	0.3	-5.5	-3.0	9.8
	Mic 4	Measured	35.1	39.8	40.6	44.8	51.0	45.3	39.9	37.8
		ISO-Wayson	35.5	38.7	37.8	37.9	51.6	51.3	40.0	18.2
		Difference	-0.4	1.1	2.8	7.0	-0.6	-6.0	-0.1	19.6
Sample 6	Mic 1	Measured	33.3	50.0	43.7	44.7	50.9	45.8	38.2	37.6
		ISO-Wayson	37.3	44.2	34.4	35.7	52.8	53.8	44.0	25.3
		Difference	-4.0	5.8	9.3	9.1	-1.9	-8.0	-5.8	12.3
	Mic 2	Measured	34.0	45.3	40.3	41.9	50.9	44.7	37.8	37.2
		ISO-Wayson	36.2	41.5	31.7	32.6	50.3	51.1	39.8	14.9
		Difference	-2.2	3.8	8.6	9.3	0.6	-6.4	-1.9	22.3
	Mic 3	Measured	32.8	46.6	48.4	48.8	54.1	48.6	41.1	38.1
		ISO-Wayson	35.7	42.8	41.0	40.7	53.8	54.2	44.4	25.7
		Difference	-2.9	3.8	7.4	8.1	0.3	-5.6	-3.3	12.4
	Mic 4	Measured	36.8	43.4	46.6	45.8	51.4	45.8	41.4	37.9
		ISO-Wayson	35.2	38.5	39.0	38.2	51.7	51.8	40.5	15.6
		Difference	1.6	4.9	7.5	7.6	-0.3	-6.1	0.9	22.3

			Frequency (Hz)							
			63	125	250	500	1k	2k	4k	8k
Average	Mic 1	Measured	38.7	46.4	43.2	47.4	52.9	48.1	39.9	37.7
		ISO-Wayson	41.9	46.3	35.6	39.8	54.5	54.4	44.3	27.5
		Difference	-3.2	0.2	7.5	7.6	-1.6	-6.3	-4.3	10.2
	Mic 2	Measured	37.2	44.1	41.0	43.6	52.4	46.0	37.8	37.1
		ISO-Wayson	40.5	43.3	32.8	36.5	51.8	51.4	39.9	17.7
		Difference	-3.3	0.8	8.2	7.1	0.6	-5.4	-2.1	19.4
	Mic 3	Measured	38.6	44.4	47.4	51.7	56.3	50.7	42.2	38.2
		ISO-Wayson	41.0	45.7	43.0	45.6	56.3	55.5	45.4	28.7
		Difference	-2.4	-1.3	4.4	6.1	0.0	-4.9	-3.3	9.6
	Mic 4	Measured	37.3	41.8	44.0	48.5	53.4	47.8	41.1	38.1
		ISO-Wayson	40.8	41.6	41.4	43.4	54.4	53.4	41.9	19.7
		Difference	-3.4	0.2	2.7	5.1	-1.0	-5.6	-0.7	18.4

Table 52, for the Crosswind Group, shows that this method on average is over-predicting for the octave band that have center frequencies 63 Hz, 125 Hz, 1 KHz, 2 KHz, and 4 KHz for the majority of the microphone locations, except Mic 3 at 1 KHz. While, on average the method is shown to under-predict for the octave band centered at 250 Hz, 500 Hz, and 8 KHz for the majority of the microphone locations, except Mic 4 at 250 Hz. It is shown that the difference between measured and predicted octave band sound levels ranged from as low as 0.2 dB(A) to as high as 15 dB(A).

Table 52: Difference Between Measured & Predicted Octave Band Sound levels dB(A)

			Frequency (Hz)							
			63	125	250	500	1k	2k	4k	8k
Sample 1	Mic 1	Measured	41.8	47.2	45.9	49.2	53.4	51.7	43.8	38.3
		ISO-Wayson	45.3	49.7	41.2	43.2	56.1	56.4	47.2	31.3
		Difference	-3.4	-2.5	4.7	6.1	-2.7	-4.7	-3.4	7.0
	Mic 2	Measured	38.4	43.8	42.0	41.1	49.7	48.7	40.2	37.7
		ISO-Wayson	44.5	47.4	38.9	40.5	54.0	54.2	43.6	22.5
		Difference	-6.1	-3.5	3.1	0.6	-4.3	-5.5	-3.3	15.2
	Mic 3	Measured	41.3	45.3	50.5	54.8	57.5	53.2	44.8	39.1
		ISO-Wayson	44.6	49.3	48.7	49.1	58.0	57.7	48.5	32.6
		Difference	-3.3	-4.0	1.8	5.7	-0.5	-4.5	-3.7	6.5
	Mic 4	Measured	37.5	41.8	44.0	50.8	52.6	48.6	41.7	38.3
		ISO-Wayson	45.1	46.0	47.9	47.7	56.9	56.5	45.9	24.8
		Difference	-7.6	-4.3	-3.9	3.0	-4.4	-7.9	-4.2	13.5
Sample 2	Mic 1	Measured	39.9	43.6	41.5	45.2	50.7	46.9	42.7	38.5
		ISO-Wayson	41.1	48.3	36.5	40.3	54.8	55.3	46.2	32.0
		Difference	-1.2	-4.7	5.0	4.9	-4.1	-8.4	-3.5	6.5
	Mic 2	Measured	35.9	40.6	38.1	38.9	48.1	45.5	38.4	37.9
		ISO-Wayson	40.0	45.5	33.8	37.2	52.3	52.7	42.2	22.8
		Difference	-4.1	-5.0	4.3	1.7	-4.2	-7.2	-3.8	15.1
	Mic 3	Measured	39.5	41.8	46.2	52.1	55.8	50.5	44.7	39.5
		ISO-Wayson	39.0	46.5	42.6	44.8	55.3	55.2	46.1	31.9
		Difference	0.4	-4.6	3.6	7.3	0.5	-4.7	-1.4	7.6
	Mic 4	Measured	35.5	38.6	40.4	48.2	51.3	46.6	42.6	38.5
		ISO-Wayson	38.0	41.7	40.3	42.0	52.7	52.5	42.0	22.6
		Difference	-2.6	-3.1	0.2	6.3	-1.4	-5.9	0.6	15.9
Sample 3	Mic 1	Measured	41.0	43.4	42.5	45.4	49.6	46.8	43.8	40.6
		ISO-Wayson	43.8	45.7	36.2	40.0	53.6	54.1	44.8	32.6
		Difference	-2.9	-2.3	6.2	5.4	-4.0	-7.3	-1.0	8.0
	Mic 2	Measured	35.7	40.7	39.0	38.6	46.0	44.0	38.7	37.5
		ISO-Wayson	42.4	42.7	33.3	36.6	50.8	51.1	40.5	23.1
		Difference	-6.7	-2.0	5.7	1.9	-4.8	-7.1	-1.7	14.4
	Mic 3	Measured	41.2	42.1	46.7	52.0	54.9	51.2	46.7	42.8
		ISO-Wayson	41.9	44.0	42.5	44.6	54.3	54.1	44.8	32.6
		Difference	-0.7	-1.9	4.2	7.4	0.7	-2.9	1.9	10.2
	Mic 4	Measured	35.1	39.3	41.0	47.9	49.8	46.0	42.1	38.9
		ISO-Wayson	40.8	39.2	40.0	41.7	51.6	51.2	40.6	23.2
		Difference	-5.6	0.2	1.0	6.2	-1.8	-5.3	1.5	15.7

			Frequency (Hz)							
			63	125	250	500	1k	2k	4k	8k
Average	Mic 1	Measured	40.9	44.7	43.3	46.6	51.2	48.5	43.4	39.1
		ISO-Wayson	43.4	47.9	38.0	41.1	54.8	55.3	46.0	32.0
		Difference	-2.5	-3.2	5.3	5.5	-3.6	-6.8	-2.6	7.1
	Mic 2	Measured	36.7	41.7	39.7	39.5	47.9	46.1	39.1	37.7
		ISO-Wayson	42.3	45.2	35.3	38.1	52.4	52.7	42.1	22.8
		Difference	-5.6	-3.5	4.4	1.4	-4.4	-6.6	-3.0	14.9
	Mic 3	Measured	40.6	43.1	47.8	53.0	56.1	51.7	45.4	40.5
		ISO-Wayson	41.8	46.6	44.6	46.2	55.9	55.7	46.4	32.4
		Difference	-1.2	-3.5	3.2	6.8	0.2	-4.0	-1.1	8.1
	Mic 4	Measured	36.0	39.9	41.8	49.0	51.2	47.0	42.2	38.6
		ISO-Wayson	41.3	42.3	42.7	43.8	53.7	53.4	42.8	23.5
		Difference	-5.3	-2.4	-0.9	5.2	-2.5	-6.3	-0.7	15.0

Table 53, for the Upwind Group, shows that this method is on average under-predicting the octave band sound levels for all the frequencies at the microphone locations, except Mic 1 at 2 KHz. It is shown that the difference between measured and predicted octave band sound levels ranged from as low as 0.4 dB(A) to as high as 28 dB(A).

Table 53: Difference Between Measured & Predicted Octave Band Sound levels dB(A)

			Frequency (Hz)							
			63	125	250	500	1k	2k	4k	8k
Sample 1	Mic 1	Measured	35.1	40.7	38.2	41.2	45.9	42.6	39.0	37.8
		ISO-Wayson	36.3	37.5	30.0	34.7	48.3	48.0	38.9	22.4
		Difference	-1.1	3.2	8.2	6.5	-2.4	-5.4	0.0	15.3
	Mic 2	Measured	39.8	38.3	38.1	35.2	44.1	39.8	37.0	37.3
		ISO-Wayson	30.3	29.9	22.5	26.8	40.9	40.4	30.0	8.5
		Difference	9.5	8.4	15.6	8.3	3.2	-0.6	7.0	28.8
	Mic 3	Measured	42.2	42.3	44.9	50.2	55.1	49.0	43.2	39.2
		ISO-Wayson	35.4	36.9	37.3	40.5	50.1	49.1	40.0	23.5
		Difference	6.8	5.5	7.6	9.8	5.0	-0.1	3.2	15.7
	Mic 4	Measured	37.8	36.1	39.4	41.9	46.9	43.0	39.1	36.8
		ISO-Wayson	30.4	28.1	30.9	33.6	43.4	42.2	31.8	10.3
		Difference	7.4	7.9	8.5	8.4	3.5	0.8	7.3	26.5
Sample 2	Mic 1	Measured	35.2	40.6	39.6	42.4	45.5	43.2	38.3	37.7
		ISO-Wayson	34.5	37.6	30.0	35.5	45.2	45.8	40.4	26.8
		Difference	0.7	3.1	9.6	6.9	0.3	-2.6	-2.1	10.9
	Mic 2	Measured	31.7	35.8	34.2	35.0	42.0	38.7	36.7	37.1
		ISO-Wayson	28.1	29.6	22.1	27.2	37.4	37.8	31.1	12.5
		Difference	3.6	6.2	12.1	7.8	4.6	0.9	5.6	24.6
	Mic 3	Measured	33.9	39.1	44.1	51.7	54.1	48.8	43.2	38.7
		ISO-Wayson	33.9	37.2	37.6	41.5	47.3	47.2	41.8	28.2
		Difference	0.0	1.9	6.4	10.2	6.8	1.6	1.4	10.5
	Mic 4	Measured	29.1	34.1	35.8	42.5	45.1	41.0	39.0	36.4
		ISO-Wayson	28.9	28.5	31.3	34.6	40.6	40.3	33.6	15.0
		Difference	0.2	5.6	4.5	7.9	4.6	0.6	5.4	21.5
Sample 3	Mic 1	Measured	38.1	41.9	40.4	44.9	48.8	46.5	44.5	38.4
		ISO-Wayson	39.5	39.7	27.0	32.0	45.9	45.3	39.9	23.2
		Difference	-1.4	2.2	13.3	12.9	2.9	1.1	4.6	15.2
	Mic 2	Measured	34.9	37.6	36.0	37.3	43.7	41.2	39.6	37.1
		ISO-Wayson	32.8	31.3	18.8	23.3	37.6	36.9	30.2	8.4
		Difference	2.1	6.3	17.3	14.0	6.1	4.3	9.4	28.7
	Mic 3	Measured	37.3	40.1	44.7	49.6	53.7	47.8	43.6	38.8
		ISO-Wayson	38.0	38.3	33.7	37.0	46.9	45.7	40.3	23.6
		Difference	-0.7	1.9	11.1	12.6	6.7	2.1	3.3	15.2
	Mic 4	Measured	32.6	34.9	37.2	43.9	47.2	42.7	40.3	36.5
		ISO-Wayson	31.9	28.5	26.2	29.0	39.1	37.7	31.0	9.2
		Difference	0.7	6.4	11.0	14.9	8.1	5.0	9.3	27.3

			Frequency (Hz)							
			63	125	250	500	1k	2k	4k	8k
Sample 4	Mic 1	Measured	39.9	39.8	41.2	41.4	47.1	44.9	42.2	37.9
		ISO-Wayson	36.3	38.9	34.9	31.3	46.2	46.7	38.0	22.1
		Difference	3.6	1.0	6.4	10.2	0.8	-1.8	4.2	15.8
	Mic 2	Measured	37.5	37.7	36.0	36.6	43.6	40.4	36.9	37.2
		ISO-Wayson	30.8	31.7	27.8	23.8	38.9	39.5	29.5	8.5
		Difference	6.8	6.0	8.2	12.8	4.7	0.9	7.4	28.6
	Mic 3	Measured	40.0	39.3	47.2	50.1	53.1	48.1	43.7	38.5
		ISO-Wayson	34.2	37.0	41.0	35.8	46.5	46.6	37.9	22.0
		Difference	5.8	2.3	6.2	14.3	6.7	1.5	5.8	16.5
	Mic 4	Measured	35.8	35.6	38.7	42.6	46.5	42.5	39.4	36.3
		ISO-Wayson	28.8	27.9	34.3	28.5	39.3	39.3	29.3	8.3
		Difference	7.0	7.7	4.4	14.1	7.1	3.2	10.1	28.0
Average	Mic 1	Measured	37.1	40.8	39.8	42.5	46.8	44.3	41.0	37.9
		ISO-Wayson	36.6	38.4	30.5	33.4	46.4	46.5	39.3	23.6
		Difference	0.4	2.4	9.4	9.1	0.4	-2.2	1.7	14.3
	Mic 2	Measured	36.0	37.4	36.1	36.0	43.4	40.0	37.5	37.2
		ISO-Wayson	30.5	30.6	22.8	25.3	38.7	38.7	30.2	9.5
		Difference	5.5	6.7	13.3	10.7	4.7	1.3	7.3	27.7
	Mic 3	Measured	38.3	40.2	45.2	50.4	54.0	48.4	43.4	38.8
		ISO-Wayson	35.4	37.3	37.4	38.7	47.7	47.2	40.0	24.3
		Difference	3.0	2.9	7.8	11.7	6.3	1.2	3.4	14.5
	Mic 4	Measured	33.8	35.2	37.8	42.8	46.4	42.3	39.4	36.5
		ISO-Wayson	30.0	28.2	30.7	31.4	40.6	39.9	31.4	10.7
		Difference	3.8	6.9	7.1	11.3	5.8	2.4	8.0	25.8

Table 54 shows that there is no significant difference between the three groups when comparing the difference between measured and predicted octave band sound levels. When comparing the results for this method with the results from the two previous methods, it seems that the ISO method with the Wayson empirical model included did not minimize the difference between measured and predicted sound levels. This is likely due to the fact that the Wayson model did not include many upwind cases when the model was developed.

Moreover, when analyzing the results from using the ISO-method to predict octave band sound levels. It was expected that the difference should increase by frequency since refraction effects increases at higher frequency. However, it appears that the ISO method works well in the middle frequencies but does not do as well at both the low and high frequencies. This is most likely an inability to handle the ground effects properly and that refraction effects are not included.

Table 54: Summary of Difference Between Measured and Predicted Octave Band Sound Levels

		63	125	250	500	1k	2k	4k	8k
Mic 1	Downwind	-1.8	1.5	8.9	8.9	-0.3	-4.9	-2.9	11.6
	Crosswind	-0.3	-1.0	7.5	7.6	-1.6	-4.6	-0.5	9.3
	Upwind	-3.1	-1.1	5.9	5.6	-3.0	-5.7	-1.8	10.8
Mic 2	Downwind	-1.2	3.0	10.3	9.2	2.7	-3.3	0.0	21.5
	Crosswind	-2.5	-0.4	7.5	4.5	-1.3	-3.5	0.2	18.0
	Upwind	-2.0	-0.8	5.8	3.2	-2.8	-6.2	-0.2	20.2
Mic 3	Downwind	-0.1	1.0	6.7	8.4	2.3	-2.6	-1.0	11.9
	Crosswind	1.0	-1.3	5.4	9.0	2.4	-1.8	1.1	10.3
	Upwind	-0.5	-0.6	4.4	8.2	2.8	-2.2	-0.1	11.0
Mic 4	Downwind	0.5	4.1	6.6	9.0	2.9	-1.7	3.2	22.3
	Crosswind	-1.6	1.3	2.8	8.9	1.2	-2.7	3.0	18.7
	Upwind	-2.9	0.3	0.5	4.7	-0.8	-4.3	1.4	19.2

Also as explained earlier, the ISO 9613-2 method was mainly developed for downwind conditions. This method does not accurately model traffic noise sources. The ISO 9613-2 method assumes that for soft ground the ground effect correction is equal to zero in the middle region between the source and the receiver region. All of these factors

contribute to the inaccurate modeling, hence the reduced error in predicted sound levels when the Wayson empirical method is applied.

However, the Wayson method did not show good results when applied to individual octave band results. Since it was not derived for this purpose, this was expected. This does show the need for correction based on octave bands.

Part of the error may have occurred as noted due to ISO 9613-2 not being a highway specific model. So to check this, the FHWA model, TNM was evaluated. The following section will illustrate the results when comparing measured sound levels to predicted sound levels using the FHWA Traffic Noise Model (TNM). TNM is the model widely used now for predicting sound levels from highway sources.

Traffic Noise Model (TNM 2.5)

Version 2.5 of the FHWA Traffic Noise Model (TNM 2.5) is the latest release of the model, promulgated in May 2005. TNM is the most used model for predicting sound levels from highway sources in the United States, being required for federal projects. Version 2.5 of the model has been shown, by El-Aassar [El-Aassar, 2005] to better predict sound levels and better account for ground effects than previous models.

This section will compare the measured sound levels and TNM predicted sound levels for each microphone of three groups: Downwind, Crosswind and Upwind. Traffic counts for five classes (automobile, medium truck, heavy truck, buses and motorcycles) were conducted during data collection, but during measurement periods there were no buses or motorcycles that passed-by and only the first three classes are presented in Table 55. The traffic counts were conducted for 15 minutes for both direction of the highway and the on-ramp simultaneously. Then, these measured traffic counts were expanded to hourly volume by multiplying the results by a factor of 4 in order to use them as input in TNM 2.5.

Table 55: Hourly Traffic Counts for All Three Groups

		NB	SB	Ramp
Downwind	Auto	504	700	148
	MT	8	11	3
	HT	6	8	3
Crosswind	Auto	432	600	127
	MT	7	10	2
	HT	5	7	2
Upwind	Auto	532	622	126
	MT	8	14	11
	HT	8	14	3

Downwind Group

A summary of the comparison of measured sound levels to TNM predicted sound levels for each microphone of the Downwind Group is illustrated in Table 56 and Figure 36.

It is shown that the predicted sound levels using TNM causes under-prediction for all microphone positions, except for Sample 5 (Mic 1 and Mic 3) where it is over predicting. This variation in Sample 5 from the other sample periods is attributed to the inversion conditions that occurred while the measurements were conducted for this sample period which worked in a synergistic way with the downwind conditions. The inversion lapse rate has affected ground effects which in turn resulted in under prediction for Mic 1 and Mic 3 and minimizing the difference between measured and predicted sound level. It is indicated that on average the difference is large between measured and

predicted sound levels. Furthermore, this difference is larger for receivers, i.e. Mic 2 and Mic 4 that are the furthest from the source. In this case, TNM proved to be less accurate when compared to results from ISO 9613-2. This analysis has illustrated that TNM prediction could have an error up to 6 dB(A), which could contribute to errors in noise mitigations measures and cost associated with noise abatement. Therefore, it is indicated that it is essential to account for the effect of atmospheric refraction due to wind gradient and lapse rate when predicting sound levels using TNM.

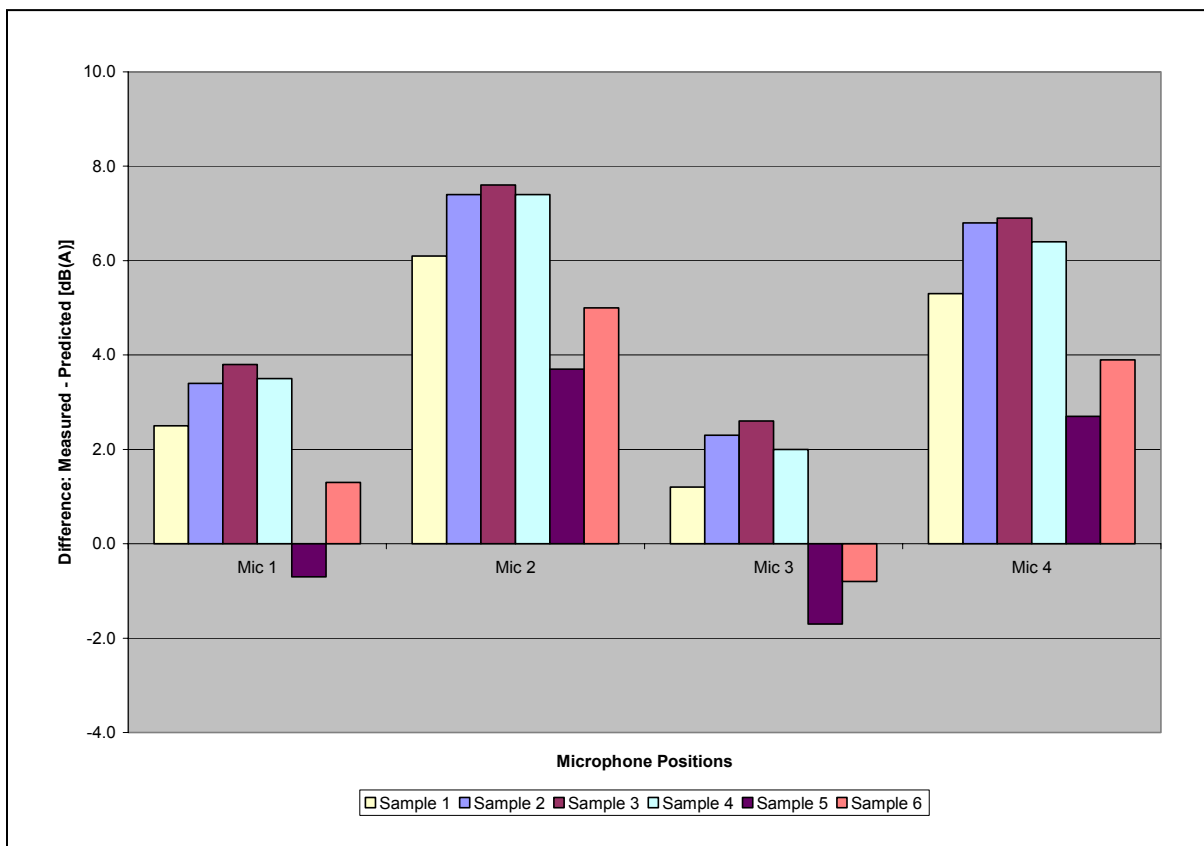


Figure 36: Difference Between Measured and Predicted Sound Levels for Downwind Group

Table 56: Difference between Measured and Predicted Sound levels dB(A) for Downwind Group

		Measured	TNM	Difference
Sample 1	Ref	69.9	71.1	-1.2
	Mic 1	56.4	53.9	2.5
	Mic 2	54.6	48.5	6.1
	Mic 3	59.4	58.2	1.2
	Mic 4	56.2	50.9	5.3
Sample 2	Ref	73.7	71.1	2.6
	Mic 1	57.3	53.9	3.4
	Mic 2	55.9	48.5	7.4
	Mic 3	60.5	58.2	2.3
	Mic 4	57.7	50.9	6.8
Sample 3	Ref	73.7	71.1	2.6
	Mic 1	57.7	53.9	3.8
	Mic 2	56.1	48.5	7.6
	Mic 3	60.8	58.2	2.6
	Mic 4	57.8	50.9	6.9
Sample 4	Ref	72.0	71.1	0.9
	Mic 1	57.4	53.9	3.5
	Mic 2	55.9	48.5	7.4
	Mic 3	60.2	58.2	2.0
	Mic 4	57.3	50.9	6.4
Sample 5	Ref	68.0	71.1	-3.1
	Mic 1	53.2	53.9	-0.7
	Mic 2	52.2	48.5	3.7
	Mic 3	56.5	58.2	-1.7
	Mic 4	53.6	50.9	2.7
Sample 6	Ref	68.4	71.1	-2.7
	Mic 1	55.2	53.9	1.3
	Mic 2	53.5	48.5	5.0
	Mic 3	57.4	58.2	-0.8
	Mic 4	54.8	50.9	3.9
Average	Ref	71.0	71.1	-0.2
	Mic 1	56.2	53.9	2.3
	Mic 2	54.7	48.5	6.2
	Mic 3	59.1	58.2	0.9
	Mic 4	56.2	50.9	5.3

Crosswind Group

Summary of the comparison of measured sound levels to TNM predicted sound levels for each microphone of the Crosswind Group is illustrated in Table 57 and Figure 37 in the same way presented for the Downwind Group.

Table 57: Difference between Measured and Predicted Sound levels dB(A) for Crosswind Group

		Measured	TNM	Difference
Average	Ref	72.3	70.5	1.8
	Mic 1	57.7	53.1	4.6
	Mic 2	53.9	47.7	6.2
	Mic 3	61.1	57.4	3.7
	Mic 4	56.4	50.1	6.3
Sample 2	Ref	70.8	70.5	0.3
	Mic 1	54.3	53.1	1.2
	Mic 2	51.5	47.7	3.8
	Mic 3	58.8	57.4	1.4
	Mic 4	54.7	50.1	4.6
Sample 3	Ref	70.2	70.5	-0.3
	Mic 1	54.2	53.1	1.1
	Mic 2	50.4	47.7	2.7
	Mic 3	58.7	57.4	1.3
	Mic 4	53.9	50.1	3.8
Average	Ref	71.1	70.5	0.6
	Mic 1	55.4	53.1	2.3
	Mic 2	51.9	47.7	4.2
	Mic 3	59.5	57.4	2.1
	Mic 4	55.0	50.1	4.9

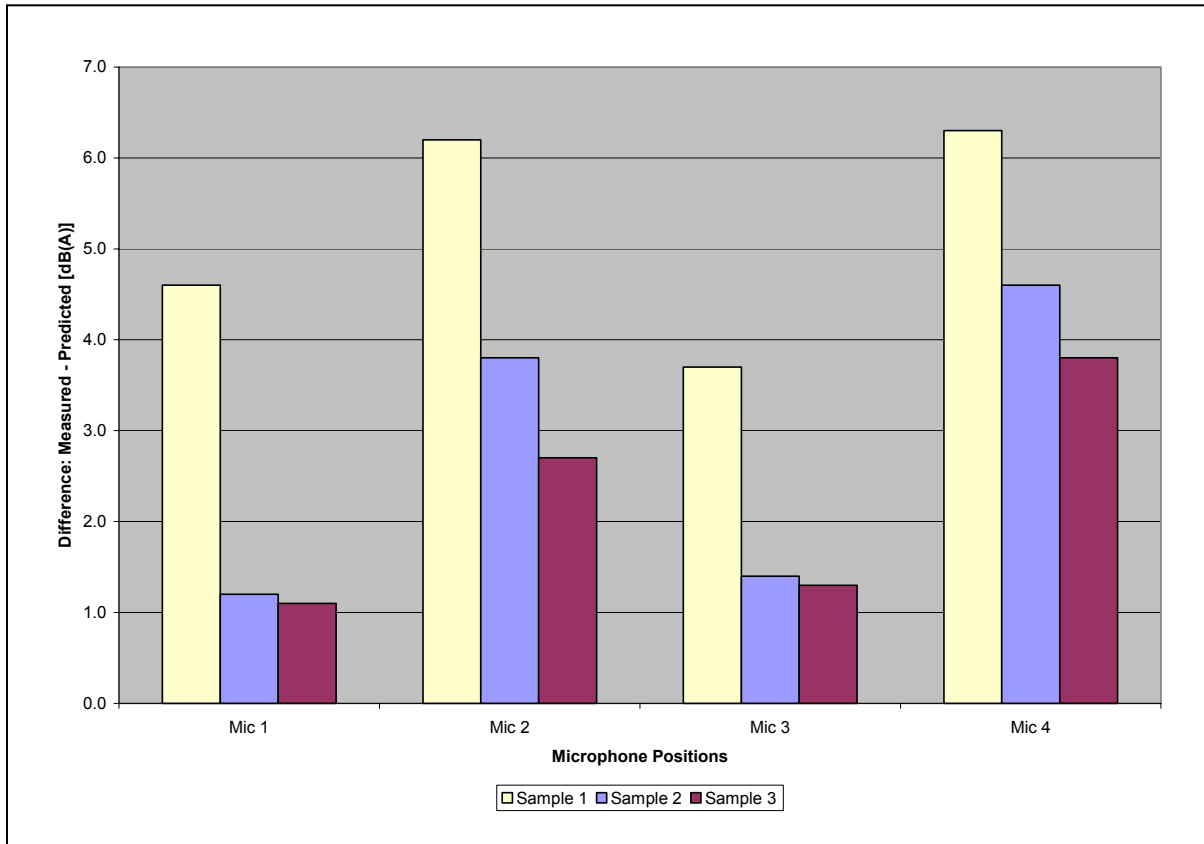


Figure 37: Difference Between Measured and Predicted Sound Levels for Crosswind Group

It is shown that the predicted sound level using TNM causes under-prediction for all microphones, except the Reference microphone in Sample 3 where it is over-predicting by 0.3 dB(A). The over-prediction is due to a slightly smaller positive U-wind component when compared to the other groups. It is shown that the differences are large when the measured and predicted sound levels are compared. Moreover, when compared to results from ISO 9613-2, it is shown that the difference between measured and predicted sound level is larger especially for the furthest microphone locations Mic 2 and Mic 4 where the failure by TNM 2.5 to account for refraction effects would be expected

to be more noticeable. It is shown from the prediction results when compared to the measurements that TNM prediction could have an error up to 5 dB(A). This is a very significant difference which could contribute to errors in noise mitigations measures and cost associated with noise abatement. Therefore, it is essential to account for the effect of atmospheric refraction due to wind gradient and lapse rate when predicting sound levels using TNM.

Upwind Group

Summary of the comparison of measured sound levels to TNM predicted sound levels for each microphone of the Upwind Group is illustrated in Table 58 and Figure 38 in the same way presented in the Downwind and the Crosswind Groups.

It is shown that the predicted sound level is over-predicting for all microphones. This shows that refraction, which should be reducing the sound levels in this case, is causing the over-prediction. It is indicated that the difference is slightly larger between measured and predicted sound levels. Of interest is Sample 4 where normal lapse rate has occurred. This has resulted in smaller difference for the microphone location closer to the ground where ground effects maybe have affected the sound levels. It is illustrated that TNM prediction is less than in the Downwind and the Crosswind Groups but could have an error up to 3 dBA, which could contribute to errors in noise mitigations measures and cost associated with noise abatement. When compared to the ISO 9613-2 method, the

results are better. This is due to the fact that the ground effects algorithm in TNM model might be better and TNM might be less prone to large variations in upwind conditions. However, it is essential to account for the effect of atmospheric refraction due to wind gradient and lapse rate when predicting sound levels using TNM.

Table 58: Difference between Measured and Predicted Sound levels dB(A) for Upwind Group

		Measured	TNM	Difference
Sample 1	Ref	70.8	71.1	-0.3
	Mic 1	50.3	54.2	-3.9
	Mic 2	48.6	48.8	-0.2
	Mic 3	57.8	58.3	-0.5
	Mic 4	50.7	51.1	-0.4
Sample 2	Ref	70.1	71.1	-1.0
	Mic 1	50.4	54.2	-3.8
	Mic 2	46.4	48.8	-2.4
	Mic 3	57.4	58.3	-0.9
	Mic 4	49.1	51.1	-2.0
Sample 3	Ref	69.2	71.1	-1.9
	Mic 1	53.4	54.2	-0.8
	Mic 2	48.4	48.8	-0.4
	Mic 3	56.6	58.3	-1.7
	Mic 4	50.8	51.1	-0.3
Sample 4	Ref	68.7	71.1	-2.4
	Mic 1	51.8	54.2	-2.4
	Mic 2	48.0	48.8	-0.8
	Mic 3	56.7	58.3	-1.6
	Mic 4	50.3	51.1	-0.8
Average	Ref	69.7	71.1	-1.4
	Mic 1	51.5	54.2	-2.7
	Mic 2	47.9	48.8	-0.9
	Mic 3	57.1	58.3	-1.2
	Mic 4	50.2	51.1	-0.9

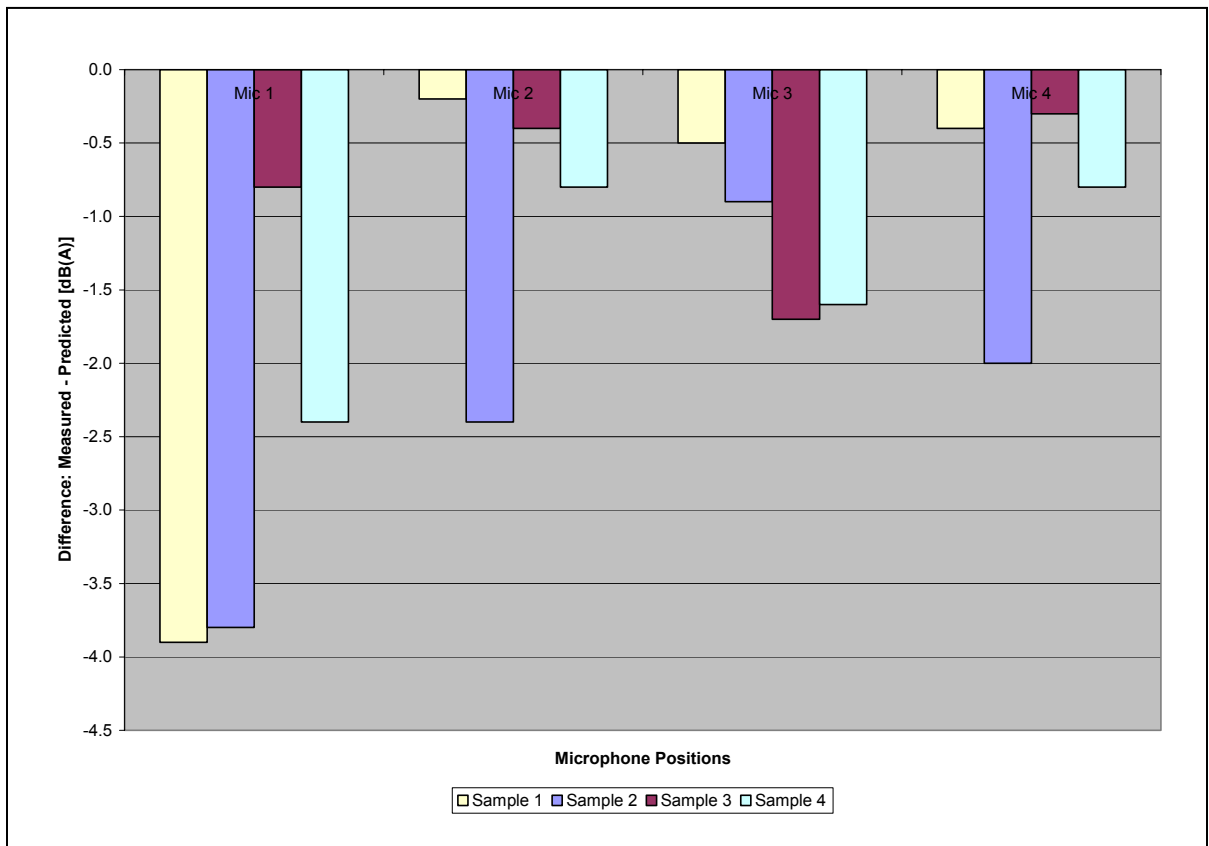


Figure 38: Difference Between Measured and Predicted Sound Levels for Upwind Group

Summary

Table 59 and Figure 39 present the summary of the difference between measured and predicted sound levels in dB(A) using TNM.

Table 59: Average Difference between Measured and Predicted Sound levels dB(A)

	Downwind	Crosswind	Upwind
Mic 1	2.3	2.3	-2.7
Mic 2	6.2	4.2	-0.9
Mic 3	0.9	2.1	-1.2
Mic 4	5.3	4.9	-0.9

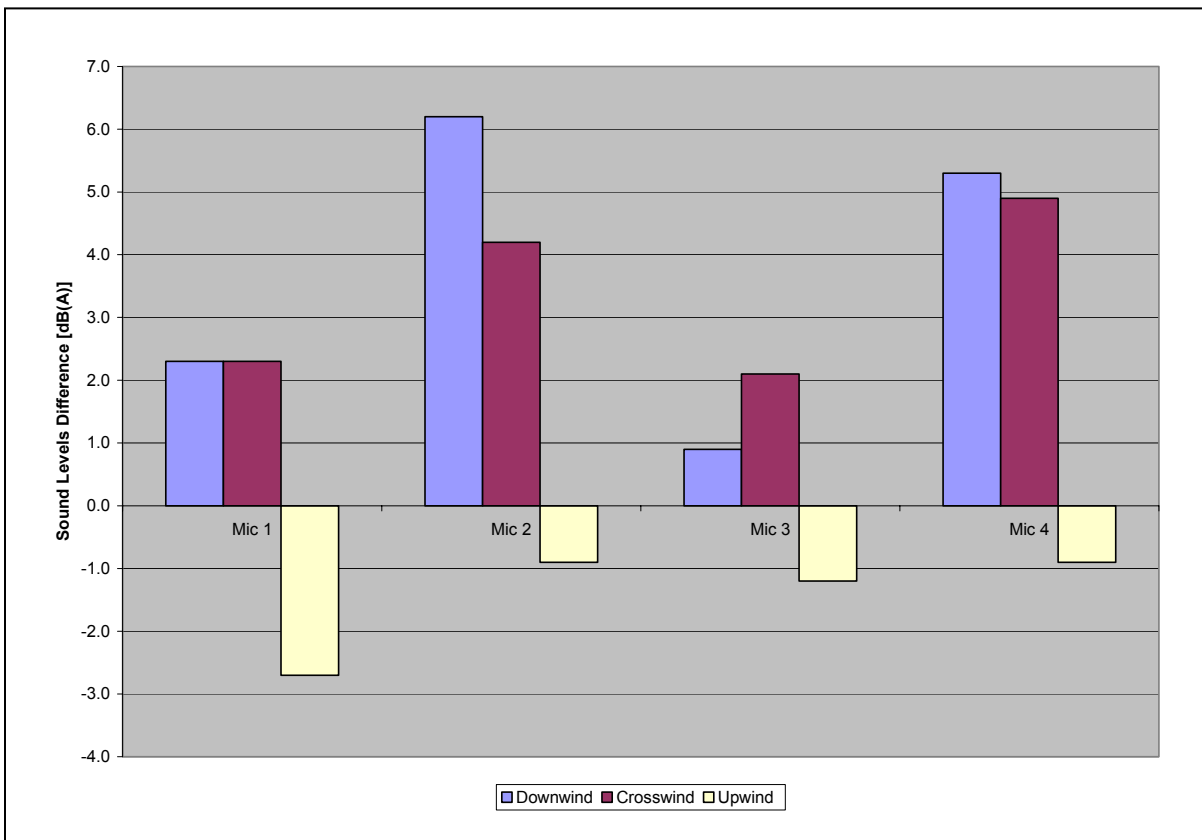


Figure 39: Average Difference between Measured and Predicted Sound levels

It is determined that TNM would generally under-predict in cases of the Downwind and the Crosswind Groups, while it would over-predict in the Upwind

Groups. This would seem to be a direct effect of refraction not being accounted for since the results are being under-predicted for downwind cases and over-predicted for upwind cases.

It could be concluded that accounting for atmospheric refraction due to wind gradient and lapse rates is essential and should not be ignored when using the widely utilized TNM model in predicting sound levels from highways. A method is needed; the following section will present a new empirical model that will account for atmospheric refraction due to lapse rate and wind gradient.

Development of An Empirical Refraction Model

The first step in the development of the model was to determine the normalized difference between predicted and measured sound levels while accounting for all propagation effects except refraction. The normalized difference might then be due only to atmospheric refraction. Manipulation of the data was accomplished by assuming refraction effects are minimal at the Reference position close to the source. This was shown to be the case previously. At the different receiver positions further away this would not be the case and difference should occur due to refraction.

The following tables present an excerpt of the sound levels for the Reference positions and the microphones positions (Mic 1, Mic 2, Mic 3, and Mic 4). Tables 60 – 64 show the measured sound levels corresponding to each frequency.

Table 60: Sample of Reference Sound Levels dB

Frequency (Hz)							
63	125	250	500	1k	2k	4k	8k
71.7	66.7	59.9	59.8	60.2	54.1	45.1	40.0
66.9	65.8	58.6	61.0	61.5	58.3	45.6	40.0
68.1	61.8	57.9	60.8	61.4	59.8	48.0	40.1
73.0	65.9	66.3	66.7	66.1	62.2	54.1	49.1
67.8	61.8	59.4	59.5	67.4	57.7	50.9	44.3
59.2	60.0	56.9	51.6	58.5	49.6	41.3	39.2
60.9	61.6	54.7	54.4	61.0	54.4	40.8	39.2
64.4	65.8	59.7	57.6	62.5	59.2	44.2	39.6
64.0	67.3	62.2	61.5	67.3	64.3	53.8	41.8
68.6	69.5	68.4	68.4	73.4	66.9	58.7	49.1
66.3	66.1	69.9	69.0	68.9	63.2	54.5	44.5
63.6	67.0	65.7	64.2	68.1	63.7	52.6	43.7
66.2	75.8	67.3	70.2	69.1	65.8	55.9	46.3
60.8	63.2	58.5	58.2	60.5	57.0	46.1	39.9
61.2	66.0	55.7	57.3	60.7	51.9	43.2	39.3
65.1	65.1	57.1	58.2	58.3	52.3	44.3	39.9
66.8	70.8	59.4	57.9	58.7	52.1	43.4	39.7

Table 61: Sample of Mic 1 Sound Levels dB

Frequency (Hz)							
63	125	250	500	1k	2k	4k	8k
62.0	57.6	51.3	51.1	52.5	45.8	37.4	38.5
61.1	58.6	51.4	51.3	53.7	47.5	38.0	38.6
59.0	57.1	50.3	50.2	56.0	48.6	37.8	38.7
59.7	57.2	51.3	49.1	54.5	47.4	38.1	38.6
59.4	59.7	49.7	47.7	53.4	46.4	38.4	38.7
60.1	60.4	48.7	48.2	51.9	45.4	38.1	38.6
64.6	58.6	48.9	47.6	52.6	45.2	38.3	38.7
60.7	58.1	48.8	48.1	53.2	47.1	39.3	38.6
57.1	57.7	48.7	48.6	52.8	47.5	39.8	38.6
59.0	57.4	49.7	48.3	51.2	46.9	38.2	38.6
59.2	55.7	49.9	50.5	52.0	46.8	37.9	38.5
58.6	57.3	47.9	48.0	52.2	46.8	38.3	38.8
62.4	60.2	48.0	49.0	54.3	46.9	38.4	38.5
67.5	65.1	49.6	51.1	54.4	46.6	38.2	38.6
67.3	63.0	47.5	49.6	54.6	47.8	39.1	38.8
63.0	59.0	47.7	50.9	54.3	45.9	38.5	38.8
66.8	56.4	46.7	49.6	53.7	47.3	38.3	38.6

Table 62: Sample of Mic 2 Sound Levels dB

Frequency (Hz)							
63	125	250	500	1k	2k	4k	8k
56.4	59.9	45.8	45.1	52.1	43.2	35.8	38.1
56.3	55.3	45.0	44.9	53.2	46.0	36.9	38.1
58.4	56.2	45.8	44.6	52.6	47.3	38.6	38.0
56.1	57.4	45.5	46.9	53.2	44.8	37.5	38.2
58.5	56.4	46.6	42.8	50.1	42.7	36.1	38.2
61.3	57.9	45.3	41.6	49.3	41.4	35.5	38.2
61.7	57.9	44.2	41.9	51.0	41.8	35.9	38.2
58.0	55.7	43.1	42.0	49.8	42.1	35.8	38.1
62.5	56.2	44.4	43.3	50.3	43.0	35.7	38.2
57.3	56.9	44.4	45.0	52.1	44.5	36.4	38.3
55.6	55.8	43.0	44.2	51.9	44.2	36.8	38.1
61.9	54.6	43.5	42.9	51.7	43.4	35.6	38.2
57.0	54.8	43.3	42.9	51.9	42.2	35.6	38.1
57.1	53.6	42.1	44.1	50.6	42.7	35.4	38.3
60.1	56.7	42.6	44.1	51.4	42.4	35.4	38.1
57.3	57.3	43.3	43.0	50.7	42.9	35.6	38.1
56.6	54.7	45.1	44.4	50.3	42.4	35.4	38.2

Table 63: Sample of Mic 3 Sound Levels dB

Frequency (Hz)							
63	125	250	500	1k	2k	4k	8k
67.8	62.0	52.5	54.5	56.2	50.3	41.1	39.4
67.9	60.5	51.7	53.0	57.4	49.5	41.0	39.4
61.0	57.4	53.0	53.5	58.1	48.7	40.7	39.4
65.0	56.6	51.5	53.8	57.2	49.4	40.5	39.2
58.8	57.4	52.9	54.7	57.5	50.9	41.8	39.2
56.1	57.5	51.5	53.0	56.9	50.2	42.0	39.4
59.5	59.7	51.3	53.2	58.6	51.6	42.8	39.4
58.8	57.2	54.0	53.3	58.5	49.7	41.1	39.6
60.8	57.0	54.3	51.3	56.1	48.9	39.4	39.1
62.6	52.8	54.1	51.2	56.1	48.3	39.5	39.3
63.2	53.1	51.7	50.4	54.5	46.4	38.7	39.1
59.4	55.4	53.1	50.5	53.8	46.3	38.9	38.9
59.4	57.0	53.0	49.5	53.6	46.5	39.2	39.0
63.9	59.6	52.1	50.4	54.6	47.7	39.1	39.1
64.0	62.6	54.2	51.1	55.9	48.9	38.9	39.1
64.7	57.1	53.7	51.5	55.4	48.4	39.6	39.2

Table 64: Sample of Mic 4 Sound Levels dB

Frequency (Hz)							
63	125	250	500	1k	2k	4k	8k
60.0	57.3	47.5	47.3	51.4	44.1	39.0	38.9
57.9	54.2	48.4	48.6	51.9	44.4	40.2	39.0
58.8	53.4	48.8	47.8	51.3	44.4	40.2	39.3
55.2	52.8	49.1	49.5	51.7	44.2	39.8	39.0
55.1	51.9	49.2	48.6	52.0	44.9	39.8	39.2
61.0	53.5	48.6	47.3	51.7	43.7	39.7	39.2
56.0	51.0	48.7	47.3	53.3	44.5	39.3	39.2
55.9	50.3	48.0	46.8	51.1	44.3	39.6	39.2
57.7	53.1	46.9	47.5	51.7	44.6	39.2	39.2
56.0	53.0	48.9	49.6	51.0	45.2	39.3	39.2
55.3	52.1	52.9	48.6	49.9	43.2	39.0	39.4
56.0	50.9	49.7	49.9	51.9	44.0	39.1	39.3
55.9	52.0	50.6	48.3	51.1	43.6	39.1	39.3
54.2	55.9	50.1	49.3	52.2	45.1	40.0	39.0
59.6	50.9	50.5	49.5	53.1	44.5	39.9	39.3
55.8	51.0	48.5	48.9	51.6	44.3	40.1	39.2
54.5	51.7	47.4	47.1	50.9	43.7	39.7	39.3

The attenuation for geometric spreading was calculated using Equation 7. The results are shown in Table 65. The calculations are based on the relative difference between the source and the receivers.

Table 65: Attenuation due to Geometric Spreading dB

Freq (Hz)	Mic 1	Mic 2	Mic 3	Mic 4
	EA (dB)	EA (dB)	EA (dB)	EA (dB)
63	7.7	10.2	7.7	10.2
125	7.7	10.2	7.7	10.2
250	7.7	10.2	7.7	10.2
500	7.7	10.2	7.7	10.2
1000	7.7	10.2	7.7	10.2
2000	7.7	10.2	7.7	10.2
4000	7.7	10.2	7.7	10.2
8000	7.7	10.2	7.7	10.2

The attenuation for atmospheric absorption was calculated using Equation 44. The results are shown in Table 66. These calculations are based on temperature and relative humidity measured during the sampling periods shown in Tables 7, 10 and 13.

Table 66: Attenuation due to Atmospheric Absorption dB

Freq (Hz)	Mic 1	Mic 2	Mic 3	Mic 4
	EA (dB)	EA (dB)	EA (dB)	EA (dB)
63	0.01	0.02	0.01	0.02
125	0.05	0.08	0.05	0.08
250	0.17	0.30	0.17	0.30
500	0.48	0.85	0.48	0.85
1000	0.94	1.67	0.94	1.67
2000	1.57	2.78	1.57	2.78
4000	3.29	5.82	3.29	5.82
8000	9.80	17.38	9.80	17.38

The next step was used to adjust for ground effects and was calculated using a custom based computer program developed by MacDonald [MacDonald, 2001]. The results are shown in Table 67 and Figure 40. These calculations are based on source and receivers height, in addition to distance between source and receivers and the ground type. Figure 40 shows how the ground effects vary and could have a substantial attenuation at the further microphone especially at the higher frequencies. The figure also shows that ground effects should be modeled accurately otherwise it is likely to cause error in predicting in sound levels as previously shown using the ISO 9613 method.

Table 67: Attenuation due to Ground Effects dB

Freq (Hz)	Mic 1	Mic 2	Mic 3	Mic 4
	EA (dB)	EA (dB)	EA (dB)	EA (dB)
63	4.3	4.0	1.9	2.6
125	0.7	-0.9	-9.1	-6.1
250	-3.5	-6.7	0.5	-4.1
500	-5.7	-8.7	2.5	3.1
1000	3.1	0.4	2.4	-6.4
2000	-1.8	5.1	3.8	-10.8
4000	0.8	-16.0	1.1	-6.1
8000	4.4	-10.8	4.5	0.9

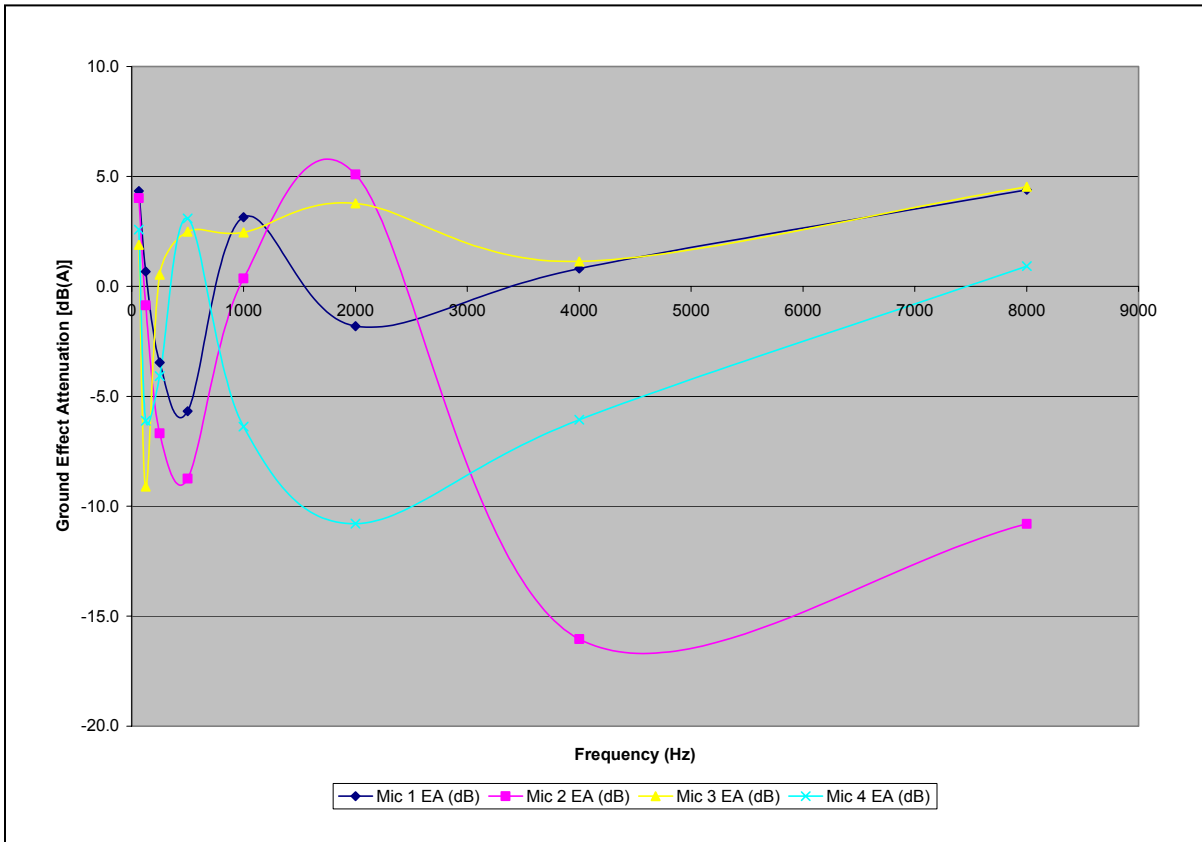


Figure 40: Attenuation due to Ground Effects

The final step was to perform A-weight adjustments as previously listed in Table 2 [ANSI, 1983]. The A-weighted adjustments are shown in Table 68.

Table 68: Attenuation due to A-weighted dB

Freq (Hz)	Mic 1	Mic 2	Mic 3	Mic 4
	EA (dB)	EA (dB)	EA (dB)	EA (dB)
63	-26.2	-26.2	-26.2	-26.2
125	-16.1	-16.1	-16.1	-16.1
250	-8.6	-8.6	-8.6	-8.6
500	-3.2	-3.2	-3.2	-3.2
1000	0.0	0.0	0.0	0.0
2000	1.2	1.2	1.2	1.2
4000	1.0	1.0	1.0	1.0
8000	-1.1	-1.1	-1.1	-1.1

Next, all of the previous attenuations were applied; geometric spreading, atmospheric absorption, ground effects, and A-weighted adjustment. The results are shown in Table 69.

Table 69: The Sum of All Attenuations dB(A)

Freq (Hz)	Mic 1	Mic 2	Mic 3	Mic 4
	EA dB(A)	EA dB(A)	EA dB(A)	EA dB(A)
63	38.2	40.4	35.8	39.0
125	24.5	25.5	14.7	20.3
250	13.0	12.4	17.0	15.0
500	5.7	5.5	13.9	17.3
1000	11.8	12.2	11.1	5.5
2000	6.3	16.9	11.8	1.0
4000	10.8	-1.0	11.1	9.0
8000	23.0	17.9	23.1	29.6

After adding the previous attenuations as shown in Table 67, they were applied to the Reference microphone position sound levels as presented in Table 58. Moreover, A-weight adjustments were also applied to the other four microphone positions as presented in Tables 59-62. After applying the corresponding attenuations to the Reference microphone, the difference was calculated by subtracting the Reference sound levels from each of the microphone positions. This remaining value only includes changes due to atmospheric refraction. The difference for each microphone location of the Downwind Group is shown in Tables 70-73.

Table 70: Sound Level Difference Between Reference & Mic 1 Downwind Group dB(A)

Frequency (Hz)							
63	125	250	500	1k	2k	4k	8k
32.2	34.0	44.4	53.1	50.3	40.1	36.3	37.5
33.9	36.4	42.0	54.6	51.5	49.1	36.9	37.6
29.9	38.7	41.7	54.6	54.9	51.0	33.7	37.7
29.0	29.7	52.5	61.1	40.6	54.9	41.2	37.3
30.9	42.5	44.5	53.5	51.6	48.9	31.8	37.6
33.9	43.8	41.1	38.8	50.3	43.6	38.5	37.6
38.5	41.1	35.7	46.9	49.9	43.1	38.8	37.7
34.0	33.8	45.2	51.1	49.6	50.9	39.3	37.6
29.5	36.7	48.2	55.6	52.2	57.3	39.0	37.5
29.3	42.7	54.8	62.8	61.2	60.2	47.3	37.3
31.5	37.4	56.4	63.4	55.5	56.2	42.0	37.4
31.6	36.7	52.1	58.5	54.2	56.7	38.2	37.7
35.7	50.5	53.8	64.6	54.3	59.0	43.7	37.3
41.4	48.7	43.2	50.8	53.0	47.5	36.9	37.6
41.2	45.5	39.9	50.2	53.2	46.1	39.3	37.8
36.5	39.1	42.0	51.0	53.5	40.2	38.2	37.8

Table 71: Sound Level Difference Between Reference & Mic 2 Downwind Group dB(A)

Frequency (Hz)							
63	125	250	500	1k	2k	4k	8k
24.9	40.4	46.7	54.2	50.0	43.3	45.6	37.0
27.8	33.9	45.3	55.5	50.9	45.7	46.0	37.0
30.5	37.9	44.4	55.3	50.0	46.9	48.5	36.8
29.4	34.1	53.4	61.3	45.5	37.4	55.0	35.9
30.8	38.2	46.0	54.0	53.6	40.7	51.8	36.8
35.2	41.0	43.3	45.5	46.3	41.9	41.0	37.1
35.6	40.5	40.8	48.7	47.0	41.4	40.1	37.1
31.2	32.1	46.6	52.1	40.4	36.1	44.6	37.0
36.3	37.0	49.2	56.1	53.3	44.4	54.8	37.0
28.2	41.3	55.5	63.1	60.6	47.8	59.7	36.0
27.1	33.4	57.1	63.7	54.9	39.0	55.5	36.7
35.7	38.6	52.8	58.8	53.8	42.7	53.5	36.9
29.4	50.1	54.4	64.9	55.2	47.3	56.9	36.5
30.7	24.3	45.4	52.6	46.8	41.3	46.7	37.2
33.9	24.3	42.3	51.6	48.3	42.8	43.4	37.0

Table 72: Sound Level Difference Between Reference & Mic 3 Downwind Group dB(A)

Frequency (Hz)							
63	125	250	500	1k	2k	4k	8k
40.4	50.9	36.7	50.0	55.3	50.7	41.4	38.4
41.5	50.2	37.4	46.6	56.4	48.4	41.2	38.4
31.4	45.9	41.4	47.8	57.3	45.3	40.0	38.4
33.9	50.9	47.8	49.1	53.2	37.7	37.6	37.9
23.9	45.9	39.4	50.4	51.3	50.7	39.8	38.1
29.0	43.1	39.5	49.7	56.4	51.0	42.8	38.4
32.8	44.3	40.7	49.7	58.0	52.2	43.6	38.4
30.6	50.7	41.7	49.2	57.6	48.2	41.5	38.6
33.7	52.4	35.7	38.4	40.3	48.5	38.8	38.0
34.1	54.8	49.7	53.6	61.1	53.4	46.6	38.0
36.1	51.3	52.0	54.6	55.1	48.8	40.9	38.0
31.9	52.2	46.2	47.5	54.2	49.7	36.3	37.8
30.2	61.2	48.6	56.1	56.1	52.6	42.9	37.9
37.7	46.9	38.8	44.2	53.0	46.3	38.5	38.1
37.7	49.7	44.2	46.2	54.7	49.4	39.1	38.1
38.1	50.0	43.1	46.3	54.7	48.8	39.7	38.2

Table 73: Sound Level Difference Between Reference & Mic 4 Downwind Group dB(A)

Frequency (Hz)							
63	125	250	500	1k	2k	4k	8k
27.5	44.9	43.2	39.3	52.0	52.1	37.7	37.9
29.6	44.7	40.8	40.8	53.9	56.8	39.3	38.0
30.2	39.5	39.1	38.4	54.1	58.4	37.1	38.3
32.6	45.1	50.5	46.6	60.0	60.9	43.2	37.9
12.6	40.2	41.6	42.8	61.4	56.1	35.6	38.2
34.8	35.9	36.9	43.8	47.2	46.0	40.0	38.2
29.2	40.3	29.3	43.3	51.5	52.4	39.6	38.2
27.9	45.3	42.8	41.1	55.7	57.8	39.1	38.2
30.6	46.6	46.2	29.4	61.4	63.0	43.0	38.2
16.5	49.0	52.8	49.4	67.8	65.7	49.2	38.1
24.6	45.4	54.1	50.7	63.2	61.9	44.1	38.4
28.4	46.5	49.8	32.8	62.2	62.4	41.1	38.3
26.3	55.6	51.5	52.3	63.4	64.6	45.9	38.3
27.0	40.1	38.7	44.8	51.8	55.3	38.7	38.0
33.3	45.4	35.4	45.4	51.1	49.2	39.8	38.3
27.2	44.4	37.7	44.2	46.7	49.8	39.8	38.2

Difference for each microphone locations for the Crosswind Group is shown in Tables 74-77.

Table 74: Sound Level Difference Between Reference & Mic 1 Crosswind Group dB(A)

Frequency (Hz)							
63	125	250	500	1k	2k	4k	8k
32.8	38.5	41.1	49.4	48.6	48.2	37.5	37.9
35.9	38.0	49.8	53.7	52.8	53.7	3.4	37.8
26.1	45.9	57.5	64.6	63.7	62.4	48.6	37.2
34.0	28.6	52.6	59.6	56.3	57.0	46.1	37.8
40.8	32.2	48.8	54.5	50.6	52.7	39.7	37.8
30.6	33.0	47.9	54.4	40.2	47.0	34.9	37.8
23.8	39.2	50.1	60.9	45.8	48.2	23.0	37.9
38.0	44.9	52.8	63.0	47.4	49.9	40.6	37.9
40.1	50.1	54.0	62.9	45.3	50.6	37.7	37.9
31.0	44.6	55.2	60.9	37.7	51.2	30.9	37.9
39.7	36.8	56.1	58.3	51.9	57.2	43.2	37.9
37.9	46.8	57.5	59.2	53.9	56.9	46.3	37.7
38.5	47.9	57.8	61.9	56.8	61.2	49.3	37.3
29.6	43.9	52.6	57.2	53.0	57.9	44.2	37.8

Table 75: Sound Level Difference Between Reference & Mic 2 Crosswind Group dB(A)

Frequency (Hz)							
63	125	250	500	1k	2k	4k	8k
38.1	36.7	41.1	47.7	48.1	47.9	39.1	37.5
37.5	37.8	50.3	53.5	51.2	47.3	49.0	37.3
24.4	38.0	58.0	64.7	63.1	30.0	60.8	32.9
24.6	34.8	53.3	59.8	54.8	38.0	58.5	36.4
32.2	39.5	50.0	54.7	42.7	44.6	53.7	37.2
26.6	41.8	49.0	54.8	50.0	45.3	47.6	37.5
28.7	36.9	50.8	61.2	47.8	45.1	51.1	37.6
32.3	45.5	53.5	63.3	46.8	44.0	55.1	37.2
36.2	49.8	54.7	63.2	44.2	38.7	53.9	37.4
31.0	45.6	55.9	61.4	45.5	41.1	52.3	37.6
32.6	34.1	56.7	59.2	51.8	41.8	56.7	37.0
22.3	43.9	58.1	60.2	53.2	39.2	59.0	36.8
31.3	47.3	58.4	62.3	56.8	48.8	61.6	35.9

Table 76: Sound Level Difference Between Reference & Mic 3 Crosswind Group dB(A)

Frequency (Hz)							
63	125	250	500	1k	2k	4k	8k
30.0	50.4	42.9	48.7	54.1	45.6	39.1	38.7
29.3	49.8	42.5	49.3	41.4	39.3	35.0	38.6
28.9	56.3	53.2	55.3	64.1	56.3	48.2	38.0
22.8	54.6	47.7	49.4	55.7	49.2	45.5	38.5
36.5	55.2	41.6	39.4	44.7	39.6	38.1	38.5
36.0	50.1	44.7	44.6	54.0	49.0	37.5	38.8
34.2	51.3	47.7	49.0	56.2	48.6	32.9	38.7
41.6	56.8	38.9	52.5	57.5	48.7	38.2	38.5
43.0	60.7	40.1	49.3	57.5	51.1	33.8	38.7
40.9	56.8	35.3	47.9	55.0	51.5	40.7	39.1
35.1	51.4	50.9	54.7	53.5	47.6	34.7	39.0
42.1	57.3	53.2	56.4	46.1	45.7	39.5	38.8
46.4	58.0	51.3	58.4	51.9	51.2	44.7	38.8
48.0	41.6	52.8	64.7	55.6	54.8	46.4	39.2
46.1	47.3	58.1	65.5	53.3	53.1	46.2	39.4
44.2	48.2	59.6	64.2	57.3	56.1	50.6	40.2

Table 77: Sound Level Difference Between Reference & Mic 4 Crosswind Group dB(A)

Frequency (Hz)							
63	125	250	500	1k	2k	4k	8k
20.9	44.0	38.4	47.2	44.3	54.4	37.2	38.5
34.1	43.8	47.5	46.0	59.9	59.1	33.4	38.4
22.1	50.6	55.4	51.7	70.1	67.7	50.6	38.4
31.0	48.7	50.2	35.8	62.9	62.3	48.1	38.2
30.2	49.1	46.5	47.0	57.3	58.0	42.1	38.4
27.6	44.0	43.6	48.1	50.5	53.3	27.4	38.4
28.8	46.3	46.6	42.7	53.5	55.1	37.3	38.3
37.9	50.6	49.5	46.9	53.7	57.2	43.6	38.4
37.8	54.8	51.0	41.6	55.1	57.8	41.1	38.4
30.1	51.4	52.8	46.5	55.6	58.0	37.2	38.4
37.5	45.7	53.6	47.3	60.2	62.8	45.6	38.5
41.3	50.1	55.2	47.7	61.5	62.5	48.2	38.5
41.0	51.5	55.3	38.2	63.9	66.5	51.1	38.4
36.1	44.8	48.0	48.4	59.9	63.2	45.8	38.4
19.1	46.3	52.6	46.6	65.5	66.3	49.8	38.4
29.2	47.0	47.0	48.2	64.9	65.5	48.2	38.4
36.5	44.5	38.4	48.1	60.5	60.3	40.5	38.5

Difference for each microphone locations for the Crosswind Group is shown in Tables 78-81.

Table 78: Sound Level Difference Between Reference & Mic 1 Upwind Group dB(A)

Frequency (Hz)							
63	125	250	500	1k	2k	4k	8k
32.4	43.1	47.5	50.6	49.5	47.4	35.3	37.7
28.2	44.7	58.3	64.8	57.8	60.2	47.6	37.3
29.6	45.4	61.1	64.3	56.6	57.5	45.5	37.4
36.0	43.8	56.2	60.3	51.7	55.2	46.2	37.3
34.4	38.5	47.5	53.6	44.2	47.8	38.4	37.5
33.4	48.1	50.3	55.5	52.3	55.8	39.2	37.6
19.5	52.8	53.2	59.9	55.9	56.3	44.6	37.4
44.9	47.2	60.0	75.4	66.3	63.6	54.7	36.0
43.8	54.4	60.4	74.7	63.3	60.0	50.1	37.3
35.7	45.0	46.1	59.7	47.4	48.5	37.8	37.5
34.8	36.4	39.1	53.1	33.6	46.8	38.3	37.8
37.8	32.0	51.8	58.9	55.5	56.7	40.4	37.4
36.8	38.3	43.6	51.9	48.6	45.8	38.9	37.6
39.9	37.6	38.5	50.2	47.3	42.8	43.6	37.8

Table 79: Sound Level Difference Between Reference & Mic 2 Upwind Group dB(A)

Frequency (Hz)							
63	125	250	500	1k	2k	4k	8k
26.0	41.0	48.8	51.0	49.4	26.1	43.5	37.0
30.6	45.1	59.0	65.0	57.4	49.4	59.8	35.3
27.6	43.7	61.7	64.5	56.2	46.3	57.9	35.9
26.1	41.2	57.0	60.6	52.5	43.8	58.6	35.6
19.7	33.3	49.2	54.1	47.2	32.3	53.0	37.0
25.8	39.2	51.5	56.0	51.7	44.3	53.3	37.0
25.6	42.6	54.0	60.2	55.9	45.3	57.3	36.5
43.0	48.6	60.6	75.6	66.0	52.9	66.6	26.1
42.0	53.6	61.0	74.9	62.9	49.2	62.3	34.8
24.7	44.1	47.7	60.0	48.3	34.5	46.7	37.1
23.2	36.6	43.1	54.0	47.7	34.9	44.0	37.0
18.1	39.3	52.8	59.3	56.1	46.2	55.3	36.5
23.2	31.0	45.8	53.3	50.2	37.3	49.9	37.0
25.7	30.9	44.0	52.9	47.7	33.6	41.4	37.0

Table 80: Sound Level Difference Between Reference & Mic 3 Upwind Group dB(A)

Frequency (Hz)							
63	125	250	500	1k	2k	4k	8k
19.4	54.0	43.2	46.2	53.0	44.8	40.5	38.5
36.2	56.9	54.3	56.3	57.6	54.1	46.8	38.2
33.7	56.5	57.1	55.9	57.0	51.6	44.9	38.4
32.4	54.7	52.3	51.7	53.4	49.2	45.8	38.2
30.4	49.2	43.8	44.3	47.1	38.8	37.5	38.2
26.9	51.3	46.4	47.0	53.3	49.7	38.2	38.3
33.0	54.1	48.9	51.6	57.0	50.5	44.2	38.4
47.7	59.7	55.9	67.2	67.1	57.9	54.4	37.1
46.7	64.5	56.2	66.5	64.0	54.2	49.9	38.1
26.7	55.5	35.4	51.1	46.2	25.9	36.9	38.6
24.1	49.1	40.6	42.5	39.6	37.5	37.6	38.5
25.7	50.6	46.2	50.3	56.4	50.7	41.0	38.4
24.0	46.2	38.4	38.9	42.9	37.9	34.4	38.4
31.1	45.7	33.8	40.4	42.0	40.8	39.1	38.4
28.7	50.9	38.4	55.2	50.7	41.4	36.3	38.3
28.7	57.4	47.3	59.7	49.5	47.6	37.7	38.4

Table 81: Sound Level Difference Between Reference & Mic 4 Upwind Group dB(A)

Frequency (Hz)							
63	125	250	500	1k	2k	4k	8k
20.0	48.4	45.9	36.1	56.6	53.1	34.9	36.2
33.3	51.2	56.4	53.1	64.3	65.5	49.6	36.2
30.5	50.8	59.1	52.6	63.1	62.9	47.5	36.1
28.2	49.0	54.3	48.6	59.6	60.8	48.3	36.2
27.7	43.5	46.3	41.4	54.6	53.9	41.7	36.2
19.1	45.6	48.8	43.7	59.4	61.2	42.2	36.2
30.6	48.4	51.3	48.2	62.9	61.8	46.8	36.5
44.4	54.1	58.0	63.8	72.7	68.9	56.6	36.0
43.5	58.9	58.4	63.1	69.7	65.4	52.2	36.0
23.1	49.9	45.0	47.9	56.3	55.1	28.4	36.2
17.0	43.3	39.6	40.9	55.2	54.4	34.1	36.3
25.5	44.9	50.0	47.2	62.9	62.5	44.5	36.4
27.9	40.4	42.5	40.1	57.0	55.4	36.5	36.4
28.2	39.9	40.5	39.1	55.0	54.0	36.6	36.3
29.9	45.3	42.9	51.8	58.7	57.3	30.6	36.3
27.1	51.8	49.8	56.3	58.8	60.5	41.1	36.5
30.9	39.2	38.1	40.2	55.5	53.1	34.5	36.3

The data presented in Tables 70-81 show that for all the groups, a difference between the calculated and measured sound levels still exists. This is due to the data being corrected for everything but refraction effects which still remain and are represented by these values.

Using this data, an empirical model incorporating the measured parameters (wind speed, wind shear, lapse rate) which affect atmospheric refraction was developed. This consisted of developing an empirical model for each octave band frequency within each group that corresponds to the difference between the Reference and each of the microphone locations after all propagation effects except refraction have been accounted for. As previously pointed out, A-weighted factors are insufficient for frequency analyses. As such, this method is octave band based.

Statistical methods used were regression analysis, Gaussian statistics, and hypothesis testing. The methods used to determine significant parameters, included multiple regression analysis for model building and other suitable statistical method such as Backward Elimination were employed to correlate the attenuation due to atmospheric refraction with the measured atmospheric parameters and derived sound level differences.

After initial statistical testing and checking residuals graphs, it was determined that the ratio of the highest difference was larger than 3 times the lowest difference, hence there was a need for transformation of the dependent variable by applying a log to the dependent variable. Moreover, after inspecting residuals graphs, it was determined the need for second order component for the dependent variables to be included in the

empirical model development. Table 82 presents an excerpt of the data from the Downwind Group used for developing the empirical model. These data are representative of the data used to develop the empirical model for the 63 Hz frequency. The data used was the wind shear, lapse rate and the wind speed (U-wind) that is in the same direction to the sound propagation path from the source to the receivers.

Table 82: Sample of Data used for Empirical Model Development for the 63 Hz

Wind Shear (m/s/m)	Lapse Rate (°C/m)	Wind Speed (m/s)
-0.231	-0.1947	0.00
-0.231	-0.1947	0.70
-0.193	-0.1947	1.06
-0.077	-0.1947	1.06
-0.116	-0.1947	1.41
-0.347	-0.1947	1.23
-0.308	-0.1947	0.88
-0.270	-0.1947	0.70
-0.154	-0.1947	1.59
-0.193	-0.1947	0.88
-0.308	-0.1947	0.70
-0.039	-0.1947	1.94
-0.308	-0.1947	1.06
-0.385	-0.1947	1.06
-0.347	-0.1947	0.88
-0.308	-0.1947	0.70
-0.385	-0.1947	0.70
-0.462	-0.1947	0.00
-0.539	-0.1947	-0.35
-0.539	-0.1947	-0.18
-0.385	-0.1947	0.18
-0.462	-0.1947	0.18
-0.462	-0.1947	0.18
-0.385	-0.1947	0.18
-0.347	-0.1947	0.18
-0.424	-0.1947	0.53
-0.077	-0.1947	1.23

The wind shear ranged from -0.86 to 0.9. 1648 cases the wind was propagating toward the receivers, while 582 cases the wind was propagating toward the source. Since wind shear was determined to be the most important variable from the measurements, the new model is very dependent on this variable. The wind component of the wind angle, in the plane of propagation was used to determine the wind shear used in development of the model.

It was decided to use the stepwise method of “backward elimination” for development of the empirical model. This method starts by incorporating all variables initially in the model, then eliminating variables that exceed a pre-determined “ α value” one at a time. The initial variable list included the U and V-wind components and also the wind direction but it has been shown through statistical testing that the U-wind component was more significant and was included in the model development. Moreover, testing of each variable for significance required going through several iterations to eliminate non-significant parameters. Testing of each variable was also accomplished to verify the results of the stepwise method. Each parameter was tested for or 95% significance, the “ α value” was set to 0.05 for the purpose of this research. After inspecting residuals graphs, a need for second order component which include second order and interaction between all independent variables was indicated. Initially, the model included all the independent variables and their second order parameters and their interactions, however after testing for significance using P- value of 0.05, some of these terms were not included in the model as it shown later in this discussion. The variables

chosen are parameters that are directly related to refraction effects as shown in the literature review. The variables chosen were Wind Shear (τ), Wind Speed (S), Lapse Rate (γ), Wind Shear² (Wshear²), Wind Speed² (S²), Lapse Rate² (γ^2), Wind Shear (τ)*Lapse Rate (γ), Wind Shear (τ)*Wind Speed (S), and Wind Speed (S)*Lapse Rate (γ). However, some of the parameters were not significant for all the frequency models when test for 95% significance. Thus, they were removed from the model after five to six iterations at the most. The best model developed from all groups is shown in Table 83. Table 83 shows each frequency equation with the coefficient for each of the parameter detailed beneath it.

Table 83: Refraction Attenuation Empirical Model for Each Frequency

Frequency (Hz)	Intercept	(τ)	(γ)	(s)	(τ) ²	(γ) ²	(s) ²	$\tau * \gamma$	$\tau * S$	$\gamma * S$
63	0.337	0.0	0	0.13	0.604	-5.57	-0.0517	-1.78	0.0	0.0
125	0.468	0.0	-4.99	-0.4	0.0	-29	0.113	0.0	-0.199	0.0
250	0.48	0.6	-4.16	-0.39	0.0	-26.6	0.0901	0.0	-0.296	0.0
500	0.463	0.0	-4.15	0.0	0.0	-16.8	-0.011	-2.94	0.0	0.725
1000	0.62	0.828	-4.26	-0.48	0.0	-32.6	0.0961	0.0	-0.321	0.0
2000	0.612	0.625	-3.07	-0.36	0.0	-22.8	0.063	0.0	-0.226	0.0
4000	0.406	-0.22	-2.59	0.0	0.0	-11.4	0.0	-2.96	0.0834	0.777
8000	0.382	0.008	-0.2	0.009	0.0201	-0.93	0.0	0.0	0.0	-0.0301

The model was tested for significance by using the t-test and it was determined that the overall model is an effective predictor. This was confirmed by a small P value

($P=0.00$) when testing the model for 95% significance ($\alpha=0.05$), using the statistical t-test method. Moreover, the overall model is adequate for prediction ($F > 5F_0$), based on results from the statistical F-test method. The model mean square error (MSE) is significantly small and was equal to 2.72 on average. In addition the average $R_{adj}^2 = 54.2\%$. Furthermore, all the β 's for the remaining independent parameters were significant and there was no multicollinearity evident when tested using the variance inflation factor (VIF) method. Hence, it could be stated the new empirical model is a useful model for prediction based on the available data.

The small R_{adj}^2 is attributed to the fact that the data used in this model were not in a time series and might have caused autocorrelation. Another reason for the low R_{adj}^2 is the small variation in lapse rate during the sampling period. Also, the atmospheric parameters were measured at a maximum elevation of 20 feet (6 m), which were discovered to be not sufficient to measure a significant lapse rate. However, this model shows that the included parameters are significant, and they could explain and interpret atmospheric refraction.

Another approach to develop the model was to investigate if the distance between the Reference and the microphone would be significant. The same steps to taken the model in Table 82 were used in addition to adding the distance as a variable. The distance was incorporated by dividing the difference in sound levels between the Reference and microphone by the corresponding distance which was 365, 708, 365 and 708 feet for Mic 1, Mic 2, Mic 3 and Mic 4 respectively. This resulted in a dB per foot approach and

assumed the effect to be linear and that the refraction effects would increase with distance. However, this approach resulted in models that were less significant statistically. The analysis was conducted for all three groups. The Downwind Group models developed for the 63, 125, 2000, and 4000 Hz frequencies, the model was not adequate for prediction ($F \ll 5F_o$), using the statistical F-test method. In addition, the R_{adj}^2 was smaller (i.e. $R_{adj}^2 = 14.2\%$ for 63 and $R_{adj}^2 = 28.3\%$ 125 Hz frequencies). Also, the Crosswind Group models for the 125, 500, and 4000 Hz frequencies, the model was not adequate for prediction ($F \ll 5F_o$), using the statistical F-test method. In addition, the R_{adj}^2 was smaller (i.e. $R_{adj}^2 = 23.4\%$ for 500 and $R_{adj}^2 = 20.1\%$ 4000 Hz frequencies). The Upwind Group models developed for the 63, 125, and 4000 Hz frequencies, the model was not adequate for prediction ($F \ll 5F_o$), using the statistical F-test method. In addition, the R_{adj}^2 was smaller (i.e. $R_{adj}^2 = 14.6\%$ for 125 and $R_{adj}^2 = 10.4\%$ 4000 Hz frequencies). These Downwind Group yielded better results than both the other two groups. This is likely due to the fact that the downwind group has more data points available to try to build the model. The poor results when distance was included could be attributed to two reasons; 1) the small difference in distance between the two tower locations and the Reference microphone position and 2) the ground effects resulting in prediction errors due to a much more complex function of distance than used here because of the refraction effects altering the grazing angle of the acoustic wave. This could have resulted in less significant statistically model when introducing distance as a variable. Hence, it was decided to focus on the previous model shown in Table 83.

The final step in the new empirical model development was to validate the model. Data collected by Wayson [Wayson, 1989] in Texas was used for validation purposes. Wayson has collected data that included temperature, wind speed and magnitude in addition to sound levels at several distances from the sources. The atmospheric parameters that included wind shear, lapse rate and the wind speed (U-wind) that is in the same direction to the sound propagation path from the source to the receivers are shown in Table 84.

Table 84: Data Collected in Texas by Wayson [Wayson, 1989]

Wind Shear (m/s/m)	Lapse Rate (°C/m)	Wind Speed (m/s)
0.031	-0.036	1.44
0.049	-0.030	1.66
0.056	-0.044	1.51
-0.017	-0.140	-1.92
-0.054	-0.137	-2.00
-0.048	-0.145	-1.62
-0.044	-0.094	-1.85
0.027	0.035	0.21
0.028	0.052	0.32
-0.086	-0.080	-2.26
-0.092	-0.095	-2.81
-0.073	-0.026	-1.20
-0.024	-0.123	-2.00
0.059	-0.107	1.00
0.069	-0.032	1.06
0.060	0.018	1.30
0.041	0.027	0.80
-0.045	-0.142	-2.49
-0.046	-0.108	-2.46
-0.046	-0.096	-2.39
0.078	-0.035	1.53
0.088	-0.125	2.00
0.126	-0.041	2.33
0.002	-0.159	2.29

Note: Lapse rates are shown here as vertical gradients instead of the more common way of normal lapse rate having a positive sign. This was done to emphasize the vertical gradient as used in the model presented here.

Wayson has calculated refraction attenuation based on the same normalization concept but using different methods in calculating ground effects and a slightly different method in calculating atmospheric attenuation.

The data shown, in Table 84, were used to predict excess refraction attenuation for each frequency band based on the new empirical model shown in Table 83. The predicted values were compared to two set of data calculated during the Wayson research effort. The first set of data is refraction attenuation based on normalization of the data that does not include ground effects. The other set of data is refraction attenuation that is based on normalization and includes ground interference.

Since the new derivation model described in this dissertation was for octave bands and the Wayson method only for A-weighted values, the prediction values had to be on a similar basis to allow comparison. The refraction attenuation effects based on the new empirical model were predicted for each frequency band, and were then summed logarithmically to a single A-weighted overall excess refraction attenuation. This allows direct comparison to the Wayson method which predicts A-weighted correction values.

The comparison between the derived empirical model for this research predicted refraction attenuation and Wayson calculated refraction attenuation is shown in Table 85. The first column (i.e. Column A) includes the predicted refraction attenuation based on the new empirical model. The second column (i.e. Column B) includes the calculated refraction attenuation not adjusted for ground effects. While the third column (i.e. Column C) includes the calculated refraction attenuation adjusted for ground effects. The difference between the predicted refraction attenuation and each of the Wayson

calculated refraction attenuation are presented in the last two columns. Some basic statistical calculations are shown at the bottom of Table 85.

Table 85: Comparison Between Empirical Model Predicted Refraction Attenuation and Wayson Calculated Refraction Attenuation

	Empirical Model	Wayson Calculated		Difference = Predicted - Calculated	
	Refraction Attenuation	Refraction Attenuation			
	W/ Ground Effects	W/o Ground Effects	W/ Ground Effects	A-B	A-C
	A	B	C		
1	9.4	-1.7	-0.7	11.1	10.1
2	9.4	-1.9	-0.9	11.3	10.3
3	9.4	-1.5	-0.5	10.9	9.9
4	9.9	-0.6	0.4	10.5	9.5
5	9.9	1.1	-0.1	8.8	10.0
6	9.8	0.3	1.3	9.5	8.5
7	9.9	4.1	5.1	5.8	4.8
8	9.4	-2.2	-1.2	11.6	10.6
9	9.3	-1.7	-0.7	11.0	10.0
10	10.0	-0.8	0.2	10.8	9.8
11	10.2	-1.9	-0.9	12.1	11.1
12	9.7	1.7	2.7	8.0	7.0
13	10.0	5.2	6.2	4.8	3.8
14	9.5	-1.0	0.0	10.5	9.5
15	9.5	3.1	4.1	6.4	5.4
16	9.3	1.0	2.0	8.3	7.3
17	9.3	-1.2	-0.2	10.5	9.5
18	10.0	1.9	2.9	8.1	7.1
19	10.1	1.9	2.9	8.2	7.2
20	10.1	0.5	1.5	9.6	8.6
21	9.4	-1.4	-0.4	10.8	9.8
22	9.4	-0.1	0.9	9.5	8.5
23	9.4	-1.2	-0.2	10.6	9.6
24	9.3	-1.5	-0.5	10.8	9.8
Max	10.2	5.2	6.2	12.1	11.1
Min	9.3	-2.2	-1.2	4.8	3.8
Avg	9.7	0.1	1.0	9.6	8.7
Std	0.3	2.0	2.0	1.9	1.9

Figure 41 shows a scatter plot between the empirical method for predicting refraction attenuation (first column) and the Wayson method for predicting refraction attenuation without ground interference included (second column). Using statistical testing, the r^2 value was 0.3 between the empirical method for predicting refraction attenuation and Wayson method for predicting refraction attenuation without ground interference included. While the r^2 value is equal to 0.2 between the empirical method for predicting refraction attenuation (first column) and the Wayson method for calculating refraction attenuation with ground effects included (third column). The r^2 value of 0.3, between the empirical method for predicting refraction attenuation and Wayson method for predicting refraction attenuation without ground interference included, indicate that a reasonable fit exist between empirical method for and the Wayson method for predicting refraction attenuation. Additionally, using the t-test for testing the null hypothesis, there is no difference between the results of the two methods. The null hypothesis was tested at 95 % level of confidence and has resulted in acceptance of the null hypothesis with $t = 0.3 < t_{0,05} = 1.68$. This tends to indicate that the agreement between results is good.

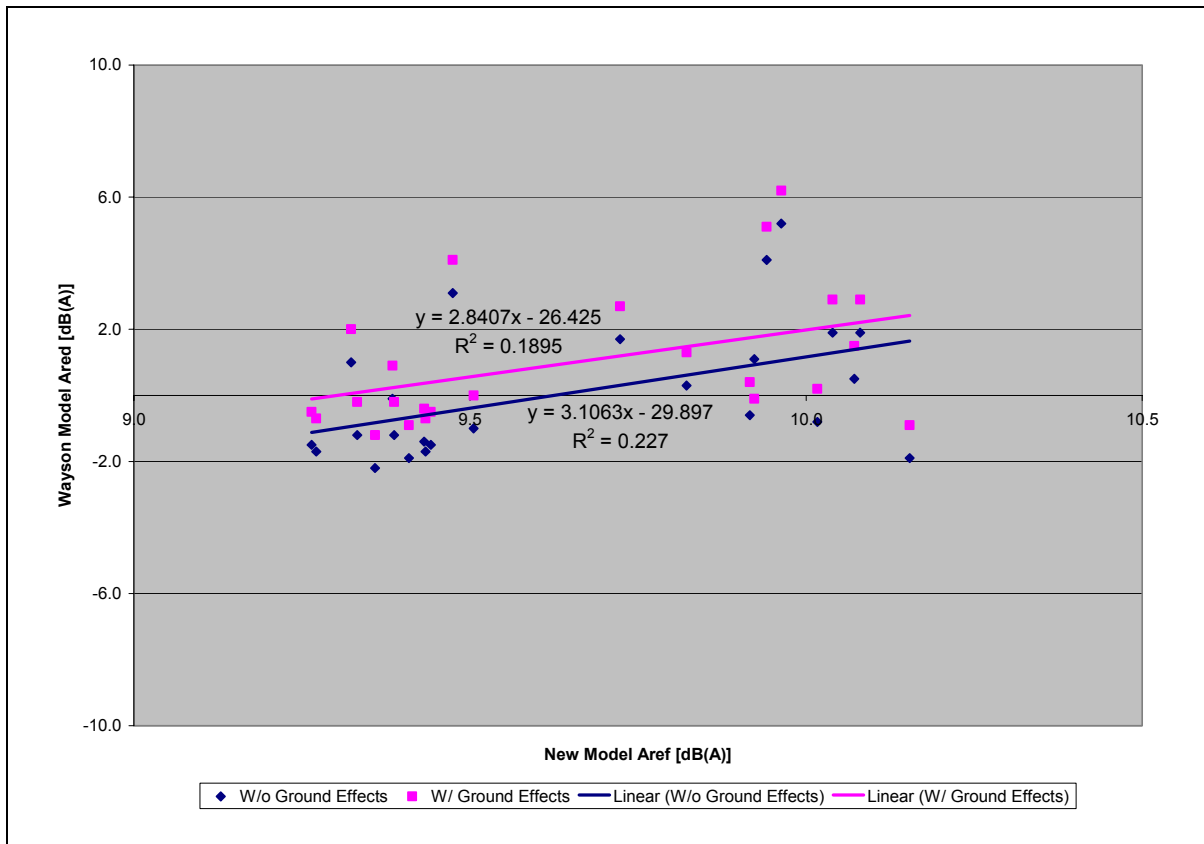


Figure 41: Scatter plot of Refraction Attenuation for both the Empirical Model and Wayson Method

Table 85 illustrates that the difference between predicted refraction attenuation and Wayson calculated attenuation (without ground effects) range from 4.8 to 12. dB(A). With an average difference of 9.6 dB(A) and standard deviation of 1.9. This difference is likely attributed to complications from ground effects modeling and to the fact that the new model used more advanced predicted values based on octave band contributions. Meanwhile, the difference between predicted refraction attenuation and Wayson calculated attenuation (with ground effects) range from 3.8 to 11.1 dB(A). With an

average difference of 8.7 dB(A) and standard deviation of 1.9. As before, ground effects appear to be key to differences between the models. This is of course quite complex and can only be assumed since proof is not possible from the data available. However, the analysis heavily indicates this parameter as the difference. The Wayson method has calculated ground effects attenuation based on the STAMINA model methodology which is the older model for predicting traffic noise. Since the Wayson research conducted in 1989, a new traffic noise model has been released (TNM) that contains an updated ground effects attenuation algorithm. The new empirical model developed for this research is based on the more updated algorithms and implemented using the software developed by MacDonald [MacDonald, 2001].

Finally, this experiment has shown that atmospheric refraction is evident with effects shown at both 440 feet (134 m) and 780 feet (238 m) from the source. The new empirical model incorporates “wind shear” and “lapse rate” terms as a function of wind speed and temperature, respectively for each octave band. This model is an attempt to predict atmospheric refraction by including the relevant parameters (e.g. wind speed, wind shear, and lapse rate) that directly affect atmospheric refraction. Table 85 illustrates that the new predicted values are comparable to the Wayson values for refraction attenuation and that the average difference when using the new empirical formula was in the order of 9.7 dB(A) as shown in Table 85. Consequently, it could be mentioned that this new empirical model is a new direction and approach in predicting attenuation due to refraction effects.

CHAPTER 5

CONCLUSIONS

There has been only limited research conducted on the effects of atmospheric refraction on traffic noise propagation behind noise barriers. This can be an important parameter even over short distance that corresponds to first and second row homes. The purpose of this research was to better understand the meteorological effects on traffic noise propagation for this relatively short propagation distance through measurements and comparison to acoustic theory.

Detailed noise and weather measurements were conducted to establish a database to allow evaluation of the problem. A comparison among the FHWA TNM and the ISO 9613-2 outdoor sound propagation prediction method was accomplished to determine the difference between the measured and predicted sound levels of existing models that do not account for refraction. In addition, the research investigated if combining the ISO meteorological correction factor or the refraction empirical model developed by Wayson with the ISO 9613-2 method would reduce the difference between measured and predicted sound levels.

This research has demonstrated that significant differences occurred between measured and predicted sound levels when using the unadjusted ISO 9613-2 method. This difference increased when the atmospheric conditions was an up wind case (i.e. the wind propagates from the receivers toward the source). The ISO 9613-2 method was

mainly developed for downwind conditions, which helps to explain why the large difference occurred between predicted and measured sound levels corresponding to upwind conditions. Furthermore, the ISO 9613-2 method assumes that for soft ground the ground effect correction is equal to zero in the middle region between the source and the receiver regions. All of these factors contributed to the inaccurate modeling of ground effects, leading to substantial difference between predicted and measured sound levels.

Combining the meteorological correction factor (C_{met}) with the ISO 9613-2 method in predicting sound pressure level did little to reduce the difference between predicted and measured sound levels did slightly improve the results. In attempting to combine the attenuation predicted by the ISO 9613-2 with Wayson empirical refraction model, some success was found for A-weighted correction, primarily in the downwind case. However, the other groups showed smaller improvement. The Wayson empirical model was developed for A-weighted application and this limitation led to a finding that a method for predicting by octave band was needed. Findings show that if the method by Wayson was to be advanced, it needed to be octave band based instead of only A-weighting. Research allowed development of an empirical model incorporating the measured parameters (wind shear, wind speed, and lapse rate) to account for the atmospheric refraction providing a method to reduce the difference in measured and predicted sound levels

The FHWA model, TNM, was also evaluated. As expected, TNM has under-predicted in cases of downwind and crosswind conditions, while it over-predicted in

cases of upwind conditions since refraction is not considered. TNM predicted levels, when compared to measured values, resulted into a comparable difference between predicted and measured sound levels. Furthermore, it was shown that refraction effects should not be ignored for highway noise modeling.

This led to the development of a new empirical model. Data analysis was done by a direct comparison of the close Reference position to the other microphone positions with corrections for all propagation parameters except refraction made at these positions. The corrections included attenuations due to geometric spreading, atmospheric absorption and ground effects. The use of the Reference position eliminated any traffic variance since a direct comparison of levels could be accomplished in real time.

The derived empirical model was developed for each octave band frequency within each of the three groups which were the Downwind, the Crosswind, and the Upwind Groups. The derived refraction effects model for each octave band then allows correction for this important phenomenon. Using logarithmic summations, the A-weighted value can also be determined after application of the A-weighting for each octave band.

After applying statistical methods and thorough statistical testing, the best model developed for each octave band is shown in details hereafter and in Table 83:

63 Hz Empirical model:

$$\text{Excess Attenuation} = 0.337 + 0.13 * S - 5.57 * \gamma^2 + 0.604 * \tau^2 - 0.0517 * S^2 - 1.78 * \tau * \gamma$$

Where:

S = wind Speed

γ = Lapse Rate

τ = Wind Shear

125 Hz Empirical model:

$$\text{Excess Attenuation} = 0.468 - 4.99 * \gamma - 0.401 * S - 29 * \gamma^2 + 0.113 * S^2 - 0.199 * \tau * S$$

250 Hz Empirical model:

$$\text{Excess Attenuation} = 0.48 + 0.6 * \tau - 4.16 * \gamma - 0.394 * S - 26.6 * \gamma^2 + 0.0901 * S^2 - 0.296 * \tau * S$$

500 Hz Empirical model:

$$\text{Excess Attenuation} = 0.463 - 4.15 * \gamma - 16.8 * \gamma^2 - 0.0111 * S^2 - 2.94 * \tau * \gamma + 0.725 * \gamma * S$$

1000 Hz Empirical model:

$$\text{Excess Attenuation} = 0.62 + 0.828 * \tau - 4.26 * \gamma - 0.475 * S - 32.6 * \gamma^2 + 0.0961 * S^2 - 0.321 * \tau * S$$

2000 Hz Empirical model:

$$\text{Excess Attenuation} = 0.612 + 0.625 * \tau - 3.07 * \gamma - 0.357 * S - 22.8 * \gamma^2 + 0.063 * S^2 - 0.226 * \tau * S$$

4 000Hz Empirical model:

$$\text{Excess Attenuation} = 0.406 - 0.224 * \tau - 2.59 * \gamma - 11.4 * \gamma^2 - 2.96 * \tau * \gamma + 0.0834 * \tau * S + 0.777 * \gamma * S$$

8000 Hz Empirical model:

$$\text{Excess Attenuation} = 0.382 + 0.00811 * \tau - 0.199 * \gamma - 0.00854 * S - 0.0925 * \gamma^2 + 0.0201 * \tau^2 - 0.0301 * \gamma * S$$

Table 83: Refraction Attenuation Empirical Model for Each Frequency

Frequency (Hz)	Intercept	(τ)	(γ)	(s)	(τ) ²	(γ) ²	(s ²)	$\tau * \gamma$	$\tau * S$	$\gamma * S$
63	0.337	0.0	0	0.13	0.604	-5.57	-0.0517	-1.78	0.0	0.0
125	0.468	0.0	-4.99	-0.4	0.0	-29	0.113	0.0	-0.199	0.0
250	0.48	0.6	-4.16	-0.39	0.0	-26.6	0.0901	0.0	-0.296	0.0
500	0.463	0.0	-4.15	0.0	0.0	-16.8	-0.011	-2.94	0.0	0.725
1000	0.62	0.828	-4.26	-0.48	0.0	-32.6	0.0961	0.0	-0.321	0.0
2000	0.612	0.625	-3.07	-0.36	0.0	-22.8	0.063	0.0	-0.226	0.0
4000	0.406	-0.22	-2.59	0.0	0.0	-11.4	0.0	-2.96	0.0834	0.777
8000	0.382	0.008	-0.2	0.009	0.0201	-0.93	0.0	0.0	0.0	-0.0301

Note: Value of 0 indicate variable not included in the model

Based on the new empirical model, the overall refraction attenuation can then be derived by summing all the A-weighted refraction corrections for all octave bands and subtracting them from the Reference position. The model was tested for significance and it was determined that the overall model is an effective predictor. The R_{adj}^2 values ranged from 40% to 72%, with the best being for the 8 KHz octave band and the worst for the 63 Hz octave band. The small R_{adj}^2 is attributed to the small variation in lapse rate and the

fact that the data used in this model were not in time series which is likely to have caused autocorrelation.

Furthermore, this model was validated against data collected in Texas by Wayson in 1989. Statistical testing has shown that the fit between the empirical method for predicting refraction attenuation and the Wayson method for calculating refraction attenuation without ground effects included resulted in an r^2 value of 0.3. When testing using the t-test for testing the null hypothesis, there is no significant difference between the results of the two methods. The results have indicated that an agreement between results is fair to good. It is thought the agreement is hindered by different methods used to predict ground effects. Additionally, the use of octave band sound levels corrections is thought to provide better results in accurately accounting for refraction effects. Additionally, the new model derived as part of this research uses a single equation for upwind and downwind propagation. This could be reevaluated in future work to determine if the equations should be separate as in the Wayson methodology.

CHAPTER 6

RECOMMENDATIONS

This work has added to the knowledge base of atmospheric effects on traffic noise propagation, but there are areas of improvement for future research. More detailed measurements, over greater time periods with more sample periods are needed to make the method more robust. Additionally meteorological measurement conducted at higher elevations above the ground may help to reduce ground effects allowing a more definite evaluation of atmospheric effects. The measurement system may need to record the meteorological data at several time periods year round in order to account for various weather conditions. Additionally, the new model derived as part of this research uses a single equation for upwind and downwind propagation. This could be reevaluated in future work to determine if the equations should be separate as in the Wayson methodology.

Moreover, the research would benefit if measurement were conducted at different locations to avoid any location bias. Research in the field of atmospheric effects on noise propagation needs to be better funded, the project was unfunded leading to time and equipment limitations, and this should lead to a better evaluation of atmospheric refraction. Finally, FHWA should strongly consider including algorithms to correct for atmospheric refraction in TNM as an option in instances where the noise consultant/researcher has observed/anticipated weather inputs and may feel that

significant atmospheric effects are occurring in the project area. This could be reevaluated in future work to determine if the equations should be separate as in the Wayson

REFERENCES

American National Standards Institute, 1978: *Method for The Calculation of The Absorption Sound by The Atmosphere*, ANSI S1.26-1978, New York.

American National Standards Institute, 1998: *Method for Determination of Insertion Loss of Outdoor Noise Barriers of All Types*, ANSI S12.8-1998, New York.

Anderson, G.S., Lee, C.S.Y., Fleming, G.G., Menge, C.W. 1998: *FHWA Traffic Noise Model, User's Guide*. FHWA-PD-96-09, U.S. Department of Transportation, Federal Highway Administration.

Attenborough, K. 1980: Propagation of Sound Above a Porous Half Space, *Journal of the Acoustical Society of America*, vol. 68(5), pp.1493-1501.

Aylor D. 1971: Noise Reduction by Vegetation and Ground, *Journal of the Acoustical Society of America*, vol. 51, pp.197-205.

Baker, R.N. 1980: The Effect of Environmental Variables on Truck Noise Emission, *Proceedings of Inter-Noise 80*, pp. 357-360.

Bass, H.E., Bolen, L.N., Cress, D., Lundien, J. and Fohr, M. 1980: Coupling of Airborne Sound into the Earth: Frequency Dependence, *Journal of the Acoustical Society of America*, vol. 67, pp. 1502-1506.

Beranek, L. 1971: *Noise and Vibration Control*, McGraw Hill Book Co.

- Bowlby, W.** 1980: *SNAP 1.1: A Revised Program and User's Manual For The FHWA Level 1 Highway Traffic Noise Prediction Computer Programs*, Report FHWA-DP-45-4. Federal Highway Administration, U.S. Department Of Transportation, Washington, D.C.
- Bowlby, W., Higgins, J., Reagan, J.** 1982: *Noise Barrier Cost Reduction Procedure: STAMINA2.0/OPTIMA: User's Manual*. FHWA-DP-58-1, U.S. Department of Transportation, Federal Highway Administration.
- Brite/Euram** 1994: *State of The Art Report and Recommendations for Practice and Further Developments*, Contract No.: BREU-CT90-0331.
- Brown, E.H. and Clifford, S.F.** 1976: On the Attenuation Of Sound by Turbulence, *Journal of the Acoustical Society of America*, vol. 60(4), pp. 788-794.
- Chernov, L.A.** 1960: *Wave Propagation in A random Medium*, McGraw Hill, New York.
- Chessel, C.I.** 1977: Propagation of Noise Along a Finite Impedance Boundary, *Journal of the Acoustical Society of America*, vol. 62(4), pp. 825-834.
- De Jong, B.A.** 1980: A New Method For Calculation of The Influence of Wind And Temperature, *Proceedings of Inter-Noise 80*, pp. 549-552.
- De Jong, B.A. vanWulfften Pathe, D.W. and Berkhout, A.J.** 1981: A New Method of Calculation of The Influence of Wind And Temperature II, *Proceedings of Inter-Noise 81*, pp. 261-264.
- DeJong, B.A., Moerkerken, J.D.** 1983: Propagation of Sound Over Grassland and Over a Barrier, *Journal of Sound and Vibration*, Vol. 86(1), pp. 23-46.

- Delany, M.E.** 1969: Range Prediction for Siren Sources, *NPL Aero Special Report 033*.
- Delany, M.E. and Bazley, E.N. 1970: Acoustical Properties of Fibrous Materials, *Journal of Applied Acoustics*, Vol. (3), pp. 105-116.
- Dickinson, P.J. and Doak, P.E.** 1970: Measurement of the Normal Acoustic Impedance of Ground Surfaces, *Journal of Sound Vibration*, vol. 13, pp. 309-322.
- Dickinson, P.J.** 1976: Temperature Inversion Effects on Aircraft Noise Propagation, *Journal of Sound Vibration*, vol. 47(3), pp. 438-443.
- Donato, R.J.** 1976: Propagation of a Spherical Wave Near a Plane Boundary with Complex Impedance, *Journal of the Acoustical Society of America*, vol. 60), pp. 34-39.
- EL-Aassar, A.A.** 2002: *Atmospheric Effects on Traffic Noise Propagation Behind Noise Barriers*, University of Central Florida, Thesis.
- Embleton, T.F.W., Olson, N., Piercy, J.E. and Rollin, D.** 1974: Fluctuations In The Propagation Of Sound Near The Ground, *Journal of the Acoustical Society of America*, vol. 55(2), pp. 485 (A).
- Embleton, T.F.W., Piercy, J.E. and Olson, N.** 1976: Outdoor Propagation over Ground Of The Finite Impedance, *Journal of the Acoustical Society of America*, vol. 59(2), pp. 267-277.
- Embleton, T.F.W.** 1980: Line Integral Theory of Barrier Attenuation, *Journal of the Acoustical Society of America*, Vol. 67(1), pp.42-45.
- Embleton, T.F.W.** 1980: Sound Propagations Outdoors-Improved Prediction Schemes For The 80's, *Proceedings of Inter-Noise 1980*, pp.17-30.

Embleton, T.F.W., Piercy, J.E. and Daigle, G.A. 1983: Effective Flow Resistivity of Ground Surfaces Determined by Acoustical Instruments, *Journal of the Acoustical Society of America*, vol. 74(4), pp. 1230-1244.

Federal Highway Administration 1977: *FHWA Traffic Noise Prediction Model*, Report FHWA-RD-77-108. Federal Highway Administration, U.S. Department of Transportation, Washington D.C.

Fleagle, R.G. and Businger, J.A. 1963: *An Introduction to Atmospheric Physics*, N.Y.

Foss, R.N. 1978: *Ground Plane Wind Shear Interaction on Acoustic Transmission*, Report No. APL-UW 7815, Washington State highway Commission, Seattle, Washington.

Gutenberg, B. 1942: Propagation of Sound Waves In the Atmosphere, *Journal of the Acoustical Society of America*, vol. 14, pp. 151-155.

Hassall, J.R. and Zaveri, K. 1979: *Acoustic noise Measurements*, 4th edition, Bruel & Kjaer.

Hibbs, B.O. and Larson, R.M. 1996: *Tire Pavement Noise and Safety Performance*, FHWA Final report, FHWA-SA-96-068.

International Organization for Standardization 1996: *Acoustics-Attenuation of Sound During Propagation Outdoors*, ISO 9613:1,1996(E), Geneva.

International Organization for Standardization 1997: *In-Situ Determination of Insertion Loss of Outdoor Noise Barriers of All Types*, ISO 10847:1997(E), Geneva.

Ingard, K.U. 1953: A Review of The Influence of Meteorological Conditions on Sound Propagation, *Journal of the Acoustical Society of America*, vol. 25(3), pp. 405-411.

- Jonasson, H.G.** 1972: Sound Reductions by Barriers on the Ground, *Journal of Sound and Vibration*, vol. 22, pp. 113-126.
- Keller, J.B.** 1962: Geometrical Theory Of Diffraction, *Journal Of Optics Society Of America*, vol. 52, pp. 116-130.
- Kneser, H.O.**, 1940: A Nomogram for Finding the Sound Absorption Coefficient in Air, *Akademie Zeit*, vol. 5, pp. 256-257.
- Kriebel, A.R.** 1972: Refraction and Attenuation of Sound By Wind and Temperature Profiles Over A Ground Plane, *Journal of Acoustical Society of America*, vol. 51(1), pp.19-23.
- Kurze, U.J. and Anderson, G.S.** 1971: Sound Attenuation by Barriers, *Applied Acoustics*, vol. 4, pp. 35-53.
- Larson, C., Israelsson, S. and Jonasson, H.** 1979: *The Effects of Meteorological Parameters on The Propagation of Noise From a Traffic Route*, Report No.54, Meteorological Institute of The University of Uppsola, Uppsola, Sweden.
- Lumley, J.L. and Panofsky, H.A.** 1964: *The Structure of Atmospheric Turbulence*, Willey, New York.
- Macdonald, J.M.** 2001: *A Comprehensive Community Noise Prediction Model*, University Of Central Florida, Dissertation.
- Nilsson, N.A.; Bennerhult, O. and Soderqvist, S.** 1980: External Tire/Road Noise: It is Generation and Reduction, *Proceedings of Inter-Noise 80*, Miami, Florida.

- Parkin, P.H. and Scholes, W.E.** 1964: The Horizontal Propagation of Sound From A Jet Engine Close to The Ground at Radlett, *Journal of Acoustical Vibration*, vol. 1, pp.1-13.
- Parkin, P.H. and Scholes, W.E.** 1965: The Horizontal Propagation of Sound From A Jet Engine Close to The Ground at Hatfield, *Journal of Sound and Vibration*, vol. 2(4), pp.353-374.
- Pierce, A.D.** 1972: Diffraction of Sound Around Corners and Wide Barriers, *Journal of the Acoustical Society of America*, Vol. 55(5), pp. 941-954.
- Pierce, A.D.** 1981: *Acoustics: An Introduction to Its Physical Principles And Applications*, McGraw Hill, New York.
- Piercy, J.E.** 1969: Role of The Vibrational Relaxation of Nitrogen in The absorption of Sound in Air, *Journal of the Acoustical Society of America*, vol. 46(3), pp.602-604.
- Piercy, J.E.** 1972: The Absorption of Sound in The Atmosphere, *Journal of the Acoustical Society of America*, vol. 52(5), pp.1310.
- Piercy, J.E., Donato, R.J., and Embleton, T.F.W.** 1976: Near Horizontal Propagation of Sound Over Grassland, *Journal of the Acoustical Society of America*, vol. 60, S2(A).
- Piercy, J.E., Embleton, T.F.W., and Sutherland, L.C.** 1977: Review of Noise Propagation in Atmosphere, *Journal of the Acoustical Society of America*, vol. 61(6), pp.1403-1418.
- Richardson, L.F.** 1920: *Some Measurements of Atmospheric Turbulence*, Phil, Transportation Royal Society, London Series A, vol. 221, pp. 1-28.

- Rudder, F.F.** 1979: *National Roadway Traffic Noise Exposure Model*. U.S. Environmental Protection Agency, Office of Noise Abatement and Control.
- Rudnick, I.** 1947: Propagation of an Acoustic Wave along a Boundary, *Journal of the Acoustical Society of America*, vol. 19(2), pp. 348-356.
- Rudnick, I.** 1951: Acoustic Wave Propagation along a Constant Normal Impedance Boundary, *Journal of the Acoustical Society of America*, vol. 23(2), pp. 546-549.
- Scholes, W.E., Salvidge, A.C. and Sarent, J.W.** 1971: Field Performance of A Noise Barrier, *Journal of Sound and Vibration*, vol. 38, pp. 281-303.
- Sommerfeld, A.** 1909: *Ann. Physics*, Leipzig, vol. 28, pp.665-736.
- Sommerfeld, A.** 1964:*Optics*, Academic Press Inc.
- Sutherland, L.C.** 1971: Scattering Attenuation of Sound In The Lower Atmosphere, *Journal of the Acoustical Society of America*, vol. 49(1), pp.129 (A).
- Sutherland, L.C., Piercy, J.E., Bass, H.E. and Evans, L.B.** 1974: Method for Calculating the absorption of Sound by The Atmosphere, *Journal of the Acoustical Society of America*, vol. 49(1), S1 (A).
- Sutherland, L.C.** 1975: Review of Experimental Data in Support of a Proposed New Method for Computing Atmospheric Loss, Department of Transportation Report TST-75-87, Department of Transportation, Washington D.C.
- Tatarski, V.I.** 1961: *Wave Propagation in A Turbulent Medium*, McGraw Hill, New York.

- Tatarski, V.I.** 1971: *The Effects Of The Turbulent Atmospheric On Wave Propagation*, Keter, Jerusalem.
- Tilliston, J.G.** 1965: Attenuation of Sound Over Snow-Covered Fields, *Journal of the Acoustical Society of America*, vol. 39, pp.171-174.
- Van Der Pol, B.** 1935: *Physica*. Vol. 2, p. 843.
- Wait, J.R.** 1970: *Electromagnetic Waves in Stratified Media*. p.5, Pergamon, New York.
- Wark, L. and Warner, C.F.** 1976: *Air Pollution: Its Origin and Control*, Harper Row, New York.
- Wayson, R.L. and Macdonald, J.M.** 1997: An Advancement in Traffic Noise Modeling: AAMA Community Noise Model 4.0, *AWMA Conference Proceedings*..
- Wayson, R.L.** 1989: *Atmospheric Effects on Traffic Noise Propagation*, Vanderbilt University, Dissertation.
- Weiner, F.M. and Keast, D.N.** 1959: Experimental Study of The Propagation of Sound Over Ground, *Journal of the Acoustical Society of America*, vol. 31, pp. 724-733.
- Wenzel, A.R.** 1974: Propagation of waves along an impedance boundary, *Journal of the Acoustical Society of America*, vol. 55(5), pp. 956-963.
- Weyl, H.** 1909: *Ann. Phys. Leipzig*, Vol. 60, pp. 95-96.
- Yoshihisa, K. and Tachibana, H.** 1984: Difference Between The Effect of Wind On Sound Propagation From A Point Source and From A Line Source, *Proceedings of Inter-Noise1984*, pp. 285-288.